LIÈGE université
Gembloux
Agro-Bio Tech

AIL
4
Water Quality

Assessing hydrodynamic soil properties and herbicides fate under contrasting long-term production systems

Clémence Pirlot

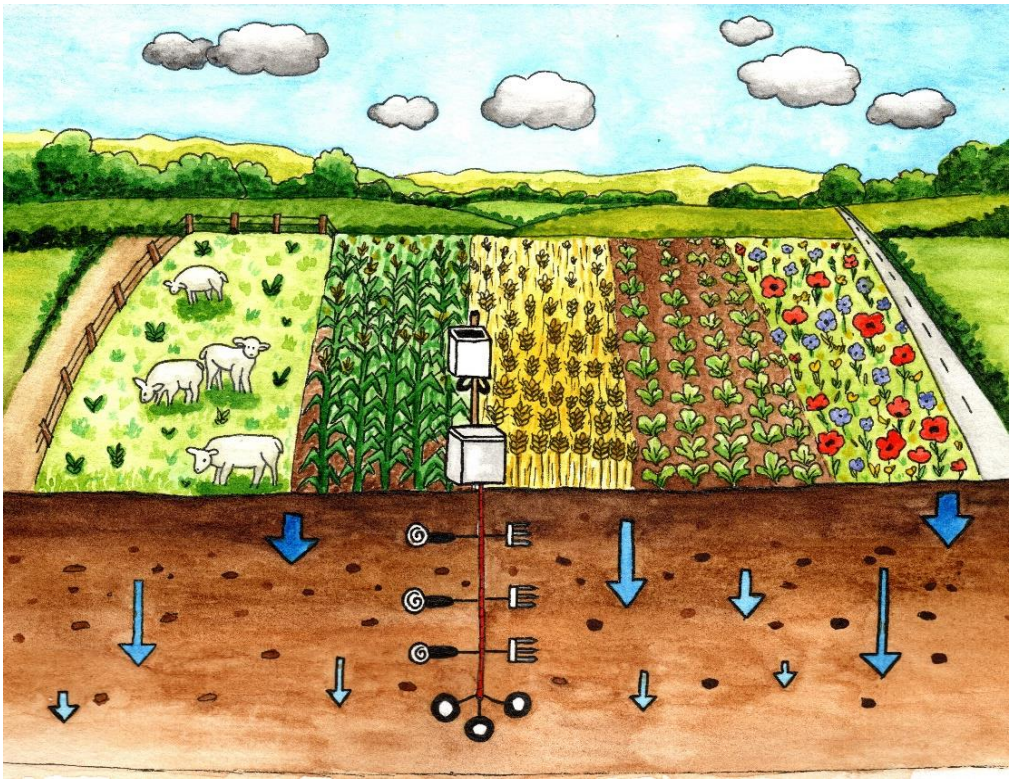

COMMUNAUTÉ FRANÇAISE DE BELGIQUE
UNIVERSITÉ DE LIÈGE – GEMBLOUX AGRO-BIO TECH

Assessing hydrodynamic soil properties and herbicides fate under contrasting long-term production systems

Clémence Pirlot

Dissertation originale présentée en vue de l'obtention du grade de doctorat en sciences agronomiques et ingénierie biologique

Promotrice : Pr. Aurore Degré
Année civile : 2025

Abstract

In the context of climate change, population growth, and degradation of natural resources, it is urgent to rethink our production systems to make them more sustainable. In this regard, a better understanding of the environmental fate of pesticides is essential. Most current studies rely on generic mobility parameters, which can result in inaccurate assessments of contamination risks. Furthermore, soil column leaching experiments are commonly conducted using a wide variety of methodologies, which may significantly influence the outcomes. Additionally, the long-term impact of agricultural practices and climatic conditions on soil hydrodynamic properties is rarely assessed directly in the field.

This thesis aims to address these gaps. First, it evaluates the impact of several commonly used leaching methodologies on experimental results. Second, it investigates the fate of eight herbicides of concern for groundwater contamination in Wallonia using undisturbed soil column experiments under various cropping systems and soil depths. Site-specific mobility parameters were derived through dual-porosity inverse modelling and compared to generic values used in Belgium and from regulatory databases. Third, this work assesses the long-term effects of production systems that incorporate sustainable agricultural practices under contrasting climatic conditions on the temporal evolution of soil water retention, using in situ monitoring. Finally, a comprehensive database was developed to document the influence of these systems on pesticide, metabolite, and nitrate leaching, as well as on soil structure and hydrodynamic properties, through high-frequency hydrological monitoring. The evolution of soil water retention curves over a three-year period was analysed and compared to laboratory-derived curves (ku-pF method) and pedotransfer function predictions from the EU-HYDI database.

Results demonstrate that soil structure, column dimensions, and sampling techniques greatly affected solute transport dynamics and water infiltration. Disturbed columns tend to underestimate rapid contaminant transport and overestimate retention, leading to biased contamination risk assessments. Shorter columns overestimated leaching potential while underestimating degradation processes. Furthermore, columns sampled with mechanical corers showed artificial preferential flow caused by vibration, compromising the representativeness of water and solute transport. These findings highlight the critical role of column design and sampling methods in leaching experiments, emphasizing the need standardised experimental protocols to improve the reliability of transport estimates.

Moreover, different soil properties and structure between soil depths had a greater impact on pesticide leaching behaviour than the cropping systems. Significant variations in pesticide transport and retention were observed between soil horizons, illustrating the inadequacy of relying solely on surface parameters for the entire soil

profile, which may lead to underestimating groundwater contamination risks. Root architecture and surface tillage were found to affect pesticide leaching dynamics, suggesting that cropping systems could serve as strategic levers to mitigate groundwater contamination. Experimental transport parameters showed discrepancies with established databases, which often overestimate retention and underestimate the production of metabolites. These study underline the need of adjusting transport parameters to site-specific conditions and systematically accounting for metabolite behaviour. Future research should focus on long-term monitoring of the effects of sustainable agricultural practices on pesticide behaviour over several seasons and for a range of soil types.

The thesis also reveals that agricultural practices and crop types have a stronger influence on soil water retention dynamics than seasonal wetting-drying cycles, plant development or interannual climatic variability. Practices such as crop differenciation, weed control, crop residue management, compaction during harvest, and the introduction of temporary grasslands induced significant changes in soil water retention capacity, persisting for more than two years in some cases. Comparisons of SWRCs showed that theoretical curves derived from PTFs poorly represent actual field conditions, especially under alternative agricultural systems. The laboratory curves are closer with similar trends but are not optimal. These findings, which are rarely documented in situ, demonstrate that soil water behaviour is far from static and sensitive to management practices. They further highlight the potential of agricultural systems as effective levers to enhance both water retention and food system resilience under future climate conditions. Therefore, to assess the relevance of future production systems, studies should focus on the impact of multi-cropping systems on water retention dynamics, continuously and directly in the field.

Finally, the comprehensive database established provides a valuable resource for supporting sustainable soil and water management decisions, support environmental protection, and improve the predictive performance of hydrological and agroecosystem models, addressing challenges such as climate resilience and food security.

Résumé

Dans un contexte de changement climatique, de croissance démographique et de dégradation continue des ressources naturelles, il devient impératif de repenser nos systèmes de production afin de les rendre plus durables. Une meilleure compréhension du devenir environnemental des pesticides est donc indispensable. Or, la majorité des études s'appuie sur des paramètres de mobilité génériques, conduisant à des estimations peu fiables des risques de contamination. Par ailleurs, les expériences de lixiviation en colonnes de sol sont réalisées selon des protocoles très variés, ce qui peut altérer fortement la qualité des résultats. De plus, l'influence des pratiques agricoles et des conditions météorologiques sur les propriétés hydrodynamiques des sols est rarement étudiée in situ sur le long terme.

Cette thèse vise tout d'abord à évaluer l'impact de plusieurs méthodologies courantes sur les résultats de lixiviation. Ensuite, elle étudie le devenir de huit herbicides préoccupants pour la qualité des eaux souterraines en Wallonie, en fonction de différents systèmes de culture et de la profondeur des horizons, à partir de colonnes de sol intactes. Les paramètres de mobilité ont été obtenus par modélisation inverse double porosité et comparés aux valeurs génériques issues des bases de données. Ensuite, la thèse explore les effets à long terme de systèmes de production intégrant des pratiques agricoles durables, sous conditions climatiques contrastées, sur l'évolution temporelle de la rétention en eau des sols. Les courbes de rétention en eau mesurées sur trois ans ont été comparées aux courbes obtenues en laboratoire par la méthode ku-pF, ainsi qu'aux prédictions issues des fonctions de pédotransfert EU-HYDI. Enfin, la base de données établie permet d'étudier l'influence de ces systèmes sur la lixiviation des pesticides, de leurs métabolites et des nitrates, ainsi que sur l'évolution de la structure et des propriétés hydrodynamiques des sols, grâce à un suivi hydrologique à haute fréquence.

Les résultats mettent en évidence l'influence déterminante de la structure du sol, de la taille des colonnes et de la méthode d'échantillonnage sur les dynamiques de transport des solutés et l'infiltration de l'eau. Les colonnes remaniées tendent à sous-estimer le transport rapide des contaminants et à surestimer leur rétention. Les colonnes plus courtes surestiment le potentiel de lixiviation et sous-estiment la dégradation des composés. De plus, les prélèvements réalisés avec un carotteur mécanique introduisent des flux préférentiels artificiels dus aux vibrations, altérant la représentativité des transferts. Ces résultats soulignent la nécessité de protocoles expérimentaux standardisés pour améliorer la fiabilité des estimations de transport.

Par ailleurs, la structure et les propriétés du sol selon la profondeur ont montré un impact plus important sur le comportement des pesticides que les systèmes de culture. Des différences marquées dans le transport et la rétention des pesticides ont été observées entre horizons, illustrant l'inadéquation des paramètres issus de la couche

superficielle pour représenter l'ensemble du profil. L'architecture racinaire et le travail superficiel influencent les dynamiques de lixiviation, suggérant que les systèmes de culture pourraient constituer des leviers efficaces pour réduire la contamination des eaux. Les paramètres expérimentaux de transport se sont souvent révélés divergents des valeurs issues des bases de données surestimant généralement la rétention et sous-estimant la formation de métabolites. Il apparaît donc essentiel d'adapter les paramètres de transport aux conditions spécifiques du site et d'inclure systématiquement les métabolites dans les évaluations de risque. Les recherches futures devraient se concentrer sur le suivi à long terme de l'influence des pratiques agricoles durables sur le devenir des pesticides, sur plusieurs saisons et types de sol.

La thèse met également en évidence une influence plus marquée des pratiques agricoles et des cultures sur la dynamique de la rétention en eau des sols que celle exercée par le développement des plantes, les cycles saisonniers d'humidification-séchage ou les conditions climatiques. Des pratiques telles que la diversification des cultures, la gestion des adventices, la restitution des résidus, le compactage en période de récolte ou l'introduction de prairies temporaires ont induit des modifications importantes de la capacité de rétention en eau, parfois durant plus de deux ans. Les comparaisons montrent que les courbes théoriques issues des fonctions de pédotransfert sont peu représentatives, notamment pour les pratiques agricoles alternatives. Les courbes mesurées au laboratoire sont plus proches mais pas optimales. Les variations temporelles observées, rarement documentées in situ, montrent que le comportement hydrique du sol est loin d'être statique. Elles soulignent que les pratiques agricoles et les cultures peuvent être de puissants leviers pour améliorer la résilience hydrique et alimentaire face aux conditions climatiques futures. Ainsi, pour évaluer la pertinence des systèmes de production de demain, il est donc indispensable d'étudier l'impact des systèmes de cultures diversifiés sur la dynamique de la rétention en eau, directement et en continu sur le terrain.

Enfin, la base de données élaborée dans cette thèse constitue une ressource précieuse pour éclairer les décisions en matière de gestion durable des sols et de l'eau, soutenir la protection de l'environnement et améliorer la performance prédictive des modèles hydrologiques et agroécosystémiques. Elle apporte des éléments-clés pour faire face aux défis de la résilience climatique et de la sécurité alimentaire.

Remerciements

À l'heure où cette thèse touche à sa fin, c'est bien plus qu'un simple chapitre qui se referme. C'est l'aboutissement de plus de cinq années intenses de travail, de réflexion, de doutes, d'essais parfois infructueux mais aussi de réussites, de découvertes, de joie et de rencontres inoubliables. Travailler sur l'eau et les sols, c'est un engagement profond envers le vivant, et cette thèse a été également une aventure humaine. Je tiens à remercier du fond du cœur toutes les personnes, proches ou lointaines, qui ont contribué, de mille façons, à rendre ce parcours possible.

Je tiens tout d'abord à remercier chaleureusement ma promotrice, Aurore Degré. Merci de m'avoir offert la chance de plonger dans cette aventure scientifique, au cœur de l'eau et des sols. Dès le début de ce projet, légèrement chamboulé par l'arrivée du Covid, tu as toujours été disponible, à l'écoute et présente dès que j'en avais besoin, malgré un agenda souvent (toujours) bien rempli. Merci pour toutes tes relectures de dernière minute (oups) malgré mes écrits d'une grande longueur. Merci pour ton soutien quand les choses n'allaient pas comme prévu ! Notamment, l'expérience en colonnes à recommencer, ce premier article qui ne cessait d'être refusé ou encore la fin du projet initial. Merci de m'avoir fait confiance une seconde fois et de m'avoir dégoté le projet AWAC pour que je puisse terminer cette thèse. Enfin, merci de m'avoir accompagnée durant ces cinq années et demie avec ce mélange de bienveillance, de rigueur et de regard critique qui m'a toujours fait progresser.

Je tiens ensuite à remercier très sincèrement les membres de mon comité de thèse, qui m'ont accompagnée tout au long de ces cinq années, avec bienveillance, encouragements et une confiance en ma thèse qui m'a portée jusqu'à la fin. Merci à Gilles Colinet pour son regard d'expert sur les sols, ses précieux conseils sur les échantillonnages, sa bonne humeur constante (pour Bob l'Éponge le jour de ma défense privée), et surtout pour avoir permis que ma thèse soit ornée d'une magnifique illustration de profil de sol ! Merci à Jeroen Meersmans pour ses conseils avisés dans son domaine d'expertise mais aussi sur la structuration de ma thèse, la gestion du temps et la publication d'articles, qui m'ont beaucoup aidée à prendre du recul et à mieux comprendre le fonctionnement du monde scientifique. Merci aussi pour les bons moments partagés, notamment lors de l'EGU. Merci à Caroline De Clerck, responsable de l'expérience EcoFoodSystem, sur laquelle repose l'ensemble de mon travail. Merci pour ta disponibilité, tes explications toujours claires, tes relectures attentives, tes encouragements et ton soutien sans faille tout au long de cette thèse. Enfin, un merci à Olivier Pigeon du CRA-W pour son expertise précieuse sur les pesticides, ses réflexions pertinentes et son aide pour les protocoles expérimentaux. Merci à vous tous d'avoir été présents, impliqués et enthousiastes, du début à la fin.

Je souhaite également remercier les membres extérieurs de mon jury pour leur disponibilité et leur implication. Merci d'avoir accepté d'évaluer mon travail, d'avoir relu attentivement ma thèse et d'y avoir apporté un regard neuf et constructif. Un

merci particulier à Valérie Pot (INRAE, France) pour sa relecture minutieuse, ses remarques pertinentes sur mes expérimentations en colonnes de sol et leur modélisation, ainsi que pour sa présence à ma défense publique. Merci également à Serge Brouyère pour l'intérêt qu'il a porté à mon travail, ses commentaires éclairants sur la portée de mes résultats, notamment en lien avec les eaux souterraines. Enfin, merci à Haissam Jijakli d'avoir accepté la présidence de mon jury.

Au-delà de l'encadrement scientifique direct, cette thèse n'aurait pas été possible sans le soutien du comité d'accompagnement du projet AIL4WaterQuality. Merci à la SPGE (Société Publique de Gestion de l'Eau) et à Nicolas Triolet et Fanny Van Wittenberge, pour avoir financé ce projet, mais aussi pour le suivi bienveillant et les retours positifs. Je remercie également Alodie Blondel et Boris Krings du CRA-W, pour leur implication dans mes expérimentations de lixiviation des pesticides et du nitrate, aussi bien au laboratoire que sur le terrain. Merci pour votre expertise, vos conseils méthodologiques, vos relectures et contributions aux protocoles, ainsi que pour tout le temps consacré aux analyses. Un grand merci aussi à Simon Dierickx de Greenotec pour son regard agronomique sur mes résultats de terrain et sa participation active à la journée de communication du projet. Enfin, je n'oublie pas Armelle Copus, Maryse Wertz, Nathalie Ducat et Céline Rentier, dont l'implication lors des réunions du comité d'accompagnement et l'intérêt pour le projet ont été très appréciés.

Un grand, grand merci à Katia Berghmans, notre super secrétaire et véritable pilier de l'axe. Merci pour ta bonne humeur contagieuse, ton efficacité redoutable et ton aide précieuse, toujours avec le sourire. Que ce soit pour mes commandes, contrats, réservations de salle, notes de débours (et bien d'autres aventures administratives), tu as toujours été là, avec patience et gentillesse. Merci aussi pour tous ces midis partagés et pour tes rires qui réchauffent le cœur du TOPO. Je souhaite également remercier Gilles Swerts et Stéphane Becquevort, techniciens de l'axe, pour leur précieuse aide tout au long de ces années. Merci pour votre soutien sur le terrain, notamment lors de l'installation du matériel de monitoring, mais aussi pour votre accompagnement lors des campagnes d'échantillonnage et des manipulations en laboratoire. Votre disponibilité, votre réactivité et votre savoir-faire ont grandement facilité le bon déroulement de mes expérimentations.

Et bien sûr, un immense merci à tous mes collègues de l'axe EESP. Merci pour tous ces moments partagés, autour d'un ordi, d'un échantillon de sol, ou d'un verre au Beer Fac. Merci pour les barbecues de l'axe, les Fac Trophy (même si le dernier manquait un peu de rigueur scientifique pour le comptage des points), et pour les super team buildings avec une mention spéciale à PEYRESQ, évidemment. Une semaine hors du temps, des éclats de rire à chaque virage, une équipe soudée comme un bon agrégat de sol et une ambiance aussi fluide qu'un ruissellement après une bonne pluie. Vous avez vraiment mis du soleil dans ma thèse. Merci pour tout.

Je voudrais maintenant remercier, du fond du cœur, l'équipe des Jeun's du topo. Merci à Benjamin, AnneK, Cailloux, SibSib, Guigui, MattMatt, Ced, Cam, Lisa et Nicolas. Il est difficile de mettre des mots sur toute la gratitude que je ressens pour vous. Merci pour chaque pause café prolongée, chaque soirée improvisée (vive Pitch Perfect), chaque éclat de rire, chaque citation ajoutée au tableau, chaque discussion sérieuse ou totalement absurde, chaque moment où vous avez su écouter, encourager, rassurer. Vous avez été des vrais rayons de soleil dans mon quotidien et transformé l'ambiance du topo en un vrai lieu de vie (et pas juste de science !). En début de thèse, le télétravail occupait une grande partie de ma semaine… aujourd'hui, je viens un maximum au bureau pour travailler à vos côtés. Vous êtes, sans aucun doute, les plus belles rencontres de ces cinq années, et je vous en serai toujours profondément reconnaissante.

Je voudrais remercier particulièrement mon tout premier TFEiste, Benjamin. Merci de m'avoir fait confiance en te lançant dans ton mémoire sur mon projet et pour ton aide sur le terrain. Tu as été le premier membre de notre petite équipe, et c'était le début d'une belle aventure ! Toujours posé, toujours partant, tu as été une vraie bouffée d'air frais dans cette thèse, merci !

Je voudrais également adresser un remerciement spécial à ma deuxième TFEiste, stagiaire éternelle de mon cœur, collègue préférée, presque amie : Anne-Catherine. Merci d'avoir accepté ce mémoire avec moi, merci pour tous les bouts de code que tu m'as concoctés avec soin, pour tes relectures toujours méticuleuses (et pour l'alignement des mes pwp) et ton aide précieuse tout au long de cette thèse. Mais surtout, merci d'avoir rejoint l'équipe du topo, et d'y avoir mis autant de lumière. Depuis ton arrivée, mes journées se sont embellies et sont devenues bien plus drôles et joyeuses. Merci pour ton écoute quand je me plains, ta bonne humeur contagieuse, tes discours de motivation (souvent bien nécessaires), tes petites attentions, ta lettre d'encouragement qui m'a fait pleurer (un peu), tes petits post-its surprises, ton sourire quand j'arrive le matin, les pauses café presque obligatoires et les soirées mémorables. Je n'oublierai jamais tout ces moments ensemble ni l'enthousiasme sincère avec lequel tu as accueilli la nouvelle de la petite brioche. Et même si tu continues de dire qu'on n'est « que collègues » pour moi, tu es devenue une amie précieuse, et je t'en remercie du fond du cœur.

Je voudrais aussi remercier deux autres collègues très spéciales à mes yeux : Cailloux et SibSib. Merci les filles pour tout ce que vous êtes. On ne se connaît pas depuis si longtemps, et pourtant, vous êtes rapidement devenues des personnes importantes dans ma vie. Merci Cailloux d'avoir été ma première coloc de bureau avec qui les discussions se faisaient aussi naturellement que les silences. Ton enthousiasme contagieux pour la recherche et la thèse m'a fait un bien fou, surtout dans les moments de doute. Merci d'avoir toujours cru en moi, de m'avoir écoutée pendant des heures, et d'avoir apporté ta bonne humeur et ton énergie au sein de notre

petite équipe du topo et d'être toujours présente et prête à aider. Merci SibSib pour ta présence lumineuse et ton soutien indéfectible. Merci pour ta chaise de psy, toujours libre pour m'écouter, pour ton appart de rêve qui nous a accueillis plus d'une fois, pour tes câlins du matin, pour tes rires qui illuminent mes journées les plus grises, et bien sûr pour tes post-its lapins, devenus des repères rassurants sur mon ordi. Merci également également d'avoir permis à la petite brioche d'avoir un premier cousin de cœur avec Podzol. Merci à vous deux pour ces dernières années, pour tous ces instants partagés, au topo comme en dehors. Vous avez mis du soleil dans cette thèse pas toujours facile, et je vous en suis profondément reconnaissante.

Aussi, un immense merci à l'ensemble de mes amis. Vous avez été un soutien indéfectible tout au long de cette thèse, et tout particulièrement dans les moments les plus compliqués. Merci pour votre écoute, vos distractions bienvenues, et votre présence, tout simplement. Un merci tout particulier à Clem B, Tanguy, Sarah, Alizé, Lise, Charles, Marine, Pauline, Tiffanie, Clem D, Manubis, Vladimir, Quentin, Nicolas, Yasmine et Jerem. Merci aussi à mes amies du hockey : Julie, Delphine, Justine, Nao, Ele et Fanny. Merci pour ces belles amitiés, certaines qui durent depuis plus de 10 ans, d'autres qui se sont tissées plus récemment mais qui comptent tout autant. Je vous aime, et je suis si heureuse de vous avoir dans ma vie.

Je voudrais maintenant remercier ma famille, et tout particulièrement mes parents, qui ont embarqué, malgré eux, dans cette aventure en même temps que moi, il y a plus de cinq ans. Merci pour votre soutien indéfectible, pour votre patience, pour vos encouragements lors des week-ends et des vacances que j'ai souvent passés à travailler. Merci pour vos conseils, vos mots rassurants dans les moments de doute, pour les distractions quand ça n'allait pas et pour avoir toujours été là, sans jamais faillir. Rien de tout cela n'aurait été possible sans vous. Merci du fond du cœur.

Mon dernier remerciement va bien sûr à la personne la plus importante de ma vie, à mon amour, mon meilleur ami, mon compagnon de route, mon pilier, et le papa de notre petit Zeze, mon Pierre. Sans toi, cette thèse n'aurait tout simplement jamais vu le jour, car je n'aurais jamais osé postuler. Tu as su m'encourager et me faire croire en moi dès le début. Tout au long de ces années, tu as toujours été là, prêt à m'aider sur le terrain, à me soutenir, à me redonner confiance quand j'en manquais. Tu as été à l'écoute dans mes moments de doute et de déprime, tu m'as redonné le sourire quand il le fallait. Merci pour toutes ces heures passées à m'écouter parler de cette thèse, pour toutes ces petites attentions, tous ces repas préparés pour me laisser travailler. Bref, merci d'être le compagnon idéal que l'on peut rêver d'avoir, tu as vécu cette thèse presque autant que moi. Merci d'avoir été aussi heureux, parfois même plus que moi, et si fier à chaque bonne nouvelle, à chaque comité, à chaque article accepté, et enfin pour cette fin de thèse. Merci pour tout, merci d'être toi. Je suis impatiente d'écrire le prochain chapitre de notre vie, avec notre petite brioche à venir, et de passer le reste de mes jours à vos côtés.

Table of contents

List of figures

List of tables

List of acronyms

BD : bulk density

BTC : breakthrough curve

CEC : cation exchange capacity

CRA-W : Centre wallon de Recherches Agronomiques

DP : dual-porosity

EFSA : European Food Safety Authority

EU : European Union

EU-HYDI : EUropean HYdropedological Data Inventory

ICLS : Integrated cop-livestock system

LOQ : limit of quantification

NT : no-till

OC : organic carbon

OM : organic matter

PPDB : Pesticides Properties DataBase

PTF : pedotransfer fonction

REF : reference

RMSE : root-mean-square-error

SAP : sustainable agricultural practices

SP : single-porosity

SSQ : sum of squares

SWRC : soil water retention curve

T1 : temporality 1

T2 : temporality 2

VWC : volumetric water content

WDs : wetting-drying cycles

Chapter 1

General introduction and objectives

1. Pesticide use: past and present

Since the dawn of agriculture, mankind has been confronted with crop-damaging organisms such as weeds and pests. The first modern pesticides were used on crops in the 19th century and these treatments expanded rapidly. After the Second World War, an increase in agricultural productivity was needed to feed the population and avoid famine, leading to the "Green Revolution". This revolution was characterised by the introduction of improved crop varieties selected for high yield, monocultures, intensive use of agrochemicals such as pesticides and fertilisers, irrigation and heavy machinery. This revolution contributed to a remarkable rise in agricultural production (Magarey et al., 2019). The use of pesticides grew with the discovery of numerous new compounds after 1950 (Oerke, 2006). These new crop varieties and agricultural environments have led to new types of weeds, requiring an increase and diversification of pesticides (Mesnage et al., 2021).

Pesticides is a broad term covering all chemicals used to kill target organisms that are harmful to crops. The term includes insecticides, fungicides, herbicides, rodenticides, molluscoids, netamiticides, plant growth regulators and other substances such as defoliants, desiccants and fumigants. The use of pesticides is an integral part of agriculture throughout the world (Pérez-Lucas et al., 2020). Pesticide use rose from 0.2 million tonnes in the 1950s to over 5 million tonnes in 2000 (Carvalho, 2017). Currently, 3.7 million tonnes of active ingredients are used every year worldwide (Hayes and Hansen, 2017; FAOSTAT, 2022). This represents a 50% increase in pesticide use since the 1990s. The main pesticide-using countries are Brazil, the USA and Indonesia, which together account for 1.6 million tonnes. Pesticide use is also high in Europe, with France in 10th place with almost 68 thousand tonnes of active ingredients (figure 1). Without pesticides, it is estimated that 78% of fruit production, 54% of vegetable production and 32% of cereal production could be lost (Lamichhane, 2017).

Herbicides are the main type of pesticide used, accounting for 55% of pesticides applied to agricultural land in 2018 (FAO, 2022). Herbicides are agrochemicals applied to prevent or interrupt the normal growth and development of unwanted plants. They are widely used to manage weeds in agriculture. In fact, weeds are responsible for an estimated 43% of crop yield losses worldwide (Oerke, 2006). Herbicides reduce the need for tillage and the energy required for mechanical weeding. They have several modes of action, but mainly focus on the physiological processes of target plants. Herbicides are classified according to whether they are applied pre-emergence or post-emergence. Pre-emergence herbicides are applied directly to the soil and prevent the germination and early growth of weed seeds. They are generally non-selective and phytotoxic to all plants. Post-emergence herbicides are applied at the start of or during cultivation and are specific to the weeds present. They are applied to the soil and to the crop.

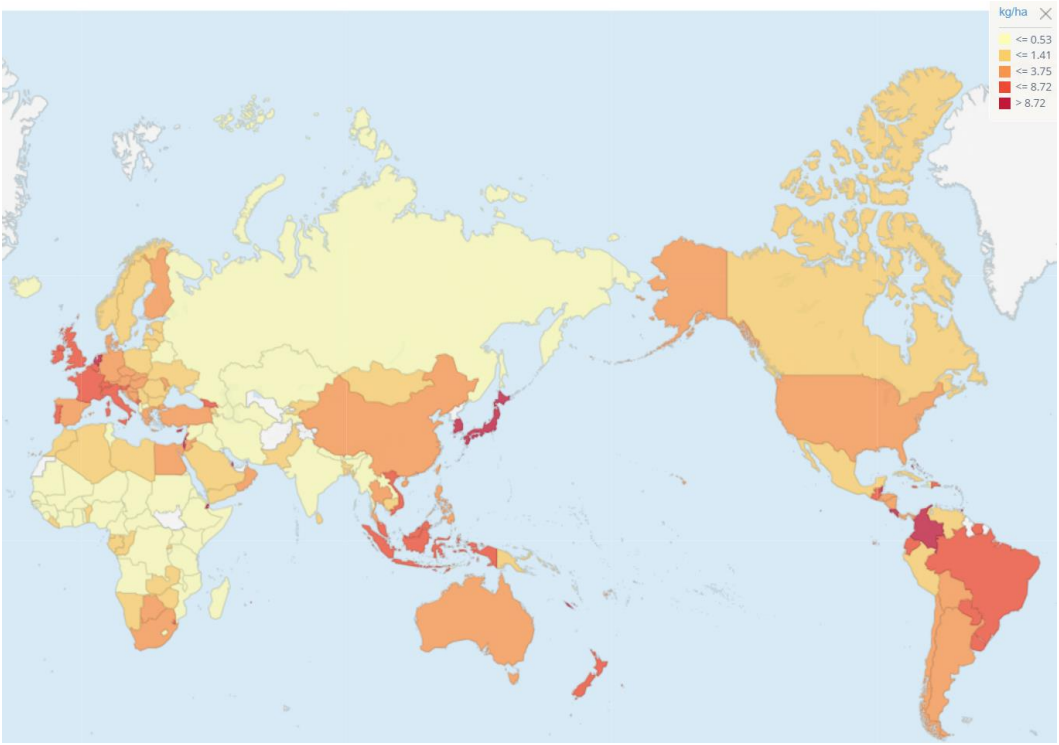

Figure 1. The use of Pesticides in 2022 (measured in kg of active ingredients/ha) (http://www.fao.org/faostat/en/#data/EP/visualize).

2. Agrochemicals use issues

From the very beginning of the intensive use of agrochemicals, their negative effects were quickly pointed out because of their high application rate, lack of selectivity and high toxicity (Smith and Secoy, 1976). Nowadays, the widespread use of these agrochemicals in natural ecosystems has had major repercussions on the environment and human health. In particular, these products can lead to the disappearance of insect populations, loss of habitat through agricultural intensification, appearance of invasive species, and soil and water pollution (Larsen et al., 2019; Sánchez-Bayo and Wyckhuys, 2019; van der Sluijs, 2020). Exposure to pesticides can also have serious consequences for human health, including vomiting, skin irritation, mental confusion, kidney problems, reproductive effects, cancer and even death (Hernández et al., 2013; Khan and Rahman, 2017).

Once applied to agricultural soils, pesticides and fertilizers can take several pathways through the environment. They can undergo a number of processes such as leaching, volatilisation, diffusion, erosion, spray drift, run-off, assimilation by microorganisms, degradation or uptake by plants (Scholtz and Bidleman, 2007). Many factors will influence the fate of pesticides such as their properties but also soil characteristics, site conditions, and pesticide application practices. Different pesticides have different environmental fates depending on their properties. Pesticides can be degraded by microorganisms, chemical reactions or light (Su et al., 2017). The persistence of pesticides in the environment long after use makes them a continuing source of exposure and bioaccumulation that can reach the food chain (Herrero-Hernández et al., 2013). Pesticides can also be adsorbed to the soil, depending on the soil pH, clay content, organic matter and soil amendments. A proportion of these pesticides will leach through the soil profile, leading to a deterioration in groundwater quality (Jurado et al., 2012; Labite et al., 2013). Indeed, high levels of pesticides and their metabolites are often found in groundwater, which is the main source of drinking water in many European countries (Köck-Schulmeyer et al., 2014; Kiefer et al., 2019; Pietrzak et al., 2019; Baran et al., 2021; EurEau, 2021). Groundwater monitoring shows systematic contamination by these products. Groundwater accounts for 30% of the world's freshwater resources. Domestic, industrial and agricultural activities depend on it. In addition, treating and restoring groundwater quality is very costly and inefficient.

In Wallonia (Belgium), almost 80% of the water used in 2019 came from groundwater. Between 2017 and 2020, pesticides were detected in 61.7% of water quality monitoring sites (figure 2).

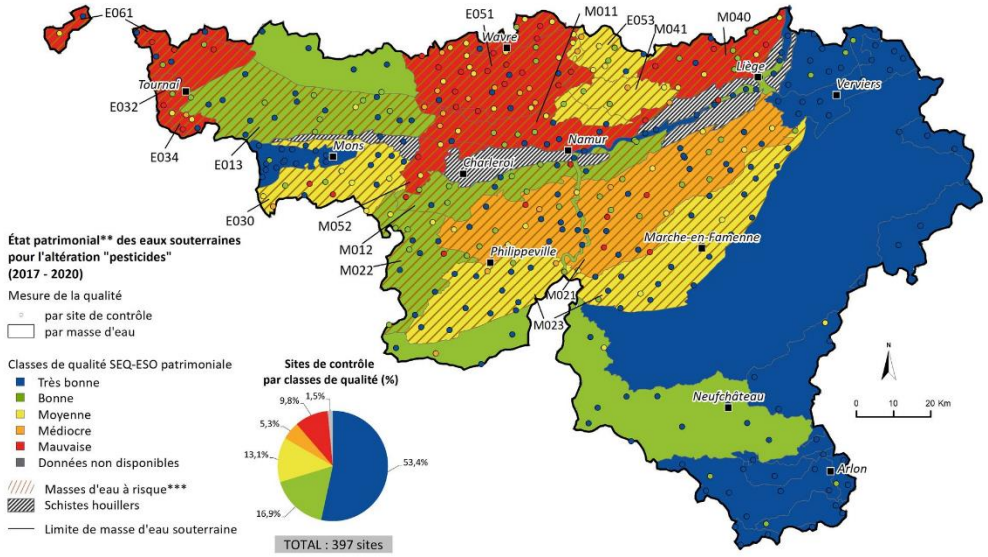

Figure 2. Impact of pesticides on groundwater quality in Wallonia. The dots represent monitoring sites. Quality classes are defined as follows: Very good in blue, Good in green, Average in yellow, Poor in orange, and Very poor in red.

3. Need for changes in agricultural systems

Without plant protection products, annual yield losses are estimated at 20-40% of overall production (FAO, 2017). In addition, these losses will increase with climate change, which contributes to disease, insect infestation and pesticide resistance (Pu et al., 2020). Climate change will also lead to more contrasting rainfall patterns, with longer and more intense droughts alternating with periods of heavy winter rainfall. Agriculture will become more dependent on available water, which will need to be managed to support the resiliency of agricultural systems (Arora, 2019). Access to food is a fundamental right, regardless of the country's economy or people's social status (FAO, 2009). Demographic growth will inevitably lead to a dramatic increase in demand for food and other resources. An increase in production, estimated at 50% by 2050, is therefore necessary to meet the nutritional needs of the future population (FAO, 2017). In this context, the perpetuation of intensive agriculture and the use of pesticides therefore seem inevitable. However, agriculture is one of the largest human interactions with the environment and the human activity with the greatest pressure on the environment. The demands placed on agricultural production systems to achieve global food security in the face of ever-increasing consumption and the degradation of natural resources are forcing us to rethink these systems and move towards more sustainable models. In agriculture, the term 'sustainable' means producing enough for the world's population while minimising environmental and

human impacts and generating a profit for producers. Assessing the sustainability of agriculture is always a vague and challenging process, but there is consensus that sustainable agriculture, by definition, must address environmental, economic and social issues in its approach (de Olde et al., 2017). The ecosystem services of agricultural land must also be taken into consideration, such as water purification, biodiversity, carbon storage, pollination and recreational areas (Tilman et al., 2001; Mesnage et al., 2021).

In order to enhance the sustainability of pesticide utilisation, a set of criteria for authorisation has been instituted within the framework of good agronomic practices and pesticide risk assessment, whether by legal means or through the implementation of policies. The European Union has promulgated regulations for the sustainable use of pesticides with a view to reducing their impact on the environment and human health. Nevertheless, these measures are not always implemented in a consistent manner at the national level, and their stipulations are not always adhered to with rigour (Swartjes and Van Der, 2020; Lykogianni et al., 2021). It has been demonstrated that, despite the existence of regulatory frameworks pertaining to the use of pesticides, these substances have been identified in groundwater sources of drinking water in the vast majority of countries worldwide (Toccalino et al., 2014; Swartjes and Van Der, 2020).

Furthermore, the agricultural sector will become increasingly dependent on available water resources, which will need to be managed in a sustainable manner to support agricultural resilience (Pereira, 2017). The main challenge for agriculture is to produce sufficient quantities in a context of increasing demand, competition for water and land resources, climate change with its uncertainties, declining ecosystem services and changing environmental regulations. Consequently, agriculture must adapt to drier periods with periodic water limitations. A key strategy to enhance the resilience of agricultural systems is the implementation of soil management practices aimed at conserving water. However, the specific strategies that are to be adopted are contingent upon the characteristics of the specific sites and regions concerned. The enhancement of resilience can be particularly bolstered by the augmentation of rainfall capture and the optimisation of soil water storage (Heitman et al., 2023). A variety of soil management solutions are available. Nevertheless, the efficacy of specific approaches varies depending on the characteristics of the soil, the prevailing climate, and the type of cropping system employed at a given location. Long-term soil management experiments and cropping system experiments can provide a comparison of different approaches under varying climatic conditions. Such experiments can facilitate comprehension of the effectiveness of specific practices. It is imperative to conduct experimental campaigns to investigate how diverse management practices influence the water cycle at the plot level (Heitman et al., 2023).

4. Ways to reduce agricultural systems' impact on water resources

Several approaches can be explored to reduce the impact of agricultural systems on water resources, both in terms of quality and quantity. Two main strategies have been identified in the context of this thesis.

4.1. A better understanding of pesticide fate in the environment

Firstly, a better understanding of the fate of pesticides within a soil profile. It is very difficult to assess it. Pesticides behave differently depending on their properties and the properties of the soil. The processes that mainly control the leaching of pesticides into groundwater are adsorption and degradation (Arias-Estévez et al., 2008; Malla et al., 2021). Adsorption depends mainly on the organic matter, clay minerals and iron/aluminium oxides present in the soil. The degree to which pesticides are adsorbed will depend on their nature and properties. Soils with higher organic matter and clay content generally retain more pesticides than other soils due to the large surface area of clay particles and organic matter (Bošković et al., 2020). Leaching will depend on the water retention of the soil, which is controlled principally by its texture, structure, organic matter and water content (Pavlis et al., 2010). Degradation will depend on chemical processes in the soil and biodegradation by soil fauna, influenced mainly by soil pH, microbial population and temperature (Mills et al., 2001).

Therefore, the fate of pesticides in the environment is difficult to predict because it depends on many environmental factors, pesticide properties, site characteristics and agricultural practices. A number of modelling tools have been developed to rapidly assess the potential risks associated with the use of pesticides on agricultural land (Kördel and Klein, 2006; Labite et al., 2011; European Commission, 2014). The most commonly used models for assessing pesticide risks are: MACRO (Water flow and solute transport in macroporous soil), PEARL (Pesticide Emission model At the Regional and Local scales), PELMO (Pesticide Leaching Model) and PRZM (Pesticide Root Zone Model) (Klein et al., 2000; Leistra et al., 2001; Larsbo and Jarvis, 2003; Carsel et al., 2005). Currently, in order to authorize a pesticide within the EU, the 9 scenarios of the FOCUS study group are used to estimate the risk of leaching for the entire geoclimatic range of Europe.

Two parameters are needed to model pesticide movements within a soil profile. These are the sorption coefficient (K_d) and the half-life of the pesticides (DT_{50}) (Kahl et al., 2015). The sorption and degradation parameters used are the result of laboratory or lysimeter experiments carried out by pesticide manufacturers at various sites in a number of European countries and compiled in databases. However, it has been shown that these scenarios with these parameters do not accurately represent the specific conditions of a country or a site (Labite et al., 2013; Cueff et al., 2020). Furthermore,

these parameters are generally estimated only for topsoil. To account for soil depth in models, the adsorption coefficient (K_d) can be converted to K_{oc} in proportion to the organic carbon content of the different soil horizons. The models will then require either a K_d per horizon, calculated based on the organic carbon content, or a single Koc that automatically adapts to the organic carbon content. In terms of degradation, this generally decreases with soil depth due to decreasing microbial activity. Therefore, correction factors can be applied to the degradation rate of pesticides depending on depth like in PEARL or PELMO (FOCUS, 2000; Katagi, 2013).

Agricultural practices and land use can affect the temporal dynamics of soil hydraulic properties and other factors such as soil structure and organic carbon content (Pirlot et al., 2024). Different crops in rotations will affect soil structure through their different root systems (Hu et al., 2009). For example, Lichter et al. (2008) found significantly larger macro-aggregates in the soil under wheat because wheat has a more horizontal root system than maize and the higher density of plants results in a denser shallow root system. Different crops also generate different soil microbial communities, with roots releasing a variety of different exudates depending on the crop. In general, earthworm abundance, diversity and activity increase under conservation agriculture (Chan, 2001; Fox et al., 2022; Lori et al., 2023). Therefore, pesticide leaching within a soil profile can be influenced by soil properties as well as land use, land management and crop characteristics (Alletto et al., 2015). As a result, the K_d and DT_{50} values found in databases are generally specific to the pesticide for a given soil type at a given depth and for a given set of agricultural practices.

It is therefore recommended by scientists and the FOCUS group that the sorption and degradation parameters required by the models should be estimated by leaching experiments on the soil under investigation (FOCUS, 2009). To adjust them, experiments can be carried out on the leaching of pesticides in soil columns (De Wilde et al., 2009; Khan and Brown, 2016; Sur et al., 2022; Imig et al., 2023b). The sorption and degradation parameters are then obtained by inverse modelling of the pesticide breakthrough curve (Mertens et al., 2009; Dusek et al., 2015).

However, soil column leaching studies in the literature have been carried out at different scales and with a wide range of technical approaches, making it difficult to compare or extrapolate results to other situations. Two types of columns are generally used to study pesticide leaching, disturbed and undisturbed columns. Disturbed columns are usually more reproducible and homogeneous than undisturbed columns. However, undisturbed columns make it possible to study the effect of agricultural practices and to approximate real conditions by taking into account preferential flows (Köhne et al., 2006; Pot et al., 2010; Cueff et al., 2020; Aliste et al., 2021). Preferential flows through soil macropores significantly reduce the retention of solutes within the soil profile and can therefore increase the risk of groundwater contamination (Koestel et al., 2013). The size of the soil columns varies greatly in the literature, with

diameters ranging from 1 to 24 cm (Beulke et al., 2001; Cherrier et al., 2005; Ortega et al., 2022) and a height ranging from 5 to 50 cm (Dusek et al., 2015; Khan and Brown, 2016; Albers et al., 2022). Various methods of sampling undisturbed columns can be found in the literature. The columns are generally pushed into the ground with a jackhammer, by hand with a hammer or with drilling equipment (Bégin et al., 2003; Vincent et al., 2007; Cueff et al., 2020).

It is therefore necessary to better understand the impact of the different methodologies on the results of the contaminant elution curves studied. In addition, it is essential to study the fate of pesticides for the specific conditions at the site of interest in order to adjust the mobility parameters derived from the modelling. These experiments will lead to a better understanding of the leaching of pesticides into groundwater, a better definition of pollution risks and improved decision-making on their application.

4.2. A transition to more sustainable and resilient production systems

Secondly, a transition from current agricultural systems to more sustainable, environmentally friendly and resilient systems. Sustainable Agricultural Practices (SAP) are emerging. According to the Food and Agriculture Organization of the United Nations, SAPs consist of 5 points: practices that conserve resources, do not degrade the environment, are technically appropriate, economically viable and socially acceptable (FAO, 2017). These practices include long-term rotations with a diversity of crops, cover crop planting such as CIPAN, no-till or reduced-till systems, systems with a livestock-crop integration, the use of reasoned inputs and agroforestry practices (Piñeiro et al., 2020). Sustainable agricultural practices protect ecosystems through a more efficient use of natural resources and strengthen the capacity to adapt to climate change (Arora, 2019; Magarey et al., 2019).

These practices are emerging. However, their impact on water resources is not yet known or has received little attention. However, the effects of these new practices on soil structure and on water and solute transport need to be investigated to assess their relevance. The effects of these alternative practices on soil structure vary and occur at different timescales. The water cycle, and therefore the amount of water that infiltrates, evaporates and is rapidly leached, depends on climate and vegetation, but also on the geometry of the soil pore space, pore size distribution and soil structure (Chandrasekhar et al., 2018; Heitman et al., 2023).

The hydraulic properties of soils are the basis for modelling water and solute fluxes to support decision-making. The hydraulic properties of soils are generally defined as the water retention function $\theta(h)$ and the hydraulic conductivity function $K(h)$ (van Genuchten, 1980). The water retention function of the soil is the relationship between

volumetric water content (θ) and water potential (h). It reflects the soil's capacity to retain water and provides information on soil structure, water retention capacity, wilting point and available water content (Rabot et al., 2018). K(h) govern the movement of water and solutes, including their infiltration into the soil.

These properties are often considered constant and measured in the laboratory or predicted by pedotransfer functions (PTFs). However, the structure of the soil and therefore its hydrodynamic properties are not static but change over time depending on agricultural practices, vegetation growth and weather conditions (Alletto et al., 2015; Tifafi et al., 2017; Huang et al., 2021; Pečan et al., 2023). This variability is usually studied by making specific measurements on samples of undisturbed soil at different times (Kool et al., 2019; Geris et al., 2021). However, the results obtained may be inconsistent due to too many different methodologies (Chandrasekhar et al., 2018). Furthermore, temporal variations in soil structure and, consequently, in the hydraulic properties of the soil are rarely included in models due to a lack of data. The exclusion of this variability can result in erroneous predictions of water and solute fluxes, consequently leading to suboptimal decision-making (Chandrasekhar et al., 2018). It is therefore essential to study the long-term temporal evolution of the hydrodynamic properties of soils directly in the field and under different cropping systems with SAPs. These experiments will make it possible to study their relevance for the future and to acquire data for implementation in the models.

5. Objectives and structure of the thesis

This thesis was written as part of the Agriculture Is Life for Water Quality (AIL4WaterQuality) project. This project was funded by the “Société Publique de Gestion de l'Eau” (SPGE). It was carried out in partnership with the Centre wallon de Recherches Agronomiques (CRA-W) for expertise and analysis of pesticides in soil and water, with Greenotec for advice and agricultural communication of the results, and with Protect'eau for the communication and diffusion of the results. The objectives of the project are to carry out long-term hydrological monitoring of EcoFoodSystem's innovative production systems, to integrate this data into an open access database, to acquire a more comprehensive analysis of the fate of pesticides that are problematic for water in Wallonia, and to obtain adjusted mobility parameters for risk assessment. The AIL4WaterQuality project provides a deeper understanding of the impact of agricultural practices on water availability and quality in soils. The results highlight the need to adopt more sustainable agricultural approaches and to use transport and degradation parameters adapted to Walloon soils in modelling and decision-making.

The present thesis will explore these different approaches in order to contribute to reducing the impact of agricultural systems on water resources, both in terms of their quality and their management in the soil. The research has several major general objectives.

For the first approach, in order to achieve a comprehensive understanding and evaluate the future of pesticides within the geo-pedological context of Wallonia, this thesis aims to:

1. Provide quantitative data on the impact of different soil column methodologies, commonly encountered in the literature, on the leaching results of solutes and on the parameters of the modelling obtained by inverse modelling. This objective focuses on the impact of soil structure, column diameter, column length, the presence of a differentiated horizon and the sampling method.

2. Evaluate the fate of eight pesticides that are problematic for groundwater using intact soil column experiments with silty soil typical of Wallonia.

3. Demonstrate the importance of considering the impact of agricultural systems and soil depth on the mobility of pesticides in the soil.

4. Obtain adsorption and degradation parameters by inverse modelling adapted to typical loamy soils of Wallonia and compare them to the values used in Belgium, as provided by the manufacturers or recorded in the Pesticides Properties DataBase for Europe.

As for the second way, to investigate the impact of a transition to more sustainable systems on soil structure, its hydraulic properties and the leaching of agrochemicals, this work seeks to:

5. Instrument the structuring EcoFoodSystem experiment, comprising four contrasting production systems including SAPs.

6. Evaluate the long-term impact of these systems and contrasting climatic conditions on the temporal evolution of soil water retention directly in the field.

7. Compare the water retention curves obtained continuously in the field with those obtained by FPT predictions and in the laboratory on preserved samples.

8. Establish a database on the impact of these systems on the leaching of pesticides and nitrate, as well as on the continuous long-term temporal evolution of the hydrodynamic properties of the soil, available to any interested user.

This thesis is structured in different chapters, as illustrated in figure 3.

Firstly, a general introduction (**Chapter 1**) will provide an overview of the context of this thesis and the related issues. This introduction will lead to the challenges of better understanding the fate of pesticides and the impact of alternative agricultural practices on the quality and management of water resources.

Then, **Chapter 2** will present the EcoFoodSystem experiment of the CARE[1] Agriculture Is Life on which this thesis is based. The production systems as well as all the agricultural practices will be presented. In addition, the instrumentation of the plots will be explained and illustrated. This chapter corresponds to objective 5 of this thesis.

The following two chapters constitute the first part of this thesis and explore a better understanding of the fate of problematic pesticides for groundwater in Wallonia.

Chapter 3 addresses objective 1. This chapter focuses on the impact of the different methodologies on the results of solute leaching experiments in soil columns. The impact of soil structure, column diameter and length, the presence of a differentiated horizon and the sampling method are analysed on the solute breakthrough curves and on the mobility parameters obtained by double-porosity inverse modelling on Hydrus 1-D.

After determining the most relevant methodology, **Chapter 4** will focus on the fate of eight pesticides that are problematic for groundwater in Wallonia in silty soils typical of the region. This chapter will address objectives 2, 3 and 4 of this thesis. Leaching experiments on these eight pesticides in undisturbed soil columns are thus carried out on three contrasting production systems of EcoFoodSystem and on the first three soil horizons. The breakthrough curves and the balances of adsorbed, degraded and eluted pesticides are analysed. Dual-porosity inverse modelling on Hydrus 1-D was used to obtain the sorption and degradation parameters of these pesticides for Wallonia and to compare them with the values used and from databases.

[1] CARE : Cellule d'appui à la recherche et à l'enseignement (Research and teaching facility)

The second part of this thesis comprises chapters 5 and 6 and will focus on hydrological monitoring of the effects of a transition to the contrasting EcoFoodSystem systems, including several sustainable agricultural practices.

Chapter 5 focuses on monitoring the temporal evolution of soil water retention in the four production systems and addresses objectives 6 and 7 of this thesis. This chapter provides an opportunity to study the long-term impact of these systems and contrasting climatic conditions between 2021, 2022 and 2023 on the temporal variability of soil water retention curves directly in the field. This research aims to assess the suitability of these systems to meet the needs of tomorrow. In this chapter, the temporal variation of retention curves obtained in the field is compared with those obtained theoretically using pedotransfer functions and in the laboratory on undisturbed soil samples.

Chapter 6 is based on all the data collected over a four-year period, from 2020 to 2024, from the hydrological monitoring of the transition to production systems. This database includes the description of the data from the water content and water potential sensors placed in the first three soil horizons. The results of nitrate and pesticide analyses in the drainage water 1.2 m below the different systems are also examined. This chapter deals with objective 8 of this thesis.

Chapter 7 provides a general discussion of all the work carried out as part of this thesis, the results obtained, their implications and the outlook for the future. Finally, **Chapter 8** concludes the dissertation.

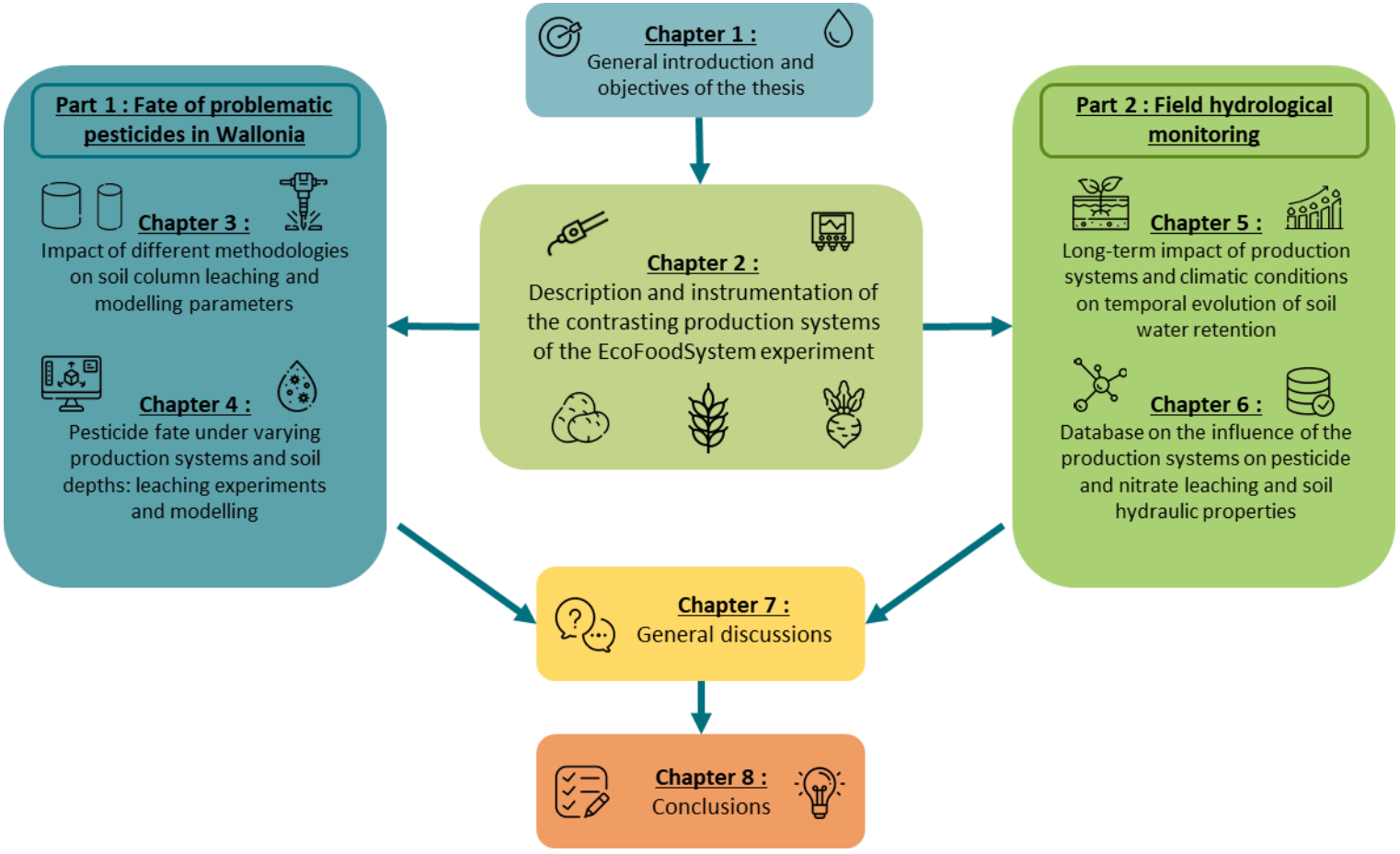

Figure 3. General structure of the thesis

Chapter 2

EcoFoodSystem field experiment: the contrasting production systems

1. Introduction

The EcoFoodSystem experimental platform was set up at the Terra research and teaching centre at Gembloux Agro-Bio Tech (Belgium) in 2020. The trial is being carried out on a 30-hectare area of the experimental farm, which is currently in the process of transitioning to zero pesticides. The objective of this initiative is to evaluate the long-term sustainability and resilience of various innovative production systems that respond to today's societal challenges. A range of indicators and measurements will be used to assess whether these rotations can meet future societal needs while preserving natural resources.

Four distinct eight-year rotations have been developed to anticipate the requirements of potential future food scenarios. These systems have been developed to align with the recommendations of the EAT-Lancet Commission for a healthy and sustainable diet (Eat Lancet Commission, 2019). They pursue environmentally-friendly agricultural practices, emphasising long crop rotations, diversified crops, intercropping and the responsible use of agrochemicals.

Adapted to the loamy region of Hesbaye, these systems have been defined through a combination of crop optimisation tools and dietary regimes. The objective of the experiment is to analyse the coherence or competition of co-evolutions between contrasting agricultural and food systems, particularly in terms of food security, crop science and environmental impact.

2. Contrasting production systems

Three contrasting production systems have been designed and implemented as part of the EcoFoodSystem experiment.

The first production system is called '**Reference**' and is described as an 'above-ground animal-plant flux' (figure 4). The animal is integrated into the system through the flow of agricultural by-products such as fodder and the input of organic matter of animal origin, such as manure. An 8-year rotation is scheduled with conventional crops (beet, wheat, potatoes, rapeseed, corn) interspersed with cover crops (intermediate crops that act as nitrate traps). This system has been implemented with two variants, with and without the use of herbicides on the plots. In the first case, only chemical herbicides are used in accordance with good agricultural practices. In the second case, no chemical pesticides are applied.

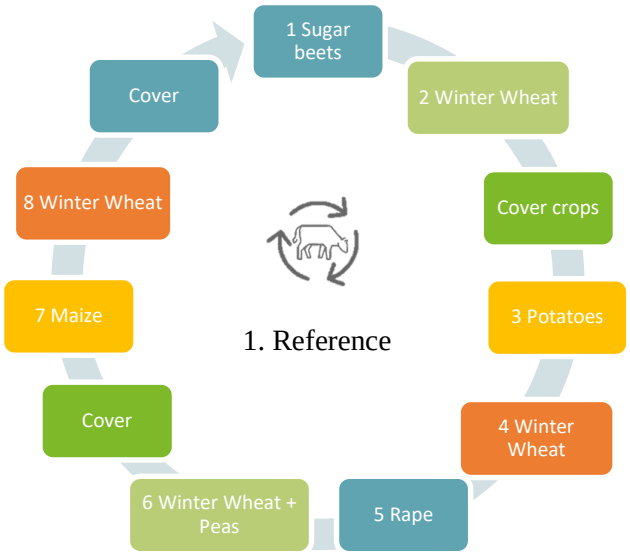

Figure 4. Reference production systems with an eight-year rotation implemented as part of the EcoFoodSystem experiment.

The second production system is called the '**Integrated Crop Livestock System (ICLS)**' and is described as 'animal-plant fluxes in agroecological interactions' (figure 5). Animals, particularly ruminants, are integrated into the system through agricultural by-product and manure flows. They are also used to control weeds by grazing temporary pastures and intercrops. This rotation is managed without the use of pesticides. An eight-year rotation is planned with conventional crops (maize, wheat, faba beans, rape) interspersed with cover crops and two and a half years of pasture.

Figure 5. ICLS production systems with an eight-year rotation implemented as part of the EcoFoodSystem experiment.

The third system is called '**Vegan**' (figure 6). It simulates agriculture in a world without animal production. No organic matter of animal origin is introduced into the system and the crops in the rotation are intended solely for human consumption. This rotation is managed without any pesticides. A rotation of 8 years is planned with various crops (camelina, wheat, faba beans, peas) with intercropping.

Figure 6. Vegan production systems with an eight-year rotation implemented as part of the EcoFoodSystem experiment.

The EcoFoodSystem experiment thus includes four contrasting rotations (with the variant of the first system). To study the impact of all the rotations earlier, they were implemented at two different times. Consequently, the four rotations were initiated simultaneously in year 1, designated temporality 1, and in year 5, designated temporality 2, across distinct plots. Consequently, after a period of four years, all the eight-year crops will have been observed once, but not under rotation conditions. The structuring experiment involves eight different plots. Winter wheat returns in all the rotations in years 2, 4 and 6 to serve as an internal reference for comparing the rotations.

The structuring experiment comprises four repetitions, i.e. four blocks of eight plots. The blocks are named 'Cimetière', 'Nationale' and 'Petit Bordia 1 and 2'. The location of the four blocks is shown in figure 7. As illustrated, the Orneau river flows from north to west, and a type IIB distant catchment prevention zone is followed by a type

IIA closer zone, designated Rabauby G1, in the north-west of the study area. The Escaille reserve is located on the periphery of the structuring experiment site.

Figure 7. Location of the four blocks of the EcoFoodSystem structuring experiment, with the catchment prevention zones in hatched red and the Escaille reserve in green crosshatching.

For the purposes of this thesis, only one block was instrumented for hydrological monitoring. In order to determine which block would be investigated, ease of access, soil type and topography were taken into consideration. To ensure easy access to the plot and easy comparison between plots, access to the land and homogeneity were the two main criteria.

Figures 8 and 9 show the main soil types in Wallonia, the soil classification codes and the topography of the site of the structuring experiment.

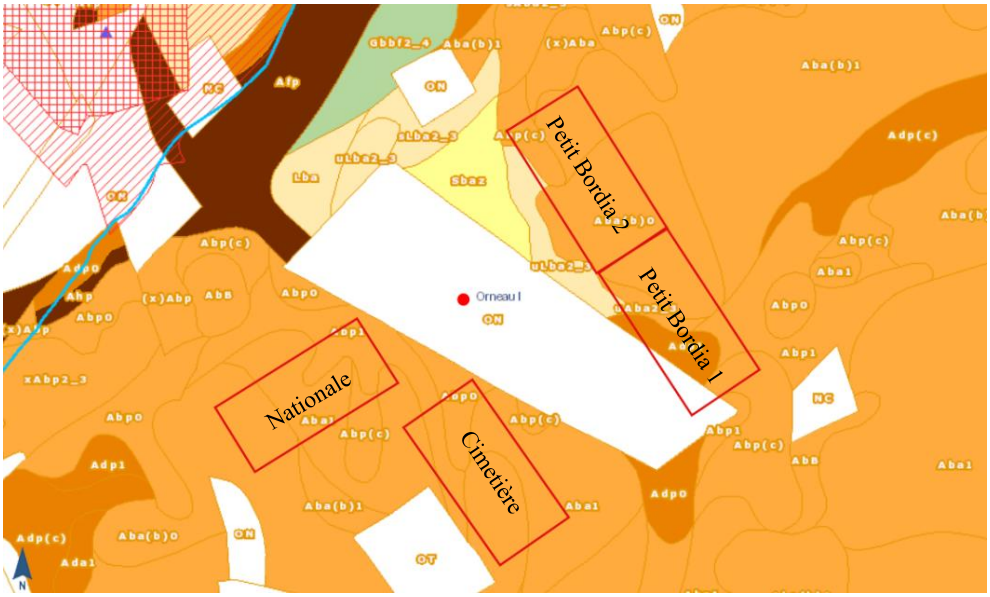

Figure 8. Map of the main soil types in Wallonia for the four blocks of the EcoFoodSystem experiment.

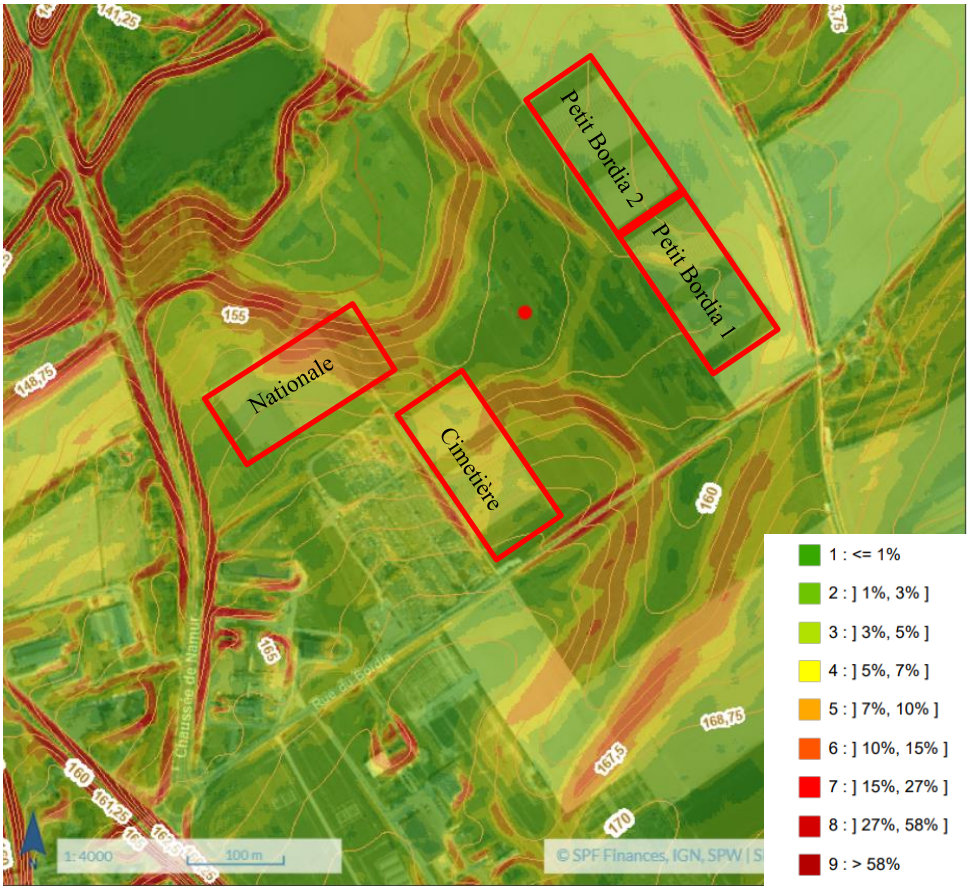

Figure 9. Digital model of percentage slopes and contour lines map for the four blocks of the EcoFoodSystem experiment.

In terms of soil type, the Petit Bordia 1 and 2 blocks are more heterogeneous than the 'Cimetière' and 'Nationale' blocks, which are entirely on loamy soils with favourable natural drainage. The 'Petit Bordia 1 and 2' blocks are also on loamy soils with moderate or imperfect natural drainage as well as on sandy-loamy soils with mainly favourable natural drainage. It should also be noted that the two 'Petit Bordia 1 and 2' blocks are further away from the path along the cemetery, which makes them more difficult to access. Consequently, these two blocks have been excluded from the study. In terms of topography, the 'Nationale' block has a steeper slope than the 'Cimetière' block. The 'Cimetière' block, located within the Gembloux cemetery, was selected for the instrumentation due to its homogeneity and accessibility.

The soil from the EcoFoodSystem experiment is a cutanic luvisol according to the World Reference Base for Soil Resources (FAO, 2015). Several soil types are found within the block. For the entire block, the soil is loamy with favourable natural drainage with a ploughed horizon Ap between 0 and 30 cm. At both ends of the block, from 30 to 60 cm, the horizon is Bt1 and after 60 cm, Bt2 with an accumulation of clay and a decrease in organic carbon content with depth. At the centre of the plot and mainly on the steepest slope, colluvial deposits are present. Between 30 and 60 cm depth, the soil contains colluvial deposits with a granulometry similar to the Ap horizon but with a decreasing organic carbon content. The Bt horizon with clay accumulation is found lower down, below 60 cm depth (Figures 10 and 11). The physico-chemical properties of the three horizons are given in Table 1. The notation is as follows: H1-3 = horizon 1 to 3.

Figure 10. Soil profile during installation of hydrological monitoring equipment

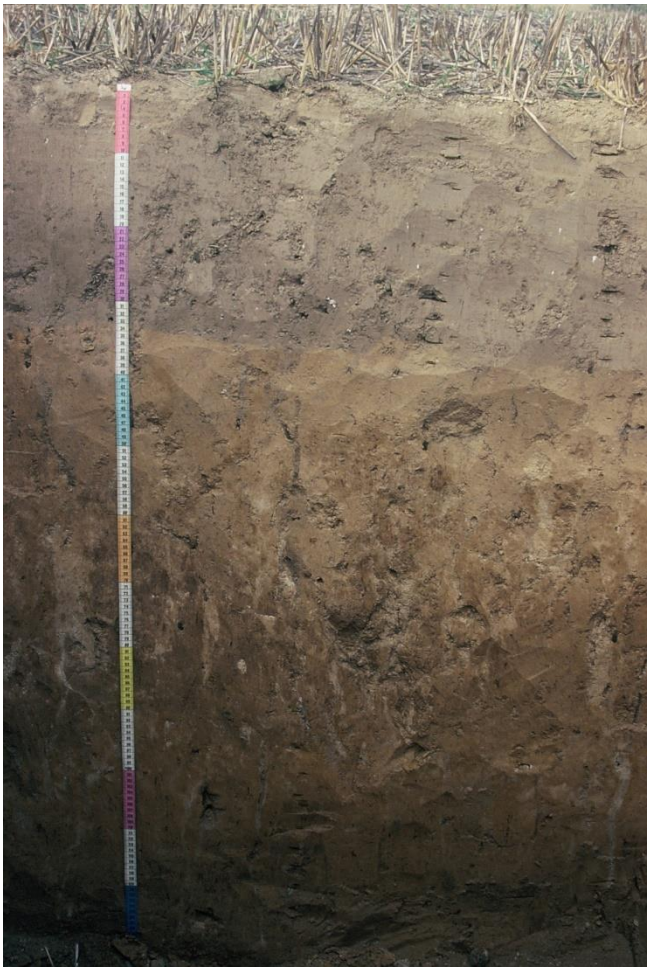

Figure 11. Luvisol soil profile, visual taken from a plot adjacent to the EcoFoodSystem experiment.

Table 1. Physico-chemical properties of the soils for three soil depths in 2021.

	H1	H2	H3
Depth	0-30	30-60	60-90
Clay (%)	13,8	13,1	19,2
Silt (%)	78,3	80,4	74,5
Sand (%)	7,9	6,4	6,2
Organic carbon (g/kg)	12,3	5,24	3,35
Cation exchange capacity (CEC) (meq/100 g)	9,4	8,3	10,6
pH water	7,6	7,8	7,9
Bulk density (g/cm³)	1,41±0,03	1,54±0,01	1,64±0,01
Porosity	0,462±0,009	0,415±0,005	0,378±0,002

The four systems with the two temporalities were implemented in September 2020 on the eight 18x84 m plots of the 'Cimetière' block. Prior to the commencement of the experiment, two years of winter wheat were cultivated on all plots between 2018 and 2020 to ensure soil homogenisation. The results of the leaf area index and aerial biomass measurements showed a high degree of uniformity in winter wheat growth across the eight plots. Before implementing the systems, ploughing and sowing of winter wheat was carried out at the end of October 2019 on the plots. The wheat was harvested and stubble was ploughed in late July 2020. An intercrop was sown at the beginning of September 2020.

3. Instrumentation

In order to investigate the impact of the transition from conventional production systems to these more sustainable systems, hydrological monitoring has been set up. Objective 5 of this thesis is to instrument the EcoFoodSystem experiment to monitor the temporal evolution of the hydrodynamic properties of the soil as well as the leaching of agrochemicals. To achieve this objective, water content and water potential sensors and solution sampling plates were required.

3.1. Sensors

MeterGroup's Teros 12 was chosen as the water content sensor (Figure 12). These sensors can also measure soil temperature and electrical conductivity. They provide water content in m³/m³ using an electromagnetic field to measure the dielectric permittivity of the surrounding medium, which is proportional to the water content. The sensor uses a frequency of 70 MHz to minimise the effects of soil texture and

salinity on the measurements, making it very accurate in most mineral soils. This probe uses a thermistor as the temperature sensor. Electrical conductivity is measured using stainless steel electrodes. The probe is also equipped with a ferrite core to avoid interference.

Figure 12. Teros 12 water content sensors from MeterGroup.

The water potential sensors chosen are Teros 21 also from MeterGroup (Figure 13). These sensors measure soil water potential in kPa and temperature. The Teros 21 sensors measure potential values over a very wide range from -9 to -2000 kPa. Measuring water potential is important because it provides information about the energy state of the water in the soil. It therefore makes it possible to determine the availability of water in the soil for plants and how it moves. In addition, the water content data combined with the water potential data makes it possible to determine the temporal evolution of the soil water retention curve.

Figure 13. Teros 21 water potential sensors from MeterGroup.

3.2. Data-logger

MeterGroup's ZL6 data loggers (Figure 14) were chosen because they provide a simple and robust connection to the Teros sensors. They are also equipped with two solar panels to recharge the internal nickel-metal hydride batteries. No other electrical installation is therefore required and these data loggers are suitable for long-term field experiments with little or no maintenance. In fact, the batteries can power the data logger for several months in winter or during prolonged periods of low light. A ZL6 data logger can connect to and record data from six different sensors.

Figure 14. ZL6 data logger from MeterGroup with integrated solar panels

3.3. Soil solution sampling plates

There are several methods for collecting water from the soil, including lysimeters, porous candles, ion exchange resins, membranes and sampling plates. Porous candles and soil sampling plates make it easy to collect water in the field. The sampling plates provide a larger sampling area than the porous candles and allow better consideration of preferential flow and soil heterogeneity (Singh et al., 2018). In addition, sampling plates are a suitable alternative to lysimeters for measuring the fate of pesticides in the environment (Kasteel et al., 2007). Porous ceramic candles are suitable for the analysis of nitrate in soil water, but not for the analysis of pesticides. This is because they can absorb more than 80% of pesticides, making them unsuitable for pesticide monitoring (Perrin-Ganier et al., 1993). This is why EcoTech Glass Sampling Plates were chosen (Figure 15). These plates are made of borosilicate multilayer glass. This construction provides high rigidity and good water absorption, as water can flow simultaneously over the entire surface of the plate. These plates have a diameter of 80 mm and a sampling area of 50 cm^2. Glass plates were chosen because, unlike ceramic or plastic plates, they are recommended for the analysis of pesticides and nitrate. This is because many soil solutes exhibit different sorption behaviour when in contact with different materials (Ciglasch et al., 2005).

These plates are connected to a vacuum system to bring the water to the surface. Each plate is connected to a water collection bottle placed in an isothermal box. This box also contains the vacuum pump and the battery. This system is adapted to long experiments in the field.

Figure 15. EcoTech glass sampling plates with its isothermal storage box containing the vacuum pump, sampling bottles and battery.

4. Experimental design

The eight plots in the Cimetière block of the structuring experiment were instrumented. In early September 2020, water content and water potential sensors were installed in each plot at depths of 30, 60 and 90 cm. All probes are connected to ZL6 data loggers. Thus, six probes were installed per plot and connected to one ZL6 data logger at the surface.

In each of the eight plots, three soil solution sampling plates were installed below the root zone, i.e. at a depth of 1.2 metres. Due to the high spatial variability of the soil, it can be difficult to accurately measure the solute concentration of water in the vadose zone (Singh et al., 2018). The three plates allow water to be collected from a larger area of soil and therefore provide a more representative measurement. An isothermal box equipped with a vacuum system can hold the collection bottles for 6 plates. A box has been installed for the plates from two plots.

A total of 24 Teros 12 water content sensors, 24 Teros 21 potential sensors, 24 soil solution sampling plates, 8 ZL6 data loggers and 4 isothermal boxes with vacuum systems were placed in the field. The experimental design is shown in Figure 16.

The block is surrounded on two sides by a flowered strip. Smaller 42x15 m plots in the middle have been demarcated as they represent the crop yield experiment of the EcoFoodSystem. The same treatments are applied to the entire 84x18 m plot. It is imperative that the small plots remain undisturbed; therefore, the installation of equipment is not permitted within them. The Teros 12 and 21 sensors, as well as the soil solution sampling plates, were therefore installed as centrally as possible in the plot, i.e. at the edge of the yield plot. The two data loggers (one per plot) and the isothermal box were placed in the middle of two plots, approximately 3 metres from the edge of the yield plots.

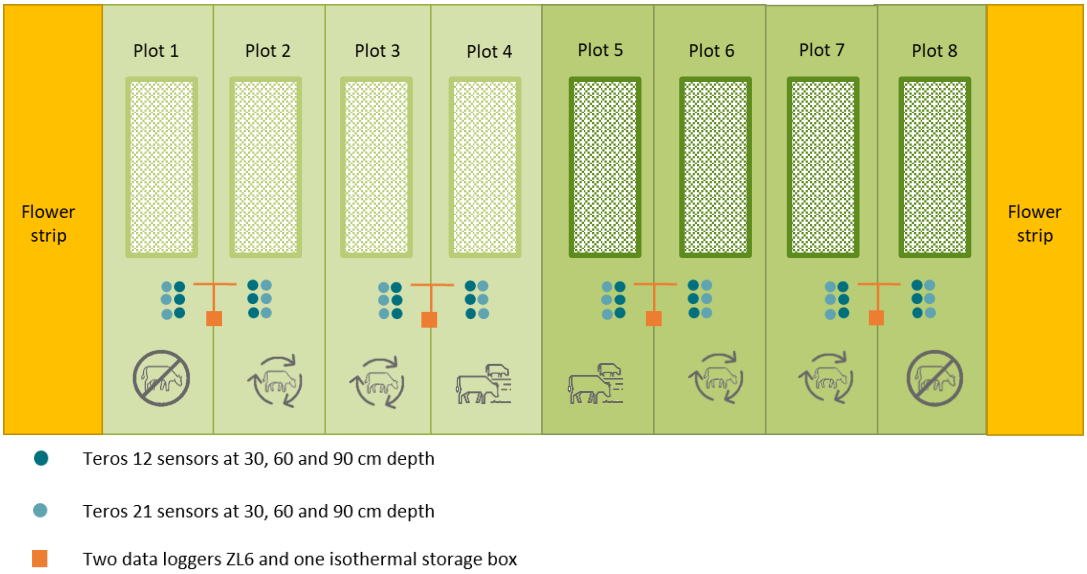

Figure 16. Experimental design for instrumenting the EcoFoodSystem plots of the "Cimetière" block.

5. Installation

The installation of all the equipment was carried out during the week commencing 31 August 2020. First, a 1.5-metre trench was dug using a mini-excavator at each of the eight plots (Figure 17).

Figure 17. Excavation of 1.5-meter-deep trenches in each of the 8 plots.

The Teros 12 and Teros 21 sensors were then installed in parallel at 30, 60 and 90 cm, at the level of the delimitation of the first three soil horizons (Figure 18). Prior to installation, the sensors were meticulously examined in the laboratory under various environmental conditions, encompassing different water contents. Subsequently, smooth surfaces were created at depths of 30, 60 and 90 cm on the left-hand side of the trenches. The Teros 12 water content sensors were then inserted into these surfaces, with the ferrite core positioned underneath to prevent any interference. On the right, precise apertures of the probes' dimensions were created at the three depths using the MeterGroup installation tool. Subsequently, soil was collected, sieved, moistened and compacted around the porous disc of each Teros 21 sensor. These steps are necessary to ensure good hydraulic contact. The sensors were then inserted into each hole.

Figure 18. Installation of Teros 12 and Teros 21 sensors in parallel in a trench on a plot at a depth of 30, 60 and 90 cm.

Prior to installation, the EcoTech soil water sampling plates were meticulously washed in accordance with the prescribed protocol to ensure the removal of any contaminants introduced during the manufacturing process. Each plate was immersed in a basin containing 0.1 M HCl, and two litres of solution were allowed to pass through the plate using a vacuum system. The plates were then immersed in a basin of deionised water, and two litres of water were allowed to percolate through the plate to rinse it. The same procedure was applied with 0.1 M NaOH.

Three tunnels were excavated at the base of each trench, at a depth of 1.2 metres (figure 19). It is imperative that the tunnels are as deep and narrow as possible. The tunnel ceiling should be smoothed with a spatula to ensure good contact with the top plate. The soil extracted from the tunnel was then sieved to 4 mm and water was added to form a slurry. This slurry guarantees a robust hydraulic connection between the plate and the undisturbed soil. The slurry is then applied to the plate, ensuring full coverage of the porous surface. The layer of mud must be sufficient to fill the gaps in the tunnel ceiling. The plate is then compressed as far as possible into the tunnel,

against the ceiling. Finally, the tunnel is refilled with the rest of the soil, sieved to 4 mm and tamped to restore its initial bulk density.

Figure 19. Installation of EcoTech soil water solution sampling plates at a depth of 1.2 m in the trenches of each plot.

The cables were then secured with strong sheaths to the data loggers or isothermal boxes (Figure 20). These sheaths were attached to the walls of the trenches with clamps. The trenches were then closed, with care taken to respect the horizons and the initial density of the soil.

Figure 20. Protection and secure fixing of cables at the edges of trenches.

Finally, the cables are conveyed to the data loggers and isothermal boxes in sheaths through trenches (Figure 21).

Figure 21. Illustration of the trenches allowing the cables from each plot to connect to the data loggers and the isothermal box located between two plots.

The sensors were connected to the various data loggers, which were mounted on poles. The sampling plate cables were also connected to the six collection bottles and to the vacuum regulating system.

On the four plots in the first season, cover crops and then sugar beets, maize and camelina were planted in year 1 for the reference, ICLS and vegan systems, respectively. In temporality 2, rape was planted in all four rotations (Figure 22).

Figure 22. Sugar beet/maize on the left for the first year of rotations in temporality 1 and rape on the right for temporality 2.

In years 2 and 4 (2022 and 2024), winter wheat, with or without peas, was planted on all eight plots for the standardisation years, except for the grazed pasture of the ICLS system in temporality 2 (Figure 23).

Figure 23. Winter wheat in years 2 and 4 of the rotations for both time periods (standardisation years).

In the third year of the project (2023), the potato and faba bean crops were sown in temporality 1, along with the maize, temporary grassland and pea crops for temporality 2 (Figure 24).

Figure 24. Potatoes on the left for temporality 1 reference and grazed meadow on the right for temporality 2 ICLS

6. Teros 12 sensors calibration

The water content sensors were calibrated after installation, as these sensors have a high degree of repeatability. The Teros 12 sensors measure volumetric water content by first measuring the dielectric permittivity of the soil. However, the measurement of the dielectric permittivity is influenced by the bulk density, texture, mineralogy and salinity of the soil. A calibration specific to the soil being studied can therefore increase the accuracy to between 1 and 2%. For the three depths at which the Teros 12 sensors were placed, namely 30, 60 and 90 cm, a soil-specific calibration had to be carried out (Figure 25).

Figure 25. Illustration of the first three soil horizons with depth limits at 30, 60 and 90 cm.

Several stages were carried out to calibrate the sensors. Firstly, soil was collected from the first three horizons. The differences between the soils at the three depths are clearly visible in terms of colour and texture, demonstrating the importance of a different calibration for each depth (Figure 26). The soil was then dried in a thin layer in an oven at 25°C, then crushed and sieved to 2 mm. After weighing a dry container, the soil was added to the container in 2 cm layers and compacted to its initial density. The container was then filled to a height of 14 cm. For the depths of 30, 60 and 90 cm, a total of 5160, 5437 and 5565 g of soil were compacted in the container with an apparent density of 1.3, 1.37 and 1.4 g/cm³ respectively.

Figure 26. Visual differences in the soil sampled at depths of 30, 60 and 90 cm for the calibration of Teros 12 sensors.

A thin layer of soil is then removed from the surface before the probe is inserted into the ground. The probe is then covered with soil and connected to a ZL6 data logger to measure the raw data without calibration. This process is carried out with 3 different Teros 12 sensors (Figure 27).

Figure 27. Calibration of a Teros 12 sensor.

Measurements were taken at 0, 10, 20, 30 and 40% soil water content. The raw data measured by the sensors were then related to the soil water content. R^2 values between 0.998 and 0.999 were obtained, demonstrating the high accuracy of the calibration (Figure 28). The calibration equations are thus obtained and can be entered directly into ZentraCloud to apply the calibration to the 24 Teros 12 sensors installed in the field.

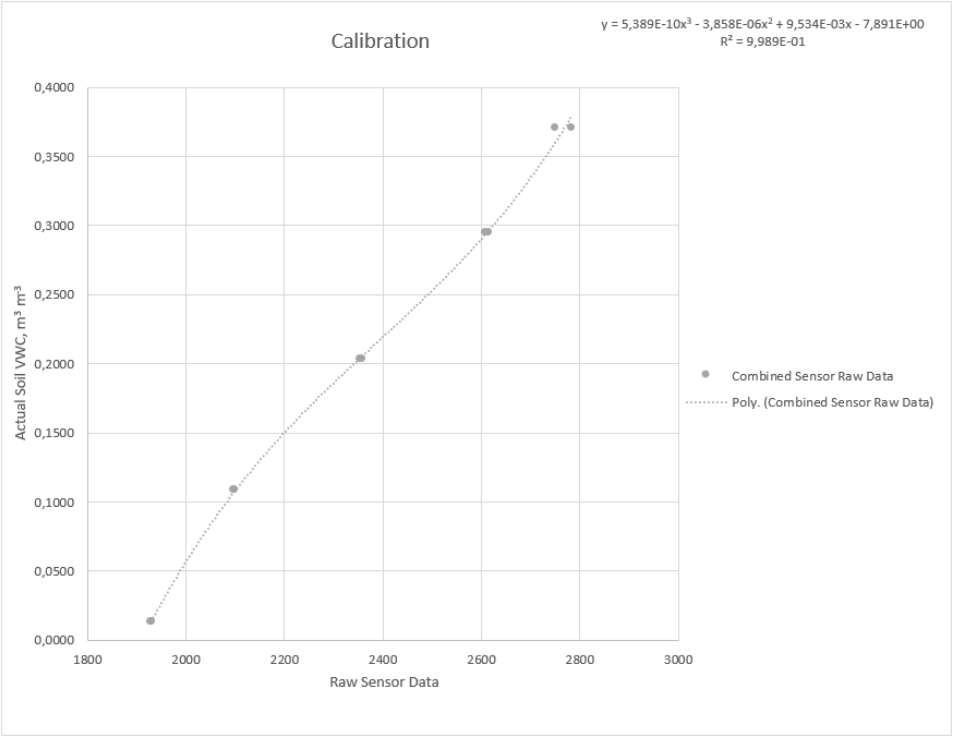

Figure 28. Equation and R^2 between the raw values measured by a Teros 12 sensor in soil 30 cm in depth and the actual water content of this soil.

7. Data collection

After the instrumentation, the data recording began. The sensors have been taking measurements every 15 minutes since September 2020. The ZentraCloud interface is used to collect the data recorded by the data loggers. This interface allows data from the data loggers to be automatically retrieved and viewed in real time. It is easy to use and also allows the loggers to be configured remotely. The graphs of each measured variable and the latest data recorded by each sensor are available in real time, allowing any problems or interruptions to be quickly identified.

Once installed, the sensors had to adapt to their new environment before providing valid measurements. During installation, the disturbance of the soil and mud on the potential sensors affected the measurements in the first few weeks after installation. In addition, the sensors were connected and disconnected several times during installation. Finally, some sensors did not record any measurements for certain periods of time. The data has been validated since October 2020.

The equipment installed, coupled with the ZentraCloud, makes it easy to acquire a very large amount of data. In fact, with a measurement interval of 15 minutes, each sensor records 4 measurements per hour, 96 measurements per day and approximately 2880 measurements per month. From October 2020 to December 2024, 148,640 measurements were taken by each sensor, for each measured quantity. The experiment involves 24 water content sensors and 24 potential sensors, so 3,567,360 water content and potential measurements have been recorded since the start of the experiment. In total, due to false contacts, cable cuts or battery discharges, only 2.7% of the data from all the sensors placed in the field could not be recorded.

Water from the plates is collected once or twice a month during the rainy season when sampling is possible. The water samples from the eight plots are split in two and put into brown bottles to prevent light from breaking down the pesticides. The first samples are taken to CRA-W (Centre wallon de Recherches Agronomiques) for analysis of pesticide concentrations. Initially, 55 pesticides were looked for in the water samples. The list of pesticides to be analysed was determined on the basis of pesticides frequently found in the water, but also on the basis of pesticides used on the plots in the last 10 years. The other half of the samples were taken to the Environment and Analysis Office in Gembloux Agro-Bio Tech to analyse the nitrate concentration.

No samples could be collected between September 2020 and March 2021. After installation, at least six months are required to ensure good hydraulic contact between the plates and the ground and to be able to extract water into the collection bottles (Singh et al., 2018). In addition, no samples could be collected between June and December 2022 due to the drought.

The columns sampled to study the impact of the methodology on the results in chapter 3 were taken at the EcoFoodsystem experimental site between June and November 2020. At this time, the plots had not yet been differentiated for temporality 1. Only the columns intended for assessing the impact of the sampling method were collected at plot T1 ref in July 2021.

The columns used in Chapter 4 to assess the fate of pesticides were taken from the the EcoFoodSystem experiment plots T1 ref, T1 ICLs and T1 vegan.

Chapter 3

Design Matters: Investigating solute leaching dynamics with multi-column experiments and dual-porosity inverse modelling

1. Synopsis

This chapter and the next constitute the first part of this thesis on a better understanding of the fate of problematic pesticides for groundwater in Wallonia.

The first step was to consider a methodology for pesticide leaching in soil columns. These experiments are the most common in the literature because they provide a reliable representation of water and solute fluxes within a soil profile. However, many different methodologies are used without apparent justification. However, these different approaches can influence the leaching results, which may lead to irrelevant transport parameters for assessing the risk of groundwater contamination.

Chapter 3 therefore fills these gaps and provides quantitative data on the effect of different methodologies often found in the literature on the leaching results of a solute and on the mobility parameters obtained by inverse modelling. Chapter 3 addresses objective 1 of this thesis and allows us to choose the appropriate methodology for the leaching experiments of problematic pesticides in Wallonia presented in chapter 4. The columns were taken from the EcoFoodsystem experimental site when the plots had not yet been differentiated for temporality 1 or from plot T1 ref with sugar beet for the last test on the sampling method.

This chapter is based on the publication: Pirlot, C., Degré, A., 2025. Design Matters: Investigating solute leaching dynamics with multi-column experiments and dual-porosity inverse modelling. CLEAN– Soil, Air, Water. Under review.

2. Abstract

Pesticide leaching experiments using soil columns are widely employed in the literature, but they are carried out with a variety of technical approaches that can strongly influence the results, leading to inaccurate transport parameter estimations. The aim of this study is to investigate and provide quantitative data on the effects of sampling method, soil structure, column size, and the presence of differentiated layers on the breakthrough curve of a solute. Leaching experiments were conducted using $CaCl_2$ as a tracer in soil columns made of silty agricultural soil. A total of 21 columns were constructed, consisting of both packed and intact core columns with diameters of 24 and 8.4 cm and heights of 20 and 35 cm (figure 29). Sampling was performed either manually or using a mechanical coring auger. Inverse modelling using Hydrus 1-D with the dual-porosity model was used to determine water and solute mobility parameters for each column. The results showed that soil structure significantly impacts solute transport dynamics and water infiltration. Disturbed columns tend to underestimate rapid contaminant transport by neglecting preferential flow and overestimate contaminant retention. Our research demonstrates that studying water

and solute fluxes in disturbed columns does not provide a reliable representation of groundwater contamination risks. Intact columns should be preferred to better approximate field conditions. Column diameter had little effect on breakthrough shape, but larger columns exhibited a greater proportion of the mobile zone, reflecting increased preferential flow. The diameter of disturbed columns had minimal impact on the $CaCl_2$ breakthrough curve, as both column diameters exhibited similar elution patterns due to the homogeneous soil matrix. While small-diameter columns adequately represent breakthrough curves in disturbed soils, they may not accurately reflect transport dynamics in structured soils, where preferential flow paths are significant. The height of intact soil columns significantly influenced the breakthrough curve shape, solute recovery, and mobility parameters. Hydrus 1-D modelling indicated that the differences were primarily due to column height rather than the plough sole. Shorter columns may overestimate solute leaching potential and underestimate solute degradation, leading to inaccurate risk assessments for groundwater contamination. Therefore, longer columns better capture natural soil heterogeneity and preferential flow, improving the reliability of transport models and environmental risk assessments. The core sampling method strongly influences the breakthrough curve and water and solute transport parameters. The percussion hammer of the mechanical corer induces vibrations, causing continuous, unnatural preferential flow and rapid elution of the majority of the solute. Hand-driven columns appear to be a better alternative for sampling intact soil cores and provide a more accurate representation of soil transport processes. This study highlights the critical role of column design and sampling methods in leaching experiments, emphasizing the need for standardized protocols to improve the accuracy of leaching results and solute transport estimations. These insights will help guide future experimental designs and enhance the reliability of contamination risk assessments.

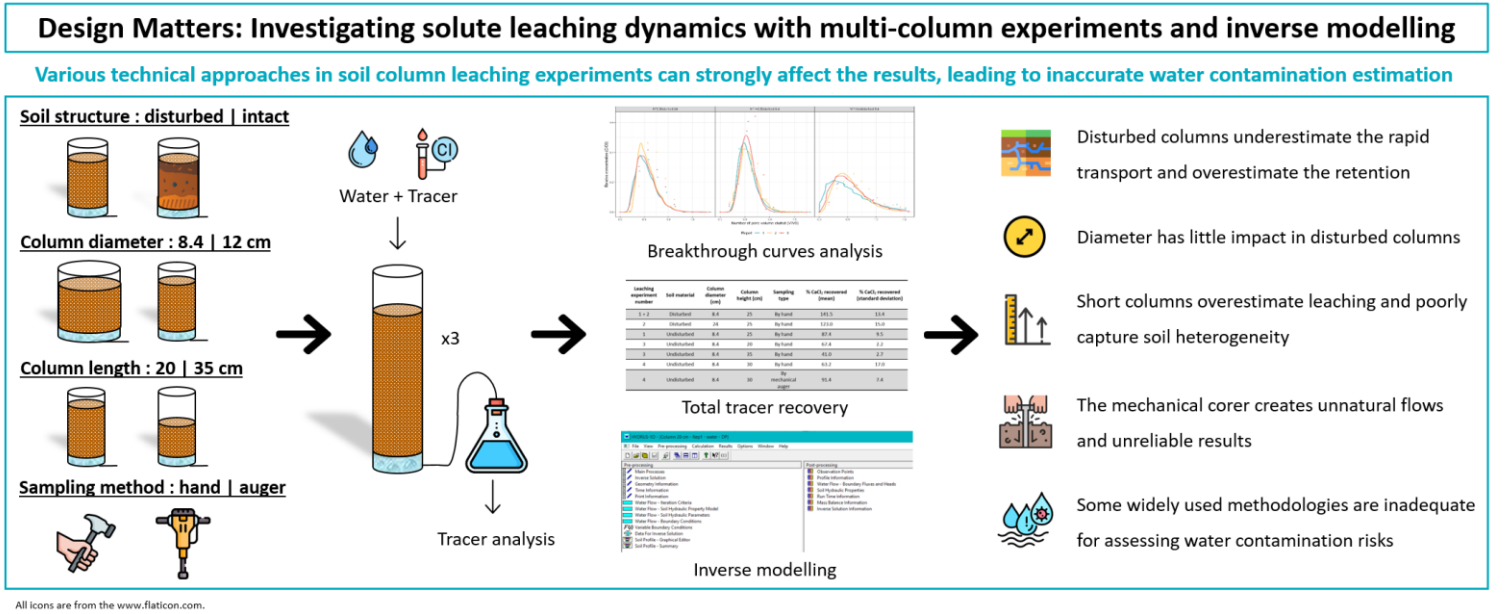

Figure 29. Graphical overview of the influence of several methodologies on the solute leaching dynamics and on the mobility parameters obtained by inverse modelling.

3. Introduction

The intensive use of pesticides on agricultural land has significantly degraded the quality of water resources through their leaching. Currently, a large number of pesticides and their metabolites are frequently detected in groundwater, the most important source of drinking water for many European countries (Kiefer et al., 2019; Pietrzak et al., 2019; Baran et al., 2021; EurEau, 2021). Many factors will influence the fate of pesticides such as their properties but also soil characteristics, site conditions, and pesticide application practices. In the last few years, numerous studies have been carried out into the fate of pesticides in soils and the impact of various organic amendments, ploughing techniques and cover crops in order to limit the leaching of these compounds into water (Barba et al., 2020; Cueff et al., 2020; Siedt et al., 2021; Imig et al., 2023a).

Furthermore, numerous modelling tools have been developed to rapidly assess the potential risks associated with the use of pesticides on agricultural land (Labite et al., 2011; European Commission, 2014; Akay Demir et al., 2019). The two processes that predominantly control the behaviour of pesticides in soils are adsorption and degradation (Arias-Estévez et al., 2008; Malla et al., 2021). Thus, the key input parameters needed for modelling pesticide transport are the sorption coefficient (K_d) and the half-life of the substance (DT_{50}). These parameters are usually obtained by inverse modelling of observed data such as breakthrough curves from field or laboratory experiments (Dusek et al., 2015; Kahl et al., 2015; Sur et al., 2022; Imig et al., 2023a). In structured soils, preferential flows such as macropores of biological or mechanical origin (earthworm galleries, cracks) can rapidly transport water and solutes deeper into the soil and increase the risk of water contamination (Köhne et al., 2009a; Varvaris et al., 2021b). Many models can be used to consider soil heterogeneity and preferential flows, such as the dual-porosity (DP) approach (Pot et al., 2005; Köhne et al., 2006). Imig et al., 2023a showed proper modelling of the peaks of several pesticides using DP inverse modelling on Hydrus 1-D.

Long-term field experiments allow researchers to get closer to reality but these are very expensive and the parameters are difficult to control due to the high soil heterogeneity and very complex boundary conditions (Dusek et al., 2011). Laboratory experiments provide relevant information on the potential mobility of pesticides (Katagi, 2013). Soil column leaching experiments are the technique most frequently encountered in the literature because they provide representations of water and solute fluxes that are closer to the actual field situation. However, studies are carried out at different scales and with a wide range of technical features, which prevents the results obtained from being compared or transposed to other situations, and makes drawing conclusions difficult.

Two types of columns are used to study pesticide leaching: packed and intact soil core columns. Packed columns are made from disturbed soil, which is dried, sieved and uniformly packed into the column (Khan and Brown, 2016; Aliste et al., 2021; Ortega et al., 2022). These columns are generally more homogeneous and reproducible than intact core columns. In order to study preferential flows, soil structure and to get closer to real conditions, a number of studies use intact soil core columns that are directly extracted from the field (Pot et al., 2010; Cueff et al., 2020; Imig et al., 2023a). Preferential flows through soil macropores significantly reduce the retention of solutes within the soil profile and can therefore increase the risk of groundwater contamination (Koestel et al., 2013). Sadeghi et al. (2000) showed that the packing of soil columns reduces leaching losses of atrazine. In addition, intact soil core columns may contain several soil layers with different properties, which will influence the leaching.

The column sizes used in pesticide leaching experiments varies widely. The diameter of the columns is usually between 8 and 10 cm but can range from 2-3 cm to over 50 cm (Albers et al., 2022; Ortega et al., 2022; Imig et al., 2023b). The length is usually between 20 and 50 cm but shorter columns of 5 to 20 cm are also very common (Dusek et al., 2015; Khan and Brown, 2016; Albers et al., 2022). From a meta-analysis of 733 soil column tracer leaching experiments, Koestel et al. (2012) showed that tracer dispersivity is positively correlated with the length and diameter of the soil column used. Bromly et al. (2007) studied the relationship between dispersivity and the properties of 291 disturbed soil columns and concluded that the column diameter was the second most important factor that determines dispersivity after clay content. Furthermore, the degree of preferential flow in intact core columns is positively correlated with the column diameter but negatively correlated with column length.

Several methods of sampling undisturbed soil columns are found in the literature. To avoid sidewall flow, the columns are usually driven directly into the soil. For large soil columns or lysimeters, a static load can be used to drive a heavy steel cylinder into the soil. Another method is to insert a beveled driving head onto a PVC tube and drive it into the ground with a jackhammer or hydraulic pressure system (Vincent et al., 2007; Pot et al., 2010). Smaller columns are usually driven in by hand with a sledgehammer (Bégin et al. 2003). To sample at deeper depths, drilling equipment can be used to drive columns into the ground. The columns can also be inserted into a steel cylinder of the same size, which is slowly driven into the ground by a mechanical shovel (Cueff et al. 2020).

Thus, varying methodologies can strongly influence the outcome of the experiment (Bromly et al., 2007). Despite some recommendations by Lewis and Sjöstrom, 2010 and correlations identified by Koestel et al., 2012, there remains limited quantitative data on how specific column designs affect solute leaching results. To date, no

standardised methodologies exist and choices regarding sampling methods, soil structure and column dimensions are often made without clear justification. However, these methodological differences can strongly influence experimental results and lead to irrelevant transport parameters for contamination risk assessment.

The objective of this study is to address these gaps by providing quantitative data on the effects of several commonly used methodologies on leaching outcomes within soil columns, as well as on the dual-porosity parameters obtained through inverse modelling. Specifically, this research investigates the impact of:

- **Soil structure**, by comparing packed and intact soil core columns derived from a silty agricultural soil.
- **Column diameter and height**, using smaller columns of 8.4 cm diameter and larger ones of 24 cm diameter, as well as columns of both 20 cm and 35 cm in height.
- **Soil layering**, by comparing a 35 cm intact soil core column with a plough sole to a 20 cm homogeneous column. Modelling with Hydrus 1-D will isolate the effects of column height and soil heterogeneity.
- **Intact core sampling method**, comparing hand-driven columns using a sledgehammer with those inserted via a mechanical auger.

By clarifying how these methodological factors influence leaching experiments and dual-porosity parameters, this study aims to support the development of standardized practices in soil column leaching research and improve the reliability of contamination risk assessments.

4. Materials and methods

4.1. Soils

All soil columns were collected from an agricultural soil located on the Agriculture Is Life experimental plots of the Terra research centre of the University of Liege in Gembloux, Belgium. The soil is a cutanic Luvisol according to the World Reference Base for Soil Resources (FAO, 2015). Its physico-chemical properties are given in Table 2. The soil is ploughed every year and shows a plough sole below 30 cm. Ploughing and sowing of winter wheat was carried out at the end of October 2019 on the plots. The wheat was harvested and stubble was ploughed in late July 2020. An intercrop was sown at the beginning of September 2020. The soil was ploughed to 30 cm and finer work with a rotary harrow at 10 cm depth was done to prepare the seedbed before sowing beet at the end of April 2021. Two hoeing operations were

carried out in June 2021. The climate is temperate oceanic with an average annual temperature of 10.2°C and an average annual rainfall of 837 mm.

Table 2. Physico-chemical properties of soil

Properties	**0-30 cm**	**30-60 cm**
Collection site	Gembloux, Belgium	
Soil type	Luvisol	
Texture	Fine silty clay	
Clay (%)	12.0	13.1
Silt (%)	80.5	80.5
Sand (%)	7.5	6.4
Bulk density (g/cm³)		
- Disturbed	1.38±0.00	-
- Undisturbed by hand	1.37±0.02	1.4
- Undisturbed by auger	1.34±0.01	-
pH water	7.8	7.8
Organic carbon (g/kg)	14.4	5.2
Organic matter (%)	2.9	1.0
CEC (meq/100g)	10.0	8.3

4.2. Column set-up

A total of 21 columns were made from Plexiglas tubes. A perforated Plexiglas plate was fixed 2 cm from the bottom of the column in order to elevate the columns and allow water to pass through. A nylon textile disc was placed between the soil and the perforated plate to prevent soil particles from being washed away. A tube was placed in the water collection area and was connected to two Erlenmeyer flasks and a vacuum pump. All columns were built in triplicate.

4.2.1. Packed columns

Six packed columns were made with soil taken from 0 to 25 cm depth in June 2020 (Figure 30). The soil was first dried at 50°C for 48 h in thin layers before being ground and sieved to 2 mm. The soil was then uniformly packed into the columns to a height of 25 cm, respecting the initial soil density of 1.38 g/cm³. The soil placed in the columns was previously weighed and added in layers of 2-3 cm in height. After each addition, the soil was evenly packed and lightly scarified on the surface to ensure good hydraulic connectivity between the soil layers (Plummer et al. 2004). Three 8.4 cm columns and three 24 cm inner diameter columns were reconstituted.

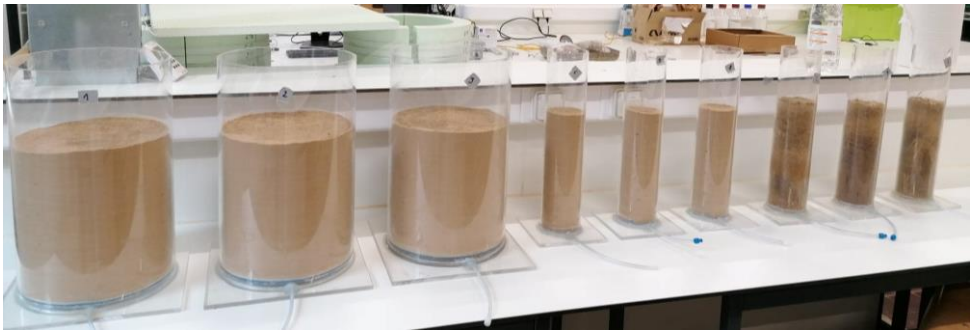

Figure 30. Illustration of the packed columns with a diameter of 24 cm and 8.4 cm and the intact columns with a diameter of 8.4 cm.

4.2.2. Intact soil core columns

Fifteen intact soil core columns were collected in 8.4 cm diameter Plexiglas tubes from the same agricultural plot as the packed columns. Twelve columns were sampled by hand and driven directly into the field using a sledgehammer and were excavated with a shovel and trowel (figure 31).

Figure 31. Removal of intact soil columns from the ground, sampled by hand.

In early August, three columns were driven in to a depth of 25 cm in order to have the same soil height as the packed columns. Then, in early November 2020, three columns were driven in up to 20 cm and three more up to 35 cm to study the impact of the height and the presence of the plough sole. In addition, three columns were sampled to a depth of 30 cm to study the impact of the sampling method in July 2021. Finally, three columns were excavated with a soil column cylinder auger. The soil column auger can be used to sample undisturbed soil columns to a depth of 1 m. The inner diameter of the auger is 90 mm. Thus, a 40 cm long Plexiglas column with an external diameter of 90 mm (84 mm internal diameter) was inserted into the auger

before sampling. Since the auger is 1 m long, a 60 cm column was placed behind the 40 cm sampling column to hold it in place. The cylinder soil column auger with a cutting head at its base was driven into the ground with a gasoline-powered percussion hammer (Cobra TT) to a depth of 30 cm. The auger was removed from the ground with a steel lifting jack. After removing the detachable lid of the auger, the soil column was carefully removed (figure 32).

Although the soil samples are referred to as 'intact soil columns' due to their preserved structural characteristics, it is important to acknowledge that some degree of disturbance is inevitably introduced during the sampling process. Inserting the plexiglass cylinder into the soil profile causes mechanical disruption, particularly along the edges of the column. While the samples retain a relatively undisturbed structure that is appropriate for investigation, they cannot be considered perfectly intact in the technical sense.

Figure 32. Sampling of intact soil columns up to 30cm depth with the gasoline-powered percussion hammer.

Immediately after excavation, the ends of the columns were sealed in order to bring them to the laboratory without disturbance. To limit possible sidewall flow, paraffin wax was poured on top of the columns at the interface between the soil column and the Plexiglas wall (Arthur et al. 1998; Isensee and Sadeghi, 1992). The columns were kept free of vegetation for the duration of the experiment.

4.3. Leaching experiment

The leaching experiments modalities are summarised in Table 3. All columns were progressively saturated by adding water above the columns and then allowed to drain freely for 24 h by gravity in order to minimise water content differences at the beginning of the experiment. All columns were then connected to a peristaltic vacuum pump to provide suction of –35 kPa at the bottom of the column to approximate the real tension conditions (Dusek et al., 2015).

Table 3. Leaching experiment summary

Leaching experiment number	Soil structure	Column diameter (cm)	Column height (cm)	Sampling type	Time of sampling	Agricutural operations
1 + 2	Disturbed	8.4	25	By hand	June 2020	
2	Disturbed	24	25	By hand	June 2020	
1	Intact	8.4	25	By hand	August 2020	Wheat harvested, stubble ploughed
3	Intact	8.4	20	By hand	November 2020	Intercrops
3	Intact	8.4	35	By hand	November 2020	Intercrops
4	Intact	8.4	30	By hand	July 2021	Soil ploughed, sugar beet planted, soil hoed
4	Intact	8.4	30	By mechanical auger	July 2021	Soil ploughed, sugar beet planted, soil hoed

The leaching experiments were performed with a tracer considered to be non-reactive, Cl_2, in the form of calcium dichlore (93% purity) from Sigma-Aldrich, USA. A 5 g/l $CaCl_2$ solution was made in a 1 l flask. Then, a 250 ml pulse of solution was added to the 3 columns of 24 cm internal diameter and a 30.6 ml pulse was added to the 18 columns of 8.4 cm diameter. The same proportion of $CaCl_2$ quantity per soil surface area was respected. The pulse was distributed manually, uniformly over the

soil column surface. Then 750 ml and 91.4 ml of water was added to the 24 and 8.4 cm diameter columns respectively to reach 2.2 cm of water.

The $CaCl_2$ leaching experiments were conducted under unsaturated conditions to simulate the situation in the vadose zone and under transient flow to imitate rain events. After 24 hours, 2.2 cm of water was applied onto the columns at a rate of 0.442 $cm.min^{-1}$. Similar simulated rainfall was applied to the columns at regular intervals. A surface water layer is built up when water is applied and gradually reduces with the water infiltration into the column. The volume of water percolated and the electrical conductivity of the percolates were measured at regular intervals of 24 to 48 hours. The volume of water percolated was measured in ml with a 250 ml graduated cylinder. The electrical conductivity was measured with a VWR® MU1600L multimeter. As the water conductivity is known, the conductivity due to tracer can be obtained. The conductivity was then converted into the concentration using a calibration curve with $CaCl_2$ concentrations of 0, 0.2, 0.4, 0.6, 0.8 and 5 $g.l^{-1}$.

4.4. Hydrus 1-D model

Hydrus 1-D is a one-dimensional finite element model that simulates water, heat and multiple solute fluxes under various saturation conditions (Šimůnek et al. 2008). All breakthrough curves were modelled to derive hydraulic and $CaCl_2$ transport parameters by inverse modelling.

4.4.1. Inverse modelling

Parameter optimisation is an indirect approach for the estimation of water and solute transport parameters from transient flow and transport data. Inverse modelling is based on numerical solutions using the Levenberg-Marquardt (LM) optimisation procedure (Marquardt, 1963). The LM algorithm minimises the differences between the observed and simulated values by iteratively adjusting the parameters of interest. This algorithm optimises the parameters by minimising the objective function φ(q,b) defined by (Šimůnek et al. 1998):

$$\Phi(q,b) = \sum_{j=1}^{m} v_j \sum_{i=1}^{n} w_{ij}\left[q_j^*(z,t_i) - q_j(z,t_i,b)\right]^2$$

Where m is the number of different sets of measurements, n is the number of observations in a particular measurement set, $q_j^*(z, t_i)$ are specific measurements at depth z and time ti for the jth measurement set, $q_j(z, t_i, b)$ are the corresponding estimated space-time variables for the optimised parameters' vector b. v_j and w_{ij} are weighting factors associated with a particular measurement set or point, respectively.

Three statistical indicators were used to assess the performance of the inverse modelling and parameter optimisation: sum of squares (SSQ), root-mean-square error (RMSE) and coefficient of determination (R^2). A sequential approach was used, where the hydraulic and transport parameters were estimated successively from the observed water flow data and then from the tracer concentration in the eluates (Šimunek et al., 2002; Imig et al., 2023b; a). This approach prevents the uncertainty in the hydraulic parameters from propagating into the uncertainty in the transport parameters (Kahl et al., 2015).

4.4.2. Dual-porosity water flow modelling

Transient water flows within the columns were simulated using the dual-porosity (DP) model. The DP approach considers the porous media to be divided into two interacting regions, partitioning the porous system into mobile and immobile regions. DP models assume that water flow is confined to the macropore or fracture domain. Water in the matrix does not move at all (van Genuchten and Wierenga, 1976; Šimůnek et al., 2003). Water can be exchanged between the two regions. We will use the subscript mo for the mobile or macropore region and im for the immobile region or soil matrix.

The total water content is given by the equation:

$$\theta = \theta_{mo} + \theta_{im} \quad 1$$

Where θ is the total soil water content (L^3/L^3) and θ_{mo} and θ_{im} are the mobile and immobile regions soil water contents respectively.

In this model, the soil water retention curve θ(h) is described by the van Genuchten (1980) equation and the hydraulic conductivity function K(h) is described with the statistical pore distribution model of Mualem (1976). These two equations contain five independent hydraulic parameters: the residual soil water content θ_r (L^3/L^3), the saturated soil water content θ_s (L^3/L^3), the hydraulic parameter n (-), the hydraulic shape parameter α (1/L) and the saturated hydraulic conductivity K_s (L/T). The pore connectivity l (-) has been estimated to be 0.5 on average for most soils (Mualem, 1976; Köhne et al., 2006). These parameters were first estimated using neural network based pedotransfer functions developed by Schaap et al. (2001) and incorporated in the Rosetta (Neural Network Predictions) module. The granulometry and bulk density of the soil columns (Table 2) were used. The parameters obtained for layer 1 of the different column types and for layer 2 are given in Table 4.

Table 4. Hydraulic parameters obtained by Rosetta for the first two layers of the studied soil

Column type	Horizon	θs (-)	θr (-)	α (1/cm)	n (-)	l (-)	Ks (cm/min)
Disturbed	0-30 cm	0.4378	0.064	0.0054	1.67	0.5	0.02139
Undisturbed by hand	0-30 cm	0.4401	0.0643	0.0053	1.6724	0.5	0.02225
Undisturbed by auger	0-30 cm	0.4471	0.0653	0.0052	1.6791	0.5	0.02504
-	30-60 cm	0.4374	0.0656	0.0055	1 .6601	0.5	0.01783

The DP model uses the Richards equation to describe water flow in the mobile region (macropores). A mass balance equation is used to describe water dynamics in the matrix (Šimůnek et al., 2003):

$$\frac{\partial \theta_{mo}}{\partial t} = \frac{\partial}{\partial z}\left[K(h)\left(\frac{\partial h}{\partial z} + cos\alpha\right)\right] - S_{mo} - \Gamma_w \qquad 2$$

$$\frac{\partial \theta_{im}}{\partial t} = -S_{im} + \Gamma_w \qquad 3$$

Where h is the water pressure head (L), *t* is time (T), *z* is the vertical coordinate (L), S_{mo} and S_{im} are the sink terms for the two regions (1/T), α is the angle between the flow direction and the vertical axis (-) and Γ_w is the rate of water transfer from the macropores to the matrix and vice versa (1/T). In the current version of Hydrus 1-D (4.17), the S_{im} term is assumed to be zero.

The mass transfer rate was assumed to be proportional to the difference in the effective saturations of the two regions using the first order rate equation (Gerke and van Genuchten, 1993a; Simunek et al., 2001):

$$\Gamma_w = \frac{\partial \theta_{im}}{\partial t} = \omega\left[S_e^{mo} - S_e^{im}\right] \qquad 4$$

Where ω is the first-order rate coefficient for water transfer between mobile and immobile regions (1/T) and S_e^{mo} and S_e^{im} are the effective fluid saturations of the mobile (macropores) and immobile (matrix) regions.

The retention curves are considered by the model to be similar for both regions. The parameters α and n of the van Genuchten equation therefore have the same value for both regions. For the mobile region (macropores) the parameters required by the model are $\theta_{r,mo}$, $\theta_{s,mo}$, α, n and K_s. For the immobile region (matrix) the parameters are $\theta_{r,im}$, $\theta_{s,im}$ and ω.

The initial values of the parameters a, n and K_s are the ones given by the Rosetta module. The parameters $\theta_{s,mo}$ and $\theta_{s,im}$ are calculated assuming a proportion of macropores of 10% of the total calculated soil porosity. Thus, $\theta_{s,mo}$ is equal to 0,1 of θ_s and $\theta_{s,im}$ to 0,9 of θ_s (Kodešová et al., 2005; Šimůnek et al., 2009). $\theta_{r,im}$ is assumed to be equal to the θ_r value of the soil obtained from the Rosetta module. $\theta_{r,mo}$ is set to zero to ensure that residual water is only present in the immobile zone of the soil (Köhne et al., 2006; Imig et al., 2023b). The first-order rate coefficient for water transfer ω was set to 0.002 min^{-1} (Köhne et al., 2004). The parameters $\theta_{s,mo}$, K_s and ω were optimised by inverse modelling of the cumulative flow measurements for each column. Then $\theta_{s,im}$ was calculated according to the equation 1. The other parameters were kept constant. Mertens et al., 2006 showed that saturated hydraulic conductivity (K_s) was the most sensitive parameter when inverse modelling was performed using eluted water volume data. For 35 cm columns, the parameters of both layers are optimised simultaneously.

4.4.3. Dual-porosity solute transport modelling

The transport of a tracer in a porous medium with variable saturation is described by the classical convection-dispersion equation where no tracer adsorption or degradation occur (Šimůnek and Genuchten, 2008):

$$\frac{\partial \theta_{mo} c_{mo}}{\partial t} = \frac{\partial}{\partial x}\left(\theta_{mo} D_{mo} \frac{\partial c_{mo}}{\partial x}\right) - \frac{\partial q_{mo} c_{mo}}{\partial x} - \Gamma_s \quad (5)$$

$$\frac{\partial \theta_{im} c_{im}}{\partial t} = \Gamma_s \quad (6)$$

$$\Gamma_s = \omega_s (c_{mo} - c_{im}) + \Gamma_w c^* \quad (7)$$

In witch, c_{mo} and c_{im} are the solute liquid concentrations of the mobile and immobile regions (M/L^3), D_{mo} is the dispersion coefficient in the mobile region, taking into account molecular diffusion and hydrodynamic dispersion (L^2/T), q_{mo} is the volumetric flux density in the mobile region (L/T), Γ_s is the solute transfer rate between the two regions (M/L^3T). ω_s is the first order chemical mass transfer coefficient (1/T) and c* is the solute concentration (M/L^3) of the mobile region c_{mo} for $\Gamma_w>0$ and of the immobile region c_{im} for $\Gamma_w<0$ (Šimůnek and Genuchten, 2008).

The dispersion coefficient of the mobile zone D_{mo} can be described as:

$$D_{mo} = D_0 \frac{\theta_{mo}^{\frac{7}{3}}}{\theta_{s,mo}^2} + \lambda_{mo}\nu \qquad 8$$

Where D_0 is the molecular diffusion coefficient in free water (L^2/T), λ_{mo} is the longitudinal dispersivity in the mobile region (L) and ν is the pore water velocity (L/T). In general, the molecular diffusion coefficient is generally of the order of 5% of the hydrodynamic dispersion coefficient (Vanderborght and Vereecken, 2007).

Dispersivity λ, molecular diffusion coefficient D_0 and first order chemical mass transfer coefficient ω_s are required. The dispersivity value is usually set at 1/10 of the column size (Šimůnek et al. 2009). Thus, for 20 and 35 cm columns, an initial dispersivity of 2 and 3.5 cm, respectively, is considered. The diffusion coefficient (D_0) is mostly of the order of 5% of the hydrodynamic dispersion coefficient (Vanderborght and Vereecken, 2007). The molecular diffusion coefficient of $CaCl_2$ is 0.0008 cm²/min (Flury and Gimmi, 2002). The initial value of the transfer coefficient ω_s has been set to 0.00001 min^{-1} (Šimůnek et al., 2009).

Finally, the observed $CaCl_2$ concentration data in the leachate were used for optimisation by inverse modelling the values of λ, D_0 and ω_s (Abbasi et al. 2003; Šimunek et al. 2002). The other parameters were fixed. For the 35 cm columns, the parameters of the first layer were adjusted first and then those of the second layer.

4.4.4. Boundary conditions

For the numerical modelling with Hydrus 1-D, columns were represented as 1D domains and discretised into 101 nodes with equal spacing. The water flow boundary condition was defined on top of the soil column as atmospheric boundary conditions with a surface water layer to allow for water build-up during time variable boundary conditions of water addition (precipitation). Thus, a flow rate of 0.442 $cm.min^{-1}$ for 5 minutes was set as a variable boundary condition at each water addition. At the bottom, the water flow boundary condition was set to constant pressure head because the vacuum pump connected to the bottom of the column induces a constant tension of −35 kPa. The solute transport boundary condition at the top of the column is a concentration flux with $CaCl_2$ applied at a concentration of 5 g/l. At the bottom of the column, a zero-concentration gradient is defined.

4.5. Data treatment and statistical analysis

Breakthrough curves were constructed using the relative concentrations (C/C_0) measured in the leachates over the cumulative relative pore volume (V/V_0). The porosity was calculated from the average bulk density for each column type (disturbed, undisturbed sampled by hand and undisturbed sampled with a mechanical auger) and the density of the soil particles and organic matter. Assuming a soil particle density of 2.65 $g.cm^{-3}$ and an organic matter particle density of 1.4 $g.cm^{-3}$, the particle density of the whole soil was found to be 2.614 $g.cm^{-3}$.

Data were processed using Rstudio v2023.12.0. The figures were plotted with ggplot2 package. The Tmin, Cpeak and Tpeak indicators were determined as the relative pore volume at the first appearance of the tracer in the eluates, the maximum relative concentration and the relative pore volume after which it was reached, for each column. To investigate the existing differences between the breakthrough curves of several soil column designs and transport parameters, analyses of variance (ANOVA) were performed. In order to compare the means of several indicators of the breakthrough curves and of dual-porosity parameters, Fisher's Least Significant Difference (LSD) method was used with the null hypothesis of equality of means and a significance level of 0.05. Normality was tested using Shapiro-Wilk and equality of variances using Levene's test. All assumptions were satisfied.

5. Results and discussion

5.1. Soil structure

Figure 33 represents the comparison of $CaCl_2$ breakthrough curves for the packed disturbed columns of 24 and 8.4 cm diameter and intact soil core columns of 8.4 cm diameter (leaching experiment n°1 and 2).

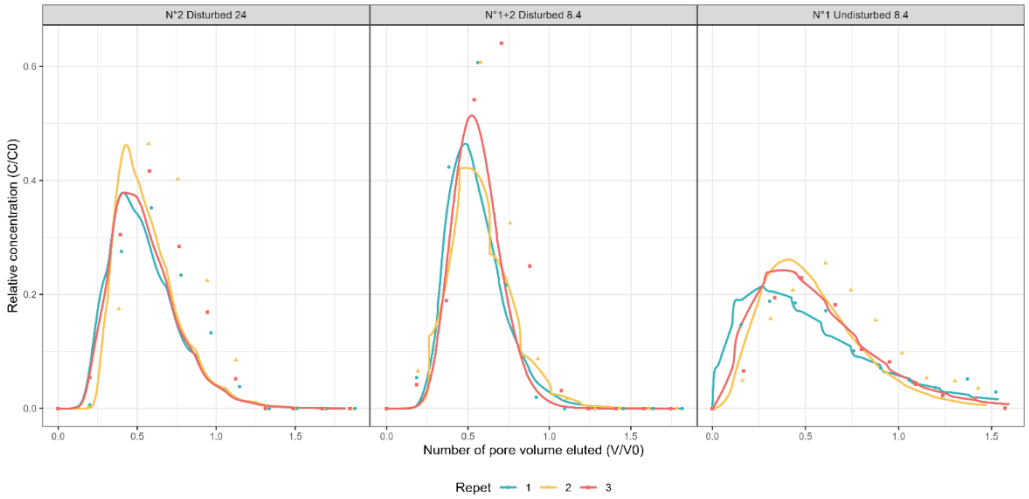

Figure 33. Measured and modelled breakthrough curves depicting the relative concentration (C/C0) in the leachates plotted as a function of the number of pore volume eluted (V/V0) for the $CaCl_2$ tracer, (a) for disturbed column of 24 cm diameter, (b) disturbed column of 8,4 cm diameter and (c) undisturbed column of 8,4 cm diameter for the three replicates. The points correspond to the measured and the lines to the modelled data.

The arrival times of the first breakthrough Tmin, the arrival time of the maximal peak concentration Tpeak, the relative maximal concentration of the peak Cpeak and the total pore volume eluted Ttot for the tracer $CaCl_2$ for the four leaching experiments are giver in table 5.

Table 5. Arrival time of the first breakthrough Tmin in pore volume, arrival time of the maximum peak concentration Tpeak in pore volume, relative maximal concentration of the peak Cpeak and total pore volume eluted Ttot for the four leaching experiments. Values correspond to the mean of the three spatial replicates with standard deviation.

Columns	Tmin	Tpeak	Cpeak	Ttot
R24	0.135 ± 0.046	0.421 ± 0.008	0.407 ± 0,040	1.86 ± 0.01
R8,4	0.152 ± 0.011	0.499 ± 0.018	0.467 ± 0.0038	1,78 ± 0.03
U8,4	0.010 ± 0.010	0.353± 0.064	0.240 ± 0.019	1.51 ± 0.06
20	0.001 ± 0,001	0.119 ± 0.025	0.492 ± 0.022	1,66 ± 0.03
35	0.003 ± 0.001	0.045 ± 0.021	0,397 ± 0.021	0.88 ± 0.05
Hand	0.021 ± 0.013	0.238 ± 0.091	0.261 ± 0.075	0.78 ± 0.06
Auger	0.002 ± 0.000	0.049± 0.028	0.516 ± 0.067	1.03 ± 0.08

Breakthrough curves show different patterns between the two soil structures (disturbed and undisturbed). The solute is found faster in the leachates with a significantly lower time (p-value = 0.002) of first breakthrough (Tmin) for the undisturbed column than for the disturbed column where it is more retained. The peak (arrival time of the maximal peak concentration Tpeak) also appeared faster for intact soil core columns than for the packed column, indicating greater retention of the solute in the disturbed soil structure.

Soil structure also influences the height and width of the breakthrough curve. The maximal concentration of the peak (Cpeak) are significantly higher (p-value = 0.0001) for the disturbed columns. Furthermore, the total amount of pore volume required to complete the pulse was significantly lower (p-value = 0.001) for packed columns with an average value of 1.205±0.098 than for intact soil core columns at 1.626±0.096. The breakthrough curves of packed columns show a Tpeak 1.41 times higher, a Cpeak (height) 1.95 times higher and a pore volume required to complete the pulse (width) 1.35 times lower than the intact columns.

The percentage of $CaCl_2$ recovered is higher (p-value = 0.002) for the disturbed columns than for the intact columns (Table 6). For the disturbed columns, an estimated percentage of $CaCl_2$ recovered exceeding 100% is obtained as a result of the electrical conductivity conversion to concentration. Soil disturbance may have resulted in the leaching of other solutes than the $CaCl_2$, previously retained within the soil matrix.

Table 6. Percentage of $CaCl_2$ recovered for all soil columns studied.

Leaching experiment number	Soil material	Column diameter (cm)	Column height (cm)	Sampling type	% $CaCl_2$ recovered (mean)	% $CaCl_2$ recovered (standard deviation)
1 + 2	Disturbed	8.4	25	By hand	141.5	13.4
2	Disturbed	24	25	By hand	123.0	15.0
1	Undisturbed	8.4	25	By hand	87.4	9.5
3	Undisturbed	8.4	20	By hand	67.4	2.2
3	Undisturbed	8.4	35	By hand	41.0	2.7
4	Undisturbed	8.4	30	By hand	63.2	17.0
4	Undisturbed	8.4	30	By mechanical auger	91.4	7.4

Very good agreement was achieved between observed and predicted cumulative outflow. The average R^2 of the water flux modelling is on average 1.00±0.00 for the disturbed columns and 1.00±0.00 for the undisturbed columns (Table 7). The K_s values for packed columns are on average significantly higher (p-value = 0.000) compared to intact soil core columns. In this way, the long tail of the intact columns' curves may be due to a higher degree of solute transport in low flow regions. Thus, water infiltration is slower at saturation for the undisturbed columns. The proportion of the mobile region is also greater for disturbed columns than for columns in undisturbed structure.

Table 7. Soil hydraulics parameters obtained by inverse modelling of cumulative outflow. Values correspond to the mean value of the three spatial replicates with the standard deviation.

Columns	θs,mo (cm^3/cm^3)	θs,im (cm^3/cm^3)	Proportion of the mobile zone (%)	Ks (cm/min)	ω (1/min)	SSQ (-)	R^2 (-)
R24	0.35 ± 0.01	0.13 ± 0.01	74.3 ± 1.3	0.105 ± 0.017	0.049 ± 0.021	0.02 ± 0.00	1.00 ± 0.00
R8,4	0.29 ± 0.02	0.19 ± 0.02	60.6 ± 4.9	0.095 ± 0.013	0.041 ± 0.040	0.01 ± 0.00	1.00 ± 0.00
U8,4	0.24 ± 0.03	0.23± 0.03	51.0 ± 5.4	0.056 ± 0.008	0.010 ± 0.004	0.01 ± 0.00	1.00 ± 0.00
20	0.21 ± 0.03	0.26 ± 0.03	43.8 ± 6.7	0.060 ± 0.002	0.028 ± 0.009	0.00 ± 0.00	1.00 ± 0.00
35 (1H)	0.17 ± 0.03	0.31 ± 0.03	35.3 ± 5.3	0.080 ± 0.004	0.000 ± 0.000	0.00 ± 0.00	1.00 ± 0.00
35 (2H)	0.18 ± 0.01	0.29 ± 0.01	38.3 ± 2.2	0.074 ± 0.005	0.003 ± 0.004	0.00 ± 0.00	1.00 ± 0.00
	0.06 ± 0.02	0.38 ± 0.02	12.9 ± 3.5	0.023 ± 0.005	0.000 ± 0.000		
Hand	0.21 ± 0.02	0.26 ± 0.02	44.4 ± 5.0	0.058 ± 0.012	0.001 ± 0.001	0.09 ± 0.05	0.99 ± 0.01
Auger	0.17 ± 0.00	0.32 ± 0.00	34.9 ± 0.5	0.112 ± 0.008	0.023 ± 0.002	0.06 ± 0.04	0.99 ± 0.01

The transport parameters fitting resulted in a proper representation of solute transport with an average R^2 of 0.89±0.06 for the disturbed columns and 0.92±0.07 for the undisturbed columns (Table 8). The dispersivity values obtained for the undisturbed columns were on average significantly higher (p-value = 0.009) at 2.89±1.20 cm compared to 0.24±0.07 cm for the disturbed columns. The dispersivity values were smaller than 1 for all the disturbed columns, indicating very low spatial heterogeneity in these columns. The diffusion coefficient shows no significant difference between the two structures. The mass transfer coefficient ω_s was significantly higher for disturbed columns than for intact columns. Thus, the dispersion is 12.3 times greater and the tracer mass transfer is 26.5 times lower for intact soil cores than for disturbed columns.

Table 8. Fitted transport parameters determined by inverse modelling of leachate concentrations on Hydrus 1-D. Values correspond to the mean value of the three spatial replicates with the standard deviation.

Columns (cm)	λ (cm)	D0 (cm²/min)	ω_s (1/min)	SSQ	R^2
R24	0.29 ± 0.10	0.000 ± 0.000	0.001 ± 0.000	0.12 ± 0.10	0.95 ± 0.04
R8,4	0.24 ± 0.07	0.009 ± 0.010	0.037 ± 0.022	0.24 ± 0.05	0.89 ± 0.06
U8,4	2.89 ± 1.20	0.002 ± 0.000	0.005 ± 0.003	0.15 ± 0.15	0.92 ± 0.07
20	3.48 ± 1.36	0.002 ± 0.003	0.000 ± 0.000	0.12 ± 0.07	0.90 ± 0.05
35 (1H)	22.6 ± 1.66	0.002 ± 0.002	0.000 ± 0.000	0.26 ± 0.06	0.80 ± 0.02
35 (2H)	17.1 ± 6.73	0.001 ± 0.000	0.000 ± 0.000	0.28 ± 0.04	0.78 ± 0.04
	0.24 ± 0.01	0.001 ± 0.000	0.000 ± 0.000		
Hand	1.42 ± 0.70	0.001 ± 0.001	0.001 ± 0.001	0.27 ± 0.21	0.84 ± 0.12
Auger	33.44 ± 7,84	0.000 ± 0.000	0.000 ± 0.000	0.14 ± 0.05	0.93 ± 0.06

Table 9 summarises the mean $CaCl_2$ recovered and the main hydraulic and transport parameters.

Table 9. Summary of average values for the recovered tracer and the main hydraulic and transport parameters for the different column types.

Columns (cm)	% $CaCl_2$ recovered	θs,mo (cm³/cm³)	Mobile zone (%)	Ks (cm/min)	ω (1/min)	λ (cm)	ω_s (1/min)
R24	141.5	0.35	74.3	0.105	0.049	0.29	0.001
R8,4	123.0	0.29	60.6	0.095	0.041	0.24	0.037
U8,4	87.4	0.24	51.0	0.056	0.01	2.89	0.005
20	67.4	0.21	43.8	0.060	0.028	3.48	0.000
35 (1H)	41.0	0.17	35.3	0.080	0.000	22.6	0.000
35 (2H)	-	0.18	38.3	0.074	0.003	17.1	0.000
	-	0.06	12.9	0.023	0.000	0.24	0.000
Hand	63.2	0.21	44.4	0.058	0.001	1.42	0.001
Auger	91.4	0.17	34.9	0.112	0.023	33.44	0.000

The results show that soil structure significantly affects the dynamics of water infiltration and solute transport. The $CaCl_2$ breakthrough curves reveal markedly different transport patterns between disturbed and intact columns. They are symmetrical for the packed columns whereas they are asymmetrically shifted to the left with a generally longer tailing for the intact soil core columns, as observed by Kamra et al. (2001) and Singh et al. (2002).

In the disturbed columns, water and solute pass through a homogeneous soil matrix with a uniform flow resulting in a gradual increase and decrease in solute concentration in the leachate. The solute is retained for longer, and all the solute comes out at the same time, generating a higher Cpeak. Higher K_s values in disturbed columns suggests that soil reorganisation favours more homogeneous and faster flow. Celestino Ladu and Zhang, 2011 also found a greater water velocity, from 2 to 10 times greater for the undisturbed columns than for the disturbed columns. However, during the column saturation, air bubbles may have been trapped, limiting the passage of water through some pores.

The asymmetry and the long tailing of the intact soil core curves for a tracer indicates the presence of physical non-equilibrium transport processes (Cox et al., 1999; Kamra et al., 2001; Pot et al., 2010). Transport is faster in intact columns with the arrival of the tracer (*Tmin*) and the peak of maximum concentration (*Tpeak*) coming earlier. The acceleration of tracer transport results from a greater degree of preferential flows through macropores. These preferential flows are generated by earthworm galleries, root holes and soil cracks. The greater dispersivity of the tracer in the undisturbed columns shows the greater degree of preferential flow in these columns, in contrast to the very low dispersivity of the disturbed columns (Koestel et al., 2013). A greater dispersivity of a solute within intact columns than in disturbed columns has also been observed by Morsali et al., 2019. Koestel et al., 2012 showed that moderate to strong preferential flows are found only in soils with more than 8 to 9% clay. The percentage of clay being 12% in the studied soil, the presence of moderate to strong preferential flows having an impact on the breakthrough curve shape is consistent.

Moreover, the solute in the soil matrix is considered immobile. The solute mass transfer coefficient between the mobile and immobile regions is lower in the conserved columns, which may explain their longer retention and the lower mass recovered. Some of the water passes through the macropores and therefore does not contribute significantly to the transport of solute that has diffused into the soil matrix (Van Beinum et al. 2006). In intact columns, the lower recovery is consistent with dispersion in the soil matrix and partial trapping of the solute in the immobile region. The tracer will emerge at different times depending on the travelled path, resulting in a more gradual elution. Greater solute retention was also observed with lower Cpeak and more widespread breakthrough curves. The wide spreading is also an indication of the heterogeneity of soil transport processes (Vincent et al., 2007). Stubble ploughing was carried out two weeks before the undisturbed columns were sampled. This operation disrupted the surface structure, limiting the continuity of the macropores along the entire length of the columns.

These results confirm that soil structure has a strong influence on solute transport dynamics and therefore on the assessment of the risk of groundwater contamination. Natural soils exhibit complex transport dynamics, with a fraction of the contaminant migrating rapidly through macropores, while another fractions remains trapped in the soil matrix. The use of disturbed columns can lead to a poor assessment of the leaching potential of contaminants under real conditions. Neglecting these preferential flows can lead to an underestimation of the risk of rapid contamination for highly mobile pollutants and an overestimation of the biodegradation or sorption of certain contaminants, due to an interaction with the soil matrix that may be less significant in real conditions. Our research shows that the study of water and solute fluxes in disturbed columns does not provide a suitable representation of the risk of groundwater contamination. The differences between the two types of columns are very pronounced in terms of the breakthrough curves and transport parameters obtained by Hydrus 1-D. Therefore, in order to better approximate real field conditions, intact columns are recommended to assess solute transport. Soil column experiments are an essential tool for modelling contaminant transport, but their design must be rigorously adapted to the objectives of the study. Accounting for soil heterogeneity and preferential transport is essential to improve the reliability of contaminant transfer models and to optimise environmental management strategies.

5.2. Column diameter

The diameter of a disturbed column has only a small influence on the shape of the breakthrough curves (leaching experiment n°2). Both the 24 and 8.4 cm diameter columns displayed symmetrical curves with similar elution patterns (Figure 33).

The solute is found at the same time (p-value = 0.573) in the leachates with a similar Tmin between the columns of 8.4 and 24 cm in diameter. Peak positions also aligned closely, with maximum $CaCl_2$ concentrations being reached after similar pore volumes (p-value = 0.092). Given that the soil in both columns was sieved to 2 mm and reconstructed to the same bulk density (1.38 g cm^{-3}), the transport velocity of solutes was expected to be uniform. Additionally, the travel distance for solute elution was identical at 25 cm for both column types, reinforcing the observed similarity in transport dynamics. Thus, the majority of the solute will emerge after a similar eluted pore volume.

The column diameter does not affect the height or the width of the curves. The maximum relative concentrations Cpeak and the total pore volume required to complete the pulse were not significantly (p-values = 0.121) different for the 24 cm and the 8.4 cm columns.

Very good agreement was achieved between observed and predicted cumulative outflow. The average R^2 of the water flux modelling is on average 1.00±0.00 for the disturbed columns (Table 7). The K_s values are on average not significantly different (p-value = 0.240) between the two diameters. However, the proportion of the mobile

zone is higher for disturbed columns of 24 cm (p-value = 0.006) with 74.3% than for columns of 8.4 cm in diameter with 60.6%. This suggests that the larger columns allowed for greater preferential flow or enhanced water movement through mobile zones.

Transport parameter fitting resulted in a satisfactory representation of solute transport with an average R^2 of 0.95±0.04 for the 24 cm diameter disturbed columns and 0.89±0.06 for the 8.4 cm diameter columns (Table 8). The average dispersivity values obtained for the 24 and 8.4 cm diameter columns were not significantly different (p-value = 0.940). Dispersivity values were less than 1 for all disturbed columns, indicating very low spatial heterogeneity in these columns. These results contrast with findings from Vanderborght and Vereecken (2007) and Bromly et al. (2007), who observed that dispersivity increases with larger lateral scales. This discrepancy is likely due to the disturbed nature of the soil structure in our experiments, which minimized lateral redistribution and dispersion, as highlighted by Koestel et al. (2012). A higher dispersivity typically reduces solute peak concentrations and smooths concentration gradients (Vanderborght and Vereecken, 2007).

The results show that for disturbed soil columns, diameter has only a limited impact on the $CaCl_2$ breakthrough curves and measured transport parameters. This similarity can be attributed to the homogeneous soil matrix across all columns. However, as highlighted in the previous section, disturbed soil columns do not adequately represent water and solute flows in natural soils, where structure plays a critical role. Thus, while column diameter has minimal influence on results obtained from homogenized soils, these results may differ significantly for columns with preserved structure. Therefore, while small-diameter columns can be sufficient for experience that need disturbed soil columns, they may not be appropriate for assessing solute transport in structured soils.

5.3. Column height and differentiated layers

Figure 34 shows the comparison of the $CaCl_2$ breakthrough curves for the 20 and 35 cm undisturbed columns. The 35 cm column includes five centimeters of plough sole between 30 and 35 cm (leaching experiment n°3). Figure 35 illustrates the 20 and 35 cm columns after sampling in the field.

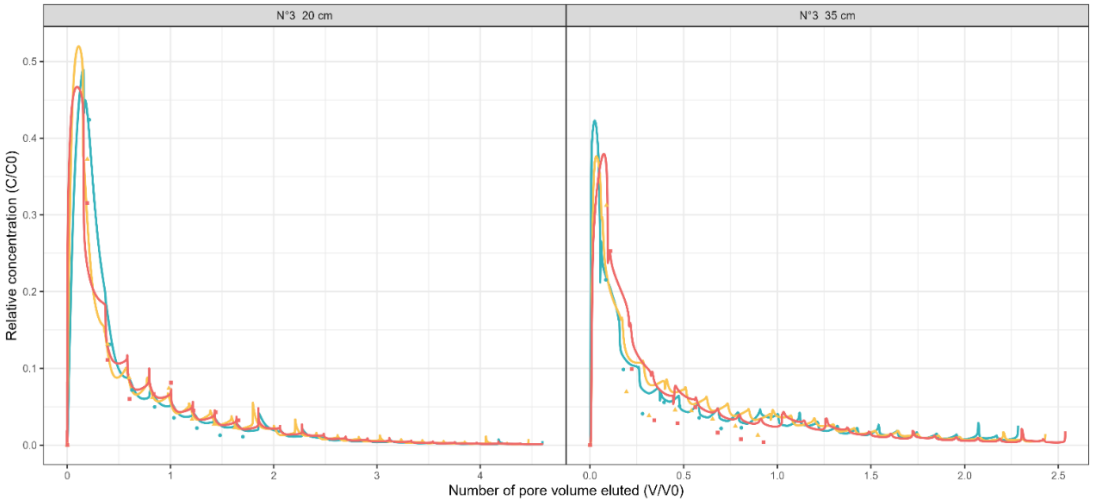

Figure 34. Measured and modelled breakthrough curves depicting the relative concentration (C/C0) in the leachates plotted as a function of the number of pore volume eluted (V/V0) for the $CaCl_2$ tracer, (a) for undisturbed column of 20 cm height and (b) for undisturbed column of 35 cm height for the three replicates. The points correspond to the measured and the lines to the modelled data.

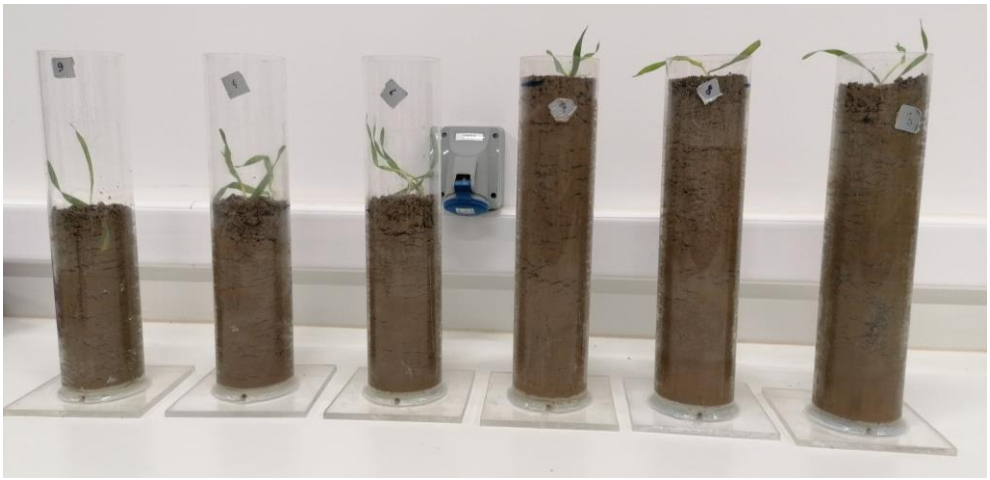

Figure 35. Illustration of the 20 and 35 cm columns after sampling in the field.

The height of the intact soil cores significantly influences the shape of the $CaCl_2$ breakthrough curves (Figure 34). All curves show pronounced asymmetry with long tails, indicating the presence of preferential flow pathways. While solutes are detected at similar times Tmin in the leachate for both the 20 cm and 35 cm columns (p-value = 0.128), the peak positions differ. The maximum $CaCl_2$ concentrations are obtained after an average pore volume that was significantly higher (p-value = 0.003), for the 20 cm columns than for the 35 cm columns. The majority of the solute is eluted with the first few centimeters of water for all columns, indicating the probable presence of continuous macropores throughout the columns. The peak position difference results from a greater pore volume in the 35 cm than in the 20 cm columns. The strong preferential flows within the columns resulted in rapid elution of solute, which may have overshadowed the real effect of height and the presence of a differentiated horizon on the shape and the position of the peak (Cueff et al. 2020). In comparison, the peak position of the intact 25 cm columns performed for leaching experiment n°1 just after stubble ploughing is on average higher. The greater asymmetry of the breakthrough curve compared to the intact columns in leaching experiment n°1 carried out just after harvesting and stubble ploughing is due to the greater importance of preferential flows. These columns were made in November, two months after an intercrop was planted, leading to the formation of aggregates and macropores mainly due to earthworm burrows and root holes. Stronger preferential fluxes are observed in soils with higher aggregate stability and greater soil structure (Porfiri et al. 2015). In addition, Koestel et al. (2012) showed that moderate to strong preferential flows are found only in soils with more than 8 to 9% clay and the percentage of clay in the studied soil is 12%. This highlights the dynamic of soil structure development, influenced by the timing of sampling and crop management practices.

The column height and the presence of a differentiated horizon significantly influence the height and the width of the breakthrough curve. The maximum relative concentrations of $CaCl_2$ were significantly higher for the 20 cm columns (p-value = 0.01), with a greater amount of $CaCl_2$ recovered (67.4 ± 2.2% compared to 41.0 ± 2.7% for the 35 cm columns; p-value = 0.0001). The total pore volume Ttot was significantly higher (p-value = 0.0001) for the 20 cm columns than for the 35 cm columns. Thus, the breakthrough curve of the 20 cm columns shows a maximum relative concentration 1.3 times higher with an amount of $CaCl_2$ recovered 1.6 times higher for a pore volume to complete the pulse 1.9 times higher than the 35 cm columns.

Regarding the optimised values of water transport, the average R^2 is 1.00±0.00, indicating the high accuracy of the water fluxes represented by the model. The modelling differentiated between the 20 cm columns, the 35 cm columns with a single horizon, and the 35 cm columns with two horizons (30 cm + 5 cm plough sole). While the mobile zone proportion was similar between the 20 cm columns and the upper 30 cm of the 35 cm columns, it was significantly reduced (12.9%, p-value = 0.0001) within the plough sole. This suggests limited solute mobility in compacted layers, potentially leading to solute retention.

The values of K_s for the 20 cm columns are on average similar with the first 30 cm of the 35 cm columns (p-value= 0.122). These values are higher than the value of 0.022 cm/min initially given by Rosetta. Strong preferential flows will result in a rapid water flow and the model increases the K_s. The plough sole has lower conductivity with an average of 0.023±0.005 cm/min, closer to the initial value.

The fitted transport parameters resulted in an appropriate representation of the transport of the solute with an average R^2 of 0.90±0.05 for the 20 cm columns, 0.80±0.02 for the 35 cm columns with one horizon and 0.78±0.04 with two horizons (Table 7). However, the high dispersivity values obtained for the columns, mainly for those of 35 cm, are beyond the range of validity and show that the dual porosity model fails to represent physical non-equilibrium processes. The dispersivity values obtained for the 20 cm columns were on average significantly lower (p-value = 0.001) compared to the horizon 1 of 35 cm columns or to the whole 35 cm columns (1H). Thus, 35 cm columns exhibit a dispersivity 6.5 times greater than 20 cm columns. The dispersivity value were smaller than 1 for the plough pan. The highest dispersivity values for the 35 cm columns show greater soil heterogeneity and higher preferential flows (Koestel et al., 2013). Vanderborght et al. (2007) and Koestel et al. (2012) demonstrated that apparent dispersivity is positively correlated with travel distance, which is consistent with our findings. In addition, the solute may have been retained in the column for a longer time by the plough pan. However, no significant difference was observed between the first 30 cm (horizon 1) and the entire 35 cm column.

Interestingly, despite the presence of the plough sole, the differences in transport behavior between the 20 cm and 35 cm columns primarily resulted from the increased soil column height. The differences in pore volume and solute dispersivity in the 35 cm columns contributed to lower $CaCl_2$ recovery and reduced peak concentrations in the leachate.

The timing of sampling in relation to cultivation operations appears to influence the solute leaching through the soil profile. Compared to the intact columns of leaching experiment n°1 performed just after a stubble ploughing that disturbed the topsoil, the solute peak arrives after a pore volume 3.0 times higher, the maximum peak concentration is 2 times lower and the dispersivity is 1.2 times lower than for the 20 cm height columns. This demonstrates how soil structure evolves over time, with macropore formation and aggregation increasing preferential flow pathways and solute mobility.

Our study showed significant differences in breakthrough curves and transport parameters between the 20-cm and 35-cm columns. Modelling on Hydrus 1-d showed that the differences are mainly due to the difference in column height and not to the presence of the plough sole. The lower pore volume eluted and the greater solute dispersivity within the 35 cm columns resulted in a lower mass of $CaCl_2$ recovered and maximum concentration peak found in the leachate. Therefore, too short soil columns may not accurately represent water and solute transport in field conditions. They could lead to overestimation of solute leaching potential and an underestimation of the degradation, which could result in inaccurate risk assessments for contaminant migration to groundwater. Therefore, longer columns that capture the heterogeneity and preferential flow dynamics of natural soils should be used to improve the reliability of transport models and environmental risk assessments.

5.4. Soil core sampling method

Figure 36 shows the comparison of the $CaCl_2$ breakthrough curves for columns collected with the mechanical soil column cylinder auger and by hand (leaching experiment n°4).

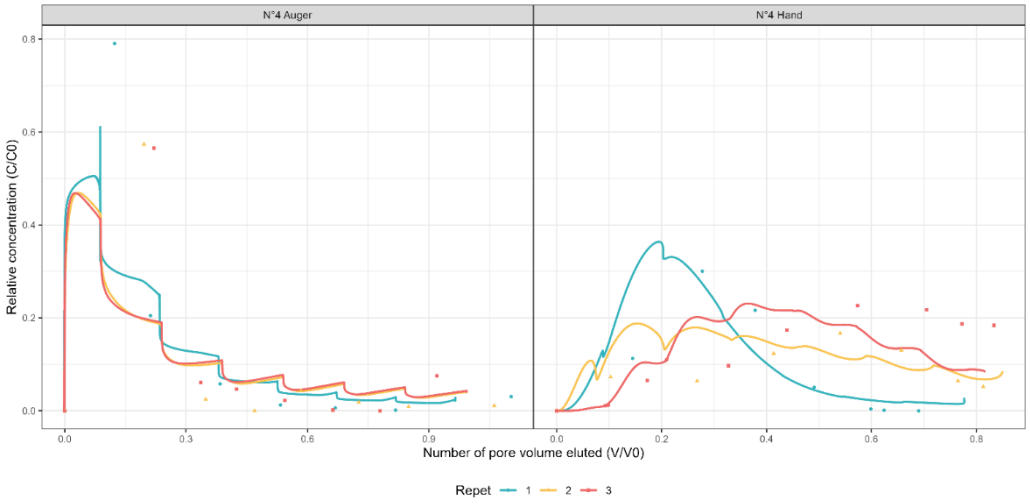

Figure 36. Measured and modelled breakthrough curves depicting the relative concentration (C/C0) in the leachates plotted as a function of the number of pore volume eluted (V/V0) for the $CaCl_2$ tracer for undisturbed column, (a) collected with the soil column cylinder auger and (b) collected by hand for the three replicates. The points correspond to the measured and the lines to the modelled data.

The sampling method has a strong influence on the overall shape of the $CaCl_2$ breakthrough curves. They are strongly asymmetrically shifted to the left for columns made with the mechanical soil column auger, indicating strong preferential flows. Breakthrough curves for columns sampled by hand are more gradual, indicating less preferential flows and a greater portion of water and solute passing through the soil matrix. The solute is found faster in the leachates with a significantly lower time (p-value = 0.045) of first breakthrough (Tmin) for the mechanical auger columns than for the hand columns where it is more retained. The peak appeared faster (p-value = 0.048) for mechanical auger columns than for the hand columns, indicating greater retention of the solute in the columns made by hand. The peak corresponds to the first water sample for the columns made with the mechanical corer indicating the presence of continuous preferential paths in the whole column that are not present in these hand-driven columns.

The sampling method also influences the height and width of the breakthrough curves. The maximum concentration of the peak (Cpeak) is significantly higher (p-value = 0.023) for the mechanical auger columns. The majority of the solute comes out very quickly from the columns sampled with the mechanical corer with an average of 91.4±7.4% of $CaCl_2$ recovered against 63.3±17.0% for the columns sampled by hand at the end of the experiment (Table 6). In addition, the total amount of pore

volume eluted (Ttot) was significantly higher (p-value = 0.025) for the mechanical auger columns. The breakthrough curves of the mechanical auger columns show a Tpeak 4.9 times lower, a Cpeak (height) 2.0 times higher and a Ttot (width) 1.32 times higher than the columns made by hands. Visually, during the experiment, significant preferential flows were present between the soil column and the Plexiglas wall of the corer columns, generating a rapid flow of water (figure 37). These continuous preferential flows are not present in the hand-driven columns. These flows are not natural and are created during the sampling with the corer. A possible cause would be the vibrations caused by the percussion hammer that is used to drive the column into the ground.

Figure 37. Illustration of intact columns extracted by hand (left and bottom) or with a mechanical auger (right and top).

The average R^2 values obtained for the optimisation of the water flow parameters are 0.99±0.01 for the columns produced by mechanical corer and 0.99±0.01 for the columns taken by hand, indicating a suitable representation for both types of columns, despite very different water flows. For the two types of column, the proportion of mobile zone is not significantly different. However, the K_s is significantly higher (p-value = 0.003) for columns made with a mechanical corer than for columns taken by hand. Thus, at saturation, the water flows 1.5 times faster in the columns taken with the mechanical corer. The continuous preferential flows explain this high hydraulic conductivity and are mainly localised along the sides of the columns.

The solute transport parameters fitting resulted in a correct representation of solute transport with an average R^2 of 0.84±0.12 for mechanical corer columns and 0.93±0.06 for hand made columns. The dispersivity, an indicator of the degree of preferential flows, is 25.3 times higher (p-value = 0.001) for the columns sampled with the corer compared to the columns driven by hand.

Interestingly, the Ks, the peak position and the maximum relative concentration of the hand-made columns are similar to the undisturbed columns of the leaching experiment n°1. These similar results may be due to agricultural operations that homogenized the topsoil 1 month before these different columns were made.

Therefore, although the mechanical corer in principle allows the sampling of undisturbed soil columns up to 1 m depth, it appears in this study that these columns do not properly represent water and solute fluxes. The vibrations of the hammer can create a gap between the soil column and the wall of the column. This gap generates continuous preferential flows and a rapid elution of the majority of the solute despite the wax poured at the soil-Plexiglas interface at the beginning of the experiment. As a result, hand-driven columns seem to be a better alternative to sample undisturbed soil columns and limit unnatural preferential flows.

6. Conclusions and perspectives

Tracer leaching experiments were performed on soil columns of different designs frequently encountered in the literature. This study shows and provides quantified data on the impact of soil structure, soil column diameter and length, as well as the presence of a plough sole and the sampling method on the leaching behaviour of a solute as well as on the dual-porosity parameters.

The difference in soil structure between disturbed and undisturbed columns significantly affects solute transport dynamics and water infiltration. Breakthrough curves of disturbed columns are symmetrical with higher peak concentrations (1.95 times) - and lower pore volumes required to complete the pulse (1.35 times). In contrast, intact columns show asymmetric curves with longer tailing, indicating non-equilibrium transport due to preferential flow through macropores. Tracer transport is faster in intact columns, with Tmin occurring 1.41 times earlier, highlighting the role of preferential pathways such as earthworm galleries and root holes. Disturbed columns have higher saturated hydraulic conductivity (K_s) and lower dispersivity (12.3 times lower), reflecting homogeneous flow with limited spatial heterogeneity. In intact columns, lower recovery and higher retention indicate immobile regions and heterogeneous transport within the soil matrix. Given these differences, intact columns should be preferred to better approximate field conditions, as disturbed columns underestimate rapid contaminant transport by neglecting preferential flow and overestimate contaminant retention. Our research shows that the study of water

and solute fluxes in disturbed columns does not provide a suitable and reliable representation of the risk of groundwater contamination.

The diameter of disturbed columns has minimal impact on $CaCl_2$ breakthrough curve shape, peak position, and width, as both 24 cm and 8.4 cm diameter columns exhibit similar elution patterns and transport velocities. However, the proportion of the mobile zone is significantly higher in larger columns (74.3% vs. 60.6%), suggesting increased preferential flow. Dispersivity remains low and comparable between diameters, reflecting homogeneous soil matrix conditions. While small-diameter columns adequately represent breakthrough curves in disturbed soils, they may not accurately reflect transport dynamics in structured soils, where preferential flow paths play a crucial role.

The height of intact soil columns significantly influences the shape of the breakthrough curve, peak position and solute recovery. In our study, 20 cm columns showed higher peak concentrations (1.3 times) and $CaCl_2$ recovery (1.6 times) compared to 35 cm columns, with 1.9 times higher pore volume to complete the pulse. This difference is due to the increased pore volume and dispersivity in the taller columns. The 35 cm columns exhibited greater solute dispersivity (6.5 times higher) and lower recovery due to increased preferential flow, particularly in the presence of a plough sole. Hydrus 1-D modelling indicated that the differences were primarily due to column height rather than the plough sole. In addition, saturated hydraulic conductivity was similar between column heights but decreased in the plough sole layer, suggesting limited mobility in compacted zones. Shorter columns may overestimate solute leaching potential and underestimate solute degradation, leading to inaccurate risk assessments for groundwater contamination. Therefore, longer columns better capture natural soil heterogeneity and preferential flow, improving the reliability of transport models and environmental risk assessments.

Sampling method significantly affects breakthrough curve shape, peak position, height and eluted pore volume. Mechanical auger columns show faster breakthrough and peak position, with higher peak concentrations and greater dispersivity (25.3 times higher) compared to hand driven columns. These differences are due to unnatural preferential flow created by vibration during auger sampling, resulting in rapid water flow along the column walls. As a result, mechanical corer columns have a higher saturated hydraulic conductivity, with water moving 1.5 times faster than in hand-driven columns. In contrast, the hand-driven columns better represent natural water and solute fluxes, producing more gradual breakthrough curves with reduced preferential flow. Despite the theoretical advantage of deeper sampling with mechanical corers, the results indicate that these columns do not properly represent water and solute fluxes. Hand-driven methods provide a more accurate representation of soil transport processes, making them the preferred choice to minimise the influence of artefacts.

This research confirms and quantifies some of the impacts of common methodological choices on pesticide leaching results. Some commonly used methodologies may not be relevant to study the mobility of solutes within a soil profile, especially if the experiment attempts to approximate field conditions. Moreover, the timing of sampling in relation to cultivation operations appears to influence the solute leaching through the soil profile. This study allows researchers to better choose the experimental design according to the purpose of their experiments. In future work, a larger number of columns and modalities should be studied to confirm the observations and to establish harmonisation functions in order to allow the combination of different approaches. By clarifying how these methodological factors influence leaching experiments and dual-porosity parameters, this work aims to support the development of standardized practices in soil column leaching research and improve the reliability of contamination risk assessments.

Chapter 4

Pesticide fate under varying cropping systems and soil depths: a study using leaching experiments and inverse modelling

1. Synopsis

After determining the most relevant methodology, **Chapter 4** will focus on the fate of eight pesticides that are problematic for groundwater in Wallonia in silty soils typical of the region. This chapter will address objectives 2, 3 and 4 of this thesis. Leaching experiments on these eight pesticides in undisturbed soil columns are thus carried out on three contrasting production systems of EcoFoodSystem and on the first three soil horizons. The breakthrough curves and the balances of adsorbed, degraded and eluted pesticides are analysed. Dual-porosity inverse modelling on Hydrus 1-D was used to obtain the sorption and degradation parameters of these pesticides for Wallonia and to compare them with the values used and from databases.

Pirlot, C., Blondel, A., Krings, B., Durenne, B., Pigeon, O., Degré, A., 2025. Pesticide fate under varying cropping systems and soil depths: A study using leaching experiments and inverse modelling. J. Contam. Hydrol. 270. https://doi.org/10.1016/j.jconhyd.2025.104526

2. Abstract

Current pesticide leaching risk assessments overlook critical site-specific factors such as soil depth and agricultural practices. Relying on transport parameters from databases or manufacturer studies, often based on limited soil types, can lead to inaccurate contamination risk estimates and ineffective protection of groundwater resources. In this study, the fate of eight pesticides of concern for groundwater was investigated under three cropping systems and three soil depths (figure 38). Leaching experiments were carried out in undisturbed columns from a loamy agricultural soil and mass balances were realized. Inverse dual-porosity modelling using Hydrus 1-D was then performed to adjust mobility parameters. The results reveal that different soil properties and structure between soil depths have a more substantial impact on pesticide leaching behaviour than the cropping systems. Significant differences in pesticide transport and retention are observed between soil horizons, illustrating the inadequacy of using surface parameters for the entire soil profile, which can lead to underestimation of groundwater contamination. Our analysis indicates that root architecture, soil properties and surface tillage can affect pesticide leaching dynamics. While short-term differences between cropping systems were limited, these factors could be important for long-term effects. The experimental transport parameters showed discrepancies with established databases, where higher adsorption and degradation could underestimate pesticide leaching and metabolites production. This study highlights the need to adapt transport parameter values for all pesticides of concern to site-specific conditions. In addition, accurate risk assessment requires advanced modelling techniques that take into account soil depth variability and local conditions to improve water protection decision-making. Future research should focus

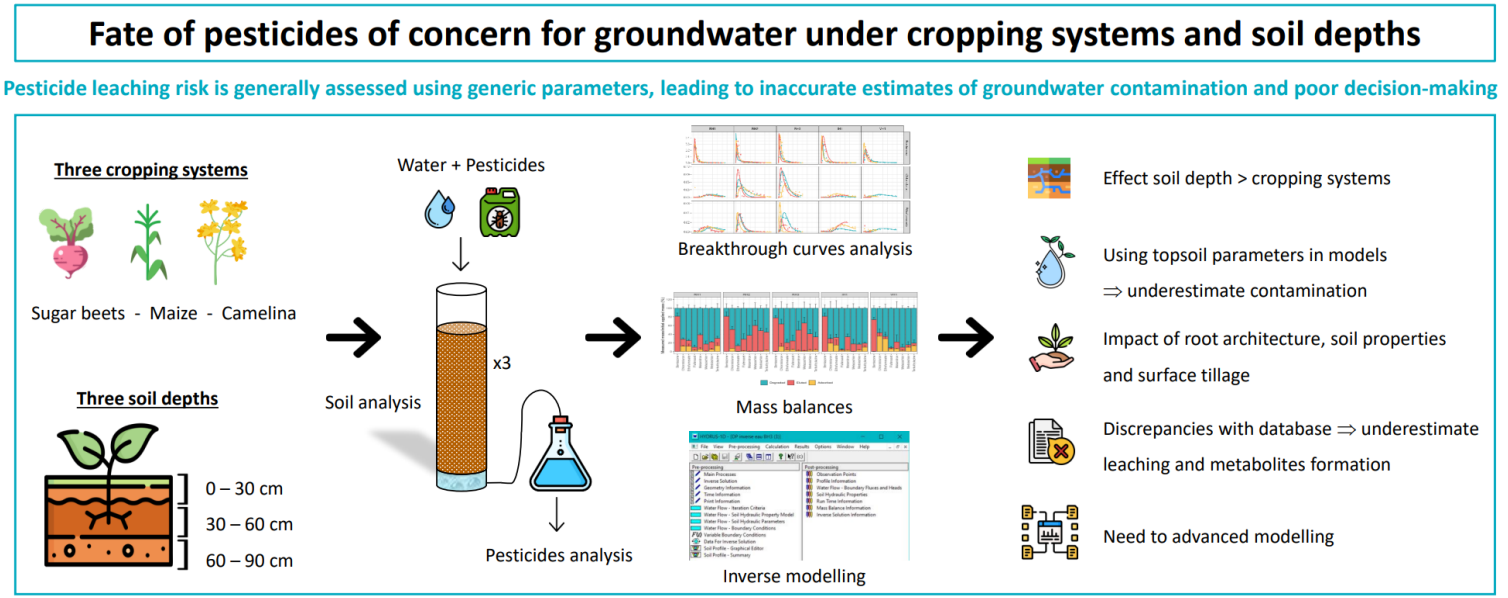

Figure 38. Graphical overview of the fate of pesticides in different cropping systems and at different soil depths.

on long-term monitoring of the effects of sustainable agricultural practices on pesticide behaviour over several seasons and for a range of soil types. Special emphasis should be placed on the role of metabolites in environmental contamination.

3. Introduction

The current use of pesticides in agricultural systems has had a negative impact on the quality of natural resources. Pesticide use in agriculture and worldwide has increased by 50% compared to the 1990s (FAO, 2022). Part of these pesticides will leach through the soil profile and lead to a deterioration of groundwater quality (Jurado et al., 2012; Labite et al., 2013). Despite a decrease in pesticide use in Europe, a large number of pesticides and their metabolites are frequently found in groundwater, which is the largest source of drinking water for many countries (Köck-Schulmeyer et al., 2014; Kiefer et al., 2019; Pietrzak et al., 2019; Baran et al., 2021; EurEau, 2021).

In Wallonia (southern Belgium), almost 80% of the water supply, especially for drinking water, comes from groundwater. Between 2017 and 2020, pesticides were detected in 61.7% of monitoring sites in measurable concentrations (SPW ARNE, 2022). Herbicides are responsible for the majority of pesticide contamination in groundwater. Among these, eight problematic pesticides were still authorised when the research was carried out: bentazone, chlorotoluron, metamitron, metazachlor, S-metolachlor, terbuthylazine, flufenacet and ethofumesate. At the European level, the Water Framework Directive (2000/60/EC) and the Groundwater Directive (2006/118/EG) seek to limit groundwater contamination by requiring groundwater monitoring and by forcing Member States to define concentration limits for pollutants (European Commission, 2000, 2006). However, inconsistencies between regulations are commonly found between soil and groundwater pesticides. As a result, worldwide regulations on soil pesticides do not take into account a sufficient number of pesticides with appropriate standard values to meet groundwater regulations and protect them effectively (Li, 2018). This is particularly the case in mixed rural and residential areas, where exposure to soil pesticides occurs indirectly. The soil-groundwater continuum needs to be properly considered in pesticide regulations (Li, 2021). To assess the risk of groundwater contamination by an active substance or its metabolites, leaching indices can be quickly calculated. However, many indices exist and the results obtained by different approaches can be contradictory (Akay Demir et al., 2019). Thus, solute leaching models relevant for the European Union are generally used to assess leaching potential (European Commission, 2014).

The two processes that predominantly control pesticide mobility within a soil profile are adsorption and degradation (Malla et al., 2021). Many factors will influence these processes such as pesticide properties but also soil characteristics, site conditions, and pesticide application practices (Arias-Estévez et al., 2008; Grodner et al., 2014). The

solubility of a pesticide in water, which refers to its ability to dissolve in water, can also determine its leaching characteristics into groundwater and its potential to run off into surface water (Rasool et al., 2022). This parameters is well characterized conversely of the two parameters needed for modelling: the sorption coefficient (K_d) and half-life time (DT_{50}) (Bewick, 1994; Wauchope et al., 2002; Katagi, 2013; Kahl et al., 2015).

The FOCUS groundwater workgroup has developed nine scenarios based on a combination of weather, soil and cropping data to represent agriculture in the European Union (FOCUS, 2009; European Commission, 2014). In order to authorize or renew the authorization of a pesticide in the EU, the 9 FOCUS scenarios are used to model the leaching risk of the active compound for the whole geoclimatic range of Europe including sorption and degradation parameters derived from laboratory and lysimeter experiments. Most of these experiments are conducted by pesticide-producing companies, such as manufacturers or registrants, at several sites within a limited number of European countries. However, this approach can be misleading. For instance, Labite et al. (2013), showed significant differences between the pesticide leaching results given by the PELMO model parameterised for soil and weather conditions specifically for the site studied in Ireland and for the EU FOCUS scenarios used. The latter overestimated leaching by 42-99%. Several studies show that pesticide properties such as K_d or DT_{50} provided by databases such as the PPDB are not always reliable for modelling pesticide fate in soils (Cueff et al., 2020; Ullucci et al., 2022; Mamy et al., 2024). They advise to determine these properties for the soil studied to have more accurate values. The FOCUS groundwater workgroup also recommends estimating the pesticide sorption and degradation parameters by inverse modelling of leaching experiments under site-specific conditions (FOCUS, 2009). However, in Belgium, pesticides transport parameters provided by manufacturers are currently still used to model the leaching risk of pesticides.

Nowadays, alternative and more sustainable agricultural practices are being developed, based on several principles such as reducing tillage, incorporating crop residues into the soil, maintaining soil cover and diversifying crops within the rotation (Verhulst et al., 2010). These practices can affect the temporal dynamics of soil hydraulic properties such as water retention and other factors such as soil structure or organic carbon content (Pirlot et al., 2024). Different crops in rotations will affect soil structure through their different root systems (Hu et al., 2009). For example, Lichter et al. (2008) found significantly larger macro-aggregates in the soil under wheat because wheat has a more horizontal root system than maize and the higher density of plants results in a denser shallow root system. Different crops also generate different soil microbial communities, with roots releasing a variety of different exudates depending on the crop. In general, earthworm abundance, diversity and activity increase under conservation agriculture (Chan, 2001; Fox et al., 2022; Lori et al., 2023). Therefore, pesticide leaching within a soil profile is influenced by soil properties as well as land use, land management and crop characteristics (Alletto et

al., 2015). As a result, the K_d and DT_{50} values found in databases are generally specific to the pesticide for a given soil type at a given depth and for a given set of agricultural practices (Weber et al., 2004; Imig et al., 2023a).

Cueff et al. (2020) showed that vertical transfer of water and pesticides in undisturbed soil columns was more pronounced in conservation agriculture production system than in conventional due to greater pore connectivity. In this context, the main risk is that preferential flows are occurring and generating a rapid vertical transfer of pesticides. Currently, the understanding of the effect of agricultural practices on pesticide leaching is unsatisfactory, which limits our ability to predict the environmental impact of cropping systems (Marín-Benito et al., 2018). Most studies try to isolate the effect of specific agricultural practices, such as tillage. However, it would be more appropriate to consider the effect of all practices to assess and compare pesticide transport under several different production systems (Willkommen et al., 2021).

The adsorption and degradation processes of pesticides will also vary with the depth of the soil. The different layers will have different textures, organic carbon contents, temperatures, pH, structure and fauna (Katagi, 2013). Available data on pesticide adsorption and degradation concern predominantly the surface soil layers and few studies are performed on the deeper soil layers. Pot et al. (2011), found different pesticide behaviors within the first three horizons of a sandy-loamy soil. Adsorption of chemicals to soil organic matter is the dominant adsorption mechanism when the organic matter fraction of the soil is higher than 2% (Arienzo et al., 1994). Adsorption will also depend on the clay and metal oxide content (Weber et al., 2004). The organic carbon content of soils tends to decrease with depth, making adsorption generally lower in deeper soil layers (Katagi, 2013). In addition, the microbial population and temperature generally decrease with depth, making biodegradation slower (Mills et al., 2001). The composition of the soil microbial community will change with depth and the abundance of some bacteria such as Gram-positive will increase with depth (Fierer et al., 2003). Moreover, earthworms, in varying abundance in different soil layers, will impact the physical properties of the soil by increasing the water infiltration rate and the macroporosity (Johnson-Maynard et al., 2007).

To investigate the movement of pesticides within a soil profile, intact soil column leaching experiments are commonly used as they allow to get closer to field conditions than laboratory batch experiments (USEPA, 2008; Katagi, 2013). Observed data such as water and solute fluxes are then used to estimate pesticide transport parameters by inverse modelling (Sniegowski et al., 2009; Dusek et al., 2015; Kahl et al., 2015; Kondo et al., 2020; Sur et al., 2022). These parameters may be difficult to obtain by field leaching experiments due to soil heterogeneity and complex boundary conditions (Dusek et al., 2011). Preferential flows will have a dominant role in the transport of water and contaminants in structured soils (Jarvis, 2007; Köhne et al., 2009a; Varvaris

et al., 2021c). The preferential pathways, mainly macropores of biological origin such as earthworm burrows, root holes and of mechanical origin such as cracks, can rapidly transport pesticides deeper and increase the risk of groundwater contamination. Different approaches can be used to take into account the heterogeneity of the matrix and the preferential flows, such as the dual-porosity approach (DP) or the double permeability approach (DPM) (Šimůnek et al., 2003). Imig et al. (2023a) determined the transport parameters of four pesticides by inverse modelling using Hydrus 1-D with herbicide concentrations in drainage water. They showed that peak concentrations in the presence of preferential flows were correctly modelled using the DP model. Hydrus 1-D was also successfully used by Pot et al. (2005) and Köhne et al. (2006) to model water and pesticide fluxes within a soil column.

Therefore, the objectives of this study are

(i) to assess the fate of eight pesticides, problematic for groundwater, using leaching experiments to obtain breakthrough curves in intact columns from a loamy agricultural soil;

(ii) to highlight the sensitivity of cropping systems and soil depth on the mobility parameters obtained by inverse modelling;

(iii) to compare those parameters with the theoretical parameters of the manufacturers, those currently used in Belgium and with the ranges of values given in the Pesticides Properties DataBase for Europe.

4. Materials and methods

4.1. Soils and cultivation practices

Soil columns were collected on an agricultural soil located on the EcoFoodSystem experimental plots (50°56'50.6"N, 4°70'93.2"E) of the Terra teaching and research centre of the University of Liege in Gembloux, Belgium. Within this experiment, three different agricultural production systems have been implemented in September 2020. The first system is called 'reference', the second system ‘Integrated Crop Livestock System (ICLS)' and the third rotation 'vegan' as presented in Chapter 2. The 'vegan' designation is derived solely from the use of crops intended exclusively for human consumption and the absence of inputs of animal products such as manure.

The climate is temperate oceanic with an average annual temperature of 10.2°C and an average annual rainfall of 837 mm. The soil is cutanic luvisol according to the World Reference Base for Soil Resources (FAO, 2015). The soil consists of a light brown Ap horizon that is ploughed up to about 30 cm. From 30 to 60 cm a lighter yellowish brown horizon AB is observed. After 60 cm there is an accumulation

horizon of light ochre clay Bt up to about 100 cm. The physico-chemical properties of the three horizons and the three cropping systems studied are given in Table 10. The notation is as follows: R = reference, I=ICLS, V=vegan, RH1-3 = horizon 1 to 3.

Table 10. Physico-chemical properties of the soils for the three cropping systems (RH1, IH1 and VH1) and the three soil depths (RH1, RH2 and RH3) at the time of sampling the columns.

	RH1	**IH1**	**VH1**	**RH2**	**RH3**
Depth	0-30	0-30	0-30	30-60	60-90
Crops	Sugarbeets	Maize	Camelina	Sugarbeets	Sugarbeets
Texture			Fine silty clay		
Clay (%)	13,8	12,3	17,2	13,1	19,2
Silt (%)	78,3	79,7	76,5	80,4	74,5
Sand (%)	7,9	7,9	6,3	60,4	6,2
Organic carbon (g/kg)	12,3	11,5	11,7	5,24	3,35
Cation exchange capacity (CEC) (meq/100 g)	9,4	8,8	10,6	8,3	10,6
pH water	7,6	7,6	7,6	7,8	7,9
Bulk density (g/cm^3)	1,41±0,03	1,64±0,01	1,59±0,04	1,54±0,01	1,64±0,01
Porosity	0,462±0,009	0,375±0,004	0,395±0,015	0,415±0,005	0,378±0,002

In July 2020, the winter wheat was harvested and stubble ploughed. Cover crops were then planted in September 2020 until the first crops of the experiment. In the first year of the rotations in 2021, sugar beet, maize, and camelina were planted in the reference, ICLS and vegan systems respectively. Tillage and soil preparation were performed on all rotations in April, 2021. In the reference system, a manure application and sowing of beets at 100,000 plants/ha was done at the end of April 2021. Then, a hoe passage was carried out at the beginning and middle of June 2021 to remove weeds mechanically between crop rows, loosening the soil surface, while avoiding the use of chemical herbicides. In the ICLS system, the application of manure and the sowing of grain corn at 100,000 plants/ha were carried out in mid-May 2021. The rotary hoe was conducted in mid-June and the hoe in late June and early July 2021. In the vegan system, camelina sowing at 3,000,000 plants/ha was completed in late April 2021. The rotary hoe was run in mid-June 2021. Harvesting and stubble plowing of the camelina was completed in early September 2021. Figure 39 shows the agricultural itineraries of the different experimental plots.

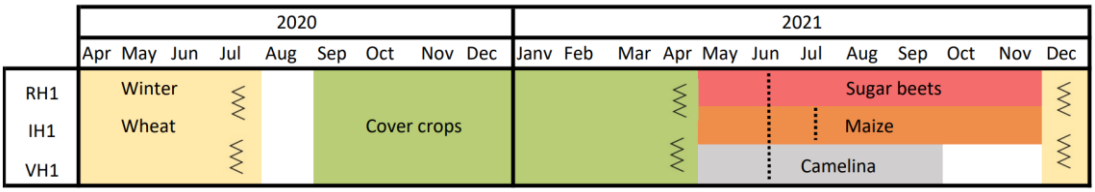

Figure 39. Technical agricultural itineraries for the three cropping systems studied.

As the cropping systems are pesticide-free, there have been no pesticide treatments since September 2020. The most recent pesticide uses studied were S-metolachlor in 2018, ethofumesate and metamitron in 2016 and metazachlor in 2013.

4.2. Undisturbed columns

A total of 15 intact soil core columns were taken using 40 cm long Plexiglas tubes with an internal diameter of 8.4 cm. Porosity was calculated from the bulk density for each column and the density of the soil particles and organic matter, assuming a soil particle density of 2.65 $g.cm^{-3}$ and an organic matter particle density of 1.4 $g.cm^{-3}$. These values have been used because they correspond to common values for silt and soil organic matter (Porfiri et al., 2015; Schjønning et al., 2017; Ruehlmann, 2020).

All columns were collected between September 8 and 13, 2021 (figure 40).

Figure 40. Plot IH1 (maize) and RH1 (beet) on 8 September 2021 during the sampling of soil columns.

Nine columns were collected in the reference innovative system where sugar beets were implanted. The columns were taken from the first three horizons, i.e. three from 0-30 cm, three from 30 to 60 cm and three from 60 to 90 cm in the reference system (figure 41). The three horizons were compared only for the reference system, as agricultural practices mainly influenced the surface horizon. Then, three columns were taken between 0 and 30 cm in the ICLS system where maize was established and three others between 0 and 30 cm in the vegan system where camelina had just been harvested. The columns were all driven in by hand. A wooden plate was placed over the columns with a piece of textile. Using a sledgehammer, they were gradually pushed into the ground to the desired depth. The surrounding soil was then removed with a shovel. Once the column was uncovered, the soil underneath was cut off with a trowel to extract it. Immediately after excavation, the ends of the columns were sealed. The columns were secured in a box to bring them to the laboratory on foot to minimize disturbance to the soil structure (Singh et al., 2002).

Figure 41. On the right, a trench 60 cm deep to sample the columns of the third horizon (RH3) and on the left, a column made at plot IH1 with the maize.

At 2 cm from the bottom of the tubes, a perforated Plexiglas plate was fixed to elevate the columns and allow water to pass through. A nylon textile disc was placed between the soil and the perforated plate to prevent soil particles from being washed away. A tube was placed in the water collection area and was connected to two Erlenmeyer flasks and a vacuum pump to provide a suction of 35 kPa to get closer to the field conditions (Dusek et al., 2015). All columns were built in triplicate.

To limit preferential flow along the column wall, paraffin was poured over the interface between the soil and the Plexiglas wall. The paraffin ensures that the water infiltrates the soil and does not flow along the wall (Isensee and Sadeghi, 1992; Arthur et al., 1998). The columns were kept free of vegetation for the duration of the experiment. Because pesticides are photosensitive, the complete experimental set-up (columns, connections, and collecting Erlenmeyer flasks) was covered with aluminium as illustrated in figure 42 (Hua et al., 2009).

The columns were gradually saturated with distilled water to ensure uniform wetting and avoid preferential flow pathways that could influence pesticide leaching dynamics (Kördel et al., 2008; Van Beinum et al., 2006). They were then drained freely without a vacuum pump for 24 hours to achieve field capacity, simulating realistic soil moisture conditions and minimizing differences in water content between columns at the beginning of the experiment (Weber et al., 2003).

Figure 42. Several columns of the pesticide leaching experiment in the laboratory.

4.3. Pesticides properties

Eight herbicides with contrasting properties were studied. These eight herbicides were chosen because they are very commonly used in agriculture and generate groundwater pollution problems in Wallonia. Collectively, they account for 20% of herbicide use in Wallonia (CORDER, 2020). In addition, they are all of different types (except metazachlor and S-metolachlor) with a wide range of solubility (6.6 to 7112 mg/l) and adsorption and degradation properties. Pesticides were used in formulation as they are applied in the field. Commercially formulated pesticides will have different mobilities and may be leached from soil columns to a greater extent than active molecules (Hua et al., 2009; Khan and Brown, 2016). The main properties of the eight herbicides from the Pesticides Properties DataBase (PPDB) (Lewis et al., 2016), as well as the recommended dose and concentrations applied to the columns are summarised in Table 11 and 12.

These eight herbicides have not been used on the plots where the columns were sampled since at least 2018. Bentazone was last used on maize in July 2005. Chlorotoluron has not been used since 2003. Ethofumesate and metamitron were last used in May 2016 on sugar beet and in May 2021 on an adjacent plot. Metazachlor was last applied in October 2013 to rapeseed. S-metolachlor was applied in May 2018 to chicory, and flufenacet and terbuthylazine were applied in June 2011 to maize.

Table 11. Main properties of the eight pesticides studied, based on the Pesticide Properties DataBase (PPDB).

Herbicide	Type	Crops	Action	Solubility in water at 20°C (mg/l)	Octanol-water partition coefficient (pH 7, 20°C)	pKa at 25°C	Henry's law constant at 25 °C ($Pa.m^3/mol$)	Persistency	Mobility	GUS index
Bentazone	Thiadiazine herbicide	Corn, rice, alfalfa, linseed, beans, …	Inhibits photosynthesis (photosystem II)	7112	-0,46 (low)	3.51 (Weak acid)	$7.20*10^{-5}$ (Non-volatile)	non-persistent	Mobile	1,95
Chlorotoluron	Urea herbicide	Cereals, potatoes, maize, vegetables	Inhibition of photosynthetic electron transport	76	2.5 (Low)	No dissociation	$9.07*10^{-7}$ (Non-volatile)	Moderately persistent	Moderately mobile	2,01
Metamitron	Triazinone herbicide	Sugar beet, Fodder beet, Red beet	Inhibits photosynthesis (photosystem II)	1770	0.85 (Low)	No dissociation	$8.95*10^{-8}$ (Non-volatile)	Moderately persistent	Moderately mobile	2,16
Metazachlor	Chloroacetamide herbicide	Oilseed rape, maize, sugarcane, cotton, …	inhibition of cell division	450	2.49 (Low)	No dissociation	$5.9*10^{-5}$ (Non-volatile)	Non-persistent	Mobile	1,75
S-Metolachlor	Chloroacetamide herbicide	Corn, soybeans, sorghum, potatoes, …	inhibition of cell division	530	3.4 (High)	No dissociation	$2.40*10^{-3}$ (Non-volatile)	Moderately persistent	Moderately mobile	2,32
Terbuthylazine	Triazine herbicide	Maize, Sorghum, Apples, Citrus, …	Inhibits photosynthesis (photosystem II)	6.6	3.4 (High)	1.9 (Weak basic)	$2.30*10^{-3}$ (Non-volatile)	Moderately persistent	Moderately mobile	2,19
Flufenacet	Anilide herbicide	Corn, Soybeans, Winter wheat, Sunflowers, …	inhibition of cell division	51	3.5 (High)	No dissociation	$1.30*10^{-3}$ (Non-volatile)	Non-persistent	Moderately mobile	2,49
Ethofumesate	Benzofuran herbicide	Sugar beet, Fodder beet, Red beet, onions, carrots, …	Inhibition of lipid synthesis	50	2.7 (Moderate)	No dissociation	$3.72*10^{-3}$ (Non-volatile)	Non-persistent	Moderately mobile	3,04

Table 12. Adsorption and degradation properties of the eight herbicides from the PPDB and concentrations used for the 5 ml pulse applied to the top of the columns. K_f is the Freundlich adsorption coefficient, n is the exponent from the Freundlich equation and DT_{50} is the half-life of the pesticide.

Herbicide	Formulation	K_f (l/kg)	1/n (β)	DT_{50} in field (days)	Recommended field application (g/ha)	Concentration of the solution applied on soil columns (mg/l)
Bentazone	Basagran SG	0.97	0.93	7.5	960 (peas)	92,7-109,6
Chlorotoluron	Chlorotoluron 500 SC	1.3	0.877	12.5	1500 (wheat)	141,1-156,2
Metamitron	Goltix 700 SC	1.09	0.81	11.1	3500 (sugar beet)	354,4-373,0
Metazachlor	Butisan S	1.02	0.993	6.8	750 (rapeseed)	57,6-84,7
S-Metolachlor	Dual Gold	0.93	0.888	21	1248 (sugar beet)	148,3-149,0
Terbuthylazine	Andes	5.1	0.93	21.8	750 (maize)	85,7-95,5
Flufenacet	Andes	4.38	0.92	39	450 (maize)	40,8-46,1
Ethofumesate	Ethomat 500	1.74	0.91	37.8	1000 (sugar beet)	65,8-125,9

4.4. Leaching experiment

An initial solution of 1L of pesticides was prepared. The concentration of pesticides in the solution was calculated to meet the maximum recommended doses per hectare (Table 12). Since bentazone is in granular form, it is added first to the 1L flask already two-thirds filled with deionized water. The other pesticides, in the form of a suspension concentrate, are added next using graduated pipettes. This order is recommended to limit the incompatibility of pesticides during mixing and to optimise the dissolution (BASF, 2017). A sample of this initial 1L pesticide mixture is analysed to quantify the exact pesticide concentrations. The solution is stored at 4°C and protected from light.

A 5 mL (0,9 mm) pesticide pulse is then applied to the column using a graduated pipette. The pulse is added drop by drop manually avoiding the outer circle of the column to avoid preferential flows. Then, 5 mL of rinse is added in the same way (Köhne et al., 2006; Van Beinum et al., 2006). The 5 ml of pulse and rinse together represent 1.8 mm of rain, which corresponds to a continuous light rain for 1 hour. The top of the column is sealed with plastic film to limit evaporation. The column was then left to stand for 24 hours. The leaching experiment was conducted under unsaturated conditions to simulate the situation in the vadose zone and under transient flow to imitate rain events. Water was added above the column at regular intervals.

The first three additions of water were of 200 mL (36 mm) each. The next additions were 400 mL (72 mm) unless there was still water at the top of the column. The chosen water inputs to the columns represent possible intense rainfall for the area under study. During intense rainfall, between 30 and 80 mm can be expected to drop (IRM, 2020). The two volumes applied to the columns correspond to a heavy rainfall of 2 mm/minute lasting 20 and 40 minutes respectively. In this case, the amount of water added depended on the amount of water still present. Eluted water samples were taken before each water application to the columns. The last samples were combined to create composite samples and to obtain the end of the breakthrough curve.

The duration of the experiment from the pulse to the last collected sample was the same for all columns, i.e. 57 days. This duration was chosen to obtain breakthrough curves in their descending part for all the pesticides and to model them more accurately. At the end of the 57-day experiment, the columns were directly disassembled and the soil was homogenized. Soil samples from each column were taken for the analysis of the residual pesticide concentrations (figure 43). The percentages of pesticides eluted in the leachates (recovered) and adsorbed within the columns, in relation to the quantity applied above the column, were calculated. The mass balance is then calculated to determine the quantity of pesticide degraded by subtracting the quantity recovered and adsorbed from the amount applied to the column. However, it should be noted that with this methodology, the non-extractable fraction of pesticide residues can be included in the degraded fraction of the mass balance.

Figure 43. Disassembly of the soil columns and homogenisation before taking samples for analysis.

4.5. Pesticide concentration measurement

The initial mixture of pesticides was analysed using UPLC-DAD (Ultra-Performance Liquid Chromatography coupled with a Diode Array Detector by Waters Acquity H class, USA). The column was an Acquity BEH (Bridged Ethylene Hybrid) C18 (50 mm x 2.1 mm (id) x 1.7 µm) with a flow rate of 0.8 mL/min. 1µL of sample was injected. Mobile phase A was H_2O with 0.1% formic acid and mobile phase B was acetonitrile. The gradient goes from 90% aqueous phase to 100% organic phase in 8 min, stays in 90% organic phase for 1 min and goes back to 90% aqueous phase for 1 min for system conditioning between injections.

After sampling at the bottom of the columns, water samples were stored at 4°C in amber glass bottles. These samples were analysed within 7 days of collection. 2 mL of acetonitrile was added to 10 mL of sample, shaken manually and then centrifuged at 4800 rcf (relative centrifugal force) for 10 min at 4°C before filtration through a 0.2µm PTFE (polytetrafluoroethylene) filter. 10µL was injected.

Water samples were analysed by liquid chromatography (Nexera X2™Shimadzu, USA) coupled to a Time-of-Flight Mass Spectrometer (Q-TOF) (X500R ABSciex, Singapore). The column used was a Waters Acquity UPLC™ HSS (High Strength Silica) T3 (100 mm x 2.1 mm i.d., 1.8 µm particle size) maintained at 40°C with a mobile phase gradient (0.3 mL/min) consisting of: MilliQ water/methanol (90/10) and 2mM ammonium formate acidified with 0.1% formic acid in lane A and methanol acidified with 0.1% formic acid in lane B. The gradient goes from 95% aqueous phase to 100% organic phase in 11 min, stays in 100% organic phase for 4 min and goes back to 95% aqueous phase in 0.5 min, then stays for 7 min for system conditioning between injections.

Soil samples were thawed and sieved 2 mm to homogenise and remove plant fragments, stones, etc. A 5 g sub-sample was then extracted using the QuEChERS method (Quick, Easy, Cheap, Effective, Rugged, and Safe) as follows: 5 mL of water was added, the sample was shaken and allowed to macerate for 30 min, then 10 mL of acidified acetonitrile (2% formic acid) was added, the sample was shaken again and allowed to macerate for 30 min. A bag of QuEChERS salts (4 g MgSO4, 1 g NaCl, 0.5 g sodium hydrogen citrate sesquihydrate, 1 g sodium citrate dihydrate) (Agilent, USA) was added and the sample was vortexed for 1 min at 20 Hz (Retch, MM400). After centrifugation at 4800 rcf for 15 min at 4°C, the supernatant was filtered through a 0.2 µm PTFE filter and transferred to a glass vial. 5 µL was injected. Soil samples were analysed using the same analytical method as water samples, except for the elution gradient. It goes from 95% aqueous phase to 100% organic phase in 8 min, stays in 100% organic phase for 3 min, goes back to 95% aqueous phase in 0.5 min and stays in this composition for 7 min for system conditioning between injections.

The acquisition of results was performed in TOF-MS (Time of Flight Mass Spectrometry) mode in electrospray positive ionisation mode (ESI+) except for bentazone which was acquired in high resolution multi reaction monitoring mode (MRMhr) in negative ionisation mode (ESI-). For quantification in water solution samples, a calibration curve was established using MilliQ water +20% acetonitrile after ensuring that there was no matrix effect. Soil quantification was performed using a matrix-matched calibration curve with a reference material, i.e. biological soil without pesticide residues. For each series of analyses, 3 spiked soil reference materials were extracted according to the protocol described above to verify the extraction efficiency. The spiked concentrations were 10, 1 and 0.2 µg/kg. Stability was checked for each injection sequence and could not exceed 20% for each active ingredient.

The limit of quantification in water and soil is given in Table 13.

Table 13. Limits of quantification (LOQ) of the eight pesticides studied in water in µg/L and in soil in µg/kg.

Pesticides	Water LOQ (µg/L)	Soil LOQ (µg/kg)
Bentazone	0.01	0.15
Chlortoluron	0.02	0.2
Flufenacet	0.01	0.2
Terbuthylazine	0.03	0.2
Metamitron	0.05	0.5
Metazachlor	0.01	0.2
Metolachlor	0.01	0.1
Ethofumesate	0.10	0.2

4.6. Water flow and pesticides transport modelling

All breakthrough curves were modelled using Hydrus 1-D. The hydraulic and transport parameters of the eight pesticides were obtained by inverse modelling. The units of length (L) are cm, the units of mass (M) are grams and the units of time (T) are days.

4.6.1. Inverse modelling

Inverse modelling is used to determine the parameters of interest from data obtained through soil column leaching experiments.

Three statistical indicators were used to assess the performance of the inverse modelling and parameter optimisation: sum of squares (SSQ), root-mean-square error (RMSE) and coefficient of determination (R^2).

Several studies suggest that both water flux data and solute concentration data are needed by models to provide a proper representation of solute transport (Coppola et al., 2009; Kahl et al., 2015; Kondo et al., 2020). A sequential or combined approach can be used, where the hydraulic and transport parameters are estimated successively or simultaneously from the observed water flux and concentration data in the eluates (Šimunek et al., 2002; Imig et al., 2023b; a). The sequential approach is commonly used because it prevents the uncertainty in the hydraulic parameters from propagating into the uncertainty of the solute transport parameters, resulting in a better fit (Abbasi et al., 2003a; Kahl et al., 2015).

4.6.2. Water flow modelling

The flow of transient water within the columns was simulated by two models: (a) single porosity (SP) et (b) dual porosity (DP) (van Genuchten and Wierenga, 1976; Šimůnek et al., 2008a, 2013). In both cases, a modified form of Richard's equation is solved.

Single-porosity model (SP)

For the single porosity model, the soil water retention curve θ(h) is described by the van Genuchten (1980) equation and the hydraulic conductivity function K(h) is described with the statistical pore distribution model of Mualem (1976) with :

$$Se = \frac{\theta - \theta_r}{\theta_s - \theta_r}, \qquad m = 1 - \frac{1}{n} \quad n > 1$$

Where S_e is the effective saturation (-), θ is the soil water content (L^3/L^3), θ_r and θ_s are the residual and saturation water contents (L^3/L^3) respectively and n and m are hydraulic parameters (-).

The five independent soil hydraulic parameters were first estimated using neural network based pedotransfer functions developed by Schaap et al. (2001) and incorporated in the Rosetta module (Table 14). The granulometry and bulk density of the soil columns (Table 10) were used. θ_s is considered to be the total porosity of the columns. θ_r has only a minor influence on water fluxes because the soil columns retain a quite high water content for the duration of the experiment. In addition, this value is generally kept constant using estimates of pedotransfer functions (Mertens et al., 2009; Sur et al., 2022). Only K_s has been calibrated using the cumulative outflow volumes of the columns. Mertens et al., 2006 showed that saturated hydraulic

conductivity (K_s) was the most sensitive parameter when inverse modelling was performed using eluted water volume data.

Table 14. Initial values of hydraulic parameters determined by the Rosetta module from granulometry and bulk density. The values of θs (third column) correspond to the total porosity of the columns, calculated from bulk density and organic matter content.

	θ_r (cm^3/cm^3)	θ_s (cm^3/cm^3)	α (1/cm)	n (-)	K_s (cm/day)
RH1	0.065 ± 0.001	0.43 ± 0.01	0.0054 ± 0.0001	1.66 ± 0.01	24.6 ± 2.5
RH2	0.061 ± 0.001	0.40 ± 0.00	0.0063 ± 0.0001	1.61 ± 0.01	14.3 ± 0.8
RH3	0.065 ± 0.000	0.39 ± 0.00	0.0068 ± 0.0001	1.56 ± 0.00	5.9 ± 0.2
IH1	0.055 ± 0.000	0.38 ± 0.00	0.0071 ± 0.0001	1.57 ± 0.01	10.6 ± 0.5
VH1	0.065 ± 0.002	0.40 ± 0.01	0.0064 ± 0.0003	1.59 ± 0.02	8.9 ± 1.5

Dual-porosity model (DP)

The dual-porosty approach is used to model water flows as in chapter 3.

For the mobile region, the parameters required for the van Genuchten-Mualem model are $\theta_{r,mo}$, $\theta_{s,mo}$, α and n and K_s. For the immobile region the required parameters are $\theta_{r,im}$, $\theta_{s,im}$ et ω. The parameters α, n and K_s are identical to those used in the SP modelling.

The parameters $\theta_{s,mo}$ and $\theta_{s,im}$ are calculated taking into account a proportion of macropores (mobile region) of 10% of the total porosity. (Kodešová et al., 2005; Šimůnek et al., 2009). $\theta_{r,im}$ is considered equal to θ_r, from the SP model (Imig et al., 2023b). $\theta_{r,mo}$ is set to zero so that residual water is only present in the immobile region (Köhne et al., 2002, 2006; Imig et al., 2023b). The first-order rate coefficient for water transfer ω was set to 0.2 day^{-1} (Köhne et al., 2004). The parameters $\theta_{s,mo}$ and ω were optimised by inverse modelling for each column. Then $\theta_{s,im}$ was calculated according to the total water content equation. The other parameters were kept constant.

4.6.3. Pesticides transport modelling

Only the DP model was used to model pesticide fluxes. The transport of solutes is described by the convection-dispersion equation. The exchange of solutes between the two liquid regions can be modelled as a first order process. Assuming that degradation is only active in the liquid phase, the governing equation is written as follows:

$$\frac{\partial \theta_{mo} c_{mo}}{\partial t} + f_{mo}\rho \frac{\partial s_{mo}}{\partial t} = \frac{\partial}{\partial x}\left(\theta_{mo} D_{mo} \frac{\partial c_{mo}}{\partial x}\right) - \frac{\partial q_{mo} c_{mo}}{\partial x} - \mu \theta_{mo} c_{mo} - \Gamma_s$$

$$\frac{\partial \theta_{im} c_{im}}{\partial t} + (1 - f_{mo})\rho \frac{\partial s_{im}}{\partial t} = \Gamma_s - \mu \vartheta_{im} c_{im}$$

$$\Gamma_s = \omega_s (c_{mo} - c_{im}) + \Gamma_w c^*$$

In witch, c_{mo} and c_{im} are the solute liquid concentrations of the mobile and immobile regions (ML-3), s_{mo} and s_{im} are the sorbed concentrations of the mobile and immobile regions(-), D_{mo} is the dispersion coefficient in the mobile region, taking into account molecular diffusion and hydrodynamic dispersion (L^2/T), q_{mo} is the volumetric flux density in the mobile region (L/T), f_{mo} is the fraction of sorption sites in contact with the mobile region (-), Γ_s is the solute transfer rate between the two regions (M/L^3T) and μ (1/T) is the first order degradation rate coefficient in the liquid phase. ω_s is the first order chemical mass transfer coefficient (1/T) and c* is the solute concentration (M/L^3) of the mobile region c_{mo} for $\Gamma_w>0$ and of the immobile region c_{im} for $\Gamma_w<0$ (Šimůnek and Genuchten, 2008).

Chemical equilibrium with Freundlich sorption isotherms are used for both regions:

$$s_{mo} = K_f c_{mo}^{\beta}$$
$$s_{im} = K_f c_{im}^{\beta}$$

With K_f the Freundlich adsorption isotherm coefficient (L^3/M) and β the Freundlich exponent 1/n (-).

The dispersion coefficient of the mobile zone D_{mo} can be described as:

$$D_{mo} = D_0 \frac{\vartheta_{mo}^{\frac{7}{3}}}{\vartheta_{s,mo}^2} + \lambda_{mo} \nu$$

Where D_0 is the molecular diffusion coefficient in free water (L^2/T), λ_{mo} is the longitudinal dispersivity in the mobile region (L) and ν is the pore water velocity (L/T). In general, the molecular diffusion coefficient is considered negligible due to its small contribution to the dispersion (Šimůnek et al., 2009). Indeed, the molecular diffusion coefficient is generally of the order of 5% of the hydrodynamic dispersion coefficient (Vanderborght and Vereecken, 2007).

The dispersivity λ, the degradation rate coefficient μ, the Freundlich adsorption coefficient K_f, the Freundlich coefficient β and the first order chemical mass transfer coefficient ω_s are required. The initial value of the transfer coefficient ω_s has been set to 0.02 day^{-1} (Šimůnek et al., 2009).

For λ, μ, Kf and β, the optimisation was performed from three initial values. In fact, local algorithms such as Levenberg-Marquardt will find a local optimum from the initial parameters entered into the model. Thus, the optimised parameters will depend on the initial values (Dubus et al., 2004). Therefore, the mean values obtained from the optimisation using three initial parameter values will be more robust. For the dispersivity, initial values of 1, 3 and 6 cm were used. This parameter was only estimated for bentazone and then kept constant for the other pesticides. This is because bentazone shows very low adsorption and can be assimilated to a tracer as observed by De Wilde et al. (2009). There are several types of tracer, with different adsorption and degradation characteristics, each suitable for different purposes.

For the eight pesticides, the initial values of μ, K_f and β were taken from the peer review of the pesticide risk assessment provided by the European Food Safety Authority (EFSA). EFSA provides conclusions to these peer reviews at the request of the European Commission. The K_f, β and half-life DT_{50} (T) values of the studies considered in the peer review, together with the corresponding country and soil type, are given in the annex 1. The Walloon Agronomical Research Centre (CRA-W) has compiled from EFSA, the values measured in the same climatic zone and for silty soils such as those found in Wallonia, Belgium. The minimum, mean and maximum values of the selected data were used as initial pesticide values for the different parameters (Table 15). The field DT_{50} were transformed into the degradation rate coefficient μ using the equation: $\mu = \ln(2)/DT_{50}$. The parameters K_f, β and μ were optimised with the three sets of input values for the fifteen columns and eight pesticides.

Table 15. Initial values of the transport parameters of the pesticides obtained from the EFSA peer reviews. The initial values are chosen as the minimum, mean and maximum of the values retained by the CRA-W for the Walloon soil-climate zone.

	K_f (cm^3/g)			β (-)			Field DT_{50} (days)		
	Min	**Mean**	**Max**	**Min**	**Mean**	**Max**	**Min**	**Mean**	**Max**
Bentazone	0.08	0.76	1.94	0.70	0.97	1,00	3.0	4.7	6.9
Metamitron	0.56	3.06	4.65	0.65	0.77	0.85	6.6	11.1	21.7
Metazachlor	0.48	2.75	3.50	0.82	0.84	0.85	5.1	8.50	14.4
S-Metolachlor	0.59	5.33	4.80	0.91	0.93	0.93	3.6	22.4	55.7
Ethofumesate	0.70	2.95	6.20	0.82	0.90	0.96	13.1	40.8	110.0
Flufenacet	1.00	5.05	14.7	0.84	0.87	0.98	13.1	27.7	54.2
Terbuthylazine	2.10	5.78	10.5	0.88	0.90	0.98	6.9	19.5	35.7
Chlorotoluron	2.70	4.52	9.60	0.82	0.87	0.93	26.0	42.0	42.0

4.6.4. Boundary conditions

For the numerical modelling with Hydrus 1-D, 30 cm columns were represented as 1D domains and discretised into 101 nodes with equal spacing of 0.3 cm. For the water flow boundary conditions, the top of the columns was set to an atmospheric boundary condition with a surface water layer to allow for water build-up during time variable boundary conditions of water addition (precipitation). At the bottom of the column, the boundary condition was set to a constant pressure head due to the vacuum pump. An initial pressure head of -510 cm was applied at the bottom of the column by the pump. The initial head at the top of the column was determined for each column as the pressure at field capacity, the columns having been saturated and drained for 24 hours prior to the start of the experiment. For the solute transport, a boundary condition flux concentration was chosen for the top of the columns. This corresponds to the pesticide pulse at the beginning of the experiment. The lower boundary condition of the columns was set to zero concentration gradient.

4.7. Data treatment and statistical analysis

Breakthrough curves were constructed by plotting the relative concentrations (C/C0) measured in the leachates against the cumulative relative pore volume (V/V0). The concentrations of pesticides found in the eluates (C) are divided by the concentrations of the pesticide pulse initially applied to the columns (C0) to obtain the relative concentrations. Based on the porosity of each column, the total pore volume (V0) was determined from the volume of the soil column. The volume of water for each sample (V) is then divided by the total pore volume (V0) to obtain the relative pore volume. This type of data allows different columns with different porosities, soil volumes and pesticides pulse concentrations to be compared. Data were processed using Rstudio v2023.12.0. The figures were plotted with ggplot2 package. The Tmin, Cpeak and Tpeak indicators were determined as the relative pore volume at the first appearance of the pesticide in the eluates, the maximum relative concentration and the relative pore volume after which it was reached, for each pesticide and column.

Analyses of variance (ANOVA) were performed to examine differences in parameters between pesticides, depths and agricultural practices over time. ANOVA tests are used to identify differences between the means of more than two groups and to establish whether these differences are due to chance or whether they reflect a meaningful difference. This test assumes that the data are normal and that the variances are equal between the groups. Normality was tested using Shapiro-Wilk and equality of variances using Levene's test. All assumptions were satisfied. ANOVA tests are regularly used to compare several factors between different soil depths and agricultural practices (de Paul Obade and Lal, 2014; Alavaisha et al., 2019; Leul et al., 2023). Fisher's Least Significant Difference method was used to compare means with the null hypothesis of equality of means and a significance level of 0.05.

5. Results

5.1. Breakthrough curves analysis

Figure 44 displays the measured and modelled breakthrough curves (BTCs) of the eight pesticides for the three agricultural systems (RH1, IH1 and VH1) and the three soil horizons (RH1, RH2, RH3). BTCs are plotted as the measured relative concentration (C/C0) versus the number of pore volume eluted (V/V0). The points correspond to the measured data and the lines to the modelled data.

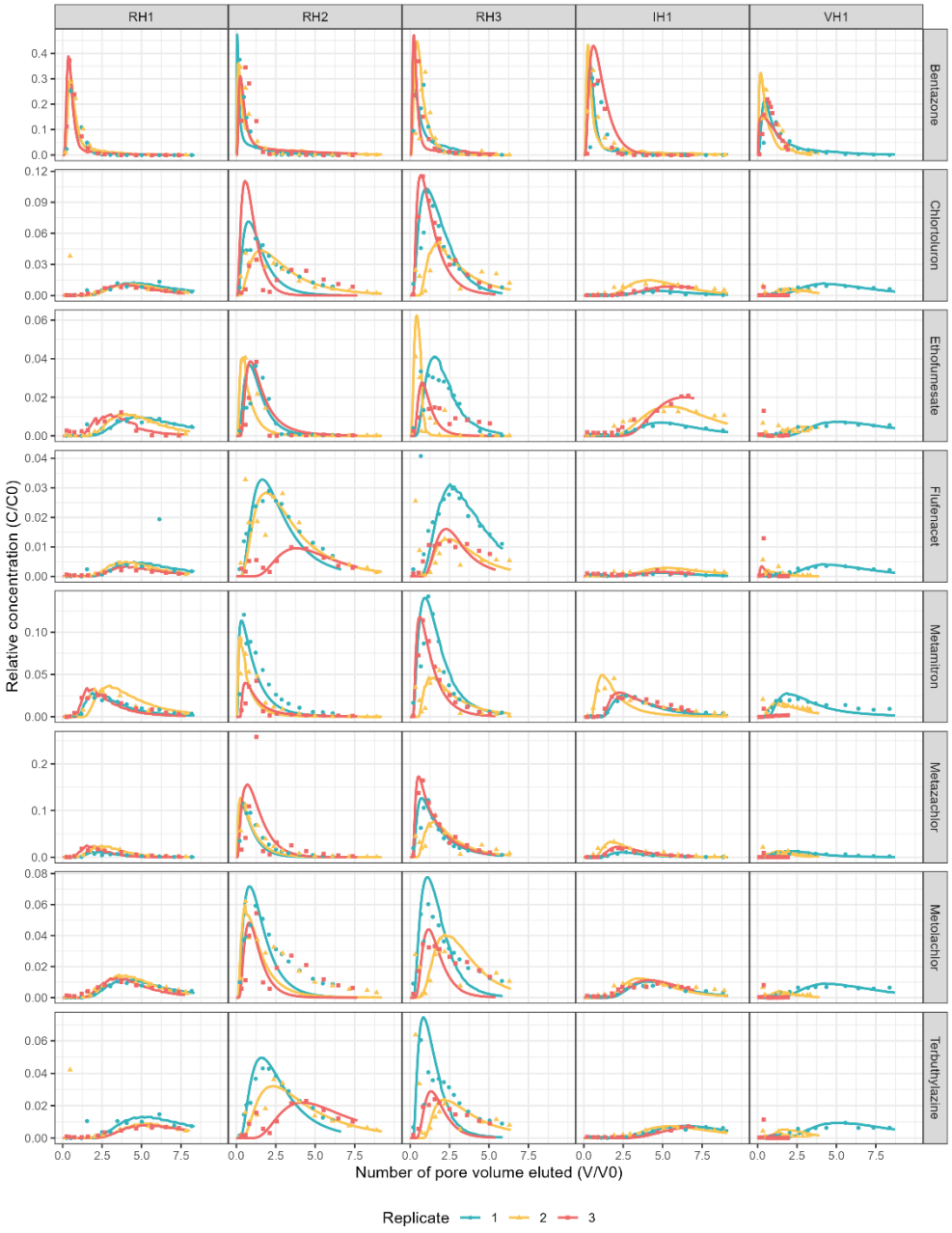

Figure 44. Measured and modelled breakthrough curves depicting the relative concentration (C/C0) as a function of the number of pore volume eluted (V/V0) for the eight herbicides, the three agricultural systems and the three horizons. The three spatial replicates are plotted. The points correspond to the measured data and the lines to the modelled data.

5.2. Breakthrough curves indicators

The arrival times of the first breakthrough Tmin, the arrival time of the maximal peak concentration Tpeak and the relative maximum concentrations of the peak Cpeak for the eight pesticides, the three production systems and the three depths are given in Table 16.

Table 16. Tmin in pore volume, Tpeak in pore volume and Cpeak for the eight pesticides, the three production systems and the three depths. Values correspond to the mean of the three spatial replicates with standard deviation.

Pesticide	Column	Tmin [-]			Tpeak [-]			Cpeak [-]		
Bentazone	RH1	0,03	±	0,01	0,45	±	0,06	0,318	±	0,052
	RH2	0,01	±	0,00	0,15	±	0,08	0,381	±	0,068
	RH3	0,01	±	0,00	0,32	±	0,08	0,391	±	0,096
	VH1	0,01	±	0,00	0,31	±	0,11	0,229	±	0,071
	IH1	0,02	±	0,00	0,42	±	0,14	0,410	±	0,029
Chlorotoluron	RH1	0,96	±	0,16	4,22	±	0,22	0,011	±	0,001
	RH2	0,06	±	0,04	0,95	±	0,42	0,075	±	0,028
	RH3	0,26	±	0,20	1,10	±	0,37	0,089	±	0,029
	VH1	0,38	±	0,16	3,09	±	1,17	0,009	±	0,003
	IH1	0,97	±	0,18	4,76	±	0,60	0,009	±	0,004
Ethofumesate	RH1	1,00	±	0,21	3,88	±	0,61	0,011	±	0,001
	RH2	0,11	±	0,08	0,71	±	0,21	0,039	±	0,002
	RH3	0,15	±	0,09	0,92	±	0,48	0,044	±	0,014
	VH1	1,21	±	0,06	3,93	±	0,97	0,006	±	0,001
	IH1	1,37	±	0,43	5,53	±	0,63	0,014	±	0,005
Flufenacet	RH1	1,29	±	0,07	4,22	±	0,22	0,004	±	0,001
	RH2	0,35	±	0,26	2,44	±	0,97	0,024	±	0,010
	RH3	0,55	±	0,11	2,35	±	0,14	0,020	±	0,008
	VH1	0,37	±	0,36	1,72	±	1,81	0,003	±	0,001
	IH1	1,12	±	0,11	4,99	±	0,22	0,002	±	0,001
Metamitron	RH1	0,90	±	0,20	2,14	±	0,63	0,033	±	0,004
	RH2	0,11	±	0,09	0,37	±	0,13	0,083	±	0,031
	RH3	0,26	±	0,15	0,92	±	0,24	0,102	±	0,040
	VH1	0,50	±	0,10	1,63	±	0,23	0,016	±	0,011
	IH1	0,86	±	0,30	2,01	±	0,59	0,035	±	0,011
Metazachlor	RH1	0,45	±	0,17	2,14	±	0,43	0,020	±	0,006
	RH2	0,02	±	0,00	0,44	±	0,18	0,132	±	0,018
	RH3	0,20	±	0,11	0,94	±	0,44	0,125	±	0,040
	VH1	0,37	±	0,13	1,64	±	0,26	0,013	±	0,000
	IH1	0,65	±	0,12	2,10	±	0,28	0,022	±	0,009
S-Metolachlor	RH1	0,85	±	0,07	3,70	±	0,21	0,013	±	0,001
	RH2	0,06	±	0,02	0,73	±	0,13	0,060	±	0,010
	RH3	0,25	±	0,10	1,49	±	0,51	0,054	±	0,017
	VH1	0,43	±	0,26	2,88	±	1,38	0,007	±	0,003
	IH1	0,88	±	0,10	3,87	±	0,35	0,011	±	0,001
Terbuthylazine	RH1	1,22	±	0,12	5,42	±	0,26	0,010	±	0,002
	RH2	0,32	±	0,24	2,70	±	1,10	0,035	±	0,011
	RH3	0,40	±	0,28	1,46	±	0,57	0,042	±	0,023
	VH1	0,51	±	0,40	2,55	±	1,69	0,006	±	0,003
	IH1	1,60	±	0,13	6,26	±	0,64	0,007	±	0,000

Pesticide breakthrough curves show varied patterns between pesticides, cropping systems and depths. All pesticides are found faster in the leachates with a significantly lower time of the first breakthrough (Tmin) for horizons 2 and 3 (RH2 and RH3) than for horizon 1 (RH1), where they are more retained. Bentazone, S-metolachlor, flufenacet and terbuthylazine were eluted faster in the vegan system (VH1) with a lower Tmin than in the reference system (RH1) and in the ICLS system (IH1). For the others, no significant difference was found between the cropping systems. The peak appeared later in the topsoil, with a significantly higher arrival time of the maximal peak concentration Tpeak for RH1 than for the deeper horizons RH2 and RH3, indicating greater retention of pesticides in the surface. For the three cropping systems, Tpeak was significantly higher for RH1 and IH1 than for VH1 for chlorotoluron, flufenacet and terbuthylazine. Ethofumesate was the exception, with a higher Tpeak for IH1 than for RH1 and VH1. No significant difference was found for the others. For all pesticides except bentazone, where no difference was observed, the maximal concentration of the peak (Cpeak) was significantly higher for RH2 and RH3 than for RH1. No significant difference in Cpeak was observed between the systems, except for bentazone, where Cpeak of IH1 was higher than that of VH1.

Bentazone is the most rapidly displaced pesticide in all columns and therefore the first compound to appear in the leachates. Its Tmin and Tpeak are lower and its Cpeak greater than those of the other pesticides. These differences are significant for RH1 and IH1 for Tmin and Tpeak and for all columns for Cpeak. Tmin was between 0.01 and 0.03 and Tpeak between 0.15 and 0.45. This means that the peak is reached after less than 0.5 pore volumes eluted, indicating non-equilibrium transport. The bentazone BTCs are strongly skewed to the left with a long tail, indicating a high degree of preferential flow within the columns. Small differences in the degree of preferential flow were observed between the production systems. However, the Cpeak of IH1 (0.410±0.029) is significantly higher than that of VH1 (0.229±0.071) for a lower of Tpeak. Between horizons, Tpeak is significantly lower for RH2 than for RH1, confirming a greater degree of preferential flow within horizon 2. After bentazone, metazachlor and metamitron generally appeared in the leachates before the other pesticides. They have a lower Tpeak and a higher Cpeak, indicating a low retention within the columns. However, these two pesticides are delayed compared to bentazone. In general, no significant differences in Tpeak and Cpeak are observed between these two pesticides, showing a similar leaching pattern. Their peaks occur after 0.44-2.14 and 0.37-2.14 pore volume for metazachlor and metamitron, respectively, for Cpeak between 0.020-0.132 and 0.016-0.102. In contrast, terbuthylazine and flufenacet are the most strongly retained within the columns. Tpeak ranged from 1.46-6.26 and 1.72-4.99 pore volume, with Cpeak values of 0.006-0.042 and 0.002-0.024 for terbuthylazine and flufenacet, respectively. Their BTCs are wider and flatter than for the other pesticides, with higher Tpeak and lower Cpeak for the majority of columns.

5.3. Pesticides mass balance

Figure 45 shows the pesticide mass balances with measured data on the percentages recovered from the leachates and remaining adsorbed in the columns, as well as the resulting degraded percentages. The behaviour of pesticides in terms of elution, adsorption and degradation varies considerably depending on the pesticide, cropping system and horizons.

The recovery rate of pesticides in the leachates was higher for RH2 and RH3 than for RH1, except for bentazone, metamitron and ethofumesate, which showed no difference. The amounts of pesticides recovered in the leachates were similar between the three cropping systems for all pesticides. Recovery rates varied considerably between pesticides. For bentazone, higher amounts were recovered than for the other pesticides in the three cropping systems, ranging from 73.4 to 81.3% of the applied amount. The second highest amount recovered in the leachates is that of metamitron, ranging from 15.5 to 33.1%. There was no significant difference between the other pesticides, which were all below 20% recovery. The pesticide with the lowest recovery from the topsoil was flufenacet for all three cropping systems, with recoveries ranging from 2.5 to 7.2%.

For RH2 and RH3, bentazone and metazachlor had a significantly higher recovery rate than the others, with 77.13-81.16% and 59.8-64.3% of the initial applied amount, respectively. The two pesticides with the lowest recoveries were flufenacet, as in the topsoil, with between 20.1 and 27.0%, and ethofumesate in last place, with between 12.6 and 16.7%.

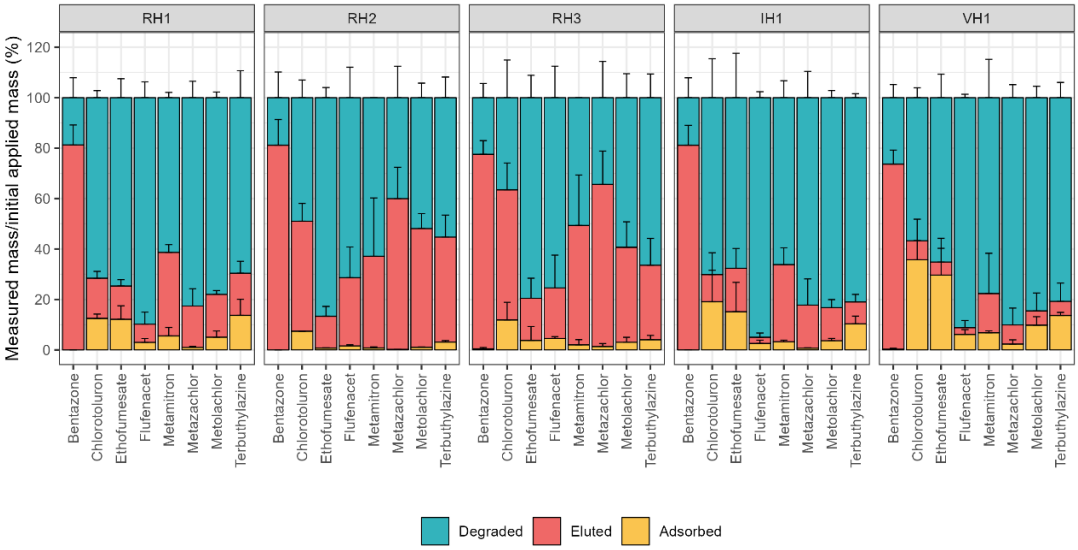

Figure 45. Pesticide mass balances with the percentage recovered in the leachates, degraded and adsorbed within the columns for the eight pesticides, the three cropping systems and the three horizons. The error bars represent the standard deviation.

For metazachlor, S-metolachlor, flufenacet, chlorotoluron and terbuthylazine, a significantly higher amount of pesticides was degraded in RH1 than in RH2 and RH3. Degradation was similar between horizons for the other pesticides and also between cropping systems for all pesticides. Within the topsoil, flufenacet and metazachlor were the most degraded pesticides with between 89.8-95.0 and 82.2-87.6% respectively. Bentazone had a significantly lower degradation percentage than the other pesticides, ranging between 18.1 and 26.7%. Metamitron was the second least degraded pesticide, ranging from 61.3 to 77.6%, but was not significantly different from the more degraded pesticides. The pesticides showed different degradation behaviour in the deeper horizons compared to the topsoil horizon. For RH2 and RH3, ethofumesate and flufenacet are significantly more degraded than the other pesticides with values between 79.5-86.7 and 71.4-75.4% respectively. The two least degraded pesticides are metazachlor and bentazone with between 34.4-40.0 and 18.8-22.5% respectively, with no significant difference between the two. Thus, except for bentazone, metazachlor changed from the most degraded pesticide in horizon 1 to the least degraded pesticide in horizons 2 and 3. The opposite trend is observed for ethofumesate, which goes from being one of the least degraded pesticides in horizon 1 to the most degraded in horizons 2 and 3.

The pesticide adsorption percentages for the different cropping systems and horizons exhibit greater variability. Except for bentazone, metazachlor and terbuthylazine, the pesticides show higher adsorption in VH1 than in RH1 and IH1. For RH1 and IH1, the most adsorbed pesticides were chlorotoluron, ethofumesate and terbuthylazine with 12.5-19.11%, 12.1-15.4% and 10.3-13.7% respectively. For VH1, only chlorotoluron and ethofumesate differed significantly from the other pesticides with 31.6 and 29.7% adsorption. The two least adsorbed pesticides, which did not differ significantly from each other or from the cropping systems, were bentazone and metazachlor with 0.0-0.3 and 3.4-6.8%, respectively. For metamitron, S-metolachlor and terbuthylazine, a higher percentage of adsorption was measured in RH1 than in RH2 and RH3. For metazachlor and flufenacet, greater adsorption was measured at 60-90 cm depth (RH3) than at 30-60 cm (RH2). Finally, bentazone, chlorotoluron and ethofumesate showed no significant differences in adsorption between the three horizons. Within RH2 and RH3, chlorotoluron was significantly more adsorbed than the other pesticides, ranging from 7.4 to 11.9%. Terbuthylazine and flufenacet followed with 3.1-4.0 and 1.6-4.6% respectively. However, their adsorption percentage was significantly higher than the other pesticides only for RH2. Finally, bentazone and metazachlor were also the least adsorbed pesticides with between 0.0-0.4 and 0.2-1.3%, respectively.

5.4. Inverse modelling parameters

5.4.1. Soil hydraulics parameters

The hydraulic parameters obtained by inverse modelling of the cumulative outflows on Hydrus 1-D for all columns are given in Table 17.

Table 17. Soil hydraulics parameters obtained by inverse modelling of cumulative outflow for the eight pesticides, the three cropping systems and the three depths. Values correspond to the mean value of the three spatial replicates with the standard deviation.

[a]parameter determined by equilibrium modelling, [b]parameters determined by DP modelling and c parameters calculated from the estimated parameters.

	$\theta_{s,mo}$[b] (cm^3/cm^3)	$\theta_{s,im}$[c] (cm^3/cm^3)	Proportion of the mobile zone[c] (%)	K_s[a] (cm/day)	ω[b] (1/day)	R^2 (-)	RMSE (cm)
RH1	0.036 ± 0.007	0.43 ± 0.01	7.8 ± 1.5	3.33 ± 0.14	0.26 ± 0.04	1.00 ± 0.00	0.02 ± 0.00
RH2	0.039 ± 0.009	0.38 ± 0.01	9.5 ± 2.1	0.89 ± 0.15	0.22 ± 0.01	1.00 ± 0.00	0.02 ± 0.01
RH3	0.028 ± 0.007	0.35 ± 0.01	7.4 ± 2.0	0.94 ± 0.21	0.17 ± 0.02	0.99 ± 0.00	0.03 ± 0.00
IH1	0.038 ± 0.003	0.34 ± 0.01	10 ± 0.8	0.94 ± 0.18	0.20 ± 0.00	1.00 ± 0.00	0.02 ± 0.00
VH1	0.035 ± 0.003	0.36 ± 0.01	8.8 ± 0.9	0.69 ± 0.46	0.20 ± 0.00	0.98 ± 0.01	0.05 ± 0.02

Good agreement was achieved between observed and predicted cumulative outflow. The R^2 is between 0.98-1.00 and the RMSE between 0.02-0.05 cm of water for all columns. The VH1 columns showed a weaker fit due to the third replicate. In fact, unlike the other two, water did not flow properly and remained stagnant on the column surface. The K_s for this column is only 0.20 cm/day for a total water outflow of 23.73 cm.

Total cumulative outflow was significantly higher for columns RH1 and IH1 with 107.8 ± 3.5 cm and 91.4 ± 15.1 cm respectively than for VH1 with 54.0 ± 37.2 cm. The cumulative outflow was also higher for RH1 than for RH3 with 64.8 ± 6.86 cm. The K_s was significantly higher for RH1 than for the other column types. Thus, in the other production systems with maize (IH1) and camelina (VH1), as well as in the deeper horizons (RH2 and RH3), water infiltration is slower at saturation. The percentage of mobile zone shows no significant differences. Significant differences were observed between the bulk densities (BD) of the columns. IH1 has the highest BD, followed by VH1 and finally RH1. At horizon level, the BDs were ranked with depth, with RH3, then RH2 and finally RH1.

5.4.2. Pesticides transport parameters

Transport parameters for the eight pesticides obtained by inverse modelling leachate concentrations are presented in Table 18. The BTCs for the eight pesticides are well described by the DP modelling, as shown by the high R^2 values, above 0.7 for most of the columns. The VH1 columns showed slightly lower R^2 values. The third replicate could only be modelled for bentazone and metamitron. For the other pesticides, no acceptable fit was obtained due to very poor water flows within this column, leading to erratic BTCs.

The dispersivity (λ) was estimated for bentazone because of its behaviour as a tracer with very low adsorption. The values were then kept constant for the other pesticides. Columns VH1 showed significantly greater dispersivity than columns IH1 and RH1, which remained close to the initial value of 3 cm. For the three horizons, a greater dispersivity was obtained for the columns from horizon 2, RH2, than for those from horizons 1 and 3 (RH1 and RH3).

The pesticide transport parameters, the Freundlich adsorption coefficient K_f, the first order degradation rate coefficient μ or the half-life DT_{50} and the first order chemical mass transfer coefficient ω_s were highly variable between columns for each pesticide.

For the horizons, the K_f of horizon 1 was always significantly higher than those of horizons 2 and/or 3 for all pesticides. For most pesticides, no significant difference was observed between the K_f for the different cropping systems. However, there were two exceptions. For metazachlor, a significantly higher K_f was obtained for RH1 columns than for IH1. In addition, for flufenacet, a higher K_f was determined for IH1

than for VH1. Between pesticides, similar trends were observed for the three cropping systems. The highest K_f values were reached for terbuthylazine with 1.48-2.25 cm^3/g, chlorotoluron with 1.57-1.88 cm^3/g and S-metolachlor with 1.44-1.71 cm^3/g. In contrast, the pesticides with the lowest K_f were bentazone with 0.17-0.22, metazachlor with 0.29-0.54 and metamiton with 0.83-1.15 cm^3/g. For RH2, terbuthylazine and flufenacet have the highest K_f of 1.17 and 1.07 g/cm^3. For RH3, the K_f of flufenacet and S-metolachlor were higher than the other pesticides with 0.77 and 0.55 cm^3/g, respectively. Bentazone remained last for RH2 and RH3 with 0.10 and 0.15 cm^3/g respectively.

Regarding the DT_{50} half-life of the pesticides, the DT_{50} of RH1 is higher than that of RH2 and/or RH3, except for metazachlor, S-metolachlor and ethofumesate. No significant differences were observed between the cropping systems for any of the pesticides. Bentazone is the only pesticide that differs significantly from the others for all columns. Its half-life was significantly higher than the other pesticides, ranging from 18.2-48.2 days for the three cropping systems in horizon 1 (RH1, IH1 and VH1), 68.6 days for RH2 and 20.8 days for RH3. However, similar trends were found between the columns. The highest DT_{50}, except for bentazone, were obtained for metamitron and terbuthylazine in all three cropping systems with 1.6-2.1 and 1.1-1.6 days respectively. Flufenacet had the lowest DT_{50} with 0.5-0.8 days. For RH2 and RH3, metazachlor had the second highest DT_{50} (6.2 and 10.6 days). Ethofumesate and flufenacet had the lowest DT_{50} with 1.4-1.5 and 2.0-2.2 days respectively.

Finally, the mass transfer coefficient ω_s shows no difference between cropping systems for the majority of the pesticides. For metazachlor, S-metolachlor and ethofumesate, a higher ω_s was obtained for columns RH1 than IH1 and/or VH1. The ω_s between horizons was similar for bentazone, metamitron and flufenacet. For the other pesticides, a higher ω_s was obtained in horizon 1 than in the other two.

Table 18. Fitted pesticide transport parameters determined by inverse modelling of leachate concentrations on Hydrus 1-D for the eight pesticides, the three cropping systems and the three horizons. Values correspond to the mean value of the three spatial replicates with the standard deviation.

Pesticide	Column	λ_{mo} [cm]	μ [1/day]	K_f [cm³/g]	β [-]	ω_s [cm³/g]	R^2 [-]	RMSE [mg/cm³]
Bentazone	RH1	2.87 ± 0.21	0.04 ± 0.02	0.22 ± 0.02	1.00 ± 0.00	0.01 ± 0.01	0.98 ± 0.01	0.04 ± 0.00
	RH2	7.02 ± 2.23	0.02 ± 0.02	0.10 ± 0.06	1.00 ± 0.00	0.02 ± 0.00	0.95 ± 0.02	0.07 ± 0.03
	RH3	4.16 ± 1.15	0.07 ± 0.06	0.15 ± 0.03	1.00 ± 0.00	0.02 ± 0.01	0.90 ± 0.06	0.09 ± 0.02
	IH1	3.00 ± 0.63	0.06 ± 0.06	0.17 ± 0.06	1.00 ± 0.00	0.03 ± 0.03	0.93 ± 0.04	0.11 ± 0.05
	VH1	5.92 ± 1.00	0.01 ± 0.00	0.17 ± 0.03	1.00 ± 0.00	0.02 ± 0.01	0.94 ± 0.01	0.09 ± 0.04
Chlorotoluron	RH1	-	0.50 ± 0.04	1.88 ± 0.08	0.92 ± 0.02	0.57 ± 0.08	0.87 ± 0.08	0.12 ± 0.02
	RH2	-	0.20 ± 0.02	0.50 ± 0.31	0.93 ± 0.03	0.21 ± 0.11	0.76 ± 0.12	0.18 ± 0.06
	RH3	-	0.15 ± 0.08	0.42 ± 0.19	0.82 ± 0.09	0.11 ± 0.02	0.83 ± 0.20	0.13 ± 0.09
	IH1	-	0.63 ± 0.16	1.78 ± 0.54	0.94 ± 0.01	0.57 ± 0.23	0.85 ± 0.07	0.15 ± 0.04
	VH1	-	0.50 ± 0.00	1.57 ± 0.31	0.94 ± 0.01	0.34 ± 0.00	0.68 ± 0.13	0.25 ± 0.08
Ethofumesate	RH1	-	0.48 ± 0.02	1.59 ± 0.36	0.90 ± 0.00	2.04 ± 1.20	0.82 ± 0.10	0.12 ± 0.05
	RH2	-	0.53 ± 0.16	0.36 ± 0.06	0.84 ± 0.05	0.40 ± 0.21	0.83 ± 0.06	0.12 ± 0.03
	RH3	-	0.53 ± 0.18	0.33 ± 0.20	0.89 ± 0.03	0.37 ± 0.14	0.61 ± 0.09	0.25 ± 0.02
	IH1	-	0.49 ± 0.15	1.67 ± 0.32	0.91 ± 0.05	0.34 ± 0.10	0.89 ± 0.06	0.12 ± 0.03
	VH1	-	0.60 ± 0.03	1.29 ± 0.49	0.76 ± 0.09	0.27 ± 0.14	0.56 ± 0.26	0.36 ± 0.21
Flufenacet	RH1	-	0.89 ± 0.06	1.66 ± 0.16	0.89 ± 0.01	0.90 ± 0.15	0.94 ± 0.02	0.11 ± 0.05
	RH2	-	0.33 ± 0.06	1.07 ± 0.26	0.90 ± 0.00	0.61 ± 0.58	0.71 ± 0.08	0.22 ± 0.04
	RH3	-	0.45 ± 0.22	0.77 ± 0.14	0.87 ± 0.03	0.26 ± 0.02	0.66 ± 0.14	0.23 ± 0.07
	IH1	-	1.38 ± 0.17	2.01 ± 0.28	0.95 ± 0.02	0.74 ± 0.34	0.57 ± 0.11	0.30 ± 0.06
	VH1	-	1.13 ±0.01	1.19 ± 0.63	0.89 ± 0.02	0.60 ± 0.16	0.66 ± 0.23	0.19 ± 0.06
Metamitron	RH1	-	0.35 ± 0.07	1.15 ± 0.14	0.75 ± 0.02	0.14 ± 0.05	0.93 ± 0.04	0.08 ± 0.03
	RH2	-	0.29 ± 0.12	0.26 ± 0.05	0.62 ± 0.06	0.16 ± 0.05	0.87 ± 0.09	0.11 ± 0.03
	RH3	-	0.17 ± 0.12	0.44 ± 0.21	0.74 ± 0.04	0.24 ± 0.15	0.83 ± 0.22	0.09 ± 0.08

	IH1	-	0.42 ± 0.11	0.86 ± 0.34	0.67 ± 0.09	0.18 ± 0.04	0.86 ± 0.08	0.13 ± 0.05
	VH1	-	0.43 ± 0.00	0.83 ± 0.03	0.72 ± 0.02	0.12 ± 0.03	0.66 ± 0.09	0.29 ± 0.06
Metazachlor	RH1	-	0.59 ± 0.22	0.94 ± 0.14	0.92 ± 0.05	0.54 ± 0.04	0.88 ± 0.07	0.11 ± 0.04
	RH2	-	0.14 ± 0.05	0.18 ± 0.01	0.87 ± 0.04	0.16 ± 0.05	0.85 ± 0.15	0.10 ± 0.06
	RH3	-	0.28 ± 0.31	0.35 ± 0.16	0.84 ± 0.01	0.03 ± 0.00	0.92 ± 0.09	0.08 ± 0.05
	IH1	-	0.59 ± 0.18	0.64 ± 0.15	0.83 ± 0.01	0.38 ± 0.16	0.91 ± 0.08	0.10 ± 0.04
	VH1	-	0.58 ± 0.16	0.69 ± 0.07	0.84 ± 0.00	0.29 ± 0.05	0.64 ± 0.08	0.23 ± 0.01
S-Metolachlor	RH1	-	0.49 ± 0.01	1.71 ± 0.12	0.92 ± 0.00	0.55 ± 0.07	0.92 ± 0.02	0.11 ± 0.03
	RH2	-	0.33 ± 0.12	0.42 ± 0.01	0.90 ± 0.04	0.18 ± 0.01	0.73 ± 0.09	0.21 ± 0.03
	RH3	-	0.26 ± 0.05	0.55 ± 0.23	0.89 ± 0.01	0.21 ± 0.02	0.73 ± 0.10	0.23 ± 0.08
	IH1	-	0.63 ± 0.11	1.44 ± 0.32	0.92 ± 0.01	0.40 ± 0.09	0.77 ± 0.10	0.18 ± 0.04
	VH1	-	0.67 ± 0.09	1.50 ± 0.43	0.93 ± 0.00	0.40 ± 0.05	0.60 ± 0.20	0.28 ± 0.11
Terbuthylazine	RH1	-	0.45 ± 0.06	2.25 ± 0.11	0.92 ± 0.00	0.59 ± 0.12	0.85 ± 0.14	0.12 ± 0.04
	RH2	-	0.17 ± 0.02	1.17 ± 0.32	0.91 ± 0.01	0.19 ± 0.04	0.77 ± 0.09	0.18 ± 0.04
	RH3	-	0.34 ± 0.04	0.46 ± 0.15	0.81 ± 0.08	0.29 ± 0.09	0.58 ± 0.09	0.29 ± 0.01
	IH1	-	0.61 ± 0.08	2.16 ± 0.68	0.91 ± 0.01	0.45 ± 0.13	0.93 ± 0.04	0.09 ± 0.02
	VH1	-	0.50 ± 0.04	1.48 ± 0.36	0.89 ± 0.01	0.41 ± 0.02	0.48 ± 0.34	0.42 ± 0.27

6. Discussion

6.1. Influence of depths on pesticide leaching

The results revealed that the differences in soil properties and structure between the three horizons resulted in more contrasting leaching behaviour than between the production systems.

Horizon 1 (0-30 cm): Despite a larger amount of outflow water and a higher Ks, greater pesticide retention is observed at the surface. The K_f obtained is systematically higher than for the deeper horizons, as reported in the literature (Felding, 1997; Deng et al., 2017). Pesticide adsorption by organic matter (OM) is the main mechanism of pesticide retention in soils when OM is greater than 2% (Arienzo et al., 1994; Arias-Estévez et al., 2008). The soil in the reference system has 2.5% OM in horizon 1, compared to only 1% and 0.7% for horizons 2 and 3, which explains the high retention of pesticides. Furthermore, horizon 1 is ploughed every year. The cultivation operations create a different structure, changing the properties of the topsoil and the macropores. Consequently, in horizons 2 and 3, a higher percentage of pesticides is recovered from the columns. However, at the end of the experience only three pesticides were significantly more adsorbed at the surface. This may be due to the higher percentage of degradation at the surface for the majority of pesticides with lower DT_{50}. In fact, microbial activity is enhanced in the topsoil, at the root-soil interface, where pesticides are retained for longer, which could explain their rapid degradation (Mills et al., 2001; Rodríguez-Cruz et al., 2006).

Horizon 2 (30-60 cm): The peak of bentazone is reached earlier in horizon 2 than in horizon 1 at similar concentrations. In addition, the percentage of mobile zone (macropores) and the dispersivity are greater in horizon 2 than in the other two horizons, reflecting a greater degree of preferential flow (Koestel et al., 2013). These results can be attributed to the large number of earthworm galleries and root holes encountered during the field investigations. Horizon 2 contains a ploughed sole over a few centimetres and is undisturbed, resulting in a greater number of macropores and pore connectivity. Undisturbed soil may increase vertical water and pesticide transfer (Soto-Gómez et al., 2019; Cueff et al., 2020). However, the leached proportions are similar to those in horizon 3 due to greater degradation.

Horizon 3 (60-90 cm): For most pesticides, greater adsorption is observed in horizon 3 than in horizon 2. This may be due to the small amount of water flowing through the soil and the pesticides retained in the immobile zone (Imig et al., 2023b). Horizon 3 is characterised by a lower porosity and transfer coefficient between the two regions, as observed by Pot et al. (2010). In addition, horizon 3 has a higher clay content of 19.2% compared to 13.8 and 13.1% for RH1 and RH2 respectively. In fact, Imig et al. (2023) have shown that finer textured soils have greater water retention. Smaller clay particles have a greater specific surface area and reduce herbicide

leaching by increasing their adsorption and enhancing their degradation in the soil (Novak et al., 2001; Mendes et al., 2016; Kumari et al., 2020). However, only the K_f of three herbicides increased from RH2 to RH3, demonstrating the complexity of their behaviour in soils.

Thus, the different soil properties and structures between the three horizons have resulted in contrasting pesticide fates. In general, only topsoil transport parameters are studied and presented in databases (Dusek et al., 2015; EFSA, 2015; Lewis et al., 2016). Furthermore, these parameters are usually considered independent of soil depth in modelling to limit the number of values to be estimated (Mertens et al., 2009; Dusek et al., 2011). However, this study shows that transport processes within the lower horizons are not negligible. Applying the values of sorption and degradation parameters from the soil surface to the entire soil profile will lead to an overestimation of pesticide degradation and adsorption. As a result, these predictions will be overly optimistic and will underestimate water contamination. The inclusion of soil properties and different soil depths in risk studies would allow more appropriate recommendations to be made on pesticide selection, dose adjustment and application periods.

However, these results must be interpreted with appropriate caution. They are based on three replicates, and the limited size of the soil columns may also depend in part on the spatial variability of the soil, given its heterogeneous nature. As a result, for some of the modalities, the standard deviations are large. Moreover, this study was carried out under controlled laboratory conditions and does not entirely reflect the complexity of natural systems. Investigating these parameters for different horizons under field conditions with more samples and considering them in pesticide leaching risk assessment and decision making is therefore essential. In addition, it should be noted that the soil profile represents a continuum between the three horizons and the quantities of pesticides entering horizons 2 and 3 will depend on the adsorption and degradation of upper horizons.

6.2. Influence of cropping systems on pesticide leaching

Agricultural practices such as tillage are known to generate different soil properties, which can influence the behaviour of pesticides in the soil (Kodešová et al., 2011; Katagi, 2013). The results indicate that production systems can generate different water fluxes and pesticide leaching dynamics.

ICLS system: In the ICLS system, the higher bentazone peak indicates a faster elution of the pesticide. The proportion of the mobile zone is higher, reaching 10% for the largest average BD, followed by the vegan and reference systems. Thus, despite a denser soil, the larger percentage of macropores generates a greater degree of preferential flow. These preferential flows may be generated by the large fibrous roots of maize as observed by Jin et al. (2018). Indeed, different root architectures and

growth stages can strongly influence the hydraulic properties of soils, especially by clogging pores, breaking aggregates or forming macropores (Ajayi et al., 2019; Lu et al., 2020). The greater connectivity of the pores in the ICLS system results in faster vertical flow, leading to a higher risk of groundwater contamination (Soto-Gómez et al., 2019).

Vegan system: Half of the pesticides eluted faster in the vegan system compared to the other systems. Nevertheless, the concentrations observed in the effluents are lower. The differences in Cpeak between the systems were generally not significant due to the large heterogeneity between the three replicates, as observed between different columns by Varvaris et al. (2021). Very low water infiltration was observed for replicates 2 and 3. The resulting K_s has a standard deviation twice as high as the other systems. This can be explained by the higher clay content of 17.2% in the vegan system compared to 13.8 and 12.3% in the reference and ICLS systems, resulting in lower leaching and a larger specific adsorption surface (Imig et al., 2023a). This high water retention for the vegan system had already been observed by Pirlot et al. (2024) in a study of water retention dynamics on the same plots. With low water flows, pesticides can also be retained longer in the immobile zone. In addition, unlike maize and beet, camelina was harvested and the stubble ploughed one week before the columns were collected. These agricultural practices may have disturbed soil structure and surface macropores, reducing pore hydraulic connectivity and soil hydraulic conductivity through the creation of a more impermeable layer (Alletto et al., 2015; Cueff et al., 2020). Post-harvest rainfall may also have destroyed some low-stability aggregates, leading to sealing of the soil surface (Holland, 2004) as observed for replicates 2 and 3 where a water layer was constantly visible on the surface. Finally, camelina has a fine root system, with 82% found in the first 30 centimetres (Gesch and Johnson, 2015; Berti et al., 2016). Fine roots can block soil pores, leading to reduced infiltration capacity (Lu et al., 2020). These low water fluxes resulted in longer pesticide/soil contact times and higher adsorption percentages for most pesticides. This higher adsorption may also be due to the higher clay content and CEC (Porfiri et al., 2015). This pesticide retention resulted in low effluent concentrations and truncated peaks, explaining the apparent early Tmin and Tpeak (Cueff et al., 2020). Dispersivity is also higher for VH1 and is almost double that of RH1 and IH1, showing that herbicide transport processes are highly heterogeneous (Vincent et al., 2007). Pesticide transfer is therefore strongly limited in the vegan system due to different soil properties and hydraulic discontinuity caused by agricultural operations.

Reference system: A greater hydraulic conductivity was observed with a higher K_s and mobile/immobile transfer coefficient than the other systems. Although there was higher porosity, the percentage of mobile zone (macropores) was lower, resulting in a reduced degree of preferential flow in comparison to the ICLS system. However, the system showed greater pore connectivity than the vegan system. Sugar beet has a main pivot root located below the plant. As a result, there are few inter-plant roots, resulting in a different soil structure compared to that of maize or camelina. Jin et al. (2018)

showed that water infiltration behaviour in soils is significantly affected by root morphological variation between crops.

Differences between systems were mainly related to crops planted, surface tillage and soil properties. However, for most of the pesticides, no significant difference was observed between the percentages of pesticides recovered and degraded or between the K_f and DT_{50} values. The production systems were only implemented for one year and the tillage practices were similar. As a result, they are probably not yet sufficiently differentiated to produce more contrasting leaching behaviour. However, the variations observed show that the production systems could have an impact in the longer term and be a lever for reducing pesticide leaching and groundwater pollution. Future studies should incorporate long-term monitoring of pesticide behaviour under different innovative production systems to assess the cumulative effects and seasonal variations in leaching dynamics. These studies could provide the basis for policies to encourage the adoption of more sustainable practices. These results must be interpreted with appropriate caution, given the small number of replicates and the limited size of the soil columns, which in some cases resulted in a large standard deviation.

6.3. Influence of pesticide properties

The properties of the pesticides themselves played a crucial role in their leaching behaviour within the same soil. In addition, the mass balances obtained do not always agree with the pesticide transport parameter values obtained. Different pesticide classifications are obtained depending on cropping systems and soil depth, highlighting the complex interaction between pesticide properties and soil characteristics.

Bentazone is the most rapidly eluted herbicide and appears tracer-like with water flow, as observed by De Wilde et al. (2009). With the low value of the K_f, its BTCs indicate a high degree of preferential flow. Koestel et al. (2012) showed that moderate to high preferential flow is found with a clay content above 8-9%. Thus, the clay content of the soils studied, ranged from 12.3 to 19.2%, results in a structured soil with stable aggregates and large pores (Bromly et al., 2007; Porfiri et al., 2015). Moreover, preferential flows may be promoted during heavy rainfall applied to the columns (ponding conditions), leading to near saturation conditions (Pot et al., 2005; Koestel et al., 2013). Between replicates, the spatial heterogeneity in the distribution of voids and macropores results in similar values, except for the peak. In fact, agricultural practices and biological activity generate heterogeneous degrees of preferential flow (Schwen et al., 2011; Singh et al., 2018). Bentazone shows very low adsorption (less than 1%) and high elution (more than 70%). These results are close to those of Boivin et al. (2004) for a silty soil after 60 days. Its K_f is the lowest and its field DT_{50} the highest, showing its high potential for leaching and groundwater contamination. These results can be explained by its high solubility in water and its

weak acid nature, with a pKa of 3.51. This means that it is primarily in the form of negatively charged ions at pH close to neutral, resulting in very low adsorption to organic matter or clay present in soils (Boivin et al., 2004; Arias-Estévez et al., 2008). The high quantities of bentazone applied to soils and leached into water can have negative impacts on non-target organisms and human health, with moderate toxicity for birds and humans (Lewis et al., 2016).

Metazachlor and metamitron are the two fastest eluted herbicides after bentazone. As in the PPDB (Lewis et al., 2016), their K_f are ranked just after bentazone. However, despite similar leaching patterns, their mass balances and soil fates are very contrasted. The percentages of metazachlor adsorbed are the lowest after bentazone in all columns, in contrast to metamitron, which is intermediate. In addition, the highest percentages of pesticide recovery in leachates were those of metamitron for topsoil (15.5-36.3%) and metazachlor (59.8-64.3%) at depth. In topsoil, the amounts of metamitron degraded are the lowest after bentazone, resulting in high leaching, in contrast to metazachlor, which shows the highest degradation percentages after flufenacet. These results could be attributed to the solubility of metamitron, which is almost four times higher than that of metazachlor (see table 2). They are in agreement with those of Mamy and Barriuso (2005) who found a low adsorption of these two pesticides in soils, with a higher adsorption and a longer half-life for metamitron than for metazachlor at the surface. Thus, metazachlor appears to be more susceptible to topsoil degradation than the other pesticides. At depth, however, the opposite trend was observed, with very little degradation of metazachlor, which ranked just behind bentazone, resulting in high leaching. Like bentazone, metamitron showed no difference in degradation or leaching between the different depth or cropping system. The mobility of metamitron in soils therefore seems to be less dependent on soil properties and biological activity than other herbicides, as observed by Cox et al. (1996). In addition, the adsorption of metazachlor appears to be more dependent on clay content than on OM content in the soil, with greater adsorption on RH3 and VH1. Both pesticides can cause moderate ecotoxicological risks to birds, fish, daphnia, bees and earthworms. Metazachlor is potentially carcinogenic for humans and may affect reproduction and development. Metamitron presents a high risk to humans as an endocrine disruptor (Lewis et al., 2016). It is therefore essential to determine the fate of these pesticides in soil and groundwater.

Terbuthylazine and flufenacet are the most strongly retained herbicides in soils. According to the PPDB, their K_f are the two highest. However, in our study these two pesticides show very different behaviours. The K_f of terbuthylazine is the highest for RH1, RH2 and IH1, but only the third highest for RH3 and VH1. The percentages adsorbed are among the three largest, but only first for RH1. Its adsorption therefore seems to depend more on the OC than on the clay content, as observed by (Kodešová et al., 2011). Terbuthylazine is a weak basic herbicide with very low solubility, explaining its low leaching. Furthermore, at a pH close to 7, its pKa of 1.9 indicates that it will mainly be in a neutral, non-ionised form. Its high octanol water partition

coefficient indicates that the pesticide is highly hydrophobic and adsorbed rapidly by organic matter. Terbuthylazine is highly toxic to humans and birds. Flufenacet is also highly toxic to humans as an endocrine disruptor.

The K_f of flufenacet is more variable, ranging from 1st for RH3 to 5th for VH1. In the topsoil, its adsorption percentages are the third lowest after bentazone and metazachlor. However, at depth it is one of the most adsorbed pesticides. Flufenacet showed greater adsorption in the RH3 and VH1 columns than in the others. Its recovery percentages are the lowest of the 8 pesticides and its degradation percentages are the highest for topsoil and the second lowest and highest at depth, after ethofumesate. Thus, flufenacet, like metazachlor, seems to be more sensitive to degradation than the other pesticides, but for all columns, and probably shows a greater affinity to clays than to OC.

Ethofumesate has the lowest recovery in the leachates at depth (12.6-16.7%) due to higher degradation (79.5-86.7%) than the others, and one of the lowest at surface due to high adsorption (12.1-29.7%). It shows a similar leaching and degradation percentage for all columns as bentazone and metamitron. Its adsorption seems to depend only on the OC content, as it shows a very low adsorption (0.73%) for RH3 compared to 29.7% for VH1, as shown by Facenda et al. (2024). Its low leaching may be due to its low water solubility, which is close to that of flufenacet. Chlorotoluron has the highest adsorption percentages for most columns (7.43 to 31.6%), with the highest values found for IH1 and VH1. The K_f values are among the three highest (1.57-1.88 cm^3/g for horizon 1 and 0.50 cm3/g for horizon 2), except for RH3. These results do not agree with the PPDB ranking, where k_f is among the lowest, just after metamitron. Kodešová et al. (2011) found large adsorption related to OM content with higher K_f for terbuthylazine, followed by chlorotoluron and finally s-metolachlor. However, the K_f rankings obtained in our study vary greatly depending on the soil depth and cropping systems.

Thus, the properties of pesticides have a major influence on their fate within the same soil. More importantly, the leaching or adsorption rates are not always in agreement with the K_f values obtained or with those of the PPDB. Different pesticide classifications are obtained depending on cropping systems and soil depth. Different adsorption mechanisms can be observed depending on the nature of the pesticide, whether or not it is ionised, and its properties such as solubility, pKa and octanol water partition coefficient. Positively ionised pesticides are more likely to be adsorbed by clays, while neutral pesticides with a high octanol water partition coefficient value are more hydrophobic and will be mainly adsorbed by organic matter. These results demonstrate the importance of studying the fate of all pesticides of environmental concern in the soils of interest to manage them more effectively. These pesticides can be highly toxic to non-target organisms such as birds and earthworms, as well as to human health. Pesticides remaining in soils can have an impact on microbial growth

and enzymatic activity, which can affect their biodegradation (Wołejko et al., 2020). In large concentrations, some pesticides can be toxic and reduce soil microbial biomass, affecting respiration, degradation of organic matter and nutrient cycling (Rose et al., 2016). It is important to mention that the toxicity of a pesticide varies depending on the way of exposure. Whether oral, dermal or respiratory, each way results in a different level of toxicity, as it influences the rate of absorption, the amount of substance absorbed and the organs affected. In animals, exposure occurs mainly through ingestion, which can be particularly toxic. Farmers are most often exposed through the skin and respiratory path during chemical spraying, which represents a high risk due to the rapid absorption of substances through these routes. On the other hand, their presence can also favour microorganisms capable of degrading them, to the detriment of other microorganisms, disrupting the established balance (Wołejko et al., 2020). Finally, the application of herbicides can lead to lower plant diversity and exudate production, and can therefore reduce the diversity and activity of soil organisms. Identifying the fate of pesticides in groundwater and soil is therefore crucial for the future.

6.4. Comparison with database

Tables 19 and 20 compare the transport parameters K_f and β, and field DT_{50} from the PPDB, the EFSA peer review for the Walloon soil-climate zone and the values used in Belgium with the results for the surface reference system.

In comparison with the databases like the PPDB or EFSA, the results indicate important differences in transport parameters for most pesticides, which may lead to underestimation of pesticide and metabolite leaching.

The K_f values obtained are within the PPDB and EFSA ranges. These ranges are indeed very broad as they are based on different studies and soils from all over Europe. Typical laboratory PPDB values are similar to our results for metazachlor and ethofumesate. They are lower for metamitron, S-metolachlor and chlorotoluron, with a larger difference for s-metolachlor. The PPBD value for s-metolachlor is the lowest of the eight herbicides studied, while our results show a high K_f, ranking third. Conversely, flufenacet and bentazone have higher PPBD K_f values. However, the EFSA values used in Belgium are all much higher than those obtained in this study. The largest differences were found for bentazone, S-metolachlor and flufenacet. The assumption of higher adsorption may lead to an underestimation of pesticide leaching and therefore groundwater contamination. Indeed, for most of the pesticides assessed in this work, EFSA concluded that the potential for groundwater contamination was low based on the 9 FOCUS scenarios, in particular for bentazone, metazachlor, chlorotoluron and terbuthylazine. Groundwater analyses in Belgium identify bentazone, chlorotoluron and terbuthylazine as major contaminants (SPW ARNE, 2022). This tends to confirm our results. These larges differences can be due to different methodologies for determining transport parameters. The parameters in the

databases are generally determined by batch adsorption in flasks, at equilibrium. These experiments are generally of short duration and maximise contact between the soil and the pesticides through agitation. Therefore, they do not take into account soil structure or preferential flow. Furthermore, as will be seen in this article, soil type and soil properties have a major influence on the fate of pesticides in soil, which can lead to significant differences in the estimated parameters. Cueff et al. (2020) also found significant differences between the transport parameters estimated for several pesticides and the PPDB. They showed that the K_d values obtained for the same soil in batch experiments did not correspond to the retardation factor obtained in undisturbed soil columns due to the soil structure.

The DT_{50} obtained for bentazone is in good agreement with the typical PPDB value. However, it is much higher than the value used in Belgium and the EFSA range. This indicates an overestimation of its degradation and therefore a possible underestimation of its leaching and contamination of groundwater. An overestimation of adsorption and degradation could have important environmental consequences for bentazone, which is very poorly retained in soils. For the other herbicides, very low DT_{50} values were obtained. They are lower than the ranges, PPDB values and values used in Belgium. The use of higher DT_{50} values leads to a possible overestimation of the leaching of these pesticides, which has less impact on the environment than the opposite for decision making purposes. However, this may lead to underestimating metabolite formation. The largest differences were found for ethofumesate, chlorotoluron and flufenacet, followed by terbuthylazine and s-metolachlor. Metabolites are generally more mobile and persistent than parent herbicides, causing significant leaching and water contamination (Lewis et al., 2016; Kiefer et al., 2019). According to EFSA studies, the metabolites of terbuthylazine, s-metolachlor and metazachlor have a high leaching potential (Brancato et al., 2017; Lentdecker et al., 2017; Alvarez et al., 2023). Along with these, metabolites of metamitron and flufenacet were classified as highly mobile in the PPDB, with high DT_{50} of up to 400 days for metolachlor ESA (Lewis et al., 2016). An investigation of novel metabolites detected in groundwater showed that those of terbuthylazine, metamitron, metazachlor and flufenacet were found at higher concentrations than the parent pesticides (Kiefer et al., 2019). It is therefore important not to underestimate the degradation of pesticides in soils. Special emphasis should be placed on the study of the fate of metabolites in soils and their measurement during monitoring, which is rarely investigated and all too often neglected.

Several sensitivity analyses have already been carried out on solute fate using Hydrus 1-D. Jian et al. (2024) showed that the adsorption coefficient K_d and the dispersivity λ are the two main parameters influencing the migration of naphthalene in soils. The concentration of the peak is the most sensitive to the concentration of the influent, followed by K_d, first order degradation rate coefficient (μ) and λ. Cheviron and Coquet (2009) also carried out a sensitivity analysis on the fate of a pesticide using the dual porosity mobile-immobile model. They found a very high sensitivity

of pesticide sorption and degradation parameters, starting with Freundlich exponent β, then K_f and finally μ. Differences in the use of adsorption and degradation parameters can therefore have a major impact on the model outputs and hence on the assessment of the potential risks of water contamination. In addition, the limitation of the dual-porosity model is that it assumes that the flow of water is limited only to the mobile region (macropores). Thus, water does not move at all in the immobile zone or soil matrix, which can only exchange, retain and store water without convective flow (Šimůnek et al., 2003). In reality, water flows in both regions of the soil, but at different rates. Some researchers even consider triple soil porosity to improve the modelling (Varvaris et al., 2021a). This limitation can lead to different behaviour of water and solute flows between reality, the database and the model values.

These results highlight the need to adapt the K_f and DT_{50} values for all pesticides and metabolites of environmental concern to the soil type studied for future modelling and decision-making. Parameter values from databases such as the PPDB or EFSA studies should be used with caution and are not always reliable. These results are in agreement with the recent study by Mamy et al. (2024) who modelled the leaching of many pesticides in soils under more sustainable agricultural practices, using three different models. They used generic transport parameters from the PPDB as used for regulatory risk assessment. They found that the models performed poorly in reproducing the concentration of pesticides in the leachates, with underestimation in most cases.

In addition, unmonitored metabolites pose a risk to water quality. Plant protection products should therefore be used more cautiously, given the difficulty and uncertainty of assessing their fate in soil and water. Studies should include the behaviour of metabolites in soils to provide a more complete picture of the potential for pesticide contamination. These products also represent a threat to microorganisms, animals and human health, particularly for farmers with high levels of exposure.

Table 19. Comparison of the K_f values and associated β values in brackets of the PPDB, the EFSA peer review for the Walloon soil-climate zone and the values used in Belgium with the results of this study for the surface reference system. For individual values, uncoloured boxes represent values similar to those obtained, less than 1.5 times higher, yellow boxes correspond to 1.5 to 2 times higher, orange boxes 2 to 3 times higher and red boxes more than 3 times higher. Ranges are shown in red if they do not include the value reported in this study. The blue boxes indicate values below the results.

	K_f (ml/g) (β)	Bentazone	Metamitron	Metazachlor	Metolachlor	Ethofumesate	Chlorotoluron	Flufenacet	Terbuthylazine
Results	RH1	**0.22 (1.00)**	**1.15 (0.75)**	**0.94 (0.92)**	**1.71 (0.92)**	**1.59 (0.90)**	**1.88 (0.92)**	**1.66 (0.89)**	**2.25 (0.92)**
PPDB	Typical lab	0.97 (0.93)	1.09 (0.81)	1.02 (0.99)	0.93 (0.89)	1.74 (0.91)	1.30 (0.88)	4.38 (0.92)	5.10 (0.93)
	Range	0.02-3.06 (0.70-1.03)	0.36-5.88 (0.67-0.95)	0.37-2.20 (0.99-1.00)	0.07-2.57 (0.55-1.35)	0.70-6.20 (0.84-0.96)	0.78-2.74 (0.83-0.93)	1.48-10.6 (0.88-0.98)	2.10-10.5 (0.88-0.98)
EFSA	Range	0.08-1.94 (0.70-1.00)	0.56-4.65 (0.64-0.85)	0.48-3.50 (0.82-0.85)	0.59-4.80 (0.91-0.93)	0.70-6.20 (0.82-0.96)	2.70-9.60 (0.83-0.93)	1.00-14.7 (0.84-0.98)	2.10-10.5 (0.88-0.98)
Belgium	Mean value	0.76 (0.97)	3.06 (0.77)	2.75 (0.84)	5.33 (0.93)	2.95 (0.90)	4.52 (1.00)	5.05 (0.87)	5.78 (0.90)

Table 20. Comparison of the DT_{50} values of the PPDB, the EFSA peer review for the Walloon soil-climate zone and the values used in Belgium with the results of this study for the surface reference system. For individual values, uncoloured boxes represent values similar to those obtained, less than 2 times higher, yellow boxes correspond to 2 to 10 times higher, orange boxes 10 to 25 times higher and red boxes more than 25 times higher. Ranges are shown in red if they do not include the value reported in this study. The blue boxes indicate values below the results.

	DT_{50} (days)	Bentazone	Metamitron	Metazachlor	Metolachlor	Ethofumesate	Chlorotoluron	Flufenacet	Terbuthylazine
Results	RH1	**18.2**	**2.1**	**1.3**	**1.4**	**1.5**	**1.4**	**0.8**	**1.6**
PPDB	Typical lab	20.0	19.0	10.8	15.0	21.6	33.5	19.7	72.0
	Range	8.0-35.0	2.2-44.5	5.5-25.3	8.0-38.0	8.5-80.5	10.3-144	7.04-37.4	38.2-167
EFSA	Range	3.0-6.9	6.6-21.7	5.1-14.4	3.6-55.7	13.1-110	26.0-42.0	13.1-54.2	6.9-35.7
Belgium	Mean value	4.7	11.1	8.5	22.4	40.8	42.0	27.7	19.5

7. Conclusions

In this study, the fate of eight pesticides of concern to groundwater was investigated under three production systems and at three soil depths. Leaching experiments in undisturbed columns, mass balances and inverse modelling using Hydrus 1-D to adjust mobility parameters were carried out. The results provide a better understanding of how cropping systems and soil properties can influence the behaviour of different pesticides in soils and highlight potential risks to the environment.

The results revealed that the differences in soil properties and structure between the three horizons resulted in more contrasting leaching behaviour than between the production systems. The soil surface retains more pesticides due to its higher organic matter content and biological activity, which enhances degradation. Horizon 2 is characterised by greater preferential flow due to the presence of more earthworm galleries and root channels, as a result of undisturbed soil. Pesticide adsorption increases in horizon 3 due to higher clay content and lower water flow, resulting in longer retention in the immobile zone. These results highlight the need to consider deeper soil horizons in pesticide leaching risk assessment, as transport processes and retention characteristics vary significantly with depth. Applying transport parameter values from the soil surface to the entire profile will result in overly optimistic predictions and will lead to an underestimation of water contamination.

Our analysis demonstrates that cropping systems can affect pesticide leaching dynamics. The findings highlight the importance of root architecture, soil properties and surface tillage in influencing water flow and pesticide transport through soil. However, the short implementation period of the production systems probably resulted in insufficient differentiation and prevented significant differences in recovery rates, degradation rates, K_f or DT_{50} values. Thus, in the long term, different agricultural systems could have a significant effect on pesticide leaching and be a lever for reducing groundwater pollution.

The properties of the pesticides themselves played a crucial role in their leaching behaviour within the same soil. In addition, the mass balances obtained do not always agree with the pesticide transport parameter values obtained or with those of the PPDB. Different pesticide classifications are obtained depending on cropping systems and soil depth, highlighting the complex interplay between pesticide properties and soil characteristics. These results demonstrate the importance of studying the fate of all pesticides of environmental concern in the soils of interest to manage them more effectively.

When compared with established databases such as the PPDB and the EFSA peer review for Europe, our results indicated discrepancies in transport parameters for most pesticides. The EFSA values used in Belgium show higher K_f than our results, which could lead to an underestimation of pesticide leaching and water contamination. In addition, except for bentazone, higher DT_{50} values were found in the databases, which could lead to an underestimation of the production and leaching of metabolites, which are more mobile and persistent than the parent pesticides. Therefore, parameters derived from databases should be used with caution and are not always reliable. Hence, this study shows the need to investigate the fate and adapt the transport values of all environmentally problematic pesticides to site-specific characteristics.

Future studies should incorporate long-term field monitoring of pesticide behaviour under different innovative production systems to assess the cumulative effects and seasonal variations in leaching dynamics. This could provide a more comprehensive understanding of pesticide persistence and mobility over time. The impact of sustainable agricultural practices should also be studied for other types of soil, with varying characteristics. Research should include a wider range of pesticides and their metabolites to help understand the leaching behaviour of different classes of chemicals and their environmental impact. In addition, a special emphasis should be placed on studying the fate of metabolites in soils. Developing advanced risk assessment models that account for soil depth variability and site-specific conditions is critical to improve predictions of groundwater contamination and inform better decision-making. This research provides some insight for developing more sustainable agricultural practices that can minimise environmental contamination while ensuring effective pest management. Such knowledge is essential for advancing policies and practices aimed at protecting environmental safety and promoting the resilience of agricultural ecosystems in the face of ongoing environmental and regulatory challenge.

Chapter 5

How does soil water retention change over time? A three-year field study under several production systems

1. Synopsis

This chapter and the next form the second part of this thesis on hydrological monitoring of the effects of a transition to contrasting EcoFoodSystem systems, including several sustainable agricultural practices.

Chapter 5 focuses on the monitoring in the field of the temporal evolution of soil water retention of four contrasting production systems at two temporalities over a period of three years. This chapter allows to respond to objectives 6 and 7 of this thesis. This work provides an opportunity to study the impact of agricultural systems on the variability of soil water retention capacity under contrasting climatic conditions between 2021, 2022 and 2023. In addition, in this chapter, the retention curves obtained in the field are compared with the curves obtained theoretically by pedotransfer functions and in the laboratory on undisturbed soil samples. This research was partly carried out by Anne-Catherine Renard as part of her master's thesis.

This chapter is based on the publication: Pirlot, C., Renard, A.-C., De Clerck, C., Degré, A., 2024. How does soil water retention change over time? A three-year field study under several production systems. Eur. J. Soil Sci., e13558 https://doi.org/10.1111/ejss.13558.

2. Abstract

Agricultural practices and meteorological conditions affect soil structure and soil hydraulic properties. However, their temporal evolution is rarely studied, and even less in the field. Thus, their dynamics are rarely taken into account in models, often leading to inconsistent results and poor decision making. In this study, the temporal evolution of water retention properties and soil structure was monitored over a 3-year period under several contrasting production systems. Soil Water Retention Curves (SWRCs) obtained directly in the field (with soil water content and potential sensors) were compared with theoretical SWRCs predicted by pedotransfer functions (PTFs) and laboratory SWRCs measured on undisturbed samples (figure 46). Bulk densities were measured every two months. Results indicate a high degree of variability in SWRCs over time and between production systems. The results suggest that variations in the soil water retention behaviour can be induced by crop differentiation, weed control, crop residue management, compaction during harvest or the introduction of temporary grassland. Contrasting climatic conditions between 2021 (water excess), 2022 (severe drought) and 2023 (intermediate) provided a unique opportunity to study the resilience of the crop systems to extreme climatic conditions. Different soil drying dynamics were observed and some agricultural practices were identified as influencing the soil water retention behaviour for at least 2 years. Comparison of

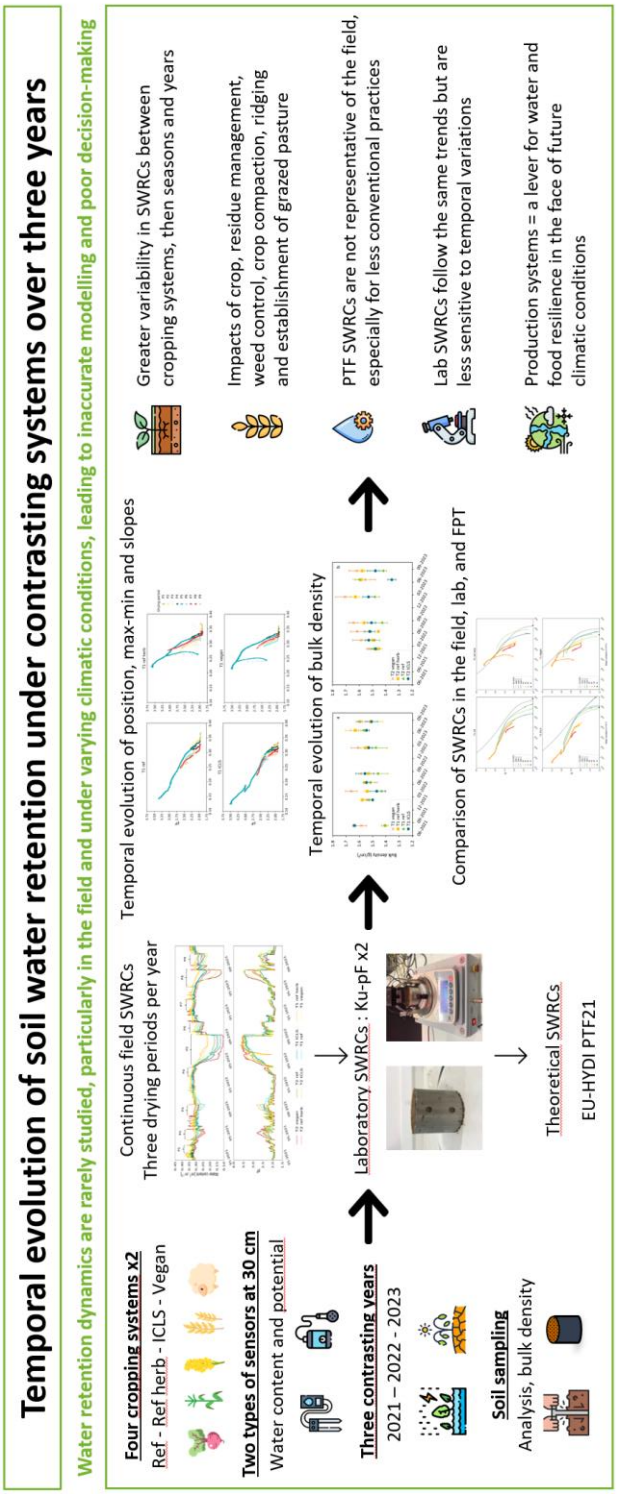

Figure 46. Graphical overview of the temporal evolution of soil water retention under contrasting production systems over three years.

SWRCs showed that the theoretical curves obtained from PTFs are not a good representation of the field SWRCs, especially for less conventional agricultural practices. The laboratory curves are closer with similar trends. However, these SWRCs are not optimal for investigating the temporal evolution of water retention properties. This research also shows that agricultural practices and crops can be levers for contributing to greater food resilience against future climatic conditions. Therefore, to assess the relevance of production systems for tomorrow's needs, studies should focus on the impact of multi-cropping systems on water retention dynamics in the field.

3. Introduction

General challenge : In the last decade, alternative agricultural practices have become more common to provide more sustainable production systems with long and diverse crop rotations, cover crops or limited chemical inputs (Piñeiro et al., 2020). In addition, climate change will put significant pressure on crop water availability due to high variability in rainfall and increased evaporation. To improve the water resilience of the system for the future, priority needs to be given to understand how these agricultural practices affect soil water behaviour (Chandrasekhar et al., 2018; Heitman et al., 2023).

Hydraulic properties: The hydraulic properties of soils are the basis for modelling water fluxes and solute transport in soils for decision-making. In particular, they influence evaporation, groundwater recharge, contaminant transport and water availability for plants (Whalley et al., 2013; Ciocca et al., 2014). A Soil Water Retention Curve (SWRC) shows the relationship between water content and matric potential and provides a better understanding of water behaviour in the soil. It gives information on soil structure, water retention capacity, wilting point and available water content (Rabot et al., 2018).

Influencing factors: The SWRC is usually considered to be an invariable soil property, determined in the laboratory or predicted by pedotransfer functions (PTFs). However, several studies have shown the influence of agricultural practices, vegetation growth and climatic conditions such as rainfall, freeze-thaw and wet-drying cycles (WDs) on soil hydraulic properties and structure (Alletto et al., 2015; Tifafi et al., 2017; Jensen et al., 2020; Alskaf et al., 2021; Huang et al., 2021; Pečan et al., 2023). The main factors influencing hydraulic properties found in the literature are:

- Tillage: Ploughing creates an abundance of large pores and unstable aggregates that collapse during rainfall. During post-tillage WDs, bulk density (ρ_b) and water retention capacity increase due to a reduction in effective soil porosity and hysteresis (Zhang et al., 2017; Huang et al., 2021). This creates a large number of interconnected pores, which improves water retention (Sandin et al., 2017; Zhang et al., 2018). After

each WDs, the steepness of SWRCs increases, indicating a reduction in the rewetting rate (Herbrich and Gerke, 2017; Kool et al., 2019). However, no-till (NT) systems have a higher water retention capacity due to the accumulation of organic matter (OM) near soil surface and a well-developed pore system (Gozubuyuk et al., 2015; Zhang et al., 2018). Retention capacity fluctuates less over time in NT due to the greater rigidity of the pore system (Huang et al., 2021). However, NT may increase the risk of compaction in the long term, resulting in finer soil porosity and greater water retention (Blanco-Canqui and Wortmann, 2020).

- Root system: Pečan *et al.*, 2023 showed that the shape of the SWRCs depends more on the root system development and environmental conditions during the seasons than on the tillage systems. Different stages of root development have also been shown to affect the hydraulic properties of soils by clogging pores, breaking up aggregates and forming macropores (Ajayi et al., 2019; Lu et al., 2020).

- Crop and rotation : Diverse crops rotations improve pore connectivity and increase OM and microbial activity, enhancing infiltration and water retention capacity (Ball et al., 2005; McDaniel et al., 2014). Crop succession affects the SWRC and a rotation with two years of grassland was found to have a higher available water retention capacity than a mixed crop rotation (Schwärzel et al., 2011; Herbrich and Gerke, 2017). When grassland was converted to bare soil, the water retention capacity decreased, whereas inverse conversion showed no change despite an increase in bulk density (Jensen et al., 2020). Bacq-Labreuil *et al.*, 2021 found an increase in porosity, pore size diversity and pore connectivity when bare soil was converted to grassland. However, soil structure was not affected by the conversion to arable crops.

- Soil compaction: After compaction on bare or covered ground (caused by machines or animals), the physical properties of the soil undergo alterations that persist for more than two years (Keller et al., 2021). The extent of these alterations depends on the compaction force applied resulting in significant differences in the physical properties of the soil. Over time, the compaction effect decreases with natural recovery (Hu et al., 2018). However, these recovery processes can take decades or even centuries (Meurer et al., 2020a; Keller et al., 2021).

The conventional approaches for investigating temporal variability: The temporal variability of hydraulic properties is generally studied in the laboratory, using small samples in undisturbed structures (Ajayi et al., 2019; Kool et al., 2019; Geris et al., 2021). The drying branch of the SWRC is obtained at different times, generally before and after the event under investigation. Then, these SWRCs are fitted with empirical models, the most widely used being the model of van Genuchten (van Genuchten, 1980; Pires et al., 2017; Jensen et al., 2019). However, the results obtained are often inconsistent between studies due to the spatial and temporal variability of soil properties or the type of measurements performed (Strudley et al., 2008; Chandrasekhar et al., 2018). Furthermore, a large variability in SWRC can be obtained between different laboratories due to non-harmonised and non-standardised procedures (Guillaume et al., 2023). Temporal variability can also be studied using

SWRCs obtained by PTFs based on easily measurable soil properties (Tóth et al., 2015). These functions represent the SWRCs with high accuracy (93%), but only for those obtained under laboratory conditions (Dashtaki et al., 2010; Ahmed et al., 2021; Tian et al., 2021).

Importance for modelling: The few studies that have included the dynamics of hydraulic properties in the models have shown better predictions and more reliable results (Schwärzel et al., 2011; Schwen et al., 2011; Alletto et al., 2015; Geris et al., 2021). The importance of developing models capable of simulating the temporal dynamics of soil hydraulic properties has been demonstrated (Hannes et al., 2016; Meurer et al., 2020b; Jarvis et al., 2022). Recently, Vogel *et al.*, 2023 presented a physically based concept to better describe these properties under non-equilibrium hydraulic conditions. However, the parameterisation of water flow and soil structure in models remains a challenge.

Comparison of field measurements with other methods: Some studies have focused on the measurement of *in-situ* SWRCs and their comparison with curves obtained in the laboratory or from PTFs (Bordoni et al., 2017; Huang et al., 2021; Pečan et al., 2023). Significant differences were observed due to hysteresis, WDs and changes in soil structure over time (Basile et al., 2003). Hysteresis describes the non-unique relationship between water content and matric potential during drying and wetting phases due to pore heterogeneity, a difference in contact angle, air entrained in the pore system and the swelling shrinking properties of the soil (Basile et al., 2003; Hannes et al., 2016; Dey et al., 2017; Zhao et al., 2020). As a result, laboratory or theoretical SWRCs failed to represent the dynamics of water retention and were insufficient to explain how agricultural practices might affect water behaviour (Alletto et al., 2015; Iiyama, 2016; Zhang et al., 2018; Hedayati et al., 2020; Ahmed et al., 2021; Huang et al., 2021; Pečan et al., 2023).

Gaps in the literature: In both cases (laboratory and field conditions), studies generally investigate the dynamic evolution of SWRCs for isolated agricultural practices, such as different types of tillage, compaction or a change in land use (Jensen et al., 2020; Huang et al., 2021; Keller et al., 2021). Yet, it is essential to examine the impact of the whole production system on the evolution of hydrodynamic properties and soil structure in order to assess its resilience for the future. Furthermore, these investigations often focus on a short-term period, such as one or two growing seasons, and on the topsoil layers (Zhang et al., 2018; Geris et al., 2021; Huang et al., 2021). However, production systems can have impacts on longer time scales and at greater depths (Wahren et al., 2009; Jirků et al., 2013; Bordoni et al., 2017).

Objectives: Therefore, this study aims:

(1) to evaluate the impact of several whole production systems and contrasting climatic conditions on the temporal evolution of SWRCs in the field over three years;
(2) to compare the field curves with those obtained by PTFs prediction and under laboratory conditions on undisturbed samples.

4. Materials and methods

4.1. Experimental setup

The experiment has been conducted on an agricultural silt soil located at the EcoFoodSystem experimental plots (50°56'50.6"N, 4°70'93.2"E) of the Terra teaching and research centre in Gembloux, Belgium. The soil used is the one described in chapter 4 for the excavation of columns in a conserved structure. Meteorological data were collected at the Ernage-Gembloux station, located less than 2 km away from the experimental plots. The physico-chemical properties of the first three soil layers were determined at the beginning of the experiment in 2021 and are given in Table 21.

Table 21. Physico-chemical properties of the three soil layers studied.

	L1	L2	L3
Depth	0-30	30-60	60-90
Texture		Fine silty clay	
Clay (%)	13,8	13,1	19,2
Silt (%)	78,3	80,4	74,5
Sand (%)	7,9	6,4	6,2
Organic carbon (g/kg)	12,3	5,2	3,4
CEC (meq/100 g)	9,4	8,3	10,6
pH water	7,6	7,8	7,9
Bulk density (g/cm³)	1,38±0,03	1,54±0,01	1,64±0,01
Porosity	0,47±0,01	0,42±0,01	0,38±0,00

The four contrasting production systems studied in this chapter are those of the EcoFoodSystem experiment described in chapter 2. These are the ‘reference’ system with or without the use of herbicides (ref/ref herb), the ‘ICLS’ system and the ‘Vegan’ system with two temporalities. This chapter is based on the Teros 12 water content

and Teros 21 water potential sensors placed at a depth of 30 cm in the eight plots. In September 2020, the four systems were implemented on eight adjacent. Two crops of each rotation were implemented each year, corresponding to two temporalities (T1 and T2).

Agricultural operations made on the eight plots during the first three years of experiment are illustrated in Figure 47.

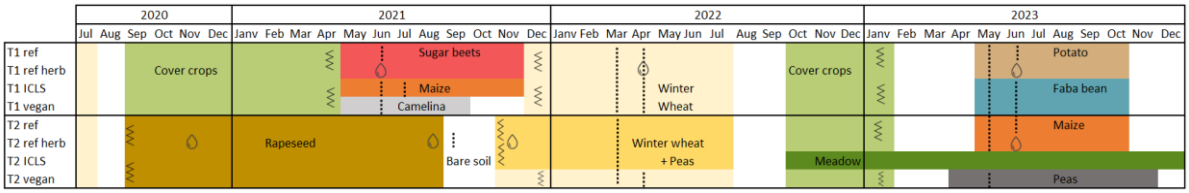

Figure 47. Agricultural practices and crops from July 2020 to December 2023 on the 8 EcoFoodSystem experimental plots. The colours represent the different crops, the zigzags indicate ploughing to a depth of 25 cm, the dotted lines refer to soil treatment (hoeing, harrowing or rotary hoeing) to a maximum depth of 5 cm and the drops correspond to herbicide application.

4.2. Meteorological conditions

The three years of measurements were very contrasted in terms of meteorological conditions. The year 2021 was a very wet year in Belgium, with total rainfall of 1039 mm. It was one of the three wettest years since 1991. Precipitation was concentrated in summer, with 410.7 mm of rain, the highest since 1833 (table 22). The year 2022 was hot and dry, with an average temperature of 12.2°C and total rainfall of 701 mm. It was one of the five driest years since 1991 and the warmest since 1833. March and July, as well as the summer, were the driest on record since 1991. The year 2023 was an intermediate one, with an average temperature of 12.2°C and total precipitation of 1011.4 mm. It was a relatively wet year, especially in spring and autumn. It was the third warmest and fourth wettest year since 1991. June and September 2023 were the hottest months on record since 1833.

Table 22. Meteorological conditions for the three years of monitoring (2021-2023) and the average between 1991 and 2020 for the four seasons. Values in red, orange and yellow indicate the highest, one of the 3 highest and one of the 5 highest values since 1991. Values in dark blue and light blue represent the lowest values and one of the 3 lowest values since 1991.

Meteorological data	**Average (1991-2020)**				**2021**				**2022**				**2023**			
	Win	Spr	Sum	Aut	Win	Spr	Sum	Aut	Win	Spr	Sum	Aut	Win	Spr	Sum	Aut
Average T° (°C)	4.1	10.5	17.9	11.2	4.7	8.8	17.8	11.5	5.5	11.3	19.6	12.8	5	10.2	18.9	13.4
Solar radiation (kWh/m²)	75.5	343.6	442.6	175.8	83	364.6	409.6	184.2	74.8	386.6	483.2	174.9	75.5	319.9	442.6	177
Total rainfall (mm)	228.6	165.6	234.2	209.3	264.1	165.6	410.7	180.6	259	108.8	110.6	210.1	214.9	241.6	279.5	283.7
Days of rainfall	55.2	43.5	42.6	48.5	54	43	50	43	55	23	24	50	54	51	45	52

4.3. Drying events

Figure 48 shows the daily rainfall, water content and matric potential measured continuously for the 8 plots at a depth of 30 cm. To compare the temporal evolution of the soil water retention between production systems, three drying events per year, 2021-2022-2023, were isolated from the continuous measurements and labelled periods P1 to P9.

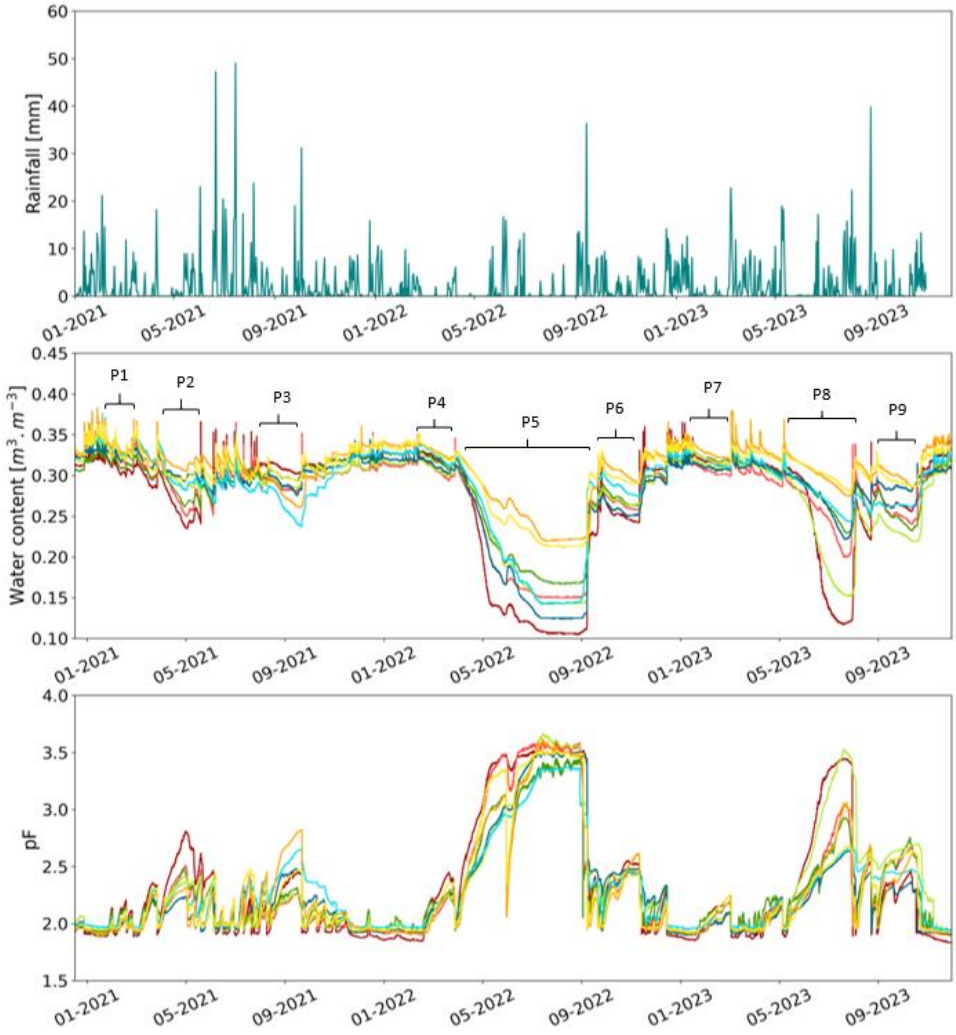

Figure 48. Daily rainfall, soil water content and matric potential from January 2021 to December 2023 for the eight plots at a depth of 30 cm. Drying events are indicated by the periods P1 to P9.

Several criteria were taken into account when selecting the drying events. Firstly, they had to lead to a reduction in water content and an increase in matric potential. Secondly, preference was given to the most pronounced drying periods. Thirdly, three events per year were chosen to ensure that the whole year was well represented. The three periods per year consecutively correspond to a winter, a spring-summer and an autumn event, respectively. The duration of the drying phases is 9, 37 and 41 days for 2021, 36, 109 and 45 days for 2022 and 46, 74 and 43 days for 2023 with most severe drying periods in spring-summer.

To compare the drying periods over time and between plots, the minimum and maximum water contents and matric potential were studied. The slopes of the SWRCs were also analysed. These slopes depend on the drying period and were therefore only compared between plots for the same drying event. To ensure that the same portion of the SWRCs were compared, the slopes were calculated using identical pF values, common to all the plots for each drying period (table 23). Some slopes could not be calculated due to similar water content values for the pF_{min} and pF_{max} of the drying period. In addition, the slopes of the P9 drying period could not be determined due to the absence of similar SWRCs portions among the eight plots in terms of pF_{min} and pF_{max} values. Slopes were calculated by dividing the difference in pF values by the difference in water content values. In the tables, the significant digits have been reduced to two, corresponding to the accuracy of the probes.

Table 23. Minimum and maximum pF values used to calculate SWRC slopes for each drying period.

Drying event number	**Common pF_{min}**	**Common pF_{max}**
P1	1.96	1.97
P2	2.05	2.24
P3	2.17	2.27
P4	1.96	2.24
P5	2.10	3.36
P6	2.24	2.43
P7	1.96	2.10
P8	1.97	2.62
P9	2.47	2.46

4.4. Soil samplings

4.4.1. Physico-chemical analysis

For plots T1 (rotations starting in year 1), soil physico-chemical properties were analysed at depths of 30, 60 and 90 cm in June 2021. They were also determined for all the plots in the end of September 2022. Soil particle size distribution was determined using the pipette method (NF X31-107), organic carbon content by dry combustion (NF EN 15936) and pH using a glass electrode (NF ISO 10390).

4.4.2. Soil bulk density and porosity

In November 2020 and September 2021, soil bulk density was determined for plots T1 using undisturbed soil columns of 8.4 cm diameter and 30 cm length. Undisturbed samples were then taken at several times in 100 cm³ Kopecky rings with a diameter of 5.1 cm and a height of 5 cm (figure 49). The rings were inserted using a special auger and hammer. The samples were then dried at 105°C for 48 hours to determine their bulk density. For all plots, samples were taken at 30 cm in three replicates in March, May, July and September 2022 and in March, July and September 2023. Samples were also taken at 60 and 90 cm in March and September 2022 and in July 2023. Soil porosity was calculated from the bulk density and assuming a soil particle density of 2.65 g/cm^3 and an organic matter particle density of 1.4 g/cm^3.

Figure 49. Sampling of the soil bulk density and preparation in the laboratory

4.4.3. Laboratory water retention curve

The SWRC in the unsaturated range was measured in the laboratory using a Ku-pF single place apparatus (Umwelt-Geräte-Technik GmbH) as illustrated in figure 50. This device is based on the simplified evaporation method with tension measurements at two depths over time during sample drying, combined with continuous weighing. The SWRC is then determined by relating the water content of the sample by weight to the average of the two potentials in kPa measured every 4 minutes from saturation to a drying limit of -90 kPa.

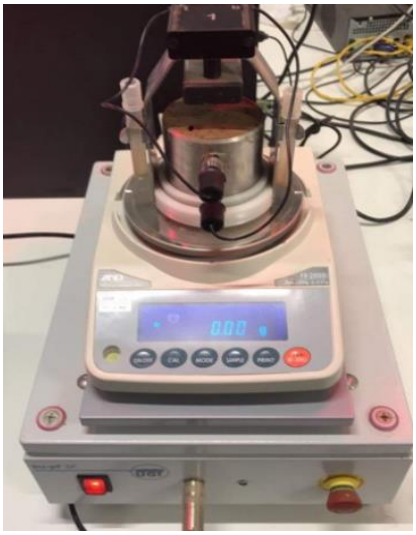

Figure 50. Ku-pF single place apparatus.

Undisturbed samples were collected in September 2022 in 250 cm^3 rings, 7.2 cm in diameter and 6.1 cm high, with two holes. Samples were taken using a guide and hammer at a depth of 30 cm in three replicates. Only the T1 plots were sampled because of their different crops in 2021. Samples were first saturated from below for 48 hours using filter mesh. The tensiometers were also saturated for 24 hours and then calibrated. They were then inserted into the holes in the ring after the soil had been drilled out. SWRCs are measured for tensions ranging from -0.5 to minimum -67.8 kPa (pF 0.70-2.83) with this apparatus (figure 51).

Figure 51. Collection of undisturbed sample to measure the SWRC in the laboratory

4.5. EU-HYDI PTF

Tóth et al., 2015 developed pedotransfer functions applicable for a wide variety of input parameters, relevant to the European continent. Data from the European Hydropedological Data Inventory (EU-HYDI), the largest hydro-pedological database in Europe, was used to train and test these functions (Weynants et al., 2013). The first version of EU-HYDI PTFs present different models and 22 classes. The soil water retention curve θ(h) can be described by the commonly used van Genuchten equation (van Genuchten, 1980). This equation contains four parameters: the residual water content θ_r, the saturated water content θ_s, the inverse of the air entry value α and the pore size distribution index n. In addition, the parameter m is calculated as 1-(1/n). In our study, PTF 21 was chosen because it can be used to determine the van Genuchten parameters from particle size distribution, bulk density and organic matter content. Using a univariate regression tree, it provides the value of θr and, using linear regression, the associated values of θs, log10(α) and log10(n-1). The theoretical EU-HYDI SWRCs for the T1 plots were estimated using particle size distributions, organic carbon content and bulk density of the samples collected at the end of September 22.

To compare field, laboratory and theoretical SWRCs, slopes were calculated for a tension between 10 and 67.8 kPa (pF 2-2.83). These common pF values allow the same part of the curve to be compared. These tension values correspond to the overlap of the SWRCs determined by field and laboratory methods.

4.6. Data treatments

Data from the water content and matric potential sensors for the 8 plots from 2021 to 2023 were processed using Python v3.9.13. The figures were plotted with seaborn and matplotlib packages. Analyses of variance (ANOVA) were performed to study differences in bulk density between plots over time. To compare the means, Fisher's Least Significant Difference method was used with the null hypothesis of equality of means and a significance level of 0.05. Normality was tested using Shapiro-Wilk and equality of variances using Levene's test. All assumptions were satisfied.

5. Results

5.1. Bulk density

The temporal evolution of soil bulk density (ρ_b) for the eight plots studied is shown in Figure 52. Statistical tests were performed on the three spatial replicates of the samples. In September 2021 for T1 plots, ρ_b is significantly higher for T1 ICLS plot with maize (1.64±0.01 g/cm³) then for T1 vegan with camelina and T1 reference with sugar beets (1.41±0.02 g/cm³).

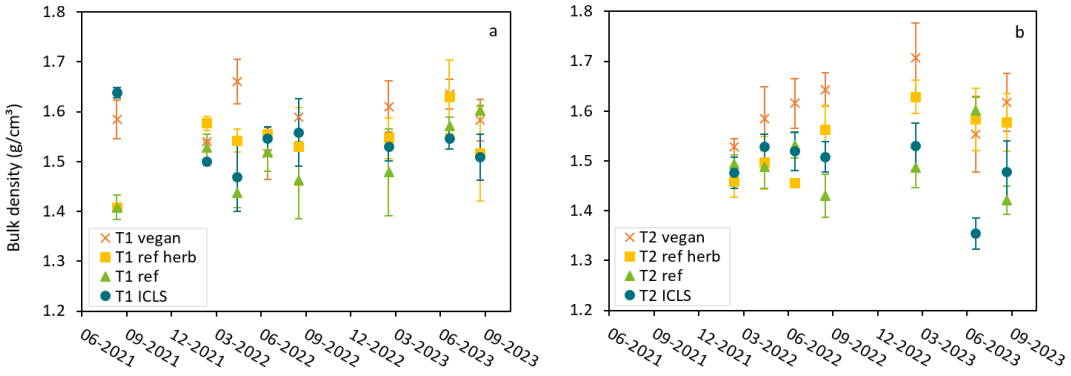

Figure 52. Bulk density of the soil in September 2021, March, May, July and September 2022 and in March, July and September 2023 at a depth of 30 cm for plots T1 (a) and T2 (b).

In 2022, four samples were taken in March, May, July and September. In March 2022, after ploughing and sowing winter wheat and winter wheat/peas, the ρ_b of T1 and T2 were close to each other. Then, in May 2022, ρ_b of T1 vegan increased to 1.66±0.05 g/cm³ and that of T1 ref dropped to 1.44±0.03 g/cm³. The ρ_b of T2 vegan increased to 1.58±0.06 g/cm³. It was significantly higher (p-value<0.05) than the other plots, except for T1 vegan. In July 2022, ρ_b were similar for all plots (p-

value>0.05) except for the higher T2 vegan and the lower T2 ref herb with 1.46±0.01 g/cm³. Finally, in September 2022, after harvesting, the ρ_b values were more differentiated, ranging from 1.46±0.08 to 1.59±0.04 g/cm³ for T1 and from 1.43±0.03 to 1.64±0.03 for T2. The ρ_b of plots T1 and T2 reference were the lowest, while those of T1 and T2 vegan are the highest.

In 2023, the three samplings were carried out in March, July and September. In March 2023, after ploughing, T1 ρ_b remained similar for all rotations while T2 ρ_b increased. The ρ_b of T2 vegan increased to 1.71±0.07 g/cm³ and was higher (p-value<0.05) than the others. Diversified crops were sown in July 2023. In general, ρ_b were similar (p-value>0.05), except for T2 ICLS planted with permanent grassland, which dropped to 1.35±0.03 g/cm³. Finally, at the end of September 2023, when crops were well developed, T1 ρ_b were generally similar (p-value>0.05), whereas T2 ρ_b were more variable. The ρ_b of T2 ref with maize decreased to 1.42±0.03 g/cm³. T2 ref and T2 ICLS were lower (p-value = 0.05) than the other plots.

Changes in bulk density are generally used to monitor the dynamics of soil structure. These results already show temporal variations in soil structure over time and between plots in response to agricultural practices. However, no clear trend was observed for the growing seasons. These results, based on three soil sampling repetitions, may also depend on spatial variability and capture random behaviour.

5.2. Temporal evolution of in-situ soil water retention curves

Tables 24 and 25 show the start and end dates of the nine selected drying events, their initial and final SWRC values (θ_{max}, θ_{min}, pF_{min} and pF_{max}) and their slope for plots T1 and T2 respectively. For each drying period, to ensure that the same portion of the SWRCs were compared, the slopes between identical pF values, common to all plots were calculated (table 23). Figure 53 shows SWRCs obtained for the nine drying events, for all plots. It should be noted that values below pF of 1.95 are displayed horizontally and represent the measurement limit of Teros 21 potential sensors.

A first observation is that the shape and the position of SWRCs varies between years, within a growing season and between plots. The years are different in terms of SWRC variability. The year 2021 shows the lowest variability in water retention capacity, but the highest variability in slope. In contrast, the year 2023 shows the greatest variability in water retention capacity, demonstrating the impact of production systems and the importance of studies over several years.

Greater variability in SWRCs was observed between plots than over time. This suggests that agricultural practices and differentiated cropping have a greater influence on soil structure than crop development, WDs and meteorological conditions. The largest differences were found between T1 and T2 plots and between T1 plots. T2 plots are generally more similar, especially in 2021 and 2022. The most different SWRCs are T1 ref with sugar beet and T1 vegan with camelina as well as T1 ref and T1 ICLS with maize in 2021. For 2022, the main differences are observed between T1 ICLS and T1 vegan, respectively with winter wheat and faba bean, and between T1 ref and ref herb without or with herbicide.

Over time, within a growing season, greater variability in SWRCs was observed between WDs, than between years. Thus, root development and WDs seem to have a greater effect on soil water retention than inter-annual meteorological conditions. Within a growing season, the greatest variation was observed for plots T2 vegan in 2022 and T1 ref herb in 2022 and 2023. Between years, the greatest differences were obtained for plots T1 ref and T1 ref herb from 2021 to 2022.

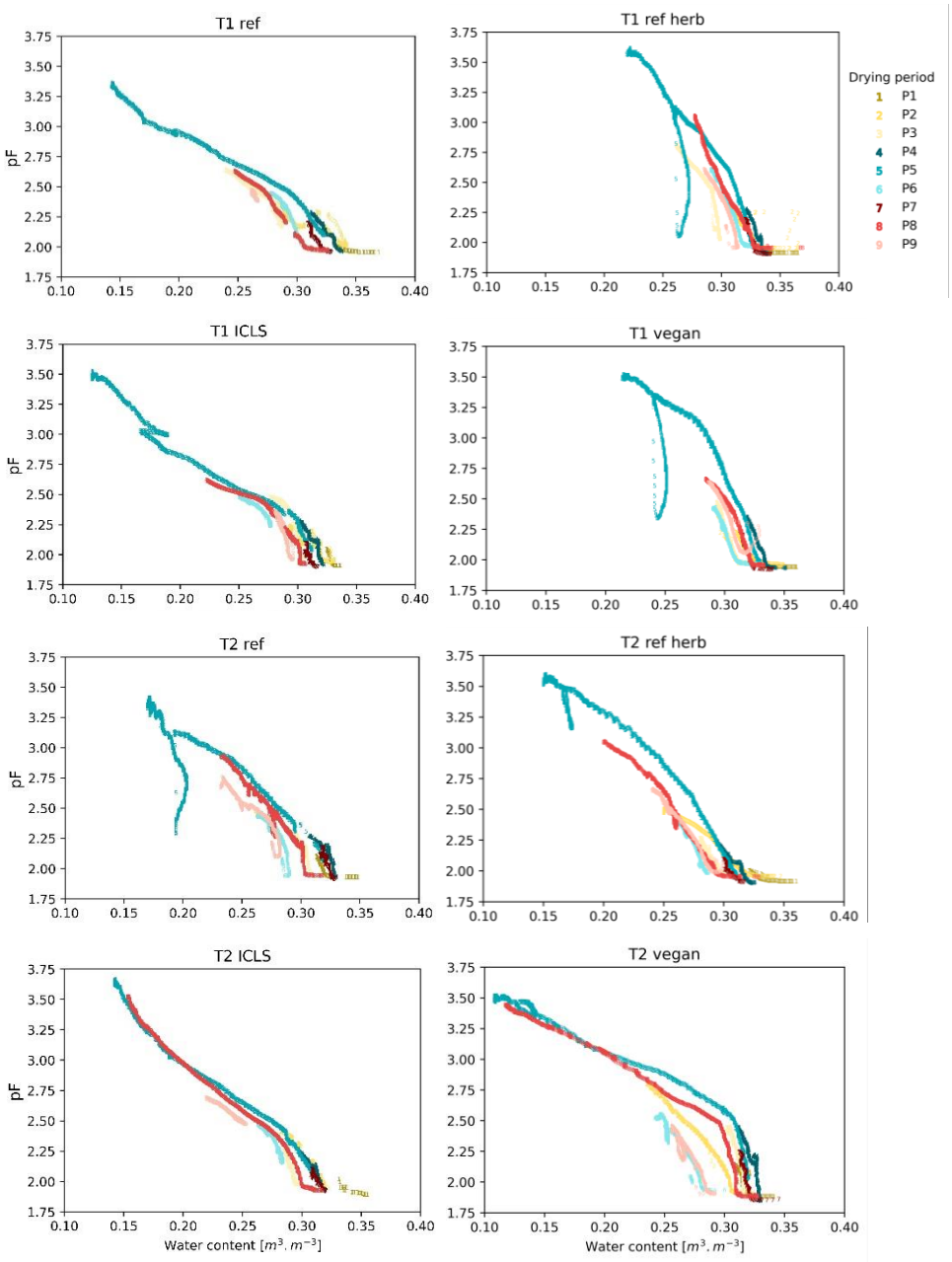

Figure 53. SWRCs for drying events P1 to P9 from 2021 to 2023 for the eight plots. The drying events are represented by numbers and the years by different colours.

Table 24. Description of the selected drying events with start and end dates, minimum and maximum soil water content (θ_{max} - θ_{min}), maximum and minimum log10 matric potential (pF) (pF_{min} - pF_{max}) and slopes calculated between identical pF values for each drying period (table 5-3) for the 4 plots of temporality 1 of the contrasting production systems studied.

Years	Event number	Start date	End date	T1 ref					T1 herb					T1 ICLS					T1 vegan				
				θ_{max}	θ_{min}	pF_{min}	pF_{max}	Slope	θ_{max}	θ_{min}	pF_{min}	pF_{max}	Slope	θ_{max}	θ_{min}	pF_{min}	pF_{max}	Slope	θ_{max}	θ_{min}	pF_{min}	pF_{max}	Slope
	P1	07-02-21	16-02-21	0.37	0.33	1.96	2.05	0.6	0.37	0.33	1.92	1.97	-	0.34	0.32	1.91	2.05	16.0	0.36	0.32	1.94	2.03	4.0
2021	P2	10-04-21	17-05-21	0.34	0.28	2.01	2.36	15.8	0.37	0.31	1.95	2.32	13.6	0.33	0.29	1.94	2.24	7.6	0.35	0.29	1.96	2.37	9.5
	P3	21-08-21	01-10-21	0.29	0.24	2.17	2.65	16.7	0.30	0.26	2.03	2.81	100.0	0.31	0.28	1.97	2.48	50.0	0.32	0.29	1.97	2.47	25.0
	P4	23-02-22	31-03-22	0.34	0.31	1.96	2.29	12.6	0.34	0.32	1.91	2.28	27.7	0.32	0.30	1.92	2.28	18.5	0.35	0.32	1.93	2.35	25.2
2022	P5	09-04-22	27-07-22	0.32	0.14	2.10	3.36	7.1	0.33	0.22	1.97	3.62	16.6	0.31	0.13	2.04	3.52	7.8	0.33	0.21	1.98	3.52	14.8
	P6	02-10-22	16-11-22	0.31	0.27	2.01	2.45	13.6	0.33	0.29	1.97	2.61	21.1	0.28	0.25	2.24	2.48	11.9	0.33	0.29	1.97	2.43	23.8
	P7	20-01-23	07-03-23	0.33	0.31	1.96	2.20	8.6	0.34	0.32	1.91	2.19	22.8	0.32	0.31	1.90	2.10	45.7	0.34	0.31	1.92	2.25	22.8
2023	P8	11-05-23	24-07-23	0.36	0.25	1.97	2.63	8.4	0.40	0.28	1.95	3.06	20.3	0.31	0.22	1.93	2.62	8.2	0.33	0.28	1.96	2.67	19.1
	P9	01-09-23	14-10-23	0.27	0.26	2.39	2.47	-	0.31	0.28	1.96	2.61	-	0.30	0.28	1.96	2.36	-	0.33	0.29	2.06	2.64	-

Table 25. Description of the selected drying events with start and end dates, minimum and maximum soil water content (θ_{max} - θ_{min}), maximum and minimum log10 matric potential (pF) (pF_{min} - pF_{max}) and slopes calculated between identical pF values for each drying period (table 5-3) for the 4 plots of temporality 2 of the contrasting production systems studied.

Years	Event number	Start date	End date	T2 ref					T2 herb					T2 ICLS					T2 vegan				
				θ_{max}	θ_{min}	pF_{min}	pF_{max}	Slope	θ_{max}	θ_{min}	pF_{min}	pF_{max}	Slope	θ_{max}	θ_{min}	pF_{min}	pF_{max}	Slope	θ_{max}	θ_{min}	pF_{min}	pF_{max}	Slope
	P1	07-02-21	16-02-21	0.35	0.31	1.93	2.11	16.0	0.36	0.32	1.92	2.00	8.0	0.36	0.33	1.90	2.02	-	0.34	0.31	1.88	2.14	16.0
2021	P2	10-04-21	17-05-21	0.31	0.26	2.05	2.48	27.1	0.35	0.25	1.96	2.51	10.6	0.32	0.28	1.95	2.42	11.2	0.32	0.24	1.90	2.81	15.8
	P3	21-08-21	01-10-21	0.31	0.29	1.97	2.31	12.5	0.30	0.28	1.99	2.27	16.7	0.30	0.28	1.98	2.27	100.0	0.32	0.30	1.91	2.45	33.3
	P4	23-02-22	31-03-22	0.33	0.31	1.93	2.27	17.3	0.33	0.29	1.90	2.24	11.5	0.32	0.30	1.93	2.24	14.6	0.33	0.31	1.85	2.45	30.8
2022	P5	09-04-22	27-07-22	0.32	0.17	2.07	3.41	8.9	0.31	0.15	1.97	3.60	10.9	0.31	0.14	2.02	3.66	8.6	0.32	0.11	2.03	3.52	7.3
	P6	02-10-22	16-11-22	0.29	0.26	1.94	2.46	10.6	0.29	0.26	1.99	2.48	14.6	0.28	0.26	2.16	2.47	13.6	0.32	0.24	1.93	2.55	10.6
	P7	20-01-23	07-03-23	0.33	0.32	1.92	2.18	45.7	0.32	0.30	1.91	2.10	19.6	0.32	0.31	1.92	2.10	19.6	0.35	0.31	1.85	2.25	68.5
2023	P8	11-05-23	24-07-23	0.32	0.23	1.94	2.93	16.2	0.33	0.20	1.95	3.05	15.1	0.32	0.15	1.93	3.53	11.8	0.33	0.12	1.88	3.44	17.5
	P9	01-09-23	14-10-23	0.28	0.23	2.10	2.76	-	0.30	0.24	1.99	2.67	-	0.25	0.22	2.47	2.69	-	0.29	0.26	1.91	2.46	-

5.2.1. Temporal evolution over WDs and years

Over time, water retention capacity, and therefore SWRCs shifts, follow the same general trend. During the course of a year, after ploughing, the SWRCs generally shift to the left during the WDs. This means that for the same value of pF, the water content decreases. Thus, the soil water retention capacity decreases between P1 and P3 for 2021, P4 and P6 2022 and P7 and P9 for 2023. The same trend is however not observed for the T1 plots in 2021. In that case, the SWRCs remain similar between P1 and P2 where cover crops are planted. In P2, before and after ploughing and sowing of crops, a discontinuity in SWRCs is observed. Then, between P2 and P3, the same pattern as in the other years is followed, with the SWRCs shifting to the left, indicating a reduction in water retention capacity.

At the beginning of each year, the SWRCs shift to the right, close to the values obtained at the beginning of the previous year. This indicates an increase in water retention capacity during winter and after the harvest. However, as the years go by, the SWRCs shift less to the right. Thus, between 2021 and 2023, decreasing water content close to saturation and retention capacity are noticed.

The steepness of the SWRCs also follows the same general trend, depending on the period and environmental conditions of the year. These differences could be due to the length of the drying periods. Therefore, slopes were only compared between plots for the same drying event. These slopes were calculated between common minimum and maximum pF values for all the plots in order to compare the same portion of the SWRCs.

5.2.2. Temporal evolution according to agricultural practices and crops

In 2021, water content (θ) generally remained above 0.25 m^3/m^3 for pF between 2 and 2.5. It should be noted that a threshold exists at pF 1.9, which corresponds to the measurement limit of the sensors. Ploughing and rapeseed sowing were carried out before P1 for plots T2. Ploughing and sowing of maize, sugar beet and camelina took place between P1 and P2 for plots T1. Crops were harvested during or after P3. For T1, the lowest θ_{min} is obtained at P3. Conversely, for T2, the lowest θ_{min} is reached at P2. However, P2 resulted in greater drying for all plots than P3.

During P2, θ_{min} ranged from 0.28 to 0.32 m^3/m^3 for T1 and from 0.24 to 0.28 m^3/m^3 for T2. T2 ref herb retains the least amount of water with a decrease of 0.1 m^3/m^3 to reach a θ_{min} of 0.24 m^3/m^3.

In contrast, at P3, θ_{min} ranged from 0.24 to 0.29 m^3/m^3 for T1 and from 0.28 to 0.30 m^3/m^3 for T2. Decreases in water content were more pronounced for T1 ref and T1 ref herb with sugar beet. The SWRC of T1 ref showed a lower water retention capacity with a flatter slope than T1 ref herb. The SWRC of T1 vegan with camelina shows the greatest water retention capacity.

In general, during 2021, the T2 SWRCs were further to the left and steeper than the T1 SWRCs, indicating a lower water retention capacity and could indicate a more compact soil.

In 2022, the spring-summer drought led to a wider range of the field SWRCs than in 2021. Winter wheat (+peas) was sown after a ploughing before P4 and harvested between P5 and P6.

P4 was the least marked drying period of 2022. θ_{min} range from 0.31 to 0.29 m^3/m^3 for pF between 1.8 and 2.4. The T1 vegan had the highest water retention capacity with a SWRC further to the right. Between P3 at the end of 2021 and P4 at the beginning of 2022, the SWRCs of T1 ref and T1 ref herb with sugar beet in 2021 had the greatest increase in water retention capacity, with a larger shift to the right than for the other plots. In addition, these two plots are steeper despite ploughing. This may indicate greater soil compaction or the influence of non-equilibrium flows and air trapped in the pore network.

P5 is the longest and most severe of the nine selected drying events. The initial θ_{max} and pF_{min} were similar for all plots. However, the final θ_{min} were highly variable between plots. They ranged from 0.13 to 0.22 m^3/m^3 for T1 and from 0.11 to 0.17 m^3/m^3 for T2 for pF between 3.4 and 3.7. For T1, θ_{min} of T1 ref herb was the highest with 0.22 m^3/m^3. Greater water retention capacity was also evident on this plot. Following, T1 vegan had a higher water retention capacity than the other T1 plots cultivated without chemical herbicide. Its θ_{min} was 0.21 m^3/m^3. T1 ref and T1 ICLS followed with lower θ_{min} of 0.14 and 0.12 m^3/m^3. T1 ICLS showed the lowest water retention capacity of all T1 plots as in P4. T2 generally retained less water than T1. T2 vegan showed the greatest drying with a drop of 0.20 m^3/m^3. It also had the lowest water retention capacity of all plots.

At the beginning of P6, the plots had not returned to near saturation water content. The θ_{max} were therefore more variable than in P4 and P5. As in P5, T2 vegan showed the greatest decrease in water content with θ falling from 0.32 to 0.24 m^3/m^3. The drying of the other plots was more similar, with decreases in θ between 0.04 and 0.02 m^3/m^3. As in P5, T1 ref herb and T1 vegan have the highest water retention capacities for similar slopes.

In 2023, crops were diversified between plots and SWRCs had varied shapes. Ploughing was carried out before P7 and sowing took place between P7 and P8. Crops were harvested after P9. P7 showed the lowest water loss of 2023 with drying between 0.01 and 0.04 m^3/m^3. The θ_{min} were between 0.31 and 0.32 m^3/m^3 for T1 and 0.30 and 0.32 m^3/m^3 for T2 for pF between 1.9 and 2.2. The retention curves were similar for all the plots.

P8 is the most significant drying event in 2023. Plots T1 ref and T1 ref herb with potato had the highest soil water retention capacity. Their θ_{min} were 0.25 and 0.28 m^3/m^3 respectively. However, T1 ref herb had a SWRC more than twice as steep as T1 ref for the same crop, indicating finer porosity. T1 vegan with faba bean followed and had the lowest decrease in θ (0.05 m^3/m^3). T1 ICLS, also with faba beans, had the lowest retention capacity of T1 plots as in 2022. However, it had one of the lowest water drying (0.09 m^3/m^3) of the plots and reached a θ_{min} of 0.22. In general, T2 plots had lower θ_{min} and water retention capacities than T1. In addition, their SWRCs were more similar to each other. The T2 vegan with peas showed the greatest decrease in θ as in 2022 (0.21 m^3/m^3) to reach a θ_{min} of 0.12 m^3/m^3. The T2 ICLS, where the grassland is established, was close with a decrease of 0.17 m^3/m^3 for a θ_{min} of 0.15 m^3/m^3.

At P9, the plots showed the lowest water retention capacities of the three years. The θ_{max} were lower than for P7 or P8. T1 ref herb and T1 vegan had the highest water retention capacities, as in 2022 and early 2023. A significant difference between T1 ref herb and T1 ref with potato was observed with higher θ_{max} and θ_{min} with herbicides. T2 had similar water retention capacities, which were still lower than T1 plots. T2 ref and ref herb with maize had the largest dryings (0.05-0.06 m^3/m^3) with θ_{min} of 0.23 and 0.24 $m^3/^3$. T2 ICLS with grazed grassland showed the lowest θ_{max} and θ_{min} and the lowest water retention capacity.

5.3. Comparison with laboratory and theoretical SWRCs

Comparisons between EU-HYDI, laboratory and field SWRCs for the year 2022 for the 4 plots T1 are shown in Figure 54. For T1 ref herb, only two replicates are shown due to inconsistent results for the third replicate. The laboratory SWRCs show variability between replicates, mainly in the wet part of the curves. However, the replicates are similar above pF 2. The laboratory curves reach a limit around pF 3 due to material limitations.

The same trends were found for the 4 plots. The EU-HYDI SWRCs are generally further to the right, showing higher water retention capacities than the reality in the field. The θ_s are larger for EU-HYDI SWRCs than for the laboratory SWRCs and are generally close to the actual measured porosity. Field SWRCs, on the other hand, are further to the left. The EU-HYDI SWRC seems to be a better fit to the field curves for the plot T1 ref herb, with the most conventional agricultural practices.

The laboratory SWRCs are between the EU-HYDI and field SWRCs. They also show higher water retention capacities than the field reality. These curves were obtained from soil samples taken at the beginning of the third drying period in 2022 (P6). However, the field SWRCs for P6 are the furthest away from the laboratory curves.

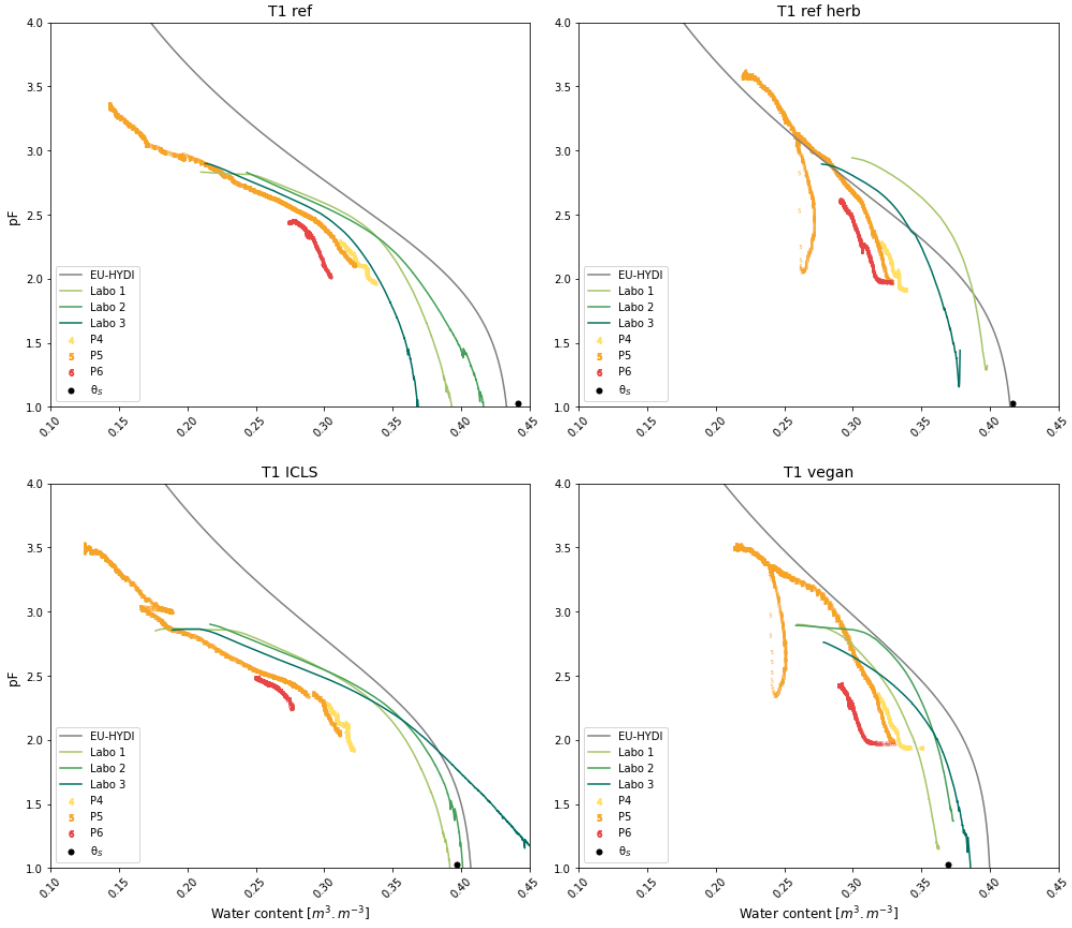

Figure 54. Comparison of SWRCs obtained by PTF EU-HYDI, in the laboratory on undisturbed samples and continuously in the field for the year 2022 and the four plots T1. The total porosity measured is shown as a black dot.

The slopes of the EU-HYDI, laboratory and field P5 SWRCs between pF 2 and 2.83 are shown in Table 24. The P5 was chosen for the comparison because it represents the most significant drying period in 2022. In addition, it allowed the slope to be calculated between the same pF values.

The slopes of the EU-HYDI SWRCs are generally lower than those of the P5 field, mainly for the T1 ref herb and T1 vegan plots. The highest slopes are for T1 ICLS and T1 vegan, due to the higher organic carbon content. The slopes of the laboratory SWRCs are also lower than those of the P5 field SWRCs, but are getting closer. Furthermore, the same trends were found, with steeper curves for T1 ref herb and T1 vegan, as observed for the field curves.

Table 26. Water contents max and min corresponding to pF of 2 and 2.83 and slope for SWRCs obtained with EU-HYDI PTF, in laboratory and in the field for the P5 drying event.

SWRC Type	Replicate	T1 ref			T1 ref herb			T1 ICLS			T1 vegan		
		θ_{max}	θ_{min}	Slope	θ_{max}	θ_{min}	Slope	θ_{max}	θ_{min}	Slope	θ_{max}	θ_{min}	Slope
FPT		0.44	0.29	5.5	0.42	0.29	6.4	0.41	0.3	7.5	0.4	0.32	10.4
Lab	1	0.36	0.21	5.5	0.39	0.33	13.8	0.36	0.24	6.9	0.34	0.29	16.6
	2	0.37	0.24	6.4	/	/	/	0.37	0.24	6.4	0.36	0.31	16.6
	3	0.34	0.23	7.5	0.36	0.3	13.8	0.37	0.22	5.5	0.36	0.28	10.4
Field	P5	0.32	0.22	8.06	0.33	0.29	21.3	0.31	0.2	7.41	0.33	0.3	27.7

6. Discussion

6.1. Temporal evolution of in-situ soil water retention curves

SWRCs varied greatly between years, seasons and plots. This shows the influence of meteorological conditions, wet-drying cycles (WDs), root development and agricultural practices on soil structure. This variability has already been reported over time and between different tillage systems (Zhang et al., 2018; Huang et al., 2021; Pečan et al., 2023).

Pečan et al., 2023 showed that root system development and environmental conditions within a season influenced soil structural dynamics and SWRC shape more than tillage system. Our study suggests that agricultural practices and crop differentiation have a greater influence on water retention dynamics than root development and WDs within a season or weather conditions between years. Crop differentiation had the most pronounced effect, followed by weed management. The results also showed a clear effect of soil compaction during harvest and of the establishment of temporary grassland.

It should be noted that the differences between plots may be partly due to spatial variability on the plots studied. The SWRCs analysed were derived from a pair of sensors per plot. The results presented therefore correspond to the volume of influence of the sensors placed in the middle of the plots. Nevertheless, the aim of this study is to investigate the temporal evolution of SWRCs. The sensors were not displaced during the experiment. The differences in the temporal evolutions between plots therefore reflect contrasting changes in soil properties.

The spatio-temporal variability of SWRCs is complex and depends on many physical phenomena. However, not all of these phenomena have been measured and therefore remain hypothetical. The interpretation of the SWRCs variability is based on knowledge of the plots and crops, visual observations and the most reasonable explanations.

6.1.1. Temporal evolution over WDs and years

Over time, greater variability in SWRCs has been observed within a growing season than between years. Thus, our study suggests a greater influence of root system development and WDs than of meteorological conditions between years.

In general, water retention capacity decreases over the growing season for relatively stable bulk densities. SWRCs start at progressively lower water contents close to saturation. After each WD, rewetting rates decrease. Similar behaviour has been observed by Herbrich and Gerke, 2017. Huang et al., 2021 reported the same trend, but only for non-tillage plots. Typically, a greater variation in water retention capacity was observed after the most intense drying event. These seasonal dynamics may reflect changes in effective wettable porosity and contact angles after each WDs as described by Herbrich and Gerke, 2017 and Lourenço et al., 2015. The lower rate of rewetting may also be due to air trapped in the soil pores during drying events (Zhao et al., 2020; Huang et al., 2021). The development of the root system and the increase of biological activity during the growing season may have led to a reduction in the water retention capacity through pore clogging, aggregates breaking up and macropores formation as described by Lu et al., 2020. Large numbers of earthworm galleries were generally observed in all plots during field sampling at 30 cm.

Each year, during the wet and vegetation-free winter period (figure 55), water retention capacity increases. Ploughing can play a role by aerating the soil to a depth of 25 cm, facilitating water infiltration. Air trapped in the pores can also be released more easily. In fact, our study shows that without winter ploughing, SWRCs are less variable over time, as observed by Huang et al, 2021. Indeed, the SWRCs of plots T1 remained similar between P1 and P2 due to the presence of the cover crops, in contrast to plots T2. The same observation was made for plot T2 ICLS where permanent grassland was established between P6 and P7.

Figure 55. Bare soil after ploughing in February 2023, with the exception of the meadow in plot T2 ICLS

6.1.2. Temporal evolution according to agricultural practices and crops

Temporal changes in SWRCs are compared with changes in bulk density. The differences observed between systems are interpreted in terms of the factors influencing the hydraulic properties.

Production systems at temporality 1

In 2021, the dynamics of water retention varied between the T1 plots depending on the crop, indicating a short-term effect (figure 56). T1 vegan with camelina had the highest water retention capacity, probably due to its shallow root system. T1 ICLS and T1 vegan generally had steeper slopes and higher bulk densities than T1 ref, indicating a more compact soil with finer porosity than under sugar beet. The lower water content in plots T1 ref and T1 ref herb may be due to greater water consumption by the beets and higher interception of rainfall by their leaves.

Figure 56. On the left, T1 plot ref herb with sugar beet and on the right T1 Vegan plot with camelina in July 2021

In 2022 and 2023, in the T1 plots without herbicide, T1 vegan had the highest water retention capacity and a steeper slope. It also had a higher bulk density of 1.66 g/cm³. As a result, the soil is more compact with finer porosity. This plot also produced the highest wheat yield in 2022 with 8.12 t/ha compared to 6.12 t/ha and 6.84 t/ha for plots T1 ref and T1 ICLS. These differences may be due to the chaffing and stubble ploughing of camelina and the use of light agricultural machinery for harvesting. A higher percentage of OM was measured in the soil of this plot in 2022 with 10.4% compared to 2.5% for T1 ref and 5.4% for T1 ICLS. In addition, this plot showed the lowest variability of SWRC over time. The pore system seems to be more stable over time. Thus, following our observations, the vegan production system at T1 should be more resilient in the face of extreme climatic conditions. Our observations are in agreement with Ball et al., 2005 who showed the importance of crop rotation and the addition of OM to the soil to preserve soil structure.

In 2022 and 2023, plot T1 ICLS had the lowest water retention capacity of the T1 plots, despite having a higher OM percentage than T1 ref and ref herb. This may be due to the large and deep root system of maize in 2021. The soil has more interconnected macropores, allowing greater water infiltration. In 2023, despite the presence of faba bean on plots T1 ICLS and T1 vegan, both plots still showed very contrasting water retention behaviour. This contrast demonstrates the influence of the 2021 crop in 2023 and therefore of the rotation in this case. As a result, this production system showed low resilience to drought for T1.

The same crops were planted on plots T1 ref and T1 ref herb. The only difference was the use of synthetic herbicides (ref herb) or shallow hoeing (ref) as weed management strategies. Over the three years, T1 ref herb showed greater water retention and less drying out. It had a higher bulk density and a steeper SWRC. As a result, the herbicide-treated plot had finer porosity and a more compact soil at 30 cm. Wheat yields in 2022 were similar (6.12 t/ha), as were OM contents (2.5 and 2.3%). The difference may be due to the higher density of weeds, whose roots took up more water, and the more frequent hoeing in T1 ref, which aerated the soil (figure 57). Indeed, 5.4 g/m² of weeds (dry matter) were measured for T1 ref herb compared to 12.9 g/m² for T1 ref.

Figure 57. On the left, plot T1 ref herb with sugar beet and herbicides and on the right plot T1 ref with sugar beet without herbicide and the presence of a large number of weeds.

Between late 2021 and early 2022, T1 ref and T1 ref herb showed a greater increase in retention capacity than the other plots. In addition, their higher bulk densities than at the end of 2021 indicate soil compaction. This compaction may be due to the harvesting of sugar beet with heavy agricultural machinery in November 2021, when the soil was very wet.

In 2023, plots T1 ref and T1 ref herb had higher θ_{max} than the other plots, despite similar bulk densities. The ridges of the potatoes aerated the soil surface, allowing water to infiltrate more easily to a depth of 30 cm. The ridges were also able to retain water for longer, thereby promoting infiltration. The difference may also be due to the lower rainfall interception of the potato crop compared to the faba beans, which contain many weeds and form a denser canopy (figure 58).

Figure 58. On the left, T1 ICLS plot with faba beans and on the right, T1 ref plot with potatoes in September 2023.

Production systems at temporality 2

Water retention behaviour of T2 plots were more similar than T1 plots and less variable over time.

Over the three years, T2 plots showed lower water retention capacity and more severe dryings than T1 plots. During rainfall, water content peaks were more pronounced in T2 than in T1. In 2021, rapeseed was sown on T2 plots from September 2020. In 2021, the rape was well developed and the roots took up more water (figure 59). In addition, the root development and the macroporosity created by the biological activity have resulted in a more aerated soil with greater water infiltration. The well-developed rapeseed crop with many weeds resulted in a denser canopy. Greater rain interception could partly explain the differences between plots T1 and T2 in 2021. The effect of the extensive root system is still visible two years after the end of the crop. The same observation was made for plot T1 ICLS in 2021 and for plots T2 ref and T2 ref herb in 2023 when maize was grown. Deeper, more developed root systems, such as those found in rape and maize crops, can lead to the formation of macropores and greater infiltration of water into the soil. Thus, different crops, and therefore different root systems, can generate different water retention dynamics in the short term.

Figure 59. T1 plots at the front with bare soil and T2 plots in the background with rapeseed already well developed in May 2021.

Permanent grassland was established on plot T2 ICLS in September 2022 (figure 60). In 2023, the pasture grazed by sheep resulted in a significant reduction in water retention capacity and bulk density. The introduction of the grassland could therefore result in soil aeration and increased deep water infiltration capacity. The fact that the soil was left undisturbed resulted in the development of interconnected macropores. These are the result of root growth, canopy density and biological activity in the soil. Our results contradict those of Jensen et al., 2020. They found an increase in bulk density and no difference in water retention capacity in the short term when a grassland was established. However, they did not plant the same species. In addition, their study focused on conversion from bare soil to grassland and not from cropland to grassland as in our case.

Figure 60. T2 ICLS plot with temporary meadow grazed by sheep.

In 2022 and 2023, the T2 vegan plot had the lowest water retention. In contrast to the other T2 plots, only winter wheat was sown in 2022. The yield was the highest of all plots with 9.36 t/ha. Its OM percentage of 2.84% was comparable to the other plots. In the year 2022, plot T2 vegan had the highest bulk density of all the plots. McDaniel et al., 2014 have shown that rotations with the number of crops and their type lead to the development of macropores due to different plant root systems and biological activity. In our study, the rape-winter wheat-pea rotation produced the lowest water retention of the plots, with the highest porosity and therefore a more aerated soil. Despite the greater water retention capacity and resilience of the vegan production system in T1, the opposite trends were observed for T2.

6.2. Comparison with laboratory and theoretical SWRCs

The theoretical SWRCs show higher water contents than the other curves. The EU-HYDI database is based on curves obtained in the laboratory using the pressure plate or sandbox method (Tóth et al., 2015). These methods tend to produce SWRCs with higher θ_s than the evaporative methods used in this paper. The steeper slope of the T1 vegan plot could be explained by the higher OC content at 30 cm, due to the shredding and stubble ploughing of the camelina straw. This profile results in greater soil water retention than the other plots.

The EU-HYDI database was chosen because it is more recent and geographically determined for Central Europe (Tóth et al., 2015). In addition, it takes into account a larger number of factors that strongly influence soil hydrological behaviour. However, the SWRCs obtained with the EU-HYDI PTFs do not provide an acceptable representation of the water retention behaviour for most of the plots. EU-HYDI SWRC fits plot T1 ref herb more closely. Therefore, these PTFs seem to better represent more conventional agricultural practices. As a result, the diversity of management practices for agricultural plots is not sufficiently integrated into the PTFs.

Laboratory SWRCs are between theoretical and field SWRCs, but still show higher water retention capacities than field measurements. Laboratory SWRCs only reflect the water retention of a soil structure condition at the time of sampling. The slopes of the laboratory SWRCs are close to those of the field and show similar trends between plots. However, they remain lower. In addition, the differences in slope between plots are less pronounced than in the field. Herbrich and Gerke, 2017 and Huang et al, 2021 also obtained steeper SWRCs in the field than in the laboratory. The higher soil water retention capacity obtained with laboratory SWRCs can be attributed to the higher water content of undisturbed samples. In fact, saturation of the samples in the laboratory occurs from below. The water flows upwards through the sample, allowing the air in the pores to escape. In the field, however, heavy rainfall usually results in rapid wetting of the soil. This traps air in the soil pores and reduces the water retention capacity. This factor is one of the main causes of the hysteresis phenomenon, which partly explains the differences between the field and laboratory curves (Hannes et al., 2016; Pečan et al., 2023). Huang et al., 2021 also observed that field SWRCs had lower θ for the same pF than laboratory SWRCs. Furthermore, they showed that the effects of different tillage practices were less visible in laboratory SWRCs than in field SWRCs. Therefore, laboratory SWRCs are not optimal for investigating the temporal evolution of water retention properties as a function of meteorological conditions and agricultural practices.

However, the laboratory SWRCs are close to the measured total porosity and allow for the lack of field data below pF 1.96. Due to the lack of field SWRC data, consistency with the laboratory SWRC for the wet part cannot be confirmed. In addition, there is still uncertainty regarding whether full saturation can be achieved in the field.

7. Conclusion

In this study, the impacts of different contrasting production systems and contrasting climatic conditions on the temporal evolution of SWRCs were analysed in the field over three years. Field SWRCs were then compared with those obtained using an EU-HYDI PTF and in the laboratory on undisturbed samples.

The results indicate a high degree of variability in SWRCs over time and between production systems. The greatest variability was found between plots, then within a season and finally between years. This study has therefore shown that agricultural practices and different crops can have a greater influence on soil water retention dynamics than the sole root development and WDs within a season or meteorological conditions between years.

Over a season, water retention decreases with wet-drying cycles (WDs) and root development. This can be due to the decrease in effective wettable porosity as a result of air trapped in soil pores and the development of macropores resulting from the root system and biological activity. After each winter, the water retention capacity increases again as a result of ploughing to 25 cm and high soil moisture. Over the years, however, a decrease in retention capacity has been observed.

Our research shows that agricultural production systems have an influence on soil water retention behaviour. The results suggest that variations in the soil water retention behaviour can be induced by crop differentiation, weed control, crop residue management, compaction during harvest or the introduction of temporary grassland. Different soil drying dynamics were observed and some agricultural practices were identified as influencing the soil water retention behaviour for at least 2 years. This study therefore shows that agricultural practices and crops can be a lever for contributing to greater food resilience against future climatic conditions. This work has shown that crops and crop rotations can affect soil water retention.

The SWRCs obtained from the EU-HYDI PTFs are not a good representation of the field SWRCs, particularly for non-conventional agricultural practices. As a result, PTFs need to integrate a wider variety of management practices for agricultural plots. The laboratory SWRCs are closer to the field curves with similar trends. However, the differences in SWRCs between different modalities may be less visible. In the short term, these curves are therefore not optimal for investigating the temporal evolution of water retention properties as a function of meteorological conditions and agricultural practices.

Therefore, in order to assess the relevance of production systems for tomorrow's needs, studies should focus on the impact of multi-crop production systems on the dynamics of soil water retention. In addition, continuous measurements of SWRCs in the field should be prioritised. Finally, the variability of soil hydraulic properties in the short, medium and long term must be taken into account in the models in order to generate more relevant management decisions.

Chapter 6

A comprehensive database for evaluating the impact of contrasting innovative agricultural systems on soil water dynamics and agrochemical leaching

1. Synopsis

Chapter 6 is based on all the data collected over a four-year period, from 2020 to 2024, from the hydrological monitoring of the transition to production systems. This database includes the description of the data from the water content and water potential sensors placed in the first three soil horizons. The results of nitrate and pesticide analyses in the drainage water 1.2 m below the different systems are also examined. This chapter deals with objective 8 of this thesis.

This chapter is based on the publication: Pirlot, C., De Clerck, C., Blondel, A., Pigeon, O., Krings, B., Colinet, G., Degré, A., 2025. A comprehensive database for measuring the impact of contrasting agricultural systems on soil water dynamics and agrochemical leaching. Geosci. Data J. Under review.

2. Abstract

Understanding the temporal evolution of soil hydraulic properties and soil structure is essential for advancing agricultural sustainability and adapting to climate change. This article presents a unique dataset resulting from the first four years of continuous hydrological monitoring of contrasting production systems using alternative agricultural practices. This database is part of the EcoFoodsystem experiment, a 16-year research initiative comprising four contrasting production systems: the reference system with and without herbicides, the integrated crop-livestock system and the vegan system. These systems include eight-year rotations implemented in two temporalities on eight loamy plots at the Terra teaching and research centre in Gembloux, Belgium. From October 2020 to December 2024, high-frequency measurements were recorded every 15 minutes using Teros 12 and Teros 21 sensors (Metergroup) installed at depths of 30, 60, and 90 cm and connected to ZL6 data logger. The dataset includes soil water content, electrical conductivity of the soil solution, soil temperature, and soil water potential measured every 15 minutes. Complementary measurements of the evolution of soil bulk density at the same depths, obtained from preserved soil cores and taken several times a year, enrich the data set. Additionally, EcoTech glass suction plates installed at 1.2 m depth in each plot provide data on leaching of pesticides, metabolites, and nitrate. This comprehensive database offers valuable insights into the temporal dynamics of soil hydraulic properties, soil structure and agrochemical leaching under diversified systems. By monitoring them at multiple depths and over time, the data can inform sustainable soil and water management practices, support environmental protection, and improve the predictive performance of hydrological and agroecosystem models. This resource is a critical tool for researchers for assessing the transition to sustainable agriculture, addressing challenges such as climate resilience, food security and environmental protection.

3. Dataset details

DOI identifiers: XX
Creator: Clémence Pirlot
Dataset correspondence : clemence.pirlot@uliege.be, aurore.degre@uliege.be
Name of dataset:
Data centre : DataVerseNL Université de Liège.
Publication year: 2025
Version : 1.0.

4. Introduction

Today, many environmental challenges depend directly on the dynamics of water in the soil. These concerns include sustainable agricultural production, food security, nutrient cycling, carbon storage, adaptation to climate change, and protection of clean water resources. Climate change will have multiple impacts on the water cycle, leading to an increase in droughts or periods of heavy rainfall (Jehanzaib et al., 2020). It is anticipated that agriculture will become increasingly dependent upon available water resources. Consequently, enhanced management strategies will be required in order to support the resilience of agricultural systems (Pereira, 2017; Arora, 2019). Additionally, the use of agrochemicals gives rise to a number of concerns pertaining to the contamination of soil and groundwater resources and to human health (Herrero-Hernández et al., 2013; WWDR, 2015; Larsen et al., 2019; Pietrzak et al., 2019; Baran et al., 2021).

A key strategy is the implementation of more sustainable agricultural systems to conserve water and limit the leaching of agrochemicals. The adoption of alternative agricultural practices is becoming increasingly widespread. These include long and diverse rotations, grazing periods, cover crops and limited use of agrochemicals (Piñeiro et al., 2020). However, further investigation is required to assess the relevance of these new practices in relation to soil structure and water and solute transport. The effects of these alternative practices on soil structure vary and occur at different timescales (Chandrasekhar et al., 2018; Heitman et al., 2023).

Hydraulic properties are the basis of water and solute flow in soils. These properties are typically defined as the soil's water retention function and its hydraulic conductivity function (van Genuchten, 1980). They will influence the water cycle with the processes of evaporation, infiltration, run-off, groundwater recharge, contaminant transport and water availability (Whalley et al., 2013; Ciocca et al., 2014). The water retention function of the soil is defined by the relationship between volumetric water content (θ) and water potential (h). The soil's capacity to retain water is reflected in its water retention potential (h), which also provides insights into its structure, water retention capacity, wilting point and available water content (Rabot et al., 2018). The

movement of water and solutes, including their infiltration into the soil, is governed by K(h).

Water content sensors are an essential tool for acquiring data at various scales, including laboratory, field, and canopy levels. Soil water potential data is also important for understanding many aspects of water behaviour, such as water retention, changes in suction stress, hydraulic conductivity, thermal conductivity and biological activity. It quantifies the change in the energy level of the soil water due to the physicochemical interactions between the soil particles and the water molecules (van Genuchten, 1980; Lu and Dong, 2015; Luo et al., 2022).

Hydraulic properties are often considered as invariable soil properties, determined on laboratory samples or using pedotransfer functions. However, several studies have shown that these properties are dynamic and will change over time (Martini et al., 2021). A variety of factors have an impact on them, including agricultural practices, crop species, the growth of vegetation and climatic conditions (Tifafi et al., 2017; Blanco-Canqui and Wortmann, 2020; Lu et al., 2020; Pečan et al., 2023; Pirlot et al., 2024). In addition, many factors will also influence the fate of agrochemicals in soils, such as their properties, soil characteristics, agricultural practices, site conditions, and application practices (Arias-Estévez et al., 2008; Grodner et al., 2014; Rasool et al., 2022; Pirlot et al., 2025a). However, the variability of soil structure and hydraulic properties is rarely studied in the field or included in models due to a lack of available data. This results in erroneous predictions and suboptimal decision-making (Chandrasekhar et al., 2018; Baroni et al., 2019).

Hydraulic properties are important for modelling water and solute flows in soils, but also for predicting and making decisions about floods, droughts, contaminations and landslides. Monitoring these properties is also a prerequisite for the calibration of remotely sensed soil moisture using satellite imaging or ground-penetrating radar (Albergel et al., 2012; Ochsner et al., 2013; Vereecken et al., 2015). Indeed, experimental approaches frequently require integration with digital models to ensure a comprehensive representation of the system's properties (Martini et al., 2021).

Accordingly, it is necessary to improve the representativeness of hydrological processes in the models, which remains one of the greatest scientific challenges (Clark et al., 2017). The necessary data include soil moisture data, groundwater measurements, soil temperature, soil water storage, etc (Wanders et al., 2014; Zink et al., 2018; Baroni et al., 2019). The performance of these hydrological models can thus be improved based on real in situ measurements at various spatial and temporal scales (Robinson et al., 2016; Clark et al., 2017). Thus, in-situ measurements of water content and water potential are an indispensable source of information (Liu et al., 2011). In addition, continuous long-term observations make it possible to reveal changes in these hydraulic properties and identify temporal trends in soil water

dynamics (Strudley et al., 2008; Vogel, 2019). The few studies that have included the dynamics of hydraulic properties in the models have shown more reliable predictions and results (Alletto et al., 2015; Geris et al., 2021).

It is therefore essential to study the long-term evolution of hydraulic properties directly in the field under contrasting cropping systems including more sustainable practices. In this article, we present the data acquired during the first four years of continuous hydrological monitoring of different production systems contrasted with sustainable agricultural practices in order to make them available to the scientific community. This monitoring will make it possible to study their relevance for the future and to acquire data for implementation in the models.

5. Data description and development

5.1. Site and experiment description

Hydrological monitoring is carried out on the EcoFoodSystem experimental plots (50°56‘50.6’‘N, 4°70'93.2'' E) of the Terra teaching and research centre in Gembloux, Belgium. The soil is agricultural silt. According to the World Reference Base for Soil Resources, the soil is a Cutanic Luvisol (FAO, 2015). The climate is temperate oceanic with an average annual temperature of 10.2°C and average annual rainfall of 837 mm. The meteorological data were collected from the Ernage-Gembloux station, located less than 2 km from the experimental plots.

Three contrasting production systems with 8-year rotations have been developed to anticipate the needs of potential future food scenarios. These systems have been developed to align with the recommendations of the EAT-Lancet Commission for healthy and sustainable eating (Eat Lancet Commission, 2019). They include more sustainable and environmentally friendly practices such as long rotations, diverse crops, intercropping and cover crops, grazing periods and the responsible use of agrochemicals.

The first system is called 'reference'. The animal is integrated into the system through the flow of agricultural by-products such as fodder and the input of organic matter of animal origin, such as manure. This system has been implemented with two variants, with (ref herb) and without (ref) the use of herbicides on the plots. In the first case, only chemical herbicides are used in accordance with good agricultural practices. In the second case, no chemical pesticides are applied. The use of other types of pesticides is prohibited. The second system is called Integrated Crop Livestock System (ICLS). In this system, the animal is integrated through grazing periods of cover crops and two-and-a-half years of temporary grassland. This rotation is managed without the use of chemical pesticides. The third rotation, called 'vegan', is based on a future where animals are no longer part of the system. The rotation is

designed to meet human nutritional needs. The 'vegan' designation is derived solely from the use of crops intended exclusively for human consumption and the absence of inputs of animal products such as manure. This rotation is also managed without the use of chemical pesticides.

In September 2020, the four rotations were implemented at two time points, corresponding to year 1 of the rotations (T1) and year 5 of the rotations (T2) on eight adjacent 18x84 cm plots. The principle was to observe all crops of the eight-year rotations in four years. All plots were homogenised with one year of winter wheat before the start of the experiment. Leaf index area and aerial biomass results showed a high degree of uniformity in wheat growth across the eight plots. In addition, winter wheat returns to all rotations every two years as an internal reference for comparison between systems.

The agricultural operations carried out on the 8 plots from September 2020 to December 2024 are illustrated in Figure 61. The detailed technical itineraries are included in the data repository.

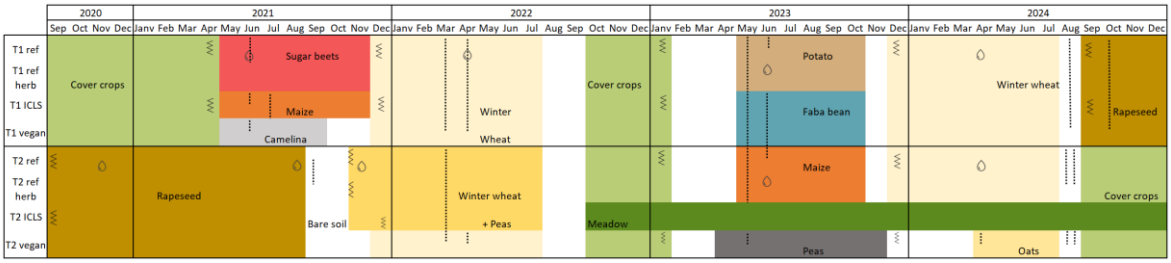

Figure 61. Agricultural operations and crops from September 2020 to December 2024 on the eight EcoFoodSystem experimental plots. The colours represent the different crops, the zigzags indicate ploughing to a depth of 25 cm, the dotted lines refer to soil treatment (hoeing, harrowing or rotary hoeing) to a maximum depth of 5 cm and the drops correspond to herbicide application.

5.2. Soil water monitoring

Hydrological monitoring was set up on the eight experimental plots to monitor the hydraulic properties of the soil in the first three horizons and the leaching of agrochemicals into the drainage water. Water content and matric potential sensors were installed, as well as soil water sampling plates.

Teros 12 capacitance sensors (Meter Group, Inc., Pullman, WA, USA) were used. They measure the volumetric water content (VWC) of the soil. These sensors use a frequency of 70 MHz to minimise the effects of texture and salinity. They measure VWC over a wide range of values between 0.00-0.70 m^3/m^3 with a resolution of 0.001 m^3/m^3 and an accuracy of 0.01-0.02 m^3/m^3 with calibration. The temperature of the

soil is also measured by means of a thermistor in the central needle, in the range -40 to 60°C. Its resolution is 0.1°C and its accuracy is 1°C from -40 to 0°C and 0.5°C from 0 to 60°C. Finally, they measure the electrical conductivity of the environment using a stainless steel electrode array in the range 0-20 dS/m with a resolution of 0.001 dS/m and an accuracy of 5% from 0-10 dS/m and 8% from 10-20 dS/m. These sensors require low power, making them suitable for permanent burial and continuous measurement over long periods.

Teros 21 soil water potential sensors (Meter Group, Inc., Pullman, WA, USA) were selected to measure soil water potential over a range of -9 to -2000 kPa (1.95-4.31 pF) with a resolution of 0.1 kPa and an accuracy of 10% between -2000 and -100 kPa and of 10%+2 kPa between -100 and -9 kPa. They also use a frequency of 70 MHz. They measure the soil temperature between -40 and 60°C with a resolution of 0.1°C and an accuracy of 1°C. They consist of two porous ceramic discs sandwiched between stainless steel screens and the circuit wide. These probes require good hydraulic contact with the surrounding soil for accurate measurements.

MeterGroup ZL6 data loggers were used to easily connect the Teros 12 and 21 sensors. The ZL6 is a data acquisition station for up to six sensors with 3.5mm stereo connectors. It also has a micro-USB port for communication with a computer. Readings can be taken from the sensors for periods ranging from 5 minutes up to 12 hours for continuous measurement. The reporting interval is one hour with the ZentraCloud, which allows to visualise and download the data. They are equipped with a 6 AA NiMH rechargeable batteries and are powered by solar panels for energy harvesting. They are shock and weather resistant.

The system used to extract water from the soil is EcoTech (EcoTech Umwelt-Meßsysteme GmbH, Bonn, Germany) glass suction plates. These consist of a multilayer borosilicate glass plate that is melted into a glass basin. This construction increases the rigidity and water uptake of the plate. They are 80 mm in diameter, allowing soil water to be sampled over an area of 50 cm^2. Unlike plastic or ceramic plates, glass plates are recommended for the analysis of pesticides and nitrate in water. The sampling plates provide a larger sampling area than the porous candles and allow better consideration of preferential flow and soil heterogeneity (Singh et al., 2018).

5.3. Experimental design and installation

The eight 84x18 m plots form a block and are surrounded by two flowered strips of the same size (figure 16). Each plot includes smaller 42x15 m plots to represent the yield experiment. This means that no equipment can be installed or samples taken in these sub-plots. Plots 1 to 4 represent rotations in the second temporality (T2) and plots 5-8 in the first temporality of the rotations (T1) with:

- Plot 1/8 = vegan rotation
- Plot 2/7 = Reference rotation with herbicides
- Plot 3/6 = Reference rotation

In the eight plots, a 1.5 m deep trench was dug with a mini-excavator at the beginning of September 2020. These trenches were dug before the start of the first year of rotations. They are located 20 m from the lower edge of the plots, at the limit of the yield experiment.

In each of the plots, three Teros 12 water content sensors were installed on one side of the trench at depths of 30, 60 and 90 cm. Flat surfaces were created at the three depths before the sensors were inserted vertically with the ferrite core on top to limit interference (figure 5). On the other side of the trench and parallel to the Teros 12, Teros 21 sensors were also placed at depths of 30, 60 and 90 cm. Precise apertures of the sensors' dimensions were created at the three depths using the MeterGroup installation tool. Subsequently, soil was collected, sieved, moistened and compacted around the porous disc of each Teros 21 sensor. These steps are necessary to ensure good hydraulic contact. The sensors were then inserted into each hole.

The soil water sampling plates were first washed in the laboratory according to the protocol described by EcoTech. The aim is to remove contaminants from the manufacturing process. Each plate was immersed in a 0.1 M HCl solution and two litres of solution were extracted through the plate using a vacuum pump. The same procedure was then carried out with deionised water, a 0.1 M NaOH solution and then again with deionised water. Three plates were placed per plot at a depth of 1.2 m. The three plates allow water to be collected from a larger surface area and provide a more representative water sample. Three 1 m deep tunnels were dug horizontally in the wall of the trench (Figure 5). The ceiling was levelled with a trowel to ensure good hydraulic contact. The soil removed from the tunnel was sieved to 4 mm and moistened to form a slurry. This slurry was applied to the entire porous surface of the plate. The plate was then pressed as deeply as possible against the ceiling of the tunnel. The slurry provided a strong hydraulic bond between the plate and the undisturbed soil above the tunnel. The tunnel was then refilled to restore the original bulk density of the soil.

The cables were then placed in protective sheaths and attached to the walls. The trenches were filled in, respecting the ground levels. Trenches 40 cm deep were used to convey the cables to the intersection between two plots. The water measurement and collection stations were installed between plots 1-2, 3-4, 5-6 and 7-8 (figure 6). The six probes (three Teros 12 and three Teros 21) in each plot were connected to a data logger. Thus, each measuring station includes two ZL6 data loggers. In addition, the plates of two plots are connected to water collection bottles and to a vacuum system with a pump in an insulated box.

A total of 24 Teros 12 and Teros 21 sensors were installed and connected to 8 ZL6 data loggers. In addition, 24 soil solution sampling plates were placed with 4 vacuum water collection systems.

After the installation, the Teros 12 were calibrated in the laboratory using three Teros 12 sensors for the soils of the three investigated horizons according to MeterGroup's instructions. Firstly, soil was collected from the first three horizons. The differences between the soils at the three depths are clearly visible in terms of colour and texture, demonstrating the importance of a different calibration for each depth. The soil was dried in a thin layer in an oven at 25°C, then crushed and sieved to 2 mm. After weighing a dry container, the soil was added to the container in 2 cm layers and compacted to its initial density. The container was then filled to a height of 14 cm. For the depths of 30, 60 and 90 cm, a total of 5160, 5437 and 5565 g of soil were compacted in the container with an apparent density of 1.3, 1.37 and 1.4 g/cm^3 respectively.

A Teros 12 probe was then inserted into the soil and connected to a ZL6 data logger to read the raw measurement from the sensor. The same process was carried out with three different sensors. Then, other measurements were taken with a soil water content of 10, 20, 30 and 40%. The raw data for the different soil moistures were then correlated using the three repetitions. The calibration equations were obtained for the three soil horizons. They were applied to all the data from the Teros 12 water content sensors. The R^2 values obtained show good sensor calibration, with values between 0.998 and 0.999.

5.4. Soil analysis and bulk density

The physico-chemical properties of the first three soil layers were determined at the beginning of the experiment in 2021 for all 8 homogeneous plots and in October 2022 for each differentiated plot. Soil particle size distribution was determined using the pipette method (NF X31-107), organic carbon content by dry combustion (NF EN 15936) and pH using a glass electrode (NF ISO 10390). The results are presented in Table 27 and Table 28.

Table 27. Physico-chemical properties of the first three soil horizons in early 2021.

Plots	Depth	Organic carbon (g/kg)	Humus (%)	pH water	Clay (%)	Silt (%)	Sand (%)
All	30	12.3	2,46	7.6	13.8	78.3	7.9
	60	5.24	1.05	7.8	13.1	80.4	6.4
	90	3.35	0,67	7.9	19.2	74.5	6.2

Table 28. Physico-chemical properties of the first three soil horizons for the eight differentiated plots in October 2022.

Plots	Depth	Organic carbon (g/kg)	Humus (%)	pH water	Clay (%)	Silt (%)	Sand (%)
T2 vegan (P1)	30	14.2	2.84	8.3	15.3	78.5	6.1
	60	4.83	0.97	8.1	20.7	76.3	3.0
	90	1.64	0.33	8.1	20.2	76.7	3.1
T2 ref herb (P2)	30	14.8	2.97	7.9	14.2	79.4	6.4
	60	4.67	0.93	8.0	15.7	80.7	3.6
	90	2.40	0.48	8.1	17.0	80.7	2.3
T2 ref herb (P3)	30	12.7	2.54	8.0	11.5	82.6	6.0
	60	5.16	1.03	7.8	11.9	84.0	4.1
	90	3.61	0.72	7.9	14.0	82.7	3.3
T2 ICLS (P4)	30	11.7	2.35	8.0	10.5	83.4	6.2
	60	2.90	0.58	7.7	11.1	84.6	4.3
	90	3.36	0.67	7.9	14.2	82.3	3.5
T1 ICLS (P5)	30	26.9	5.38	8.0	11.3	82.9	5,8
	60	3.71	0.74	8.0	11.6	83.8	4.6
	90	3.63	0.73	8.0	14.5	81.8	3.6
T1 ref (P6)	30	12.6	2.53	7.9	14.3	79.4	6.3
	60	5.95	1.19	7.8	14.6	78.9	6.5
	90	2.73	0.55	7.8	20.2	76.7	3.0
T1 ref herb (P7)	30	11.5	2.30	7.8	15.1	79.1	5.8
	60	4.54	0.91	7.8	22.0	75.3	2.7
	90	2.38	0.48	7.9	23.1	73.9	3.0
T1 vegan (P8)	30	52.2	1.,44	8.1	11.4	85.4	3.2
	60	3.22	0.64	8.0	21.9	75.2	3.0
	90	1.72	0.34	7.9	20.6	76.3	3.1

To monitor the evolution of soil structure, bulk density measurements were carried out on the 8 plots at depths of 30, 60 and 90 cm. Undisturbed samples were collected in 100 cm^3 Kopecky rings with a diameter of 5.1 cm and a height of 5 cm. The rings were inserted using a special auger and hammer. The soil in the rings was levelled in the laboratory. The samples were then dried at 105°C for 48 hours and weighed with and without the ring to determine their bulk density. Soil porosity was calculated from the bulk density, assuming a soil particle density of 2.65 g/cm^3 and an organic matter particle density of 1.4 g/cm^3.

6. Data collection

6.1. Sensors data

Teros 12 and Teros 21 sensors have been recording high-frequency measurements every 15 minutes since their installation in September 2020 with data stored via ZL6 data loggers. Following installation, a short adaptation period was necessary to allow the sensors to stabilize in their new soil environment. During this time, soil disturbance and residual mud around the sensors may have temporarily influenced measurement accuracy. As a result, only data collected from October 2020 onwards were validated and included in the dataset. This database includes the measurements of the 24 Teros 12 sensors and the 24 Teros 21 sensors installed in the eight plots at a depth of 30, 60 and 90 cm from October 2020 to December 2024. Each sensor records four measurements per hour, 96 measurements per day and approximately 2880 measurements per month. Thus, over the period of time of the database, 148,640 measurements were taken by each sensor, which makes 3,567,360 measurements of water content, matric potential, soil temperature and soil electrical conductivity. Despite the robustness of the setup, around 2.7% of the data was lost due to minor technical issues such as loose contacts, battery failures, or disturbances during farming operations.

The years 2021 to 2024 were very contrasting in terms of meteorological conditions. 2021 was a wet year in Belgium with total precipitation of 1039 mm. It was one of the three wettest years since 1991. Rainfall was concentrated in the summer, with 410.7 mm of rain, making it the wettest summer since 1833. The year 2022 was warmer and drier, with total rainfall of 701 mm. It was one of the three driest years since 1991. The year 2023 was more moderate, with 1011.4 mm of precipitation, making it the fifth wettest since 1991, with very dry and hot months of June and September. The year 2024 was the wettest since 1991, with 1170.7 mm.

Figures 62, 63 and 64 show the precipitation, water content, matric potential (pF), electrical conductivity and soil temperature data for sensors at 30 cm, 60 cm and 90 cm depth for the eight plots from October 2020 to December 2024. For Teros 21 sensors, the range of measured values is technically limited to 1.95 pF.

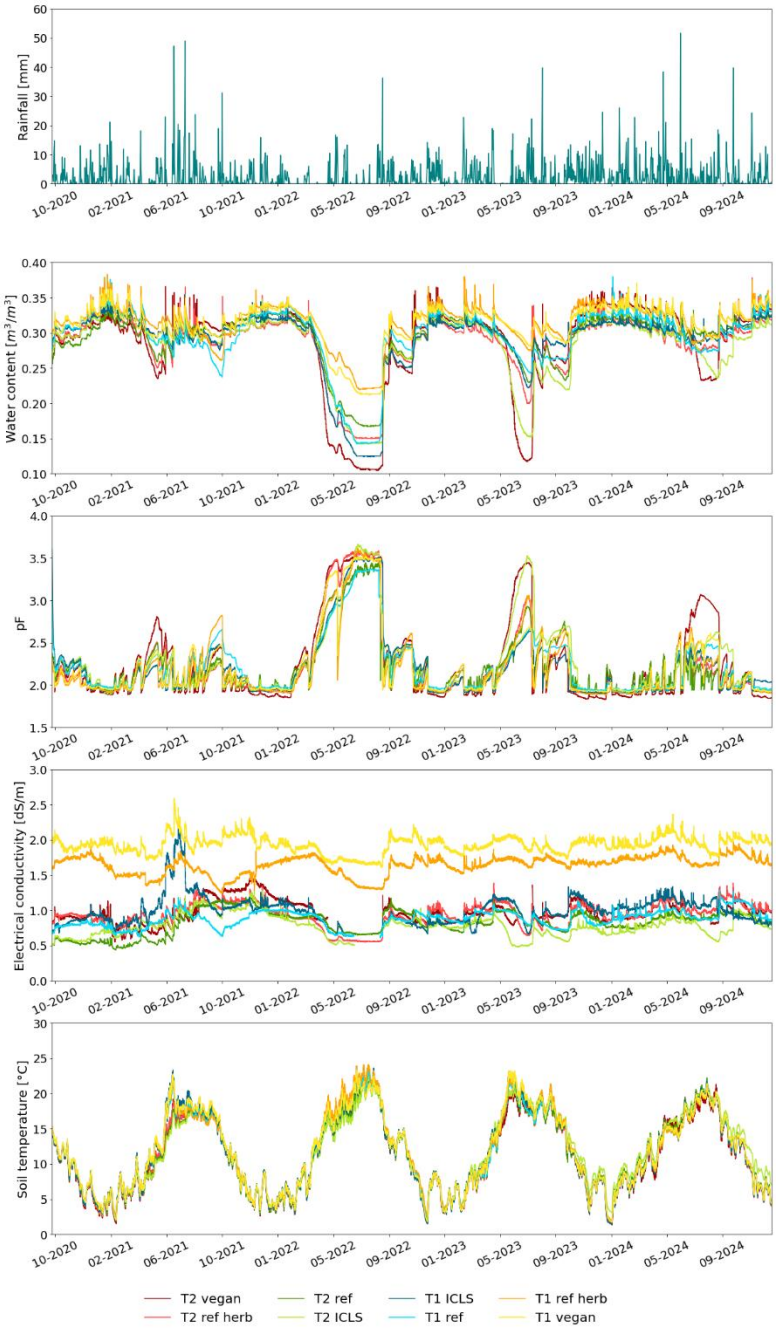

Figure 62. Precipitation and temporal evolution of soil water content, matric potential (pF), electrical conductivity and temperature data from sensors at a depth of 30 cm for the eight plots from October 2020 to December 2024.

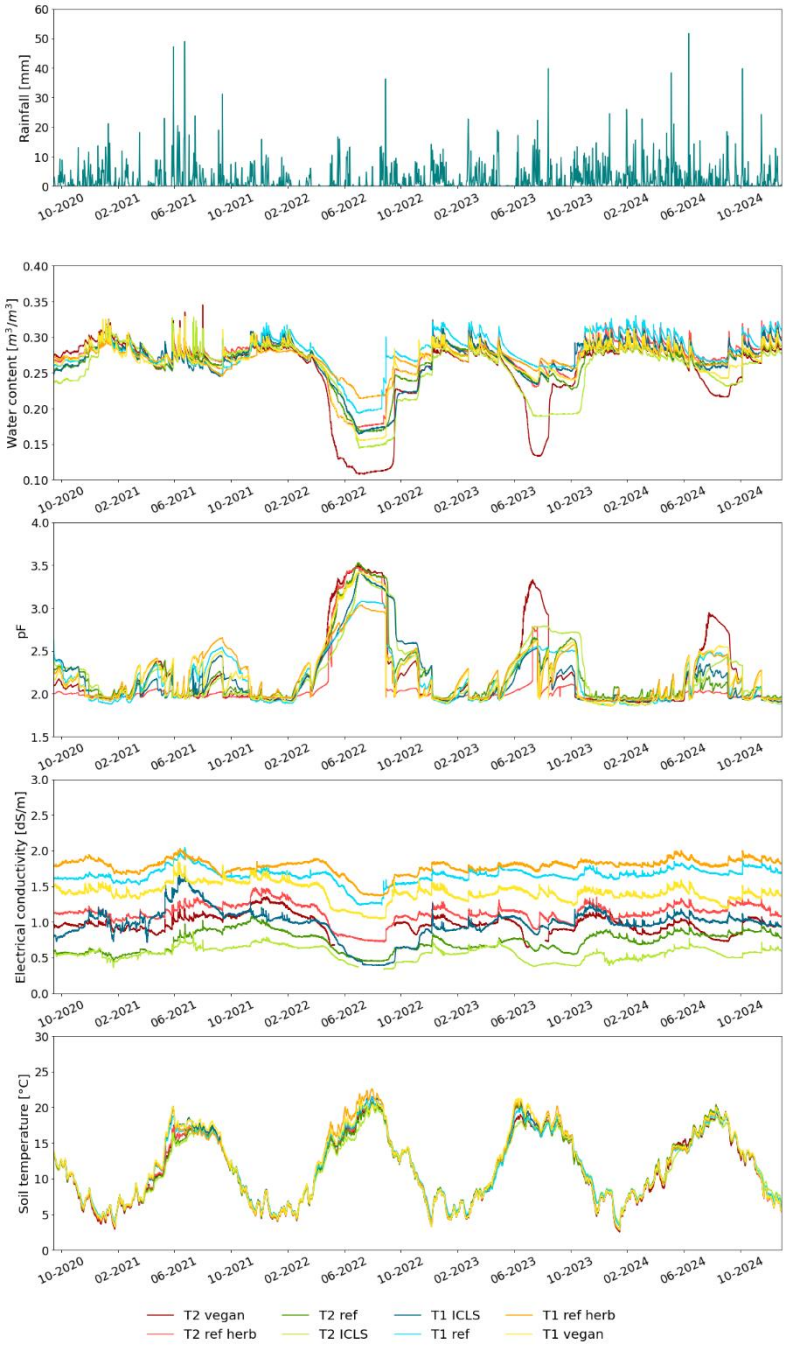

Figure 63. Precipitation and temporal evolution of soil water content, matric potential (pF), electrical conductivity and temperature data from sensors at a depth of 60 cm for the eight plots from October 2020 to December 2024.

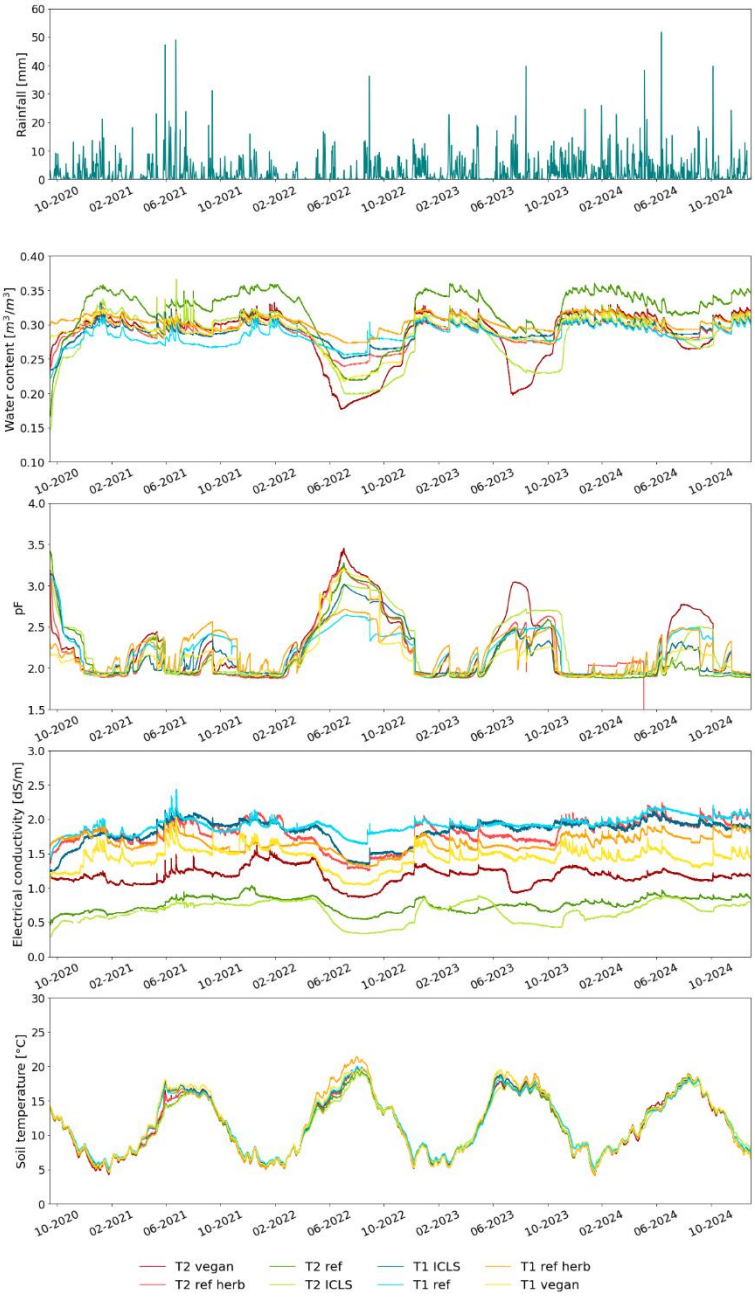

Figure 64. Precipitation and temporal evolution of soil water content, matric potential (pF), electrical conductivity and temperature data from sensors at a depth of 90 cm for the eight plots from October 2020 to December 2024.

Significant differences are observed between plots with different crop rotations and agricultural practices, between years and between depths.

At a depth of 30 cm, the lowest water content values were obtained for T2 vegan (P1) from 2021 to 2024. The two years with the most pronounced periods of soil drought were 2022 and 2023, with minimum water contents of 0.105 and 0.117 m^3/m^3, respectively. The maximum water contents were obtained for the T1 ref herb system (P7) from 2021 to 2023, with water contents of 0.383, 0.366 and 0.38 m^3/m^3, respectively. In 2024, the maximum water content of 0.38 m^3/m^3 was obtained for T1 ref (P6). The matric potential values follow the same trend as those for water content, with significant differences between plots and years. The pF values show a limit of the sensors towards pF of 1.83-1.84 in practice in the field. Unlike water content, the highest maximum drought pF values are not achieved by T2 vegan every year but by various systems over the four years. Thus, the maximum values are obtained for T1 ref herb with 2.82 in 2021, for T2 ICLS with 3.67 and 3.53 in 2022 and 2023, and for T2 vegan with 3.07 in 2024. The electrical conductivity values of the soil solution differ significantly between plots. The lowest values were obtained on plot T2 ref in 2021 with 0.44 dS/m, followed by T2 ICLS from 2022 to 2024 with 0.50, 0.48 and 0.55 dS/m respectively. The highest values were obtained for plots T1 vegan and then T1 ref herb. The maximum values for T1 vegan are 2.59, 2.22, 2.09 and 2.36 from 2021 to 2024. Soil temperature is more consistent across the eight plots. At 30 cm depth, the minimum temperatures recorded were 1.5 in 2021 and 2022, 2.8 in 2023 and 1.3°C in 2024. The maximum soil temperatures reach 23.3 in 2021, 24.1 in 2022, 23.2 in 2023 and 22.2°C in 2024.

At a depth of 60 cm, the measurements show delayed peaks that occur later than at a depth of 30 cm. The peaks are also broader and less extreme. The systems therefore respond more slowly to changes at a depth of 60 cm. However, significant differences between plots and years are observed, especially during the drying phases. The minimum soil water content values obtained were 0.235 for T1 ICLS, followed by 0.108, 0.133 and 0.216 m^3/m^3 from 2022 to 2024 for T2 vegan. The T2 vegan system therefore has the lowest soil water content in most years at a depth of 30 cm. The minimum water content is generally higher than at 30 cm, except for 2024. The maximum water contents are obtained for different plots than at horizon 1. They are 0.345 for T2 vegan in 2021, 0.324 for T2 ref herb in 2022 and 0.322 and 0.330 m^3/m^3 for T1 ref in 2023 and 2024. For all years they are lower than the maximum values obtained at a depth of 30 cm. The lowest pF values obtained are for T1 ref in 2021 and 2022 and for T1 vegan in 2023 and 2024. The highest pF values corresponding to periods of drought are obtained for T1 ref herb with 2.65 in 2021, T2 ref with 3.53 in 2022 and T2 vegan with 3.33 and 2.95 for 2023 and 2024. The maximum pF values are all lower than those at a depth of 30 cm, which corresponds to the observations of the minimum water content values. The plots with the lowest water content in 2021 and 2022 are not those with the highest soil matric potential values, unlike in 2023 and 2024 with the T2 vegan system. There are marked differences between plots in

terms of the electrical conductivity of the soil solution, especially at depths greater than 30 cm. The lowest values are always obtained for T2 ICLS with 0.36, 0.34, 0.38 and 0.39 dS/m between 2021 and 2024. They are lower than at a depth of 30 cm. The highest values are obtained for plot T1 ref herb, which was the second highest at 30 cm. The values range from 2.05 in 2021, 1.89 in 2021 and 2022, and 2.00 dS/m in 2024. These values are also lower than the maximum values obtained at 30 cm. Soil temperatures are similar for all plots, with minima of 2.9, 3.3, 4.2 and 2.5°C between 2021 and 2024. The maximum temperatures recorded are 20.2, 22.6, 21.3 and 20.4°C between 2021 and 2024. These values are also less extreme than at a depth of 30 cm.

At a depth of 90 cm, the same trends as between 30 and 60 cm continue, with peaks of wetting and drying that are more delayed in relation to the rainfall. These peaks are also less pronounced and broader. However, significant differences between plots are still observed. Water content data reached a minimum of 0.266 m^3/m^3 in 2021 for T1 ref, then 0.177, 0.197 and 0.264 m^3/m^3 for T2 vegan between 2022 and 2024, as at 30 and 60 cm depth. The minimum values are all higher than at 30 or 60 cm depth, indicating less drying of the soil at depth. The maximum values are 0.366 m^3/m^3 for T2 ICLS in 2021, then 0.359, 0.360 and 0.360 for T2 ref between 2022 and 2024. The maximum water contents are lower than those obtained at a depth of 30 cm, but higher than those obtained at 60 cm. The minimum values of the matric potential at pF are obtained for T2 ref herb in 2021 and 2022, and T2 ref in 2023 and 2024. These values are similar to those obtained at a depth of 60 cm and indicate the measurement limit of the sensors. The maximum values are obtained at pF of 2.56 for T1 ref herb in 2021, then 3.45, 3.04 and 2.77 for T2 vegan between 2022 and 2024. The same trends are therefore observed for the plots in terms of maximum pF at depths of 60 and 90 cm. The maximum values corresponding to droughts are lower than at depths of 30 or 60 cm. The electrical conductivity data show minimum values for T2 ICLS between 2021 and 2024 with 0.54, 0.33, 0.42 and 0.52 dS/m, as at 30 and 60 cm depth. The highest values are observed for T1 ref in 2021 and 2022 with 2.44 and 2.13 dS/m and for T2 ref herb in 2023 and 2024 with 2.10 and 2.24 dS/m. These values are higher than at a depth of 60 cm. As far as temperatures are concerned, the minimum and maximum values are less extreme than at shallower depths. The minimum temperatures are 4.2, 5, 5.3 and 4.1°C between 2021 and 2024. The maximum temperatures are 18.1, 21.4, 19.5 and 18.9°C.

6.2. Bulk density data

The evolution of the soil bulk density between 2021 and 2024 for the eight plots is illustrated in Figures 65, 66 and 67 for depths of 30, 60 and 90 cm, respectively.

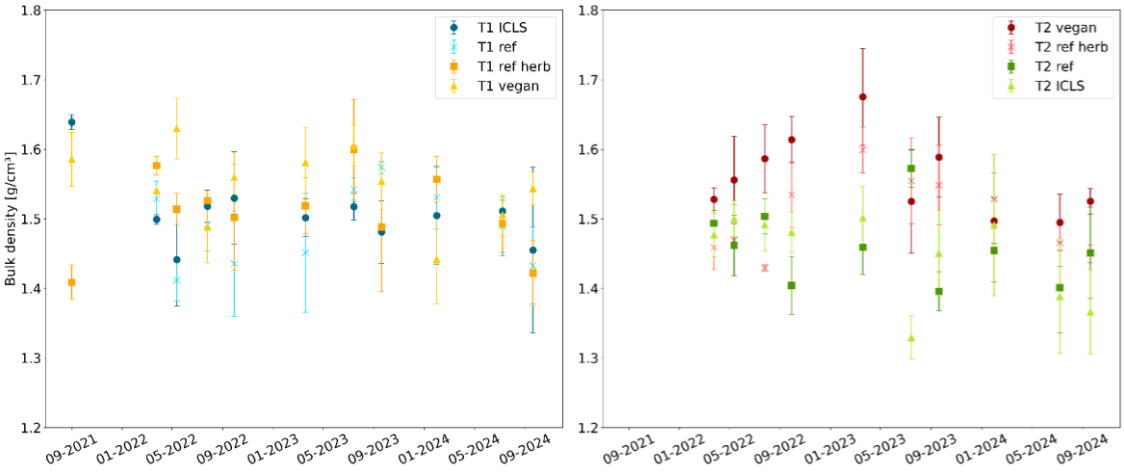

Figure 65. Temporal evolution of soil bulk density between 2021 and 2024 for the eight plots (T1 and T2) at a depth of 30 cm.

At a depth of 30 cm, plots 5 to 8 of temporality 1 were sampled in three replicates in early September 2021. Subsequently, all plots were sampled in March, May, July and September 2022, March, July and September 2023 and January, July and September 2024, also in triplicates. The three replicates were sampled in a triangular pattern at the plot level. Samples were taken at 60 and 90 cm depth in September 2021, March and September 2022, July 2023 and July 2024, without repetition.

Bulk densities vary considerably over time and between plots, demonstrating soil structure dynamics. These changes can be attributed to meteorological conditions as well as different crop rotations and agricultural practices on the plots. In September 2021, the average bulk density of plot T1 ICLS was the highest at 1.64 g/cm³, compared to 1.41 g/cm³ for plots T1 ref herb and T1 vegan. No bulk density was measured for the T2 plots. In March 2022, the bulk densities of the plots were closer to each other for both temporalities, with a maximum of 1.58 for T1 ref herb and a minimum of 1.46 g/cm³ for T2 ref herb. In May 2022, the T1 plots differed with values up to 1.63 g/cm³ for T1 vegan and 1.41 g/cm³ for T1 ref. The bulk density of the T2 plots were closer and remained between these two extremes. In July 2022, the T2 plots differ with values ranging from 1.59 g/cm³ for T2 vegan to 1.43 g/cm³ for T2 ref herb, while the T1 plots are close with values ranging from 1.49 to 1.53 g/cm³. Finally, in

September 2022, the extremes were still found in the T2 plots, with a maximum of 1.61 for T2 vegan and 1.40 g/cm³ for T2 ref. In the T2 plots, T2 vegan always had the highest bulk density in 2022. In March 2023, while the bulk density of the T2 plots all increased compared to September 2022, those of temporality 1 remained more constant. The maximum was reached by T2 vegan, again with 1.75 g/cm³, and the minimum was 1.45 g/cm³ for T1 ref. In July 2023, the bulk densities of the T1 plots increased, while those of the T2 plots decreased. The values ranged from 1.61 for T1 vegan to 1.33 g/cm³ for T2 ICLS. At the end of 2023, in September, the bulk densities of the soils ranged from 1.59 for T2 vegan, which had risen again, to 1.40 g/cm³ for T2 ref. In January 2024, the bulk densities were more uniform, with a maximum of 1.53 g/cm³ for T1 ref herb and a minimum of 1.44 g/cm³ for T1 vegan. In July 2024, the bulk densities of the T2 plots all decreased significantly, with values ranging from 1.39 g/cm³ for T2 ICLS to 1.49 g/cm³ for T2 vegan. The values for the T1 plots were very similar, ranging from 1.49 to 1.51 g/cm³. Finally, in September 2024, the bulk densities differed significantly between plots, with a minimum of 1.37 for T2 ICLS and a maximum of 1.54 g/cm³ for T1 vegan.

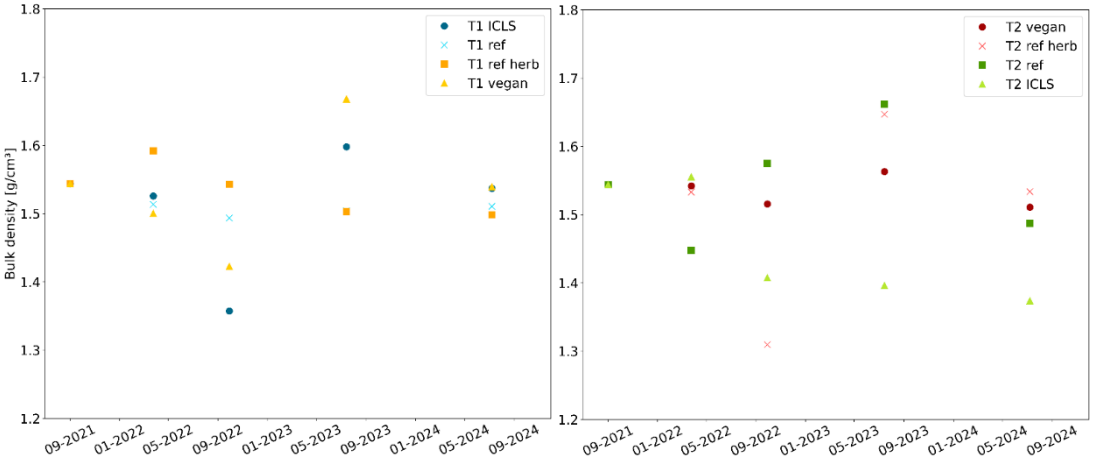

Figure 66. Temporal evolution of soil bulk density between 2021 and 2024 for the eight plots (T1 and T2) at a depth of 60 cm.

At a depth of 60 cm, the soil was considered to have a more uniform structure at the start of the experiment. A sample was taken from the block of eight plots with an apparent density of 1.54 g/cm³. In March 2022, after one year of crop differentiation, the bulk densities remained similar, with a minimum of 1.45 g/cm³ for T2 ref and a maximum of 1.59 g/cm³ for T1 ref herb. In September 2022, after a year of standardisation with winter wheat, the bulk densities differed significantly. For T1, the values ranged from 1.36 for T1 ICLS to 1.54 g/cm³ for T1 ref herb, which

remained the highest of the T1 plots. In the T2 plots, the values were more dispersed, ranging from 1.31 g/cm³ for T2 ref herb to 1.58 g/cm³ for T2 ref. Then, in 2023, during a year of crop differentiation, the bulk densities were higher than in 2022 for most of the plots. The values ranged from 1.40 for T2 ICLS to 1.67 g/cm³ for T1 vegan. Finally, in 2024, the year of the winter wheat standardisation, soil densities on most plots decrease and become more homogeneous. They ranged from 1.50 for T1 ref herb to 1.54 for T1 vegan and from 1.37 for T2 ICLS to 1.53 g/cm³ for T2 ref herb.

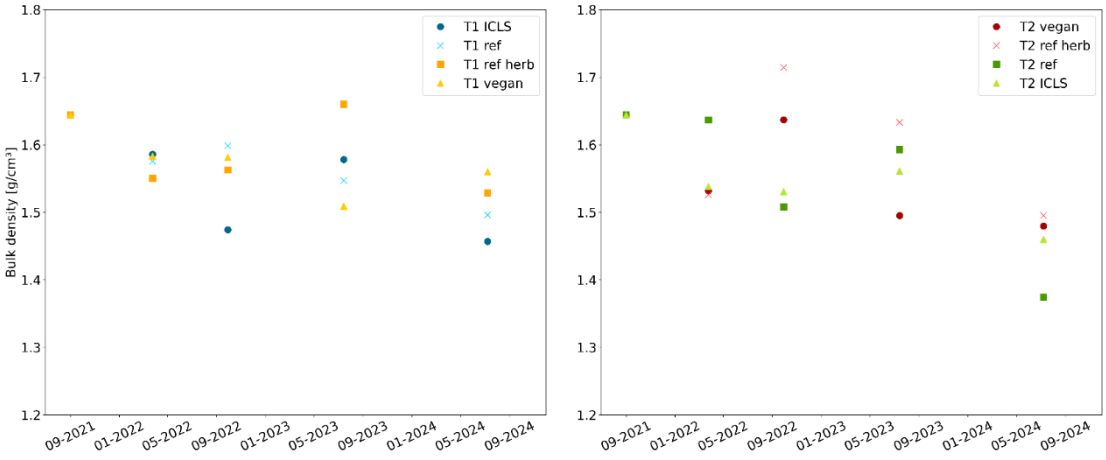

Figure 67. Temporal evolution of soil bulk density between 2021 and 2024 for the eight plots (T1 and T2) at a depth of 90 cm.

At a depth of 90 cm, the bulk densities are generally higher and more homogeneous than at depths of 30 or 60 cm. A sample was taken from the block of eight plots with a bulk density of 1.64 g/cm³, much higher than at 30 or 60 cm depth during the same period. In March 2022, the bulk density of the plots is lower and more homogeneous. For plots T1, it ranges between 1.55 and 1.59 g/cm³. They are generally lower for the T2 plots, ranging between 1.53 and 1.54 g/cm³, except for T2 ref, which remained at 1.64 g/cm³. In September 2022, after the year of standardisation, the densities differed more significantly, as at 60 cm. The density of the T1 plots remained more similar, between 1.56 and 1.60 g/cm³, except for the T1 ICLS plot with 1.47 g/cm³. The T2 plots are more heterogeneous, with 1.51 and 1.53 g/cm³ for the T2 ref and T2 ICLS plots and 1.64 and up to 1.71 g/cm³ for T2 vegan and T2 ref herb. In 2023, densities ranged from 1.50 g/cm³ for T2 vegan to 1.66 for T1 ref herb. Finally, in 2024, all bulk densities decreased significantly compared to 2023, as at a depth of 60 cm, mainly for T2. The plots range from 1.37 g/cm³ for T2 ref to 1.56 g/cm³ for T1 vegan.

6.3. Soil water sampling data

The water samples from the eight plots are split in two and put into brown bottles to prevent light from breaking down the pesticides. The first samples are for pesticide and metabolite analysis. Initially, 55 molecules were looked for in the water samples. The list of compounds to be analysed was determined on the basis of pesticides frequently found in the water and of pesticides used on the plots in the last 10 years. Then, the list was reduced to 25 compounds (table 29) based on those found in the first water samples and applied to plots T1 ref herb and T2 ref herb with herbicides. The other half of the samples were taken to nitrate analysis.

Table 29. List of 25 compounds analysed in water at a depth of 120 cm.

Compounds analysed	Limit of quantification (µg/L)
2,6-dichorobenzamide	0,050
Bentazone	0,008
Chloridazon	0,006
Clomazone	0,050
Clopyralide	1,000
Cloquintocet-mexyl	0,050
Desmediphane	0,500
Desphenyl-Chloridazon	0,021
Dimethenamide-P	0,044
Ethofumesate	0,050
Florasulam	0,050
Fluazifop-P-butyl	0,020
Flufenacet	0,010
Iodosulfuron-methyl-sodium	0,050
Mefenpyr-diethyl	0,050
Mesosulfuron-methyl	0,180
Metamitron	0,025
Metazachlore	0,020
metazachlore ESA	0,051
Metolachlore	0,025
metolachlore ESA	0,050
Metsulfuron-methyl	0,020
Phenmediphane	0,500
Pyroxsulam	0,014
Pendimethaline (since 2022)	0,050

No samples could be collected between September 2020 and March 2021. After installation, at least six months are required to ensure good hydraulic contact between the plates and the ground to extract water into the collection bottles (Singh et al., 2018). In addition, no samples could be collected between June and December 2022 due to the drought. In 2021, seven samples were taken in March, May, June, July, September, October and December. Three samples were then taken in 2022, in January, March and May. Three samples were also taken in 2023, in January, April and November. In the end, only seven compounds, in addition to nitrate, were found in soil water in concentrations exceeding their quantification limits. These were Chloridazon, Desphenyl-chloridazon, Metazachlor, Metazachlor ESA, Metolachlor, Metolachlor ESA, Ethofumesate and Metamitron. All values for each sample are available in the database.

Low concentrations of Chloridazon were found in all samples in 2021, except for T1 ref (figure 68). This pesticide has not been applied to the plots since April 2012. Concentrations ranged from 0 to 0.034 µg/l in 2021. In 2022, concentrations decreased, with many values below the limit of quantification and a maximum of 0.019 µg/l. Finally, in 2023, concentrations remained similar and did not exceed 0.021 µg/l. Its metabolite, Desphenyl-chloridazon, showed much higher concentrations for all plots. Maximum concentrations are 16.2 µg/l in 2021, then drop to 10.9 µg/l in 2022 and 6.8 µg/l in 2023.

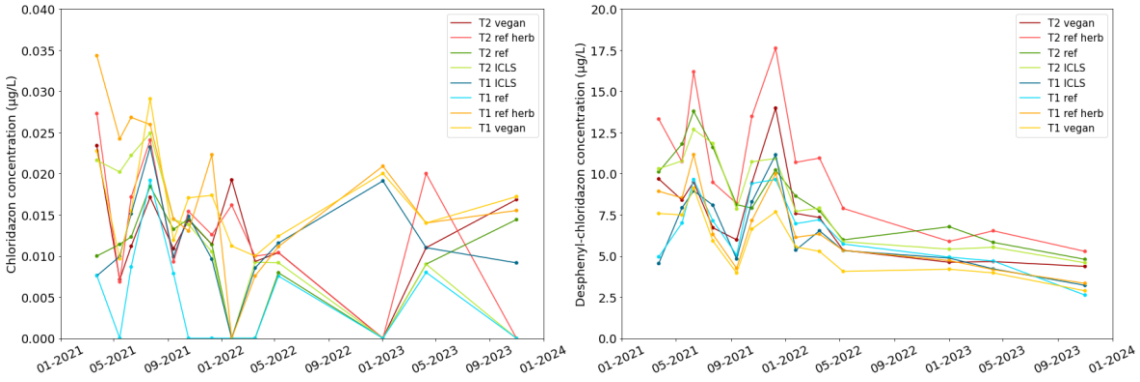

Figure 68. Concentrations of Chloridazon and Dephenyl-chloridazon in µg/l found in soil water samples between 2021 and 2023 for the eight plots. Values of zero are those measured below the limit of quantification at 0.006 and 0.021 µg/l, respectively.

Metazachlor was applied on plot T2 ref herb in November 2020. Concentrations above the limit of quantification were found in March 2021 for T2 vegan and in May 2021 for T2 vegan and T2 ref herb. It was also found in high concentrations in September 2021 for T1 ref and in December 2021 for T2 vegan and T2 ref herb with a peak of 3.883 µg/l. Its main metabolite, metazachlor ESA, was found in high concentrations in all samples on plot T2 ref herb with a peak of 24.452 µg/l in June 2021 (figure 69).

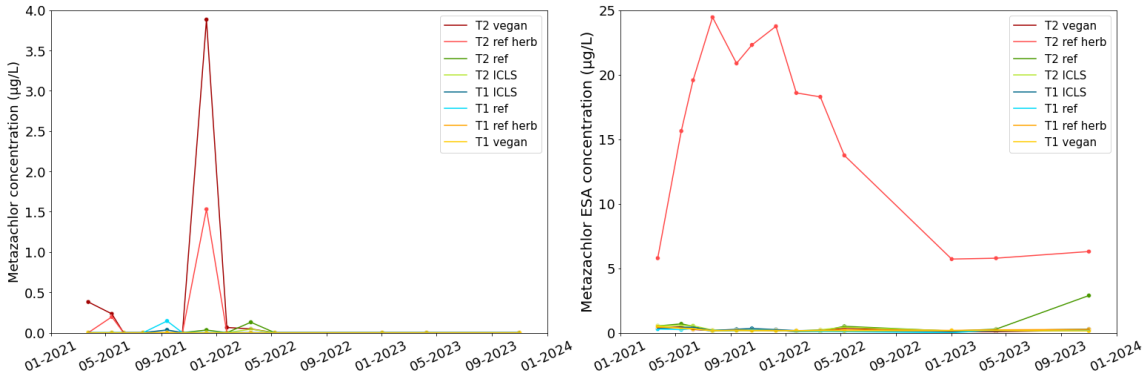

Figure 69. Concentrations of Metazachlor and Metazachlor ESA in µg/l found in soil water samples between 2021 and 2023 for the eight plots. Values of zero are those measured below the limit of quantification at 0.020 and 0.051 µg/l, respectively.

Metolachlor was only detected above its quantification limit in 2022 and 2023 in a few samples with a high concentration of 2.128 µg/l found only in March 2022 for T2 ref. It was applied in May 2018 on all plots for the last time. Its main metabolite, Metolachlor ESA, was found in high concentrations on all plots in March, May and June 2021, with a maximum of 7.923 µg/l. High concentrations were also found in September, October and December 2021, except for plots T2 ref and T2 ICLS. In 2022 and 2023, lower concentrations were found in samples, ranging from 0.128 to 2.592 µg/l (figure 70).

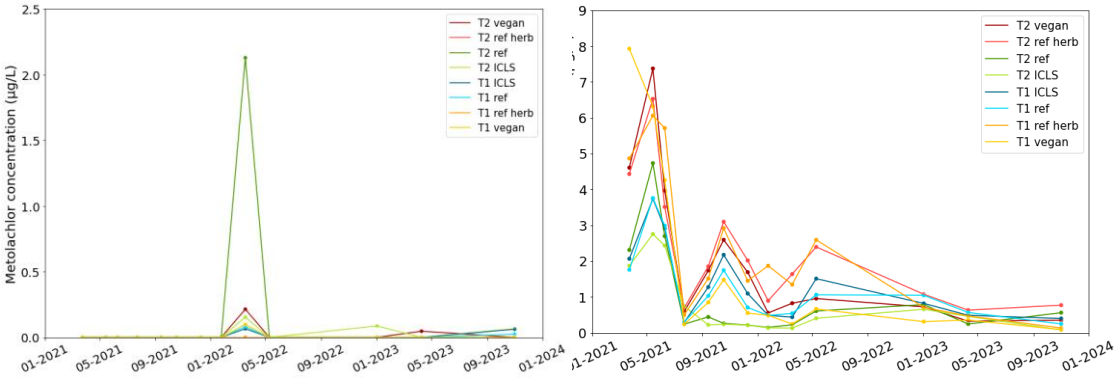

Figure 70. Concentrations of Metolachlor and Metolachlor ESA in µg/l found in soil water samples between 2021 and 2023 for the eight plots. Values of zero are those measured below the limit of quantification at 0.025 and 0.050 µg/l, respectively.

Ethofumesate, Metamitron, Phenmediphan and Metsulfuron-methyl were applied together on T1 ref herb on sugar beet on 20 and 30 May and then on 8 June 2021. Phenmediphan and Metsulfuron-methyl were never found in concentrations above their quantification limit. Ethofumesate was found only in low concentrations in three samples from different plots. Metamitron was detected at higher concentrations of up to 0.213 µg/l in plots T1 ICLS and T1 ref herb in June 2021 and then in T1 ref in December 2021.

Nitrate concentrations vary depending on the season, meteorological conditions, different crop inputs and residue management (figure 71). Between March and June 2021, low levels of nitrate were found in water at a depth of 1.2 m. Then, in July and September, levels increased and exceeded 25 mg/l in most samples, with a maximum of 43.0 mg/l for T1 ref herb. In October and December, nitrate concentrations increased in all plots except T1 ref and T2 ref herb with sugar beet, which decreased sharply and did not exceed 20.1 mg/l. The other two T1 plots showed a moderate increase, with maximum values of 48.3 and 39.1 mg/l for T1 ICLS (maize) and T1 vegan (camelina). The T2 plots with rapeseed in 21 increased more drastically, with values ranging from 36.8 to 69.3 mg/l in December. From January to May 2022, nitrate levels rose in all plots under winter wheat. The T1 ref and T1 ref herb plots remained at lower levels, with maximum concentrations of 27.5 and 30.9 mg/l respectively in May. T1 ICLS and T1 vegan increased more markedly, with maximum values of 78.1 and 67.2 mg/l. All T2 plots had higher nitrate concentrations throughout 2022, with peaks between 120.6 and 153 mg/l in May. In 2023, concentrations fell until April, ranging from 0.10 for T1 ICLS to 58.2 mg/l for T2 vegan, before rising again in November 2023, peaking at 79.9 for T2 ICLS with the meadow.

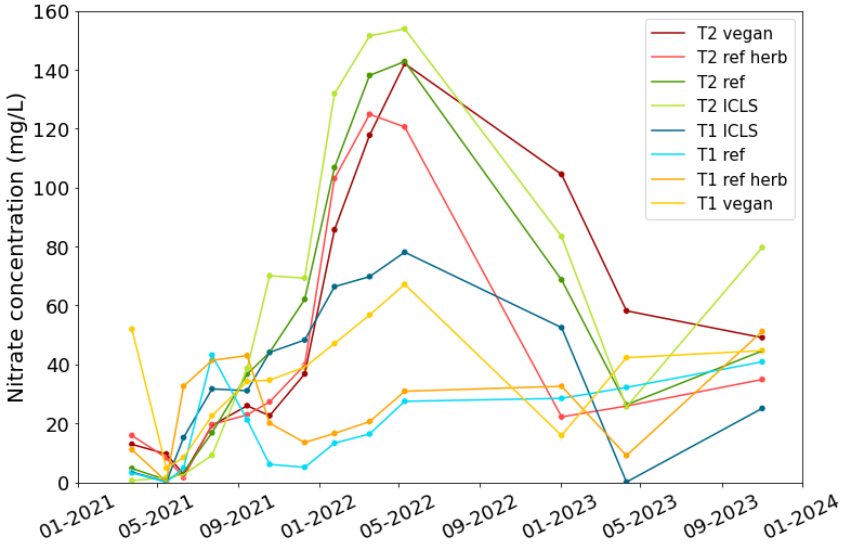

Figure 71. Nitrate concentrations in mg/l found in soil water samples between 2021 and 2023 for the eight plots. Values of zero are those measured below the limit of quantification at 0.10 mg/l.

7. Dataset access

The overall data is accessible at the DataVerseNL online data repository under a non-restrictive CC by 4.0 licence, which allows any interested user to access the data.

Firstly, the dataset includes eight files in Excel format. Each file contains data from six sensors connected to a single data logger for one plot. The first column contains the data logger number and the timestamps in the format YYYY-MM-DD hh:mm:ss from 2020-10-01 00:00:00 to 2021-12-31 23:45:00. Columns 2-4 represent data from the Teros 12 sensor at a depth of 30 cm with 'Water content m^3/m^3', 'Soil Temperature °C' and 'Saturation Extract EC mS/cm'. Columns 5-7 and 8-10 show the same data for Teros 12 sensors placed at depths of 60 and 90 cm. Columns 11-12, 13-14 and 15-16 show the data taken by the Teros 21 sensors at depths of 30, 60 and 90 cm with 'pF suction' and 'Soil Temperature °C'. Columns 17 and 18 show barometer data from the data logger with 'Reference Pressure kPa' and 'Logger Temperature °C'. These eight files will be updated annually until the end of the production system rotations, i.e. until at least 2028.

The second Excel file contains three sheets with the bulk density results between 2021 and 2024 at depths of 30, 60 and 90 cm respectively. The first column corresponds to the sampling date in YYYY-MM-DD format, the second to the plot and the third to the bulk density value obtained in g/cm³.

The third Excel file contains the results of the analyses of pesticides, metabolites and nitrate in soil water samples taken at 1.2 m depth. The file consists of the sampling date in YYYY-MM-DD format, the plot and the results of the seven pesticides/metabolites in µg/l and the nitrate in mg/l.

The fourth Excel file contains daily weather data from 1 October 2020 to 31 December 2024. The file consists of the date in YYY-MM-DD format, the maximum, minimum and average air temperatures in °C, the number of hours of sunshine, the wind speed in km/h, the relative humidity in % and the precipitation in mm. The data comes from the Ernage weather station of the Royal Meteorological Institute of Belgium, available in open access at: https://opendata.meteo.be. The data is also available in hourly and 10-minute formats.

Finally, a Word document summarises the complete technical itinerary for the eight plots, including dates and agricultural practices such as crop sowing and harvesting, soil cultivation, and the application of nitrogen inputs and herbicides.

8. Potential dataset use and reuse

Hydraulic properties such as water retention and hydraulic conductivity are key to understand water and solute fluxes in soils. The data from the water content and potential sensors provided in this database offer the opportunity to study the long-term in-situ temporal evolution of these hydraulic properties under real agricultural conditions (Pirlot et al., 2024). These dynamics are central to multiple important processes of the water cycle, including run-off, infiltration, contaminant transport, water availability for crops, and groundwater recharge.

Understanding the temporal evolution of these properties is essential for promoting sustainable agriculture that is more resilient to climate change. By capturing these variations over four years across diverse production systems, this dataset enables researchers to assess the effects of transitioning from conventional to alternative agricultural practices on soil hydraulic behavior and structure. It provides insights into how different crops and agricultural practices influence soil water dynamics, structural evolution, and agrochemical leaching. Additionally, it supports the evaluation of system resilience under varying climatic conditions, including the

extremes rainfalls and droughts observed between 2021 and 2024, thereby helping to identify practices that optimise water retention and minimise pollutant transfer.

A major strength of this dataset lies in its depth measurements, down to 90 cm, allowing researchers to study not just surface processes but also the propagation of climatic and management effects into deeper soil horizons. The inclusion of soil water sampling plate data at 1.2 m depth further enriches the resource by enabling the monitoring of residual pesticide and metabolite leaching, even years after their use has ceased. This is particularly valuable for understanding persistent groundwater contamination. Moreover, the dataset can support the calibration of remote sensing techniques (e.g. satellite-based or ground-penetrating radar measurements) by providing ground-truth reference data. It also offers a robust basis for improving the temporal representation of hydrological and agroecosystem models, enhancing their predictive reliability for water-related risks such as droughts and floods.

This resource a valuable and multi-purpose tool for scientists, modellers, and environmental managers. This database is useful for advancing research on climate-resilient and environmentally sustainable agriculture, contributing to global efforts in food security, water conservation, and pollution mitigation.

Chapter 7

General discussion and perspectives

The intensive use of pesticides and fertilisers since the 19th century has had negative repercussions on the environment, biodiversity and human health (Larsen et al., 2019; Sánchez-Bayo and Wyckhuys, 2019; van der Sluijs, 2020). These compounds are frequently found in groundwater, the largest source of drinking water for European countries (WWDR, 2015; EurEau, 2021). In Wallonia, nitrate and herbicides are the main contaminants of groundwater (SPW ARNE, 2022). However, without these products, annual yield losses are estimated at 20-40% of global production (FAO, 2017). Additionally, climate change will lead to contrasting climatic conditions and make agriculture more dependent on water availability (Arora, 2019). So, to move forward towards more sustainable systems that address environmental, economic, and social issues, agriculture needs to be rethought (de Olde et al., 2017).

Several approaches can be explored to reduce the impact of agricultural systems on water quality and management. This thesis focuses on two main strategies.

Firstly, chapters 3 and 4 focus on achieving a better understanding of the environmental fate of pesticides. The fate of pesticides and their leaching into groundwater is dependent on numerous factors and therefore difficult to predict. The required parameters must be adjusted to the specific site conditions through leaching experiments and inverse modelling (Dusek et al., 2015; Sur et al., 2022; Imig et al., 2023a). These experiments allow for a more accurate estimation of pollution risks and enhanced decision-making processes. However, these studies are conducted on different scales and using a wide range of technical approaches, which can impact the results. In this context, it is imperative to enhance our comprehension of the impact of diverse methodologies on contaminant leaching outcomes.

Secondly, chapters 5 and 6 focus on the transition of agricultural production systems towards more sustainable and climate-resilient systems. Agricultural practices could contribute to the protection of ecosystems through enhanced efficiency in the utilisation of natural resources and increased capacity to adapt (Arora, 2019; Magarey et al., 2019). More sustainable practices are emerging, but their impact on water and solute flows in soils is not yet known and has received little attention. Nevertheless, these practices will influence soil structure and hydraulic properties over time. It is generally assumed that these properties remain unaltered and, as such, they are measured in the laboratory or predicted using pedotransfer functions. Research into temporal changes is typically conducted through the measurement of samples with undisturbed structure, collected at various temporal periods, with a focus on specific practices (Kool et al., 2019; Geris et al., 2021). It is therefore essential to study the long-term temporal evolution of soil hydrodynamic properties directly in the field, under various cropping systems incorporating more sustainable practices. These experiments will help assess their relevance for the future and provide data for implementing this variability in models.

1. A better understanding of pesticide fate in the environment

The primary objective of the first approach is to achieve a better understanding and assess the fate of pesticides in the geo-pedological context of Wallonia. This section comprises multiple sub-objectives. Chapter 3 provides quantitative data on the impact of different soil column methodologies, frequently encountered in the literature, on solute leaching results and on mobility parameters obtained by inverse modelling. Chapter 4 then assesses the fate of eight problematic herbicides in groundwater using leaching experiments on intact soil columns with loamy agricultural soil typical of Wallonia. It also focuses on the impact of agricultural practices and soil depth on pesticide mobility. Finally, this chapter undertakes a comparative analysis of the mobility parameter values obtained with those used in Belgium, as provided by manufacturers and recorded in the Pesticide Properties Database for Europe in order to assess their relevance.

Do different methodologies really affect the results of solute leaching in soil columns?

Since the 1950s, a large number of articles have been published on the results of soil column experiments. Despite this, no attempt has been made to standardise or compile best practices (Lewis and Sjöstrom, 2010). Even a simple review of the literature reveals a bewildering array of technical approaches. However, these could influence the results, leading to transport parameters that are not relevant for assessing water contamination risks (Bromly et al., 2007; Lewis and Sjöstrom, 2010). Some recommendations have been made by Lewis and Sjöstrom, 2010 and correlations identified by Koestel et al., 2012. However, there is very little quantitative data on how a specific design can affect results. Methodological choices are therefore often made without clear justification.

The findings of this chapter suggest that some methodologies frequently employed in the literature significantly influence the outcomes and may not be pertinent for studying contaminant behaviour. The results showed that soil structure greatly affect solute transport dynamics and water infiltration. Disturbed columns tend to underestimate the rapid transport of contaminants and overestimate their retention in soils, failing to provide a reliable representation of groundwater contamination risks. Moreover, shorter columns resulted in greater leaching and recovery of the solute due to lower dispersivity. They tend to overestimate leaching potential and underestimate retention. Nevertheless, a significant number of new studies use disturbed columns or very small columns to examine the transport of some pollutants in soils and into water. In a recent study, Aliste et al., 2021, for example, examined the mobility of four

insecticides and their main reaction products. In order to ascertain the amounts leached from the soil profile, experiments were conducted in disturbed soil columns measuring 5 cm in diameter and 30 cm in length. Ortega et al., 2022 studied the mobility of copper and several fungicides applied to vineyards, depending on different types of cover crops. The experiments were also carried out on disturbed columns of 15 cm in diameter and 20 cm in length on which cover crops were sown.

Despite their lack of realism, disturbed columns are generally preferred due to their homogeneous structure and greater reproducibility. They are also easier to construct at a large scale than undisturbed columns. In addition, they could facilitate the standardisation of methods through a harmonised column design protocol. These columns are ideal for comparing several pesticides or modalities, which explains their widespread use in the literature. By contrast, undisturbed columns are more suitable for location-specific experiments. They enable the impact of soil structure and preferential flows to be examined (Jarvis, 2020; Varvaris et al., 2021b). To get closer to real conditions, a number of studies use intact soil core columns that are extracted directly from the field (Cueff et al., 2020; Imig et al., 2023a; Pot et al., 2010). The main disadvantage of these columns is their poor reproducibility due to soil heterogeneity. Therefore, a larger number of columns may be required to obtain consistent results. Additionally, extracting bigger columns can be challenging (Corwin, 2000). Finally, while the soil samples are referred to as 'intact soil columns' because their structural characteristics are preserved, it is important to acknowledge that some degree of disturbance is inevitably introduced during sampling. Inserting the plexiglass cylinder into the soil profile causes mechanical disruption, particularly along the edges of the column (Isensee and Sadeghi, 1992; Lewis and Sjöstrom, 2010; Katagi, 2013). While the samples retain a relatively undisturbed structure that is suitable for investigation, they cannot be considered perfectly intact in a technical sense.

In this thesis, intact columns were chosen for pesticide leaching experiments. One of the objectives was to demonstrate the impact of cropping systems and soil depth, which influence soil structure and properties, on the leaching of problematic herbicides in Wallonia (Hu et al., 2009; Alletto et al., 2015; Cueff et al., 2020; Fox et al., 2022). In addition, the second main objective was to adapt the mobility parameters of these pesticides to enable more realistic risk assessments. Conditions closer to those in the field were therefore more relevant to this study. Thus, although this research highlights the importance of standardising practices, which is more implementable with disturbed columns, it supports the use of intact columns to obtain more accurate analyses of water contamination risks. However, undisturbed columns in the laboratory also have limitations. They do not allow for the study of the impact of vegetation growth, soil drying-wetting cycles, seasonal and diurnal changes, and natural precipitation. Outdoor lysimeters have been developed to reduce the gap between data obtained in the laboratory and directly in the field (Šimůnek et al., 2008b; Katagi, 2013). These lysimeters are ideal for long-term field experiments that

aim to analyse water balance and evapotranspiration, measure water flows, and develop crop responses and hydrological models. They are also well-suited to monitor pesticide movements (Chen et al., 2008; Bergström et al., 2011; Imig et al., 2023a). However, these lysimeters require installation at the start of the experiment, which is more difficult to set up and much more expensive than soil columns (Singh et al., 2018). Therefore, column design must be carefully considered based on assumptions and experimentation, as no single methodology will be suitable for all applications.

This work has limitations and the results should therefore be considered with caution.

A larger number of columns should be studied to confirm the observations. Three repetitions are the acceptable minimum number for studying the effect of these different methods. However, when using intact columns, a larger number of columns would provide more reliable results due to the high heterogeneity of the soils.

In addition, the column diameter factor was only tested with disturbed columns, which resulted in few differences, unlike the height of the columns in intact structure. The reasons are mainly practical: to make it easier to reconstruct wider columns. However, it also depended on the order in which the experiments were carried out. Thus, columns of several diameters were made before the results of the impact of soil structure were available, and intact columns were selected for the following experiments. Koestel et al., 2012 showed that dispersivity depended on the height and diameter of the columns. In addition, Bromly et al., 2007 identified column diameter as the second most influential factor affecting solute dispersivity in soil columns. The degree of preferential flow in intact columns depends on column height and diameter. Thus, different intact column diameters could lead to more pronounced differences, which would be worth investigating.

Furthermore, only two modalities were considered for each factor. These modalities were chosen based on those most commonly used in the literature. However, analysis of a wider range of modalities, such as several techniques for creating disturbed or intact columns, as well as more different column diameters and lengths, would permit the establishment of harmonisation functions. These functions would make it easier to compare the results of several studies and choose the most appropriate methodology for the experiment. Moreover, in addition to the factors studied in this chapter, many others vary in the literature, such as the method of column construction, the materials used for the columns, the boundary conditions, and the saturation and water content conditions of the columns fo example (Lewis and Sjöstrom, 2010; Katagi, 2013; Singh et al., 2018).
Finally, this study used the dual porosity model to obtain the adjusted hydraulic and tracer mobility parameters for the columns. This physically based model considers the impact of preferential flows and non-equilibrium physical transport. DP models

assume that water flow is confined to the macropore domain, though water can be exchanged between the two regions (van Genuchten and Wierenga, 1976; Šimůnek et al., 2003). The model has been used in numerous studies to describe the movement of pesticides in structured soils, achieving good results (Gärdenäs et al., 2006; Varvaris et al., 2021b; Imig et al., 2023a). However, the very high dispersivities obtained when investigating the effect of column height, particularly for 35 cm columns, demonstrate that the model is unable to accurately represent the considerable preferential flows present in these columns. Therefore, this approach does not seem sufficient for these columns, which exhibit significant physical non-equilibrium processes. An alternative approach would be to consider a dual-permeability model or a triple porosity model incorporating a region of immobile water (Šimůnek and Genuchten, 2008; Köhne et al., 2009b). The dual-permeability model considers two pore domains, with water flowing rapidly in the macropore domain and more slowly in the matrix or micropore domain (Gerke and van Genuchten, 1993b; Gerke and Köhne, 2004). These models may be more appropriate for these columns. Indeed, they have provided better predictions during significant preferential flows in some studies (Kodešová et al., 2005; Pot et al., 2005; Köhne et al., 2006; Varvaris et al., 2021a). The dual permeability model with more parameters to estimate was tested but did not provide valid results and less accurate predictions. In fact, the number of parameters that can be optimised simultaneously may depend on the availability of measurement data used in the objective function and on the uncertainty of the estimated parameters (Abbasi et al., 2003b).

Do cropping systems and soil depth affect the fate of eight pesticides in soil columns and their mobility parameters?

Chapter 4 focuses on the fate of eight problematic herbicides in a typical Walloon loamy soil that were still authorised at the start of the experiment. This chapter investigates in particular the influence of the three contrasting EcoFoodSystem production systems and the first three horizons on the breakthrough curves, mass balances and mobility parameters obtained by dual-porosity inverse modelling on Hydrus 1-D. Indeed, pesticide leaching risk assessments do not generally take into account site-specific factors such as soil depth or agricultural practices. However, the use of generic mobility parameters can lead to inaccurate contamination estimates and ineffective protection of water resources (Labite et al., 2013; Cueff et al., 2020; Mamy et al., 2024).

In general, only topsoil parameters are considered and presented in databases for pesticide risk assessment studies (EFSA, 2015; Lewis et al., 2016). Adsorption and degradation are generally higher at horizon 1 due to higher organic matter content and more intense biological activity, as observed in this study (Mills et al., 2001; Katagi, 2013). However, this thesis shows that the transport processes and fate of pesticides within the lower horizons are complex and cannot be ignored. Applying topsoil

mobility parameters to the entire profile will lead to an overestimation of pesticide adsorption and degradation, underestimating the risk of groundwater contamination. In horizon 2, for example, significant preferential flows are observed due to the undisturbed nature of this soil layer, which can lead to rapid pesticide leaching. These results may partly explain the high concentrations still found in groundwater despite contamination risk assessments and the resulting regulations. Nevertheless, there are approaches that allow deeper horizons to be considered based on topsoil parameters. To account for soil depth in models, the adsorption coefficient (K_d) can be converted to K_{oc} in proportion to the organic carbon content of the different soil horizons. The models will then require either a K_d per horizon, calculated based on the organic carbon content, or a single K_{oc} that automatically adapts to the organic carbon content. In terms of degradation, this generally decreases with soil depth due to decreasing microbial activity. Therefore, correction factors can be applied to the degradation rate of pesticides depending on depth like in PEARL or PELMO (FOCUS, 2000; Katagi, 2013).

Regarding the influence of cropping systems, the results indicate that they can generate different water flow and pesticide leaching dynamics with the differences mainly due to root architecture, surface tillage and soil properties. However, only minor changes in mass balances and mobility parameters were found, probably due to insufficient differentiation between the systems. Nevertheless, it has been shown that different crop rotations influence soil structure depending on their root systems (Lichter et al., 2008; Hua et al., 2009). These results are consistent with the findings of the thesis, which showed that maize's large roots generate more macropores, greater connectivity of the pores and cause pesticides to leach more quickly. Chapter 5 also supports the observation of lower water retention in the plots with maize, as revealed by sensors data. In addition, very low water infiltration was observed in the columns of the vegan system, as shown in Chapter 5, which demonstrates that this system has the highest water retention capacity. Pesticide transfer is therefore limited in this system. This can be attributed to the fine, dense roots of the camelina near the surface, which can block the pores (Lu et al., 2020). Different crop rotations can also impact the fauna, particularly the microbial communities in the soil (Fox et al., 2022; Lori et al., 2023). Consequently, in the medium to long term, more contrasting pesticide leaching behaviour could be observed between cropping systems, potentially becoming a lever for reducing groundwater contamination.

The properties of pesticides have a major influence on their fate within the same soil. More importantly, the leaching or adsorption rates are not always in agreement with the K_f values obtained or with those of the PPDB. Different pesticide classifications are obtained depending on cropping systems and soil depth. Different adsorption mechanisms can be observed depending on the nature of the pesticide, whether or not it is ionised, and its properties such as solubility, pKa and the octanol-water partition coefficient. Positively ionised pesticides are more likely to be adsorbed by clays, while neutral pesticides with a high octanol-water partition coefficient value

are more hydrophobic and are mainly adsorbed by organic matter. For instance, bentazone exhibits very low adsorption and high elution in all columns. This can be explained by its high water solubility and its weak acid nature, with a pKa of 3.51. This means that it primarily exists in the form of negatively charged ions at pH close to neutral, resulting in very low adsorption to organic matter or clay present in soils (Boivin et al., 2004; Arias-Estévez et al., 2008). The adsorption of terbuthylazine depend more on the OC than on the clay content, as observed by Kodešová et al., 2011. Terbuthylazine is indeed a weak basic herbicide with very low solubility, which explains its low leaching. Furthermore, at a pH close to 7, its pKa of 1.9 indicates that it will mainly exist in a neutral, non-ionised form. Its high octanol-water partition coefficient indicates that the pesticide is highly hydrophobic and is rapidly adsorbed by organic matter. Conversely, flufenacet and metazachlor exhibited greater adsorption in the horizon 3 and vegan system columns than in the others. Therefore, these herbicides appear to have a greater affinity for clays than for OC. These results highlight the importance of studying the fate of all environmentally relevant pesticides in soils to enable more effective management.

This thesis demonstrates the importance of considering deeper soil horizons in pesticide fate to better understand and include the different transport, retention and degradation dynamics within the entire soil profile. This will enable more relevant recommendations to be made on pesticide selection, dose adjustment and authorised application periods. In addition, future risk assessments should incorporate long-term monitoring of pesticide fate under different cropping systems to encourage the adoption of more sustainable agricultural practices, thereby reducing water contamination. Finally, in order to manage them more effectively, it is necessary to study the behaviour of all problematic compounds under site-specific conditions.

However, it should be noted that the mass balances for the adsorption, elution and degradation of pesticides were calculated after 57 days of experimentation. Adsorption/desorption phenomena may have occurred during this period, but these were not measured. Consequently, the dynamics of the adsorption processes were not investigated. Furthermore, degradation percentages were not measured but calculated by subtracting the eluted and adsorbed quantities from the total quantities applied to the columns. Therefore, the proportion of herbicides that remained adsorbed in the soil and were non-extractable was considered degraded. Finally, a mixture of eight herbicides was applied to the columns simultaneously, which may have resulted in competition for adsorption sites between the herbicides. These limitations may explain why low percentages of adsorbed pesticides were found for most herbicides.

Do the mobility parameters obtained for Walloon agricultural soils correspond to the generic parameters used in Belgium or given in databases?

Chapter 4 also provided pesticide mobility parameters suitable for soils typical of the loamy agricultural region of Wallonia. Risk assessment and authorisations for pesticide use are determined based on modelling of pesticide fate in soils. The parameters used are often derived from experiments carried out by manufacturers and compiled in peer reviews of pesticide risk assessments provided by the European Food Safety Authority and in databases such as the Pesticide Properties Database (EFSA, 2015; Lewis et al., 2016).

The results highlighted significant differences in transport parameters for most pesticides. The EFSA values used in Belgium for the same soil type and climate zone show higher adsorption coefficients, which could lead to an underestimation of pesticide leaching into groundwater. These results are consistent with recent findings by Mamy et al. (2024) who modelled the fate of several pesticides under different agricultural practices. They showed that the generic transport parameters of the PPDB did not provide a reliable representation of the concentrations actually found in the column leachates, underestimating them in most cases.

For the majority of pesticides studied in this thesis, such as bentazone, chlorotoluron and terbuthylazine, the EFSA peer review based on the 9 FOCUS scenarios, concluded that they had a low potential for groundwater contamination, renewing their authorisation. However, groundwater analyses in Belgium identify bentazone, metazachlor, chlorotoluron and terbuthylazine as major contaminants (SPW ARNE, 2022). These conflicting results may be due to the use of inappropriate transport parameters, but also to different testing methods. Indeed, they are generally determined by batch adsorption or degradation experiments maximising contact between the soil and the pesticide, under laboratory conditions, at equilibrium and over short periods, as recommended by the Organisation for Economic Cooperation and Development (OECD, 2000, 2002). In these experiments, soil structure and preferential flows are not taken into account and these experiments generally overestimate the adsorption and degradation of compounds. These batch experiments deviate even further from the reality in the field than experiments in disturbed soil columns, also recommended by the OECD (OECD, 2004). However, Chapter 3 demonstrated that this type of experiment does not provide a reliable representation of the risks of groundwater contamination. Cueff et al., 2020 also showed a discrepancy between the adsorption coefficient values obtained by batch and by leaching in intact soil columns.

In addition, generic half-lives found in this thesis are higher for most herbicides, indicating an underestimation of pesticide degradation and metabolite production. Underestimating metabolite production leads to significant pollution from these compounds. Metabolites are generally more mobile and persistent in soil than their parent compounds (Lewis et al., 2016; Kiefer et al., 2019). According to EFSA studies, the metabolites of terbuthylazine, s-metolachlor and metazachlor have a high leaching potential (Brancato et al., 2017; Lentdecker et al., 2017; Alvarez et al., 2023). Along with these, metabolites of metamitron and flufenacet were classified as highly mobile in the PPDB, with high DT_{50} of up to 400 days for metolachlor ESA (Lewis et al., 2016). An investigation of novel metabolites detected in groundwater showed that those of terbuthylazine, metamitron, metazachlor and flufenacet were found at higher concentrations than the parent pesticides (Kiefer et al., 2019). The Sol-Phy-Ly project analysed the long-term fate of numerous herbicides using field lysimeters on a plot adjacent to the EcoFoodSystem experiment investigated in this thesis. The results showed significant concentrations of metabolites in the water years after their last use. Metazachlor ESA had average annual concentrations at a depth of 2 m between 100 and 1000 ng/L, even though the last treatment had been carried out around 15 years earlier. The metabolite of metolachlor, metolachlor ESA, showed concentrations between 2,000 and 10,000 ng/L when used every two years. After fifteen years without use, concentrations remained around 500 ng/L (Vandenberghe et al., 2024). These results are consistent with those of the AIL4WaterQuality project, which this thesis supports. Only a few parent pesticides were found in the water at a depth of 1.2 metres, and then only in very low concentrations. One example is chloridazon, which was last used in 2012. Metabolites were found in higher concentrations. Desphenyl-chloridazon exceeded the threshold concentration in most samples. Higher concentrations were mainly observed in plot T2, where greater leaching of contaminants from the soil was evident. In contrast, plot T1 vegan shows lower concentrations, resulting from lower water infiltration and greater retention capacity, as observed in Chapter 5. Although metazachlor was applied to rapeseed in plot T2 in 2020, high concentrations were only found in March and May 2021, after the harvest. However, its metabolite, metazachlor ESA, was found in samples from this plot until the end of 2023, with concentrations exceeding 6 µg/L. The same is true for metolachlor, which has not been applied since 2018. Its metabolite, metolachlor ESA, was found at significant concentrations until the end of 2022, after which it fell below 1 µg/l in 2023 (Pirlot and Degré, 2023).

The threshold values for most metabolites are different and higher than those for parent pesticides because they are considered less toxic, in accordance with the precautionary principle. For example, the threshold values for metazachlor ESA and metolachlor ESA are 0.5 µg/L and 1 µg/L, respectively (Arrêté Du Gouvernement Wallon du 07 juin 2018). However, these metabolites have been shown to be toxic to aquatic organisms and earthworms. Furthermore, there is a lack of data on these metabolites to estimate their toxicity to human health (Lewis et al., 2016). It is

therefore important not to underestimate the degradation of pesticides in soils. Special emphasis should be placed on the study of the fate of metabolites in soils and their measurement during monitoring, which is rarely investigated and too often neglected.

Pesticide leaching modelling in soil columns is strongly influenced by the sorption coefficient and half-life, but also by dispersivity. These parameters are among the most sensitive for modelling leachates concentrations (Cheviron and Coquet, 2009; Jian et al., 2024). Thus, even minor differences in the values of these parameters can have a major impact on pesticide risk assessments.

These results highlight the need to adapt the K_f and DT_{50} values for all pesticides and metabolites of environmental concern to the soil type studied for future modelling and decision-making. These results may explain why pesticides that are problematic for the environment and human health are still in use today and why more effective policies are not being implemented. Hearings on pesticides and their effects on health and the environment are being held in June and July 2025 in Wallonia, demonstrating the pressing nature of the issue. The outcome is not very positive. In addition to their impact through leaching into water, pesticides are also dangerous in our food, an issue not addressed in this thesis. Biomonitoring in Wallonia shows widespread contamination with significant repercussions for children and pregnant women, but also for farmers, who are on the front line.

Plant protection products must therefore be used with greater caution, given the difficulty and uncertainty of assessing their fate. Studies must also more systematically include the behaviour of metabolites to provide a more complete picture of the fate of pesticides and their degradation products. The methodologies used to assess mobility parameters must be adjusted and closer to the field conditions in order to more accurately represent the risks of water contamination by these substances. Longer-term lysimeter studies, such as those conducted in the Sol-Phy-Ly project under field conditions, are required to monitor the behaviour of pesticides in different cropping systems, climatic conditions and soil types. Such studies would inform recommendations for more sustainable agricultural practices for pesticide management.

Nevertheless, the findings and values of the parameters found in this thesis must be interpreted and used with cautionas this study has several limitations.

Firstly, the soil column methodology used in this experiment may have impacted the results. Following the conclusions of Chapter 3, columns with a diameter of 8.4 cm, a height of 30 cm and an intact structure were used. Despite the recommendations of the FOCUS groundwater working group to use intact soil column experiments to determine mobility parameters, these small columns under laboratory conditions can also strongly influence the findings (FOCUS, 2009). To get closer to reality, many

studies focus on the fate of pesticides in larger outdoor lysimeters (Mertens et al., 2009; Schuhmann et al., 2019; Imig et al., 2023a). Although these require more investment to set up, they offer a satisfactory compromise between controlled laboratory and natural field conditions. They enable the impact of agricultural practices and climate on the fate of pesticides in soil to be investigated.

On top of that, the mobility parameters obtained in this thesis are only suitable for soils typical of the loamy agricultural region of Wallonia. However, Wallonia also has more clayey soils, such as in the Fagnes-Famenne or in the herbagère region, with greater retention potential. Sandier soils are found in the north of Wallonia in the sandy, sandy-loam and Campine Hennuyère regions, mainly with higher infiltration potential and therefore potentially higher pollution levels. Indeed, the aquifers most affected are the "Sables bruxelliens" in the Haine and Sambre basins, the "Sables du Bruxellien" and the Cretaceous in the Geer basin (SPW ARNE, 2022). These different soil textures and properties will impact the behaviour of pesticides and therefore their mobility parameters.

Then, the results are based solely on three repetitions of small-scale columns and depend on spatial soil variability. Thus, for some modalities such as camelina columns, standard deviations are large. They are also based on a single column sample. However, Chapter 3 showed contrasting leaching results for the same solute and the same plot depending on the sampling date of the columns and the cultivation operations.

Furthermore, this study was conducted under laboratory conditions, at a relatively constant temperature with theoretical rainfall, and therefore does not fully reflect the complexity of natural systems. Furthermore, the study does not analyse degradation, obtained by balancing leached and adsorbed quantities, nor metabolites their evident impact.

Also, no analysis of herbicides in the soil was carried out at the start of the experiment. However, the risk of contamination of the columns by the eight herbicides studied is low. Indeed, these eight herbicides have not been used on the plots where the columns were sampled since at least 2018. Bentazone was last used on maize in July 2005. Chlorotoluron has not been used since 2003. Ethofumesate and metamitron were last used in May 2016 on sugar beet and in May 2021 on an adjacent plot. Metazachlor was last applied in October 2013 to rapeseed. S-metolachlor was applied in May 2018 to chicory, and flufenacet and terbuthylazine were applied in June 2011 to maize.

Finally, mobility parameters were obtained by double porosity inverse modelling using the initial parameters used in Belgium. This model assumes that water flow is limited to the mobile part of the soil, at the macropore level. Thus, the water in the

matrix is considered immobile and can only exchange with the mobile zone (Šimůnek et al., 2003). In reality, water will flow in both regions at different rates. This choice of model therefore makes strong assumptions about how water and solutes flow within a soil profile. Some research is exploring triple porosity models to improve the representativeness of soil structure (Pot et al., 2005; Köhne et al., 2006; Varvaris et al., 2021a). Furthermore, this 1-D model only considers vertical flows downwards through the column. However, in reality, lateral transfers also occur in soils, causing contamination of surrounding plots and surface water. These flows can be taken into account in larger-scale studies such as lysimeters, which can be inclined to represent the topography of the site. Furthermore, 2-D or 3-D models exist to simulate these different transfers (Šimůnek et al., 2016; Singh et al., 2018; Varvaris et al., 2021a). However, the main difficulties in using more complex models are determining the appropriate initial parameterisation and simultaneously predicting the parameters of preferential transport, sorption and degradation of pesticides with accuracy (Köhne et al., 2009a).

2. A transition to more sustainable and resilient production systems

The main objective of this section is to study the impact of different production systems on the variability of soil water retention capacity under contrasting climatic conditions. The second objective is to compare the retention curves obtained in the field with those obtained by pedotransfer function or under laboratory conditions on undisturbed samples. The third objective is to develop a database on the long-term temporal dynamics of soil hydraulic properties, soil structure and agrochemicals leaching directly in the field.

How does soil water retention change over time, depending on agricultural practices and climatic conditions?

Chapter 5 focuses on improving our understanding of soil water retention dynamics in relation to agricultural practices and climatic variability. To this end, field monitoring of the temporal evolution of water retention in four contrasting production systems, based on the diets of tomorrow, with two temporalities was conducted over a three-year period. In a context of climate change and transition towards more sustainable agricultural practices, it is crucial to understand the impact of entire production systems on soil water dynamics in order to assess their long-term relevance.

The results of this thesis reveal a high degree of variability in soil water retention curves (SWRCs). The greatest variability is observed between systems, followed by

variations during a single season, and finally interannual differences. These findings thus highlight a stronger influence of agricultural practices and crop types on soil water retention dynamics than that of plant development, seasonal wetting-drying (WD) cycles, or contrasting climatic conditions across years. Practices such as crop differentiation, weed control, crop residue management, compaction during harvest, and the introduction of temporary grasslands induced significant changes in water retention capacity, with some effects persisting for at least two years. It shows that the effects of production systems are not limited to a single growing season, but can be part of slow and gradual changes in the physical properties of the soil. Recent studies have also highlighted the influence of certain agricultural practices and climatic conditions on the evolution of soil structure and hydraulic properties (Alletto et al., 2015; Tifafi et al., 2017; Jensen et al., 2020; Alskaf et al., 2021; Huang et al., 2021; Pečan et al., 2023). However, these studies tend to offer limited insight into the behaviour of entire cropping systems, as they rely on undisturbed soil samples collected at shallow depths and over short time periods, focusing on a single practice (Geris et al., 2021; Huang et al., 2021). This study highlights that agricultural practices and different crops can be levers for enhancing water and food resilience against future climate conditions.

However, these results should be interpreted with caution given some methodological limitations. Firstly, although the systemic approach adopted is relevant for studying the combined effects of management practices at the system level, it makes it difficult to accurately assign observed effects to a specific practice or factor on soil water dynamics. Secondly, intra-plot spatial variability was not investigated, as the study relied on a single pair of water content–matric potential sensors per plot. This limits the representativeness of some observations, even though the differences in SWRCs observed appear to reflect real structural contrasts. Thirdly, the measurement range of matric potential sensors is limited to 1.95 pF, which restricts the analysis of near saturation states, where water infiltration into the soil is often critical. Furthermore, observations focused on the 0–30 cm horizon, despite evidence from previous studies indicating that agricultural practices can affect soil structure at greater depths, particularly beyond 60 cm. In addition, the spatio-temporal variability of SWRCs is complex and depends on many factors. However, not all of these influencing factors and processes were measured, meaning that some interpretations remain hypothetical. Finally, this study covers the first three years of a complete eight-year crop rotation. Year four, during which winter wheat will be grown across all plots, will provide an opportunity to validate or challenge some of the trends already identified.

This study represents a first step towards a deeper understanding of the temporal dynamics of soil water retention in contrasting agricultural production systems. However, several ways for further investigation should be considered to strengthen and broaden the scope of this work.

Firstly, it is essential to continue monitoring throughout the entire eight-year crop rotation in order to better understand the long-term effect of the studied systems on soil structure and water retention capacity. Structural effects on water retention may be progressive, cumulative or delayed, and long-term observation is necessary to distinguish transient trends from long-lasting. Furthermore, although readings were taken at a depth of 30 cm (horizon 1), sensors were also placed at depths of 60 and 90 cm, enabling analysis of SWRC evolution at greater depths. This approach would provide a better understanding of vertical water redistribution processes, deep rooting dynamics and the effects of agricultural practices at different soil depths. Another aspect for improvement concerns the number of spatial repetitions. This study is based on the instrumentation of a single block of eight plots, whereas the full experimental setup includes four similar blocks. Extending the instrumentation to the other blocks would enhance the robustness of the results with regard to spatial variability and allow a more accurate quantification of the effects of management practices. Increasing the number of sensors per plot would enable better characterisation of intra-plot variability. Concerning the agricultural practices studied, it would be relevant to investigate even more innovative or alternative systems, such as agroforestry, perennial crops, permanent cover cropping or no-till systems. These approaches, which are more challenging in terms of sustainability, may induce even more diverse dynamics in soil hydraulic properties and deserve to be integrated into similar research protocols. From a methodological perspective, another important approach would be to analyse the wetting phases of the soil water retention curves. So far, only drying phases have been considered (three per year), but the wetting phases can provide complementary information on the soil's water uptake dynamics and the restoration of functional porosity. Such analyses would also make it possible to take into account hysteresis effects, which are often overlooked but are fundamental to understanding the actual soil behaviour under natural conditions. Then, it would be valuable to combine these hydrological observations with other measurements, such as mechanical resistance or biological indicators (microbial activity, root development), in order to better link changes in water retention to integrated physical and biological processes. The integration of flow measurements could also improve the quantification of the agricultural consequences of the observed variations. Finaly, it would be interesting to study the effect of these systems in other pedological contexts. This thesis is based on loamy soils typical of the agricultural region of Wallonia. These deep loamy soils have a good balance between water retention and infiltration capacity and are among the most resilient soils to extreme climatic conditions. However, Wallonia also has more clayey soils, such as in the Fagnes-Famenne region, which are more susceptible to saturation. Sandier soils are also present in the north and south, with lower available water for plants and greater sensitivity to soil drought (Pirlot et al., 2025b).

Soil hydraulic properties are essential for understanding and modelling water flow and solute transport in soils. However, the high variability in soil structure and

hydraulic properties highlighted in this thesis is rarely taken into account in models, mainly due to a lack of data and the complexity of the processes occurring in agricultural soils. However, the few studies that have included the dynamics of these properties have shown better predictions and more reliable results (Meurer et al., 2020a; Geris et al., 2021; Jarvis et al., 2022). The dynamics of hydraulic properties can be taken into account by FPTs based on the variability of bulk density or organic carbon content. Van Genuchten parameters can then be modified in hydrological models to represent this variability (Geris et al., 2021; Huang et al., 2021). More complex models that consider the dynamics of soil structure induced by biological activity or OM turnover are beginning to emerge (Meurer et al., 2020a; b). In particular, they take into account root growth, which compresses or blocks pores, root decay, which creates biopores, bioturbation by soil fauna, and aggregation due to the decomposition of OM by soil microorganisms. More recently, Jarvis et al. (2024) developed a new soil-crop model called "USSF - Uppsala model of Soil Structure and Function" which integrates the effects of soil structure dynamics on water and organic matter. These are studied in response to the activity of biological agents such as earthworms or plant roots, as well as physical processes such as ploughing or WD cycles, and at seasonal to decadal timescales. This thesis therefore demonstrates the importance of collecting data on these temporal dynamics in order to develop more reliable models, currently under development for assessing the relevance of soil and crop management practices for the future.

Do SWRCs obtained by pedotransfer functions or laboratory measurements match those obtained continuously, directly in the field?

As already observed in Chapter 3 for the assessment of water and solute fluxes within a soil column, different methodologies can lead to contrasting results. In general, the temporal variability of SWRCs is studied in the laboratory using undisturbed samples taken at multiple times during the practice under study (Kool et al., 2019; Geris et al., 2021). However, the results obtained may be inconsistent between studies due to different sampling timing or types of measurements performed (Chandrasekhar et al., 2018). SWRCs are also often obtained by PTFs from easily measurable soil properties (Tóth et al., 2015; Szabó et al., 2021). This study therefore compared SWRCs obtained by EU-HYDI PTFs based on texture, organic carbon and bulk density, SWRCS obtained in the laboratory by ku-pF on undisturbed samples, and SWRCs obtained continuously, directly in the field for the same period.

The results indicate that SWRCs obtained by PTFs did not accurately represent SWRCs in the field. It has been shown that the use of PTFs to represent soil water dynamics leads to a large margin of error and high variability depending on the choice of PTF (Weihermüller et al., 2021; Hessine et al., 2025). These functions, developed

from large databases, struggle to capture the effects of agricultural practices, particularly when they deviate from conventional references. In order to improve the predictions and reliability of PTFs, predictors of soil structure dependent on agricultural practices should be added (Vereecken et al., 2010; Zhang and Schaap, 2019; Ramos et al., 2023). Furthermore, the incorporation of a greater diversity of agricultural practices into databases is essential, based on real field data.

SWRCs obtained in the laboratory are closer to those in the field and show similar trends. However, differences between plots are less visible. Thus, these curves do not seem optimal for investigating the temporal evolution of water retention properties as a function of agricultural practices. In addition, methodological biases may arise depending on the method used (ku-pF, sandbox, pressure plate, etc.) or the timing of sampling. This makes it difficult to compare studies and limits the ability to detect subtle or progressive trends.

In contrast, continuous field measurements allow real-time monitoring of changes in hydraulic properties over the seasons and during crop management operations. They incorporate the cumulative effect of wetting-drying cycles, root development, compaction and tillage operations. This approach also eliminates biases related to sample processing, measurement protocols, and temporal heterogeneity between studies. It therefore provides a more realistic and integrated view of soil water behaviour, which is essential for understanding the impact of agricultural practices and climate on soil structural dynamics. However, several other areas of research could have been explored. Firstly, it would be useful to test and compare the SWRCs obtained with several recent PTFs in order to identify their ability to represent different cropping systems. Second, sampling and analysis of samples preserved in their intact structure at several times during the year would allow for a better study of the seasonal dynamics of SWRCs in the laboratory and provide a more relevant comparison with field curves. Finally, it would also be useful to compare several SWRC analysis techniques in the laboratory, such as pressure plates or sandboxes.

In the face of growing challenges in modelling water and solute dynamics, and in predicting water availability in agriculture, it has become essential to inform models with data that reflects actual field conditions. However, the current lack of continuous and representative datasets remains a significant obstacle (Alletto et al., 2015; Meurer et al., 2020b; Jarvis et al., 2024). Addressing this issue necessitates a rethink of experimental protocols and the harmonisation of methodologies to better capture the temporal variability of agricultural practices. This thesis emphasises the importance of long-term in situ monitoring in multi-crop systems for improving model reliability and water management. Moving beyond static or punctual measurements of soil hydraulic properties, it advocates integrating variability into modelling tools to enable more accurate predictions and support informed decision-making, ultimately leading to more resilient and sustainable agricultural systems.

Publication of a database for assessing the impact of contrasting production systems on soil water dynamics and agrochemical leaching

This thesis wraps up with the publication of all the data collected over four years, from 2020 to 2024, from the hydrological monitoring of EcoFoodSystem contrasting production systems, a 16-year research initiative. This database includes the long-term temporal dynamics of soil hydraulic properties, soil structure and chemical leaching directly in the field. The installation of 24 Teros 12 water content sensors and 24 Teros 24 potential sensors, coupled with monitoring of bulk density and input leaching, constitutes an integrated approach that is still rarely found in the literature.

This comprehensive database is a valuable resource for understanding the temporal variability of hydraulic properties, which are too often considered static in agricultural models and decision-making (Chandrasekhar et al., 2018; Baroni et al., 2019). It opens the way to a better understanding of the interactions between agricultural practices, water dynamics, soil structure and the fate of agrochemicals, in the context of the transition to more sustainable agricultural systems and adaptation to climate change.

The results of Chapter 5 confirm the value of rejecting a static or snapshot view of soil hydraulic properties. These properties vary depending on climatic conditions, crop succession, weed management, soil cover, tillage practices and biological processes such as root development. Furthermore, measurements taken at different depths (up to 90 cm for moisture and potential, and 1.2 m for leaching) provide a better understanding of the vertical propagation of the effects of agricultural practices and extreme climatic events. This multi-depth approach enhances the ability to analyse water dynamics at the soil profile scale, an aspect that is often neglected in conventional studies focusing on surface layers. The integration of leaching data (nitrates, pesticides, metabolites) via sampling plates also allows for better characterisation of the transfer of pollutants to groundwater. This information is essential for assessing the environmental impact of agricultural systems and informing input management policies. The high variability of climatic observations (droughts, excess water) over the 2020-2024 period provides additional value for adapting practices to climate change.

Part of the data in this database has already been used in Chapter 5 of this thesis. However, many questions could still be answered using such a database. The prospects would be to analyse the influence of contrasting production systems and climatic conditions on the temporal evolution of hydraulic properties at depths of 60 and 90 cm. These results could then be compared with those obtained at the surface to identify any similarities or discrepancies. In addition, the impact of agricultural

practices on soil hysteresis could also be studied. Finally, it would be useful to study in more detail the effect of a transition to more sustainable systems on the exhaustion of metabolites and pesticides and on nitrate leaching.

This type of dataset is fundamental for integrating temporal variability in hydraulic properties into hydrological and agroecosystem models, which are often constrained by a lack of continuous, long-term in situ data (Clark et al., 2017; Baroni et al., 2019; Vogel, 2019). In particular, it can be used to refine water retention and hydraulic conductivity curves by incorporating their seasonal and annual variability, and to better predict episodes of runoff, drought or landslides. It can also be useful for calibrating remotely sensed soil moisture using satellite imaging or ground-penetrating radar (Albergel et al., 2012; Ochsner et al., 2013; Vereecken et al., 2015). Finally, this database is designed to be long-term, with monitoring beyond 2024 as part of the EcoFoodSystem experiment. It offers interesting prospects for studying longer-term trends, at least over eight years, in water dynamics and their link to full crop rotations. It will also enable data sharing within the scientific community on issues related to agroecological transition, water management and the sustainability of agricultural systems.

This comprehensive database will be available to all interested users and will be updated until at least 2028. This resource is a valuable and multi-purpose tool for scientists, modellers, and environmental managers, for advancing research on climate-resilient and environmentally sustainable agriculture, contributing to global efforts in food security, water conservation, and pollution mitigation.

General discussion on the resilience of EcoFoodSystem production systems

The database presented in chapter 6 can therefore help identify the agricultural practices most likely to limit the transfer of pollutants, optimise water retention and strengthen the resilience of agroecosystems to climate uncertainties. Through the analysis of water retention dynamics in Chapter 5 between 2021 and 2023, the study of herbicide behaviour in soil columns in 2021 in Chapter 4, and the monitoring of pesticide, metabolite and nitrate leaching in drainage water between 2021 and 2023 in Chapter 6, significant differences between EcoFoodSystem systems were highlighted. The concentrations of metabolites, pesticides and nitrate found in the samples are analysed in detail in the AIL4WaterQuality project report (Pirlot and Degré, 2023).

Over these three years, the T1 vegan system appears to be the most resilient in terms of hydrology. Camelina was planted on this system in 2021. It showed the greatest water retention capacity, with more compact soil and finer porosity. Furthermore,

during soil column leaching experiments, this system exhibited reduced water flow and lower herbicide elution, which was retained for a longer period in the immobile zone. Lower metabolite concentrations were also found in the drainage water at a depth of 1.2 metres. The majority of camelina roots are finer and within the first 30 centimetres, which leads to reduced water infiltration. Additionally, this plot exhibited a higher clay content, resulting in finer porosity and a higher CEC. Finally, pesticide transfer was limited due to hydraulic discontinuity caused by agricultural operations prior to the experiment. Despite the absence of fertilisation in 2021, however, nitrate concentrations above the 50 mg/l threshold and higher than those observed in plots T1 ref and ref herb were evident in 2022. This may be due to nitrate being released from the camelina or stubble. Nevertheless, nitrate residues were highest in the T1 plots in 2022. In 2022 and 2023, this system still demonstrated the greatest water retention capacity, with finer porosity and higher bulk density than the other plots. In 2022, the standardisation year, this plot produced the highest wheat yield of the T1 plots at 8.12 t/ha, with a higher organic matter content of 10.4%. The same trends continued in 2023 with faba bean. Therefore, the T1 vegan system incorporating camelina at the beginning of the rotation, involving chaffing and stubble ploughing, demonstrated a highly stable pore system, exhibiting the least water variability over time, and possessing soil properties conducive to subsequent crops in the rotation. Therefore, this system is likely to be the most resilient to extreme climatic conditions.

Conversely, the T1 ICLS system appears to be the least resilient of the T1 systems. In 2021, when maize was growing, its water retention capacity was intermediate between those of the T1 vegan and T1 ref systems. This system exhibited faster herbicide elution in soil columns with a larger mobile zone. Additionally, significant nitrate application to the maize resulted in higher concentrations in the 1.2 m drainage water than in the other T1 rotations. Nitrate residues in 2022 were comparable to those in the other plots. In 2022, when growing winter wheat, and in 2023, with faba beans, the T1 ICLS system demonstrated the lowest water retention capacity, with greater variability and more significant increases and decreases in water content. The presence of greater macropores causes preferential flows. This may be due to the large, fibrous, deep roots of the maize in 2021 causing more connectivity between the macropores, thereby enhancing and increasing water infiltration rates. These larger vertical flows pose a greater risk of groundwater contamination in this system. Therefore, this system is likely to be the least resilient to the extreme climatic conditions of T1 systems.

In 2021, the T1 ref system with sugar beet shows less compact soil than the T1 vegan or T1 ICLS systems, with better hydraulic conductivity and greater transfer between the mobile and immobile zones. Despite this, the system exhibits fewer preferential flows and lower herbicide elution in columns, as well as greater water retention than the T1 ICLS system. Nitrate concentrations in drainage water remain low, mainly due to lower fertilisation than in the T1 ICLS system or T2 rotations, and are below those of other plots. From 2021 to 2023, the T1 ref herb system showed greater water retention capacity and lower soil drying than systems without herbicide

use. The low presence of weeds and the absence of frequent hoeing, as in rotations without herbicides, may have resulted in a different soil structure that is more compact, with greater, but finer, porosity. Thus, the reference system shows intermediate drought resilience with its herbicide variant, which is more stable over time and could be more resilient.

Regarding T2 rotations, these are more similar to each other and demonstrate lower water retention capacities than T1 rotations from 2021 to 2023. Soil droughts are more severe for these rotations, with more pronounced peaks in water content during the rainy season. Rapeseed planted at the beginning of the 2021 rotation resulted in high macroporosity and rapid water infiltration, due to its well-developed, deep root system. These effects are still visible two years later in the rotation. A similar observation was made with maize in the T1 ICLS system in 2021 and in the T2 ref and T2 ref herb systems in 2023, albeit to a lesser extent. Generally, higher nitrate concentrations were found at a depth of 1.2 metres in the T2 plots due to the heavy fertilisation of the rapeseed and the rapid transport of nitrate by high water infiltration. However, in 2022, nitrate residues in the soil after rapeseed were higher for the subsequent crop. Therefore, planting rapeseed at the beginning of the rotation appears to have a detrimental effect on the systems' water retention capacity and hydrological resilience to drought.

Of the T2 rotations, the vegan T2 had the lowest water retention capacity and experienced the most pronounced soil drying in 2022 and 2023. Unlike the other systems incorporating winter wheat and peas in 2022, this system involved the cultivation of wheat alone. Therefore, the rapeseed, wheat and pea rotation appears to be the least resilient of the eight rotations examined when faced with extreme climatic conditions.

The evolution of water content during the most severe droughts of 2024 and 2025 for the eight plots is illustrated in Figures 72 and 73, respectively.

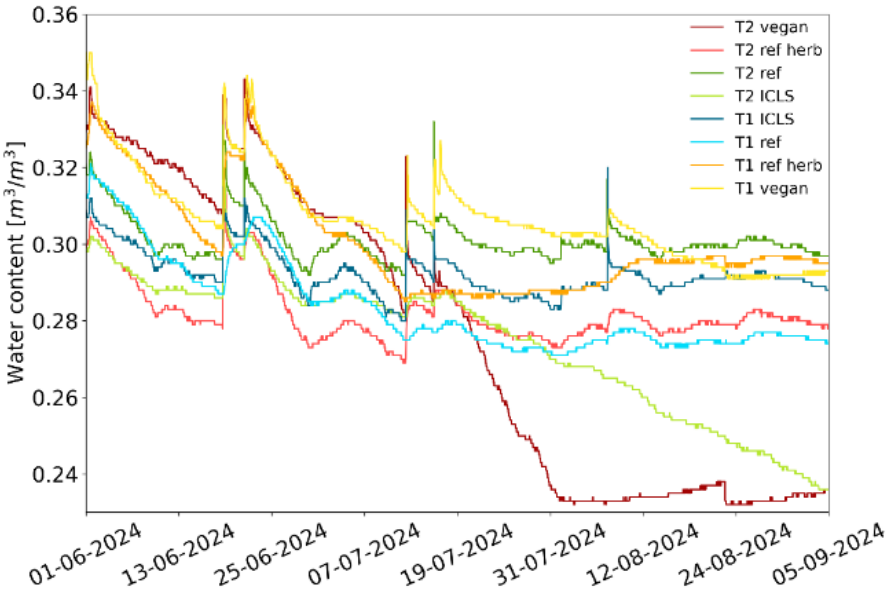

Figure 73. Evolution of water content in the eight plots during the soil drying period from June to September 2024.

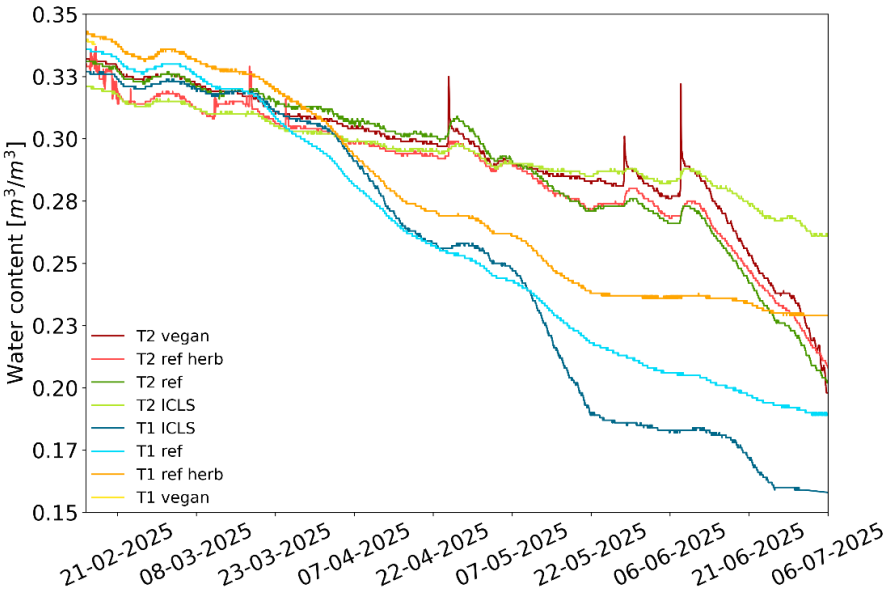

Figure 72. Evolution of water content in the eight plots during the soil drying period from February to July 2025

In 2024, the year of standardisation with winter wheat, except for T2 vegan with oats, the same trends appear to continue. The T1 plots show lower overall soil drying out, with higher water contents than T2. The T1 ref herb and T1 vegan plots still demonstrate greater soil water retention, followed by the T1 ICLS plot. As in August 2023, the T1 ref plots show greater drying out than the T1 ICLS plots. Potato cultivation in 2023 may have altered the soil structure, influencing its water retention capacity. The T2 plots exhibit more contrasting behaviour, probably due to the varied crops in 2023. T2 ref shows better water retention and a more stable water content, while T2 ref herb exhibits more pronounced drying out. Despite the planting of maize in 2023, these two plots are above some of the T1 plots. As in 2023, the T2 ICLS and T2 vegan plots show the lowest water retention, drying out significantly, mainly after the July 2024 harvest. The T2 ICLS plot showed more pronounced drying out due to temporary grassland being established with sheep grazing, as observed in 2023. The dense cover can pump more water. Additionally, the lack of tillage may have resulted in greater biological activity and connected macropores, leading to increased water infiltration.

Between February and July 2025, significant soil drought was observed. Until early April, the water content remained consistently high across all plots. In the fifth year of the rotation cycle, crops in temporalities 1 and 2 were reversed compared to 2021. Since September 2024, rapeseed has been planted on plots T1. Plots T2 had a cover crop established until April 2025, after which sugar beet, maize and camelina were planted. Interestingly, trends opposite to those observed in 2021–2024 emerged. Between March and June 2025, the T1 plots dried out faster and more significantly than the T2 plots. Thus, the introduction of rapeseed has reversed the trends, reducing the water retention capacity of these plots and their resilience to drought. These observations confirm the influence of rapeseed cultivation in crop rotations. The T1 ICLS plot, which showed the most significant drying out of the T1 plots between 2022 and 2024, has the lowest water retention and content, reaching 0.16 m^3/m^3. The T1 ref herb plot continues to demonstrate the highest water retention of the T1 plots. Therefore, despite the influence of rapeseed on soil water retention dynamics, crops from previous years help to mitigate its impact. The T2 plots demonstrate greater resilience to drought, maintaining high water content until mid-June 2025 before declining. These plots remain close to each other. T2 ref and T2 ref herb show the lowest water content, indicating the potential impact of sugar beet crops with abundant weeds. In contrast, the T2 ICLS plot shows the highest water retention, with water content remaining above 0.28 m^3/m^3 despite maize being planted. Therefore, establishing temporary grassland in 2022 and 2023 appears to have created a more stable pore structure, enabling high water retention to be maintained during maize cultivation.

Therefore, caution should be exercised when drawing conclusions about how resilient systems are to climatic conditions and their ability to mitigate water pollution. Trends are emerging in the first part of the rotation, from 2021 to 2024. However, changes appear to be taking place after the fifth year. Consequently, a more thorough analysis of the systems after the full eight-year rotation period seems more relevant and reliable. Nevertheless, the impact of certain agricultural practices has already been highlighted, as has the importance of crop succession in relation to soil and water dynamics in the short and medium term.

This thesis demonstrates that it is possible to design agricultural systems that are both more environmentally sustainable and more resilient to climate variability, without compromising the ability to meet the nutritional needs of the population. The cropping systems investigated were specifically designed to align with the EAT-Lancet Commission's recommendations for a healthy and sustainable diet, exploring several dietary trajectories, including reference systems, integrating livestock system, as well as entirely without animal (vegan) systems. Contrary to the commonly held view that environmental sustainability and food security are mutually exclusive, this thesis highlights the potential of certain alternative production systems to reconcile these objectives. By incorporating more diverse agricultural practices, reducing reliance on synthetic inputs, and improving water retention capacity, these systems emerge as promising levers to enhance water management in agriculture, mitigate diffuse pollution risks, and strengthen the resilience of agroecosystems. This work thus shows that sustainable agricultural pathways can simultaneously address the challenges of food production, public health, and natural resource preservation.

To finish, this thesis finally explores two ways of reducing the impact of agricultural systems on water resources in terms of quantity and quality. These are: firstly, improving our understanding of the fate of pesticides; and secondly, investigating the impact of more sustainable agricultural practices on soil structure dynamics, hydraulic properties, and agrochemical leaching. However, other approaches could have been considered. Firstly, more optimal fertilisation management could have been considered. Nitrate and phosphorus are major contaminants of both groundwater and surface water. Secondly, improving soil vegetation cover would limit the risk of runoff, erosion, and the leaching of plant protection products. Thirdly, the impact of landscaping and agroecological infrastructure on water and contaminant flows in the soil should be studied. Creating grassy buffer zones, hedges, wooded strips, filter ditches or agroforestry areas could help conserve water. The thesis could also have examined the effect of soil compaction on its hydraulic properties. The effectiveness and leaching of biocontrol products could then be explored as an alternative to conventional pesticides. Lastly, the thesis could have examined runoff and shallow water flows in soils, which transport agrochemicals into surface waters.

Chapter 8

Conclusions

To address the challenges posed by climate change, water resource contamination, and the need for a transition to more sustainable production systems, this thesis aims to provide a more realistic analysis of soil water dynamics and contaminant behaviour. Two approaches to reducing the impact of agricultural systems on water quality and management are explored. The first approach is to improve our understanding of the fate of pesticides in the environment. This will be achieved by studying the leaching of problematic herbicides in undisturbed soil columns at various depths and under different cropping systems in Wallonia. The second approach involves analysing the temporal dynamics of soil water during the transition to contrasting, more sustainable production systems through continuous hydrological monitoring in the field.

Firstly, tracer leaching experiments were performed on soil columns of different designs frequently encountered in the literature to obtain quantitative data and dual-porosity parameters. The results showed that soil structure greatly affected solute transport dynamics and water infiltration. Undisturbed columns provide a more realistic representation of field conditions, accounting for soil heterogeneity and preferential flows. Disturbed columns tend to underestimate the rapid transport of contaminants and overestimate their retention in soils, failing to provide a reliable representation of groundwater contamination risks. The differing diameters of disturbed columns did not have a significant impact on leaching results. In contrast, different heights of undisturbed columns had a significant impact on solute transport. Shorter columns resulted in greater leaching and recovery of the solute due to lower dispersivity. They tend to overestimate leaching potential and underestimate retention. Longer columns better capture the natural heterogeneity of the soil, improving the reliability of transport models and environmental risk assessments. Finally, the sampling method had a major effect, with columns sampled using a mechanical corer showing very significant preferential flows due to vibrations and failing to accurately represent water and solute flows. Therefore, some commonly used methodologies may not be relevant to study the mobility of solutes within a soil profile, especially if the experiment attempts to approximate field conditions. Moreover, the timing of sampling in relation to cultivation operations appears to influence the solute leaching through the soil profile. This study allows researchers to better choose the experimental design according to the purpose of their experiments.

Secondly, the fate of eight pesticides of concern to groundwater was investigated under three production systems and at three soil depths with leaching experiments in undisturbed columns, mass balances and inverse dual-porosity modelling to adjust mobility parameters. The results revealed that the differences in soil properties and structure between the three horizons resulted in more contrasting leaching behaviour than between the production systems. The topsoil retains more pesticides due to its high organic matter content and biological activity, which promotes degradation. Significant preferential flows are observed in horizon 2 due to the undisturbed nature of this soil layer. Pesticide adsorption increases in horizon 3 due to its higher clay content and lower water flow, resulting in greater retention. This study shows that the

transport processes and fate of pesticides within the lower horizons are complex and cannot be ignored. Applying topsoil mobility parameters to the entire profile will lead to an overestimation of pesticide adsorption and degradation, underestimating the risk of groundwater contamination. These results may partly explain the high concentrations still found in groundwater despite contamination risk assessments and the resulting regulations. Our analysis also demonstrates that cropping systems can affect pesticide leaching dynamics. The findings highlight the importance of root architecture, soil properties and surface tillage in influencing water flow and pesticide transport through soil. Thus, in the long term, different agricultural systems could have a significant effect on pesticide leaching and be a lever for reducing groundwater pollution. The results also highlighted significant differences in transport parameters for most pesticides when compared with established databases such as the PPDB and the EFSA peer review for Europe. The values used in Belgium show higher adsorption coefficients, which could lead to an underestimation of pesticide leaching into groundwater. In addition, generic half-lives are higher for most herbicides, indicating an underestimation of pesticide degradation and metabolite production. Therefore, parameters derived from databases should be used with caution and are not always reliable. Hence, this study shows the need to investigate the fate and adapt the transport values of all environmentally problematic pesticides to site-specific characteristics.

Thirdly, the impacts of different contrasting production systems and contrasting climatic conditions on the temporal evolution of SWRCs were analysed in the field over three years. Field SWRCs were then compared with those obtained using an EU-HYDI PTF and in the laboratory on undisturbed samples. The analysis shows a high degree of variability in SWRCs, both over time and between cropping systems. The greatest variability was found between plots, then within a season and finally between years. This study has therefore shown that agricultural practices and different crops can have a greater influence on soil water retention dynamics than the sole root development and WDs within a season or meteorological conditions between years. Practices such as crop differentiation, weed control, crop residue management, compaction during harvest, and the introduction of temporary grasslands induced significant changes in water retention capacity, with some effects persisting for at least two years. These seasonal dynamics, rarely documented in situ, show that soil water behaviour is far from static and depends on climate, crop type and agricultural practices. This study highlights that agricultural practices and different crops can be levers for enhancing water and food resilience against future climate conditions. In addition, the SWRCs obtained from the EU-HYDI PTFs did not accurately represent SWRCs in the field, particularly for non-conventional agricultural practices. As a result, PTFs need to integrate a wider variety of management practices for agricultural plots. The laboratory SWRCs are closer to the field curves with similar trends. However, the differences in SWRCs between different modalities may be less visible. In the short term, these curves are therefore not optimal for investigating the temporal

evolution of water retention properties as a function of meteorological conditions and agricultural practices.

Finally, this thesis wraps up with the publication of all the data collected over four years, from 2020 to 2024, from the hydrological monitoring of contrasting production systems by EcoFoodSystem, a 16-year research initiative. A major strength of this dataset lies in its depth measurements, down to 90 cm, allowing researchers to study not just surface processes but also the propagation of climatic and management effects into deeper soil horizons. The inclusion of soil water sampling plate data at 1.2 m depth further enriches the resource by enabling the monitoring of residual pesticide and metabolite leaching, even years after their use has ceased. This database includes the long-term temporal dynamics of soil hydraulic properties, soil structure and chemical leaching directly in the field. This resource is a valuable and multi-purpose tool for scientists, modellers, and environmental managers, for advancing research on climate-resilient and environmentally sustainable agriculture, contributing to global efforts in food security, water conservation, and pollution mitigation.

In conclusion, this thesis demonstrates the importance of clarifying how different methodologies can impact results and develop standardised practices for research into pollutant leaching in soil columns in order to improve the reliability of contamination risk assessments. This study also demonstrates the importance of considering deeper soil horizons in pesticide fate to better understand and include the different transport, retention and degradation dynamics within the entire soil profile. This will enable more relevant recommendations to be made on pesticide selection, dose adjustment and authorised application periods. This research therefore supports the importance of adapting sorption and degradation parameters for all problematic pesticides and metabolites to the specific characteristics of the site under study for future modelling and decision-making. Aiming to improve water management in agriculture, this thesis emphasises the value of continuous, long-term measurements under real field conditions in multi-crop production systems. It is becoming necessary to move beyond static or punctual approaches of hydraulic properties and to integrate their variability into modelling tools to generate more relevant decision-making to promote more resilient, efficient and sustainable agriculture. The research also proves that it is possible to design agricultural systems that are both more environmentally sustainable and more resilient to climate variability, without compromising the ability to meet the nutritional needs of the population.

References

Abbasi, F., D. Jacques, J. Simunek, J. Feyen, and M.T. van Genuchten. 2003a. Inverse Estimation of Soil Hydraulic and Solute Transport Parameters from Transient Field Experiments: Heterogeneous Soil. Am. Soc. Agric. Eng. 46(4): 1097–1111. doi: 10.13031/2013.13961.

Abbasi, F., J. Simunek, J. Feyen, M.T. Van Genuchten, and P.J. Shouse. 2003b. Simultaneous Inverse Estimation of Soil Hydraulic and Solute Transport Parameters from Transient Field Experiments: Homogeneous Soil. Am. Soc. Agric. Eng. 46(4): 1085–1095. doi: 10.13031/2013.13960.

Ahmed, A., J. Bin Alam, P. Pandey, and S. Hossain. 2021. Estimation of unsaturated flow parameters and hysteresis curve from field instrumentation. MATEC Web Conf. 337: 8.

Ajayi, A.E., R. Horn, J. Rostek, D. Uteau, and S. Peth. 2019. Evaluation of temporal changes in hydrostructural properties of regenerating permanent grassland soils based on shrinkage properties and μCT analysis. Soil Tillage Res. 185(June 2018): 102–112. doi: 10.1016/j.still.2018.09.005.

Akay Demir, A.E., F.B. Dilek, and U. Yetis. 2019. A new screening index for pesticides leachability to groundwater. J. Environ. Manage. 231(November 2018): 1193–1202. doi: 10.1016/j.jenvman.2018.11.007.

Alavaisha, E., S. Manzoni, and R. Lindborg. 2019. Different agricultural practices affect soil carbon, nitrogen and phosphorous in Kilombero -Tanzania. J. Environ. Manage. 234(January): 159–166. doi: 10.1016/j.jenvman.2018.12.039.

Albergel, C., P. de Rosnay, C. Gruhier, J. Muñoz-Sabater, S. Hasenauer, et al. 2012. Evaluation of remotely sensed and modelled soil moisture products using global ground-based in situ observations. Remote Sens. Environ. 118: 215–226. doi: 10.1016/j.rse.2011.11.017.

Albers, C.N., U.E. Bollmann, N. Badawi, and A.R. Johnsen. 2022. Leaching of 1,2,4-triazole from commercial barley seeds coated with tebuconazole and prothioconazole. Chemosphere 286(P2): 131819. doi: 10.1016/j.chemosphere.2021.131819.

Aliste, M., G. Pérez-Lucas, I. Garrido, J. Fenoll, and S. Navarro. 2021. Mobility of insecticide residues and main intermediates in a clay-loam soil, and impact of leachate components on their photocatalytic degradation. Chemosphere 274. doi: 10.1016/j.chemosphere.2021.129965.

Alletto, L., V. Pot, S. Giuliano, M. Costes, F. Perdrieux, et al. 2015. Temporal variation in soil physical properties improves the water dynamics modeling in a conventionally-tilled soil. Geoderma 243–244: 18–28. doi: 10.1016/J.GEODERMA.2014.12.006.

Alskaf, K., S.J. Mooney, D.L. Sparkes, P. Wilson, and S. Sjögersten. 2021. Short-term impacts of different tillage practices and plant residue retention on soil physical properties and greenhouse gas emissions. Soil Tillage Res.

206(104803): 1–12. doi: 10.1016/j.still.2020.104803.

Alvarez, F., M. Arena, D. Auteri, M. Binaglia, A.F. Castoldi, et al. 2023. Peer review of the pesticide risk assessment of the active substance S-metolachlor excluding the assessment of the endocrine disrupting properties. 21(January). doi: 10.2903/j.efsa.2023.7852.

Arias-Estévez, M., E. López-Periago, E. Martínez-Carballo, J. Simal-Gándara, J.C. Mejuto, et al. 2008. The mobility and degradation of pesticides in soils and the pollution of groundwater resources. Agric. Ecosyst. Environ. 123(4): 247–260. doi: 10.1016/j.agee.2007.07.011.

Arienzo, M., T. Crisanto, M.J. Sánchez-Martín, and M. Sánchez-Camazano. 1994. Effect of Soil Characteristics on Adsorption and Mobility of (14C)Diazinon. J. Agric. Food Chem. 42(8): 1803–1808. doi: 10.1021/jf00044a044.

Arora, N.K. 2019. Impact of climate change on agriculture production and its sustainable solutions. Environ. Sustain. 2(2): 95–96. doi: 10.1007/s42398-019-00078-w.

Arthur, E.L., P.J. Rice, P.J. Rice, T.A. Anderson, and J.R. Coats. 1998. Mobility and Degradation of Pesticides and Their Degradates in Intact Soil Columns. In: Führ, F., Hance, R., Plimmer, J., and Nelson, J., editors, The lysimeter concept, environmental behavior of pesticides. American Chemical Society, Washington DC. p. 88–114

Bacq-Labreuil, A., A.L. Neal, J. Crawford, S.J. Mooney, E. Akkari, et al. 2021. Significant structural evolution of a long-term fallow soil in response to agricultural management practices requires at least 10 years after conversion. Eur. J. Soil Sci. 72(2): 829–841. doi: 10.1111/ejss.13037.

Ball, B.C., I. Bingham, R.M. Rees, C.A. Watson, and A. Litterick. 2005. The role of crop rotations in determining soil structure and crop growth conditions. Can. J. Soil Sci. 85(5): 557–577. doi: 10.4141/S04-078.

Baran, N., N. Surdyk, and C. Auterives. 2021. Pesticides in groundwater at a national scale (France): Impact of regulations , molecular properties, uses, hydrogeology and climatic conditions. Sci. Total Environ. 791: 148137. doi: 10.1016/j.scitotenv.2021.148137.

Barba, V., J.M. Marín-Benito, M.J. Sánchez-Martín, and M.S. Rodríguez-Cruz. 2020. Transport of 14C-prosulfocarb through soil columns under different amendment, herbicide incubation and irrigation regimes. Sci. Total Environ. 701: 1–8. doi: 10.1016/j.scitotenv.2019.134542.

Baroni, G., B. Schalge, O. Rakovec, R. Kumar, L. Schüler, et al. 2019. A Comprehensive Distributed Hydrological Modeling Intercomparison to Support Process Representation and Data Collection Strategies. Water Resour. Res. 55(2): 990–1010. doi: 10.1029/2018WR023941.

BASF. 2017. Formulations WG : Préparation de la bouillie de pulvérisation. Ecully, France.

Basile, A., G. Ciollaro, and A. Coppola. 2003. Hysteresis in soil water characteristics as a key to interpreting comparisons of laboratory and field measured hydraulic

properties. Water Resour. Res. 39(12): 1–12. doi: 10.1029/2003WR002432.

Bégin, L., J. Fortin, and J. Caron. 2003. Evaluation of the Fluoride Retardation Factor in Unsaturated and Undisturbed Soil Columns. Soil Sci. Soc. Am. J. 67(6): 1635–1646. doi: 10.2136/sssaj2003.1635.

Van Beinum, W., S. Beulke, C. Fryer, and C. Brown. 2006. Lysimeter experiment to investigate the potential influence of diffusion-limited sorption on pesticide availability for leaching. J. Agric. Food Chem. 54(24): 9152–9159. doi: 10.1021/jf061850m.

Bergström, L., E. Börjesson, and J. Stenström. 2011. Laboratory and Lysimeter Studies of Glyphosate and Aminomethylphosphonic Acid in a Sand and a Clay Soil. J. Environ. Qual. 40(1): 98–108. doi: 10.2134/jeq2010.0179.

Berti, M., R. Gesch, C. Eynck, J. Anderson, and S. Cermak. 2016. Camelina uses, genetics, genomics, production, and management. Ind. Crops Prod. 94: 690–710. doi: 10.1016/j.indcrop.2016.09.034.

Beulke, S., C.D. Brown, C.J. Fryer, and A. Walker. 2001. Lysimeter study to investigate the effect of rainfall patterns on leaching of isoproturon. Pest Manag. Sci. 58(1): 45–53. doi: 10.1002/ps.419.

Bewick, D. 1994. The Mobility of Pesticides in Soil — Studies to Prevent Groundwater Contamination. Chem. Plant Prot. 9: 57–86. doi: 10.1007/978-3-642-79104-8_2.

Blanco-Canqui, H., and C.S. Wortmann. 2020. Does occasional tillage undo the ecosystem services gained with no-till ? A review. Soil Tillage Res. 198(October 2019): 104534. doi: 10.1016/j.still.2019.104534.

Boivin, A., R. Cherrier, C. Perrin-Ganier, and M. Schiavon. 2004. Time effect on bentazone sorption and degradation in soil. Pest Manag. Sci. 60(8): 809–814. doi: 10.1002/ps.889.

Bordoni, M., M. Bittelli, R. Valentino, S. Chersich, and C. Meisina. 2017. Improving the estimation of complete field soil water characteristic curves through field monitoring data. J. Hydrol. 552: 283–305. doi: 10.1016/j.jhydrol.2017.07.004.

Bošković, N., K. Brandstätter-Scherr, P. Sedláček, Z. Bílková, L. Bielská, et al. 2020. Adsorption of epoxiconazole and tebuconazole in twenty different agricultural soils in relation to their properties. Chemosphere 261. doi: 10.1016/j.chemosphere.2020.127637.

Brancato, A., D. Brocca, L. Bura, A. Chiusolo, D.C. Marques, et al. 2017. Peer review of the pesticide risk assessment for the active substance terbuthylazine in light of confirmatory data submitted. 15(May). doi: 10.2903/j.efsa.2017.4868.

Bromly, M., C. Hinz, and L.A.G. Aylmore. 2007. Relation of dispersivity to properties of homogeneous saturated repacked soil columns. Eur. J. Soil Sci. 58(1): 293–301. doi: 10.1111/j.1365-2389.2006.00839.x.

Carsel, R., J.C. Imhoff, P.R. Hummel, J.M. Cheplick, and D.J. A.S. 2005. PRZM-3, A Model for Predicting Pesticide and Nitrogen Fate in the Crop Root and Unsaturated Soil Zones: Users Manual for Release 3.12.2. Athens, GA.

Carvalho, F.P. 2017. Pesticides, environment, and food safety. Food Energy Secur.

6(2): 48–60. doi: 10.1002/fes3.108.

Celestino Ladu, J.L., and D.R. Zhang. 2011. Modeling atrazine transport in soil columns with HYDRUS-1D. Water Sci. Eng. 4(3): 258–269. doi: 10.3882/j.issn.1674-2370.2011.03.003.

Chan, K.Y. 2001. An overview of some tillage impacts on earthworm population abundance and diversity - Implications for functioning in soils. Soil Tillage Res. 57(4): 179–191. doi: 10.1016/S0167-1987(00)00173-2.

Chandrasekhar, P., J. Kreiselmeier, A. Schwen, T. Weninger, S. Julich, et al. 2018. Why we should include soil structural dynamics of agricultural soils in hydrological models. Water 10(1862): 1–18. doi: 10.3390/w10121862.

Chen, X., Z.-C. Zhang, X.-N. Zhang, Y.-Q. Chen, M.-K. Qian, et al. 2008. Estimation of Groundwater Recharge from Precipitation and Evapotranspiration by Lysimeter Measurement and Soil Moisture Model. J. Hydrol. Eng. 13(5): 333–340. doi: 10.1061/(asce)1084-0699(2008)13:5(333).

Cherrier, R., A. Boivin, C. Perrin-Ganier, and M. Schiavon. 2005. Sulcotrione versus atrazine transport and degradation in soil columns. Pest Manag. Sci. 61(9): 899–904. doi: 10.1002/ps.1105.

Cheviron, B., and Y. Coquet. 2009. Sensitivity Analysis of Transient-MIM HYDRUS-1D: Case Study Related to Pesticide Fate in Soils. Vadose Zo. J. 8(4): 1064–1079. doi: 10.2136/vzj2009.0023.

Ciglasch, H., W. Amelung, S. Totrakool, and M. Kaupenjohann. 2005. Water flow patterns and pesticide fluxes in an upland soil in northern Thailand. Eur. J. Soil Sci. 56(6): 765–777. doi: 10.1111/j.1365-2389.2005.00712.x.

Ciocca, F., I. Lunati, and M.B. Parlange. 2014. Effects of the water retention curve on evaporation from arid soils. Geophys. Res. Lett. 41(9): 3110–3116. doi: 10.1002/2014GL059827.

Clark, M.P., M.F.P. Bierkens, L. Samaniego, R.A. Woods, R. Uijlenhoet, et al. 2017. The evolution of process-based hydrologic models: Historical challenges and the collective quest for physical realism. Hydrol. Earth Syst. Sci. 21(7): 3427–3440. doi: 10.5194/hess-21-3427-2017.

Coppola, A., V. Comegna, A. Basile, N. Lamaddalena, and G. Severino. 2009. Darcian preferential water fl ow and solute transport through bimodal porous systems : Experiments and modelling. J. Contam. Hydrol. 104(1–4): 74–83. doi: 10.1016/j.jconhyd.2008.10.004.

CORDER. 2020. Estimation quantitative des utilisations de produits phytopharmaceutiques par les différents secteurs d'activité en Wallonie.

Corwin, D.L. 2000. Evaluation of a simple lysimeter-design modification to minimize sidewall flow. J. Contam. Hydrol. 42(1): 35–49. doi: 10.1016/S0169-7722(99)00088-1.

Cox, L., M.J. Calderón, M.C. Hermosín, and J. Cornejo. 1999. Leaching of Clopyralid and Metamitron under Conventional and Reduced Tillage Systems. J. Environ. Qual. 28(2): 605–610. doi: 10.2134/jeq1999.00472425002800020026x.

Cox, L., A. Walker, M.C. Hermosin, and J. Cornejo. 1996. Measurement and

simulation of the movement of thiazafluron, clopyralid and metamitron in soil columns. Weed Res. 36(5): 419–429. doi: 10.1111/j.1365-3180.1996.tb01671.x.

Cueff, S., L. Alletto, M. Bourdat-Deschamps, P. Benoit, and V. Pot. 2020. Water and pesticide transfers in undisturbed soil columns sampled from a Stagnic Luvisol and a Vermic Umbrisol both cultivated under conventional and conservation agriculture. Geoderma 377(August): 114590. doi: 10.1016/j.geoderma.2020.114590.

Dashtaki, S.G., M. Homaee, and H. Khodaverdiloo. 2010. Derivation and validation of pedotransfer functions for estimating soil water retention curve using a variety of soil data. Soil Use Manag. 26(1): 68–74. doi: 10.1111/j.1475-2743.2009.00254.x.

Deng, H., D. Feng, J. xiong He, F. ze Li, H. mei Yu, et al. 2017. Influence of biochar amendments to soil on the mobility of atrazine using sorption-desorption and soil thin-layer chromatography. Ecol. Eng. 99: 381–390. doi: 10.1016/j.ecoleng.2016.11.021.

Dey, P., P. Sundriyal, and S.K. Sahoo. 2017. Science of Lagging Behind- Hysteresis in Soil Moisture Characteristic Curve - A Review. Int. J. Curr. Microbiol. Appl. Sci. 6(10): 151–156.

Dubus, I.G., S. Beulke, C.D. Brown, B. Gottesbüren, and A. Dieses. 2004. Inverse modelling for estimating sorption and degradation parameters for pesticides. Pest Manag. Sci. 60(9): 859–874. doi: 10.1002/ps.893.

Dusek, J., M. Dohnal, M. Snehota, M. Sobotkova, C. Ray, et al. 2015. Transport of bromide and pesticides through an undisturbed soil column: A modeling study with global optimization analysis. J. Contam. Hydrol. 175–176: 1–16. doi: 10.1016/j.jconhyd.2015.02.002.

Dusek, J., M. Dohnal, T. Vogel, and C. Ray. 2011. Field leaching of pesticides at five test sites in Hawaii: Modeling flow and transport. Pest Manag. Sci. 67(12): 1571–1582. doi: 10.1002/ps.2217.

Eat Lancet Commission. 2019. Healthy Diets From Sustainable Food Systems : Summary.

EFSA. 2015. Conclusion on the peer review of the pesticide risk assessment of the active substance bentazone. EFSA J. 13(April). doi: 10.2903/j.efsa.2015.4077.

EurEau. 2021. Europe's Water in Figures An overview of the European drinking water and waste water sectors. Brussels.

European Commission. 2000. Directive 2000/60/EC of the European Parliament and of the Council of 23 October 2000 establishing a framework for Community action in the field of water policy.

European Commission. 2006. Directive 2006/54/EC of the European Parliament and of the Council of 12 December 2006 on the protection of groundwater against pollution and deterioration.

European Commission. 2014. Assessing Potential for Movement of Active Substances and their Metabolites to Ground Water in the EU.

Facenda, G., R. Celis, B. Gámiz, and R. López-Cabeza. 2024. An enantioselective

study of the behavior of the herbicide ethofumesate in agricultural soils: Impact of the addition of organoclays and biochar. Ecotoxicol. Environ. Saf. 270(September 2023). doi: 10.1016/j.ecoenv.2023.115870.

FAO. 2009. How to Feed the World in 2050.

FAO. 2015. World reference base for soil resources 2014 - International soil classification system for naming soils and creating legends for soil maps.

FAO. 2017. The future of food and agriculture: trends and challenges.

FAO. 2022. Pesticides use, pesticides trade and pesticides indicators – Global, regional and country trends, 1990–2020. Rome, Italy No. 46: 13. https://www.fao.org/documents/card/es/c/cc0918en/%0Ahttp://www.fao.org/documents/card/en/c/cc0918en.

FAOSTAT. 2022. Land, Inputs and Sustainability / Pesticides Use - Metadata. Pestic. Use. https://www.fao.org/faostat/en/#data/RP/visualize.

Felding, G. 1997. Pesticide adsorption as a function of depth below surface. Pestic. Sci. 50(1): 64–66.

Fierer, N., J.P. Schimel, and P.A. Holden. 2003. Variations in microbial community composition through two soil depth profiles. Soil Biol. Biochem. 35(1): 167–176. doi: 10.1016/S0038-0717(02)00251-1.

Flury, M., and T.F. Gimmi. 2002. Solute Diffusion. In: Jacob, H. and Clarke, G., editors, Methods of Soil Analysis. Soil Science Society of America. p. 1323–1351

FOCUS. 2000. FOCUS groundwater scenarios in the EU review of active substances.

FOCUS. 2009. Assessing Potential for Movement of Active Substances and their Metabolites to Ground Water in the EU.

Fox, A., F. Widmer, and A. Lüscher. 2022. Soil microbial community structures are shaped by agricultural systems revealing little temporal variation. Environ. Res. 214(P3): 113915. doi: 10.1016/j.envres.2022.113915.

Gärdenäs, A.I., J. Šimůnek, N. Jarvis, and M.T. van Genuchten. 2006. Two-dimensional modelling of preferential water flow and pesticide transport from a tile-drained field. J. Hydrol. 329(3–4): 647–660. doi: 10.1016/j.jhydrol.2006.03.021.

van Genuchten, M.T. 1980. A Closed-form Equation for Predicting the Hydraulic Conductivity of Unsaturated Soils. Soil Sci. Soc. Am. J. 44: 892–898. doi: 10.2136/sssaj1980.03615995004400050002x.

van Genuchten, M.T., and P.J. Wierenga. 1976. Mass transfer studies in sorbiong porous media. Soil Sci. Soc. Am. J. 40(4): 473–480.

Geris, J., L. Verrot, L. Gao, X. Peng, J. Oyesiku-Blakemore, et al. 2021. Importance of short-term temporal variability in soil physical properties for soil water modelling under different tillage practices. Soil Tillage Res. 213(July): 105132. doi: 10.1016/j.still.2021.105132.

Gerke, H.H., and M.T. van Genuchten. 1993a. Evaluation of a first-order water transfer term for variably saturated dual-porosity flow models. Water Resour. Res. 29(4): 1225–1238. doi: 10.1029/92WR02467.

Gerke, H.H., and M.T. van Genuchten. 1993b. A dual-porosity model for simulating the preferential movement of water and solutes in structured porous media. Water Resour. Res. 29(2): 305–319. doi: 10.1029/92WR02339.

Gerke, H.H., and J.M. Köhne. 2004. Dual-permeability modeling of preferential bromide leaching from a tile-drained glacial till agricultural field. J. Hydrol. 289(1–4): 239–257. doi: 10.1016/j.jhydrol.2003.11.019.

Gesch, R.W., and J.M.F. Johnson. 2015. Water use in camelina-soybean dual cropping systems. Agron. J. 107(3): 1098–1104. doi: 10.2134/agronj14.0626.

Gozubuyuk, Z., U. Sahin, M. Cemal, and I. Ozturk. 2015. The influence of different tillage practices on water content of soil and crop yield in vetch – winter wheat rotation compared to fallow – winter wheat rotation in a high altitude and cool climate. Agric. Water Manag. 160: 84–97. doi: 10.1016/j.agwat.2015.07.003.

Grodner, M.L., W.B. Richardson, D.J. Boethel, and P.D. Coreil. 2014. Protecting Groundwater from Pesticide Contamination Groundwater. Louisiana Coop. Ext. Serv. LSU AgCenter Res.: 1–4.

Guillaume, B., H. Aroui Boukbida, G. Bakker, A. Bieganowski, Y. Brostaux, et al. 2023. Reproducibility of the wet part of the soil water retention curve: A European interlaboratory comparison. Soil 9(1): 365–379. doi: 10.5194/soil-9-365-2023.

Hannes, M., U. Wollschlager, T. Wohling, and H.-J. Vogel. 2016. Revisiting hydraulic hysteresis based on long-term monitoring of hydraulic states in lysimeters. Water Resour. Res. 52: 3847–3865. doi: 10.1111/j.1752-1688.1969.tb04897.x.

Hayes, T.B., and M. Hansen. 2017. From silent spring to silent night: Agrochemicals and the anthropocene. Elementa 5. doi: 10.1525/elementa.246.

Hedayati, M., A. Ahmed, M.S. Hossain, J. Hossain, and A. Sapkota. 2020. Transportation Geotechnics Evaluation and comparison of in-situ soil water characteristics curve with laboratory SWCC curve. Transp. Geotech. 23(March): 100351. doi: 10.1016/j.trgeo.2020.100351.

Heitman, J.L., D. Kool, and H.D.R. Carvalho. 2023. Soil management considerations for water resiliency in a changing climate. Agron. J. 115: 2127–2139. doi: 10.1002/agj2.21425.

Herbrich, M., and H.H. Gerke. 2017. Scales of Water Retention Dynamics Observed in Eroded Luvisols from an Arable Postglacial Soil Landscape. Vadose Zo. J. 16(10): 1–17. doi: 10.2136/vzj2017.01.0003.

Hernández, A.F., F. Gil, M. Lacasaña, M. Rodríguez-Barranco, A.M. Tsatsakis, et al. 2013. Pesticide exposure and genetic variation in xenobiotic-metabolizing enzymes interact to induce biochemical liver damage. Food Chem. Toxicol. 61: 144–151. doi: 10.1016/j.fct.2013.05.012.

Herrero-Hernández, E., M.S. Andrades, A. Álvarez-Martín, E. Pose-Juan, M.S. Rodríguez-Cruz, et al. 2013. Occurrence of pesticides and some of their degradation products in waters in a Spanish wine region. J. Hydrol. 486: 234–245. doi: 10.1016/j.jhydrol.2013.01.025.

Hessine, R., S. Ben Mariem, S. Ghannem, S. Mouelhi, and S. Kanzari. 2025. Assessing the effect of pedotransfer functions on modeling of soil water dynamics. J. Appl. Water Eng. Res. 9676. doi: 10.1080/23249676.2025.2463901.

Holland, J.M. 2004. The environmental consequences of adopting conservation tillage in Europe: Reviewing the evidence. Agric. Ecosyst. Environ. 103(1): 1–25. doi: 10.1016/j.agee.2003.12.018.

Hu, W., M. Shao, Q. Wang, J. Fan, and R. Horton. 2009. Temporal changes of soil hydraulic properties under different land uses. Geoderma 149(3–4): 355–366. doi: 10.1016/j.geoderma.2008.12.016.

Hu, W., F. Tabley, M. Beare, C. Tregurtha, R. Gillespie, et al. 2018. Short-Term Dynamics of Soil Physical Properties as Affected by Compaction and Tillage in a Silt Loam Soil. Vadose Zo. J. 17(1): 1–13. doi: 10.2136/vzj2018.06.0115.

Hua, R., N.H. Spliid, K. Heinrichson, and B. Laursenb. 2009. Influence of surfactants on the leaching of bentazone in a sandy loam soil. Pest Manag. Sci. 65(8): 857–861. doi: 10.1002/ps.1763.

Huang, X., H. Wang, M. Zhang, R. Horn, and T. Ren. 2021. Soil water retention dynamics in a Mollisol during a maize growing season under contrasting tillage systems. Soil Tillage Res. 209(January): 104953. doi: 10.1016/j.still.2021.104953.

Iiyama, I. 2016. Differences between field-monitored and laboratory-measured soil moisture characteristics. Soil Sci. Plant Nutr. 62(5–6): 416–422. doi: 10.1080/00380768.2016.1242367.

Imig, A., L. Augustin, J. Groh, T. Pütz, M. Elsner, et al. 2023a. Fate of herbicides in cropped lysimeters: 2. Leaching of four maize herbicides considering different processes. Vadose Zo. J. 22(5): 1–14. doi: 10.1002/vzj2.20275.

Imig, A., L. Augustin, J. Groh, T. Pütz, T. Zhou, et al. 2023b. Fate of herbicides in cropped lysimeters: 1. Influence of different processes and model structure on vadose zone flow. Vadose Zo. J. 22(5): 1–13. doi: 10.1002/vzj2.20265.

IRM. 2020. Caractéristiques des paramètres climatiques. Inst. R. Météorologique. https://www.meteo.be/fr/unpublish/climat-general-en-belgique/parametres.

Isensee, A.R., and A.M. Sadeghi. 1992. Laboratory apparatus for studying pesticide leaching in intact soil cores. Chemosphere 25(4): 581–590. doi: 10.1016/0045-6535(92)90289-4.

Jarvis, N.J. 2007. A review of non-equilibrium water flow and solute transport in soil macropores: Principles, controlling factors and consequences for water quality. Eur. J. Soil Sci. 58(3): 523–546. doi: 10.1111/j.1365-2389.2007.00915.x.

Jarvis, N.J. 2020. A review of non-equilibrium water flow and solute transport in soil macropores: principles, controlling factors and consequences for water quality. Eur. J. Soil Sci. 71(3): 279–302. doi: 10.1111/ejss.12973.

Jarvis, N., E. Coucheney, E. Lewan, T. Klöffel, K.H.E. Meurer, et al. 2024. Interactions between soil structure dynamics, hydrological processes and organic matter cycling : A new soil-crop model. Eur. J. Soil Sci. 75(e13455): 1–

24. doi: 10.1111/ejss.13455.

Jarvis, N., J. Groh, E. Lewan, K.H.E. Meurer, W. Durka, et al. 2022. Coupled modelling of hydrological processes and grassland production in two contrasting climates. Hydrol. Earth Syst. Sci. 26(8): 2277–2299. doi: 10.5194/hess-26-2277-2022.

Jehanzaib, M., M.N. Sattar, J.H. Lee, and T.W. Kim. 2020. Investigating effect of climate change on drought propagation from meteorological to hydrological drought using multi-model ensemble projections. Stoch. Environ. Res. Risk Assess. 34(1): 7–21. doi: 10.1007/s00477-019-01760-5.

Jensen, J.L., P. Schjønning, C.W. Watts, B.T. Christensen, and L.J. Munkholm. 2020. Short-term changes in soil pore size distribution: Impact of land use. Soil Tillage Res. 199(January): 104597. doi: 10.1016/j.still.2020.104597.

Jensen, J.L., C.W. Watts, B.T. Christensen, and L.J. Munkholm. 2019. Soil Water Retention: Uni-Modal Models of Pore-Size Distribution Neglect Impacts of Soil Management. Soil Phys. Hydrol. 83: 18–26. doi: 10.2136/sssaj2018.06.0238.

Jian, M., Y. Che, M. Gao, X. Zhang, Z. Zhang, et al. 2024. Migration of naphthalene in a biochar-amended bioretention facility based on HYDRUS-1D analysis. J. Environ. Manage. 369(August): 122383. doi: 10.1016/j.jenvman.2024.122383.

Jin, X., W. Liu, C. Chen, J. Liu, Z. Yuan, et al. 2018. Effects of three morphometric features of roots on soil water fl ow behavior in three sites in China. Geoderma 320(October 2017): 161–171. doi: 10.1016/j.geoderma.2018.01.035.

Jirků, V., R. Kodešová, A. Nikodem, M. Mühlhanselová, and A. Žigová. 2013. Temporal variability of structure and hydraulic properties of topsoil of three soil types. Geoderma 204–205: 43–58. doi: 10.1016/j.geoderma.2013.03.024.

Johnson-Maynard, J.L., K.J. Umiker, and S.O. Guy. 2007. Earthworm dynamics and soil physical properties in the first three years of no-till management. Soil Tillage Res. 94(2): 338–345. doi: 10.1016/j.still.2006.08.011.

Jurado, A., E. Vàzquez-Suñé, J. Carrera, M. López de Alda, E. Pujades, et al. 2012. Emerging organic contaminants in groundwater in Spain: A review of sources, recent occurrence and fate in a European context. Sci. Total Environ. 440: 82–94. doi: 10.1016/j.scitotenv.2012.08.029.

Kahl, G.M., Y. Sidorenko, and B. Gottesbüren. 2015. Local and global inverse modelling strategies to estimate parameters for pesticide leaching from lysimeter studies. Pest Manag. Sci. 71(4): 616–631. doi: 10.1002/ps.3914.

Kamra, S.K., B. Lennartz, M.T. Van Genuchten, and P. Widmoser. 2001. Evaluating non-equilibrium solute transport in small soil columns. J. Contam. Hydrol. 48(3–4): 189–212. doi: 10.1016/S0169-7722(00)00156-X.

Kasteel, R., T. Pütz, and H. Vereecken. 2007. An experimental and numerical study on flow and transport in a field soil using zero-tension lysimeters and suction plates. Eur. J. Soil Sci. 58(3): 632–645. doi: 10.1111/j.1365-2389.2006.00850.x.

Katagi, T. 2013. Soil column leaching of pesticides. Rev. Environ. Contam. Toxicol. 221: 1–105. doi: 10.1007/978-1-4614-4448-0_1.

Keller, T., T. Colombi, S. Ruiz, S.J. Schymanski, P. Weisskopf, et al. 2021. Soil

structure recovery following compaction: Short-term evolution of soil physical properties in a loamy soil. Soil Sci. Soc. Am. J. 85(4): 1002–1020. doi: 10.1002/saj2.20240.

Khan, M.A., and C.D. Brown. 2016. Influence of commercial formulation on leaching of four pesticides through soil. Sci. Total Environ. 573: 1573–1579. doi: 10.1016/j.scitotenv.2016.09.076.

Khan, M.S., and M.S. Rahman. 2017. Pesticide residue in foods: Sources, management, and control.

Kiefer, K., A. Müller, H. Singer, and J. Hollender. 2019. New relevant pesticide transformation products in groundwater detected using target and suspect screening for agricultural and urban micropollutants with LC-HRMS. Water Res. 165: 114972. doi: 10.1016/j.watres.2019.114972.

Klein, M., J. Hosang, H. Schäfer, B. Erzgräber, and H. Resseler. 2000. Comparing and evaluating pesticide leaching models. Results of simulations with PELMO. Agric. Water Manag. 44(1–3): 263–281. doi: 10.1016/S0378-3774(99)00095-5.

Köck-Schulmeyer, M., A. Ginebreda, C. Postigo, T. Garrido, J. Fraile, et al. 2014. Four-year advanced monitoring program of polar pesticides in groundwater of Catalonia (NE-Spain). Sci. Total Environ. J. 470–471: 1087–1098. doi: 10.1016/j.scitotenv.2013.10.079.

Kodešová, R., M. Kočárek, V. Kodeš, O. Drábek, J. Kozák, et al. 2011. Pesticide adsorption in relation to soil properties and soil type distribution in regional scale. J. Hazard. Mater. 186(1): 540–550. doi: 10.1016/j.jhazmat.2010.11.040.

Kodešová, R., J. Kozák, J. Šimůnek, and O. Vacek. 2005. Single and dual-permeability models of chlorotoluron transport in the soil profile. Plant, Soil Environ. 51(7): 310–315. doi: 10.17221/3591-pse.

Koestel, J.K., J. Moeys, and N.J. Jarvis. 2012. Meta-analysis of the effects of soil properties, site factors and experimental conditions on solute transport. Hydrol. Earth Syst. Sci. 16(6): 1647–1665. doi: 10.5194/hess-16-1647-2012.

Koestel, J.K., T. Norgaard, N.M. Luong, A.L. Vendelboe, P. Moldrup, et al. 2013. Links between soil properties and steady-state solute transport through cultivated topsoil at the field scale. Water Resour. Res. 49(2): 790–807. doi: 10.1002/wrcr.20079.

Köhne, J.M., S. Köhne, and H.H. Gerke. 2002. Estimating the hydraulic functions of dual-permeability models from bulk soil data. Water Resour. Res. 38(7): 26-1-26–11. doi: 10.1029/2001wr000492.

Köhne, J.M., S. Köhne, B.P. Mohanty, and J. Šimůnek. 2004. Inverse Mobile-Immobile Modeling of Transport During Transient Flow: Effects of Between-Domain Transfer and Initial Water Content. Vadose Zo. J. 3(4): 1309–1321. doi: 10.2136/vzj2004.1309.

Köhne, J.M., S. Köhne, and J. Šimůnek. 2006. Multi-process herbicide transport in structured soil columns: Experiments and model analysis. J. Contam. Hydrol. 85(1–2): 1–32. doi: 10.1016/j.jconhyd.2006.01.001.

Köhne, J.M., S. Köhne, and J. Šimůnek. 2009a. A review of model applications for

structured soils: b) Pesticide transport. J. Contam. Hydrol. 104(1–4): 36–60. doi: 10.1016/j.jconhyd.2008.10.003.

Köhne, J.M., S. Köhne, and J. Šimůnek. 2009b. A review of model applications for structured soils: a) Water flow and tracer transport. J. Contam. Hydrol. 104(1–4): 4–35. doi: 10.1016/j.jconhyd.2008.10.002.

Kondo, K., Y. Wakasone, K. Iijima, and K. Ohyama. 2020. Inverse modeling of laboratory experiment to assess parameter transferability of pesticide environmental fate into outdoor experiments under paddy test systems. Pest Manag. Sci. 76(8): 2768–2780. doi: 10.1002/ps.5824.

Kool, D., B. Tong, Z. Tian, J.L. Heitman, T.J. Sauer, et al. 2019. Soil water retention and hydraulic conductivity dynamics following tillage. Soil Tillage Res. 193(June): 95–100. doi: 10.1016/j.still.2019.05.020.

Kördel, W., and M. Klein. 2006. Prediction of leaching and groundwater contamination by pesticides. Pure Appl. Chem. 78(5): 1081–1090. doi: 10.1351/pac200678051081.

Kumari, U., S.B. Singh, and N. Singh. 2020. Sorption and leaching of flucetosulfuron in soil. J. Environ. Sci. Heal. - Part B Pestic. Food Contam. Agric. Wastes 55(6): 550–557. doi: 10.1080/03601234.2020.1733363.

Labite, H., F. Butler, and E. Cummins. 2011. A review and evaluation of plant protection product ranking tools used in agriculture. Hum. Ecol. Risk Assess. 17(2): 300–327. doi: 10.1080/10807039.2011.552392.

Labite, H., N.M. Holden, K.G. Richards, G. Kramers, A. Premrov, et al. 2013. Comparison of pesticide leaching potential to groundwater under EU FOCUS and site specific conditions. Sci. Total Environ. 463–464: 432–441. doi: 10.1016/j.scitotenv.2013.06.050.

Lamichhane, J.R. 2017. Pesticide use and risk reduction in European farming systems with IPM: An introduction to the special issue. Crop Prot. 97: 1–6. doi: 10.1016/j.cropro.2017.01.017.

Larsbo, M., and N. Jarvis. 2003. MACRO 5.0. A model of water flow and solute transport in macroporous soil. Technical description. Uppsala, Sweden.

Larsen, A.E., M. Patton, and E.A. Martin. 2019. High highs and low lows: Elucidating striking seasonal variability in pesticide use and its environmental implications. Sci. Total Environ. 651: 828–837. doi: 10.1016/j.scitotenv.2018.09.206.

Leistra, M., A.M.A. van der Linden, J.J.T.I. Boesten, A. Tiktak, and F. van den Berg. 2001. PEARL model for pesticide behaviour and emissions in soil-plant systems ; Descriptions of the processes in FOCUS PEARL v 1.1.1. Wageningen.

Lentdecker, D., M. De Maglie, D.C. Marques, F. Crivellente, M. Egsmose, et al. 2017. Peer review of the pesticide risk assessment for the active substance metazachlor in light of confirmatory data submitted. 15(April). doi: 10.2903/j.efsa.2017.4833.

Leul, Y., M. Assen, S. Damene, and A. Legass. 2023. Effects of land use types on soil quality dynamics in a tropical sub-humid ecosystem, western Ethiopia. Ecol. Indic. 147(January): 110024. doi: 10.1016/j.ecolind.2023.110024.

Lewis, J., and J. Sjöstrom. 2010. Optimizing the experimental design of soil columns in saturated and unsaturated transport experiments. J. Contam. Hydrol. 115(1–4): 1–13. doi: 10.1016/j.jconhyd.2010.04.001.

Lewis, K.A., J. Tzilivakis, D.J. Warner, and A. Green. 2016. An international database for pesticide risk assessments and management. Hum. Ecol. Risk Assess. 22(4): 1050–1064. doi: 10.1080/10807039.2015.1133242.

Li, Z. 2018. A health-based regulatory chain framework to evaluate international pesticide groundwater regulations integrating soil and drinking water standards. Environ. Int. (October): 1253–1278. doi: 10.1016/j.envint.2018.10.047.

Li, Z. 2021. Regulation of pesticide soil standards for protecting human health based on multiple uses of residential soil. J. Environ. Manage. 297(June): 113369. doi: 10.1016/j.jenvman.2021.113369.

Lichter, K., B. Govaerts, J. Six, K.D. Sayre, J. Deckers, et al. 2008. Aggregation and C and N contents of soil organic matter fractions in a permanent raised-bed planting system in the Highlands of Central Mexico. Plant Soil 305(1–2): 237–252. doi: 10.1007/s11104-008-9557-9.

Liu, Y.Y., R.M. Parinussa, W.A. Dorigo, R.A.M. De Jeu, W. Wagner, et al. 2011. Developing an improved soil moisture dataset by blending passive and active microwave satellite-based retrievals. Hydrol. Earth Syst. Sci. 15(2): 425–436. doi: 10.5194/hess-15-425-2011.

Lori, M., M. Hartmann, D. Kundel, J. Mayer, R.C. Mueller, et al. 2023. Soil microbial communities are sensitive to differences in fertilization intensity in organic and conventional farming systems. FEMS Microbiol. Ecol. 99(6): 1–13. doi: 10.1093/femsec/fiad046.

Lourenço, S.D.N., N. Jones, C. Morley, S.H. Doerr, and R. Bryant. 2015. Hysteresis in the Soil Water Retention of a Sand–Clay Mixture with Contact Angles Lower than Ninety Degrees. Vadose Zo. J. 14(7): 1–8. doi: 10.2136/vzj2014.07.0088.

Lu, N., and Y. Dong. 2015. Closed-Form Equation for Thermal Conductivity of Unsaturated Soils at Room Temperature. J. Geotech. Geoenvironmental Eng. 141(6): 1–12. doi: 10.1061/(asce)gt.1943-5606.0001295.

Lu, J., Q. Zhang, A.D. Werner, Y. Li, S. Jiang, et al. 2020. Root-induced changes of soil hydraulic properties – A review. J. Hydrol. 589(125203): 1–13. doi: 10.1016/j.jhydrol.2020.125203.

Luo, S., N. Lu, C. Zhang, and W. Likos. 2022. Soil water potential: A historical perspective and recent breakthroughs. Vadose Zo. J. (February): 1–39. doi: 10.1002/vzj2.20203.

Lykogianni, M., E. Bempelou, F. Karamaouna, and K.A. Aliferis. 2021. Do pesticides promote or hinder sustainability in agriculture? The challenge of sustainable use of pesticides in modern agriculture. Sci. Total Environ. 795: 148625. doi: 10.1016/j.scitotenv.2021.148625.

Magarey, R.D., S.S.H. Klammer, T.M. Chappell, C.M. Trexler, G.R. Pallipparambil, et al. 2019. Eco-efficiency as a strategy for optimizing the sustainability of pest management. Pest Manag. Sci. 75(12): 3129–3134. doi: 10.1002/ps.5560.

Malla, M.A., S. Gupta, A. Dubey, A. Kumar, and S. Yadav. 2021. Contamination of groundwater resources by pesticides. INC.

Mamy, L., and E. Barriuso. 2005. Glyphosate adsorption in soils compared to herbicides replaced with the introduction of glyphosate resistant crops. Chemosphere 61(6): 844–855. doi: 10.1016/j.chemosphere.2005.04.051.

Mamy, L., J.M. Marín-benito, L. Alletto, E. Justes, M. Ubertosi, et al. 2024. Measurement and modelling of water flows and pesticide leaching under low input cropping systems. Sci. Total Environ. 957(November). doi: 10.1016/j.scitotenv.2024.177607.

Marín-Benito, J.M., M.J. Sánchez-Martín, J.M. Ordax, K. Draoui, H. Azejjel, et al. 2018. Organic sorbents as barriers to decrease the mobility of herbicides in soils. Modelling of the leaching process. Geoderma 313(May 2017): 205–216. doi: 10.1016/j.geoderma.2017.10.033.

Marquardt, D.W. 1963. An algorithm for least-squares estimation of nonlinear parameters. J. Soc. Indust. Appl. Math. 11(2): 431–441. doi: 10.1137/0111030.

Martini, E., M. Bauckholt, S. Kögler, M. Kreck, K. Roth, et al. 2021. STH-net: A soil monitoring network for process-based hydrological modelling from the pedon to the hillslope scale. Earth Syst. Sci. Data 13(6): 2529–2539. doi: 10.5194/essd-13-2529-2021.

McDaniel, M.D., L.K. Tiemann, and A.S. Grandy. 2014. Does agricultural crop diversity enhance soil microbial biomass and organic matter dynamics? A meta-analysis. Ecol. Appl. 24(3): 560–570. doi: 10.1890/13-0616.1.

Mendes, K.F., M.H. Inoue, M.O. Goulart, R.F. Pimpinato, and V.L. Tornisielo. 2016. Leaching of a Mixture of Hexazinone, Sulfometuron-Methyl, and Diuron Applied to Soils of Contrasting Textures. Water. Air. Soil Pollut. 227(8). doi: 10.1007/s11270-016-2954-4.

Mertens, J., G. Kahl, B. Gottesbüren, and J. Vanderborght. 2009. Inverse Modeling of Pesticide Leaching in Lysimeters: Local versus Global and Sequential Single-Objective versus Multiobjective Approaches. Vadose Zo. J. 8(3): 793–804. doi: 10.2136/vzj2008.0029.

Mertens, J., R. Stenger, and G.F. Barkle. 2006. Multiobjective Inverse Modeling for Soil Parameter Estimation and Model Verification. Vadose Zo. J. 5(3): 917–933. doi: 10.2136/vzj2005.0117.

Mesnage, R., A. Székács, and J.G. Zaller. 2021. Herbicides: Brief history, agricultural use, and potential alternatives for weed control. Herbic. Chem. Effic. Toxicol. Environ. Impacts: 1–20. doi: 10.1016/B978-0-12-823674-1.00002-X.

Meurer, K., J. Barron, C. Chenu, E. Coucheney, M. Fielding, et al. 2020a. A framework for modelling soil structure dynamics induced by biological activity. Glob. Chang. Biol. 26(10): 5382–5403. doi: 10.1111/gcb.15289.

Meurer, K.H.E., C. Chenu, E. Coucheney, A.M. Herrmann, T. Keller, et al. 2020b. Modelling dynamic interactions between soil structure and the storage and turnover of soil organic matter. Biogeosciences 17(20): 5025–5042. doi: 10.5194/bg-17-5025-2020.

Mills, M.S., I.R. Hill, A.C. Newcombe, N.D. Simmons, P.C. Vaughan, et al. 2001. Quantification of acetochlor degradation in the unsaturated zone using two novel in situ field techniques: Comparisons with laboratory-generated data and implications for groundwater risk assessments. Pest Manag. Sci. 57(4): 351–359. doi: 10.1002/ps.306.

Morsali, S., H. Babazadeh, S. Shahmohammadi-Kalalagh, and H. Sedghi. 2019. Simulating Zn, Cd and Ni Transport in Disturbed and Undisturbed Soil Columns: Comparison of Alternative Models. Int. J. Environ. Res. 13(4): 721–734. doi: 10.1007/s41742-019-00212-w.

Mualem, Y. 1976. A New Model for Predicting the Hydraulic Conductivity of Unsaturated Porous Media. Water Resour. Res. 12(3): 513–522. doi: 10.1029/WR012i003p00513.

Novak, S.M., J. Portal, and M. Schiavon. 2001. Influence of Soil Aggregate Size on Atrazine and Trifluralin. Bull. Environ. Contam. Toxicol. (August 2000): 514–521. doi: 10.1007/s00128-001-0037-7.

Ochsner, T.E., M.H. Cosh, R.H. Cuenca, W.A. Dorigo, C.S. Draper, et al. 2013. State of the Art in Large-Scale Soil Moisture Monitoring. Soil Sci. Soc. Am. J. 77(6): 1888–1919. doi: 10.2136/sssaj2013.03.0093.

OECD. 2000. Test No. 106: Adsorption - Adsorption - Desorption Using a Batch Equilibrium Method. Paris.

OECD. 2002. Test No. 307: Aerobic and Anaerobic Transformation in Soil. Paris.

OECD. 2004. Test No. 312: Leaching in Soil Columns. Paris.

Oerke, E.C. 2006. Crop losses to pests. J. Agric. Sci. 144(1): 31–43. doi: 10.1017/S0021859605005708.

de Olde, E.M., H. Moller, F. Marchand, R.W. McDowell, C.J. MacLeod, et al. 2017. When experts disagree: the need to rethink indicator selection for assessing sustainability of agriculture. Environ. Dev. Sustain. 19(4): 1327–1342. doi: 10.1007/s10668-016-9803-x.

Ortega, P., E. Sánchez, E. Gil, and V. Matamoros. 2022. Use of cover crops in vineyards to prevent groundwater pollution by copper and organic fungicides. Soil column studies. Chemosphere 303(February). doi: 10.1016/j.chemosphere.2022.134975.

de Paul Obade, V., and R. Lal. 2014. Soil quality evaluation under different land management practices. Environ. Earth Sci. 72(11): 4531–4549. doi: 10.1007/s12665-014-3353-z.

Pavlis, M., E. Cummins, and K. McDonnell. 2010. Groundwater vulnerability assessment of plant protection products: A review. Hum. Ecol. Risk Assess. 16(3): 621–650. doi: 10.1080/10807031003788881.

Pečan, U., M. Pintar, and D. Kastelec. 2023. Variability of in situ soil water retention curves under different tillage systems and growing seasons. Soil Tillage Res. 233(105779): 1–13. doi: 10.1016/j.still.2023.105779.

Pereira, L.S. 2017. Water, Agriculture and Food: Challenges and Issues. Water Resour. Manag. 31(10): 2985–2999. doi: 10.1007/s11269-017-1664-z.

Pérez-Lucas, G., M. Gambín, and S. Navarro. 2020. Leaching behaviour appraisal of eight persistent herbicides on a loam soil amended with different composted organic wastes using screening indices. J. Environ. Manage. 273(June). doi: 10.1016/j.jenvman.2020.111179.

Perrin-Ganier, C., M. Schiavon, J.M. Portal, C. Breuzin, and M. Babut. 1993. Porous cups for pesticides monitoring in soil solution - Laboratory tests. Chemosphere 26(12): 2231–2239. doi: 10.1016/0045-6535(93)90349-A.

Pietrzak, D., J. Kania, G. Malina, E. Kmiecik, and K. Wator. 2019. Pesticides from the EU First and Second Watch Lists in the Water Environment. Clean – Soil, Air, Water 47(7): 13. doi: 10.1002/clen.201800376.

Piñeiro, V., J. Arias, J. Dürr, P. Elverdin, A.M. Ibáñez, et al. 2020. A scoping review on incentives for adoption of sustainable agricultural practices and their outcomes. Nat. Sustain. 3(10): 809–820. doi: 10.1038/s41893-020-00617-y.

Pires, L.F., J.A.R. Borges, J.A. Rosa, M. Cooper, R.J. Heck, et al. 2017. Soil structure changes induced by tillage systems. Soil Tillage Res. 165: 66–79. doi: 10.1016/j.still.2016.07.010.

Pirlot, C., A. Blondel, B. Krings, B. Durenne, O. Pigeon, et al. 2025a. Pesticide fate under varying cropping systems and soil depths: A study using leaching experiments and inverse modelling. J. Contam. Hydrol. 270(September 2024). doi: 10.1016/j.jconhyd.2025.104526.

Pirlot, C., and A. Degré. 2023. Rapport final – projet AIL4WaterQuality.

Pirlot, C., M. Harchies, and A. Degré. 2025b. Diagnostic de vulnérabilités pour augmenter la résilience wallonne à travers l'adaptation aux changements climatiques : Sols sensibles et stratégiques face au changement climatique - Rapport méthodologique.

Pirlot, C., A.-C. Renard, C. De Clerck, and A. Degré. 2024. How does soil water retention change over time? A three-year field study under several production systems. Eur. J. Soil Sci. e13558: 0–20. doi: 10.1111/ejss.13558.

Plummer, M.A., L.C. Hull, and D.T. Fox. 2004. Transport of Carbon-14 in a Large Unsaturated Soil Column. Vadose Zo. J. 3(1): 109–121. doi: 10.2136/vzj2004.1090.

Porfiri, C., J.C. Montoya, W.C. Koskinen, and M.P. Azcarate. 2015. Adsorption and transport of imazapyr through intact soil columns taken from two soils under two tillage systems. Geoderma 251–252: 1–9. doi: 10.1016/j.geoderma.2015.03.016.

Pot, V., P. Benoit, M. Le Menn, O.M. Eklo, T. Sveistrup, et al. 2010. Metribuzin transport in undisturbed soil cores under controlled water potential conditions: Experiments and modelling to evaluate the risk of leaching in a sandy loam soil profile. Pest Manag. Sci. 67(4): 397–407. doi: 10.1002/ps.2077.

Pot, V., J. Šimůnek, P. Benoit, Y. Coquet, A. Yra, et al. 2005. Impact of rainfall intensity on the transport of two herbicides in undisturbed grassed filter strip soil cores. J. Contam. Hydrol. 81(1–4): 63–88. doi: 10.1016/j.jconhyd.2005.06.013.

Pu, J., Z. Wang, and H. Chung. 2020. Climate change and the genetics of insecticide

resistance. Pest Manag. Sci. 76(3): 846–852. doi: 10.1002/ps.5700.

Rabot, E., M. Wiesmeier, S. Schlüter, and H.J. Vogel. 2018. Soil structure as an indicator of soil functions: A review. Geoderma 314(November 2017): 122–137. doi: 10.1016/j.geoderma.2017.11.009.

Ramos, T.B., H. Darouich, and M.C. Gonçalves. 2023. Development and functional evaluation of pedotransfer functions for estimating soil hydraulic properties in Portuguese soils: Implications for soil water dynamics. Geoderma Reg. 35(July): e00717. doi: 10.1016/j.geodrs.2023.e00717.

Rasool, S., T. Rasool, and K.M. Gani. 2022. A review of interactions of pesticides within various interfaces of intrinsic and organic residue amended soil environment. Chem. Eng. J. Adv. 11(April): 100301. doi: 10.1016/j.ceja.2022.100301.

Robinson, N.J., P.G. Dahlhaus, R.J. MacEwan, and J.K. Alexander. 2016. Soil data for biophysical models in Victoria, Australia: Current needs and future challenges. Geoderma Reg. 7(3): 259–270. doi: 10.1016/j.geodrs.2016.03.004.

Rodríguez-Cruz, M.S., J.E. Jones, and G.D. Bending. 2006. Field-scale study of the variability in pesticide biodegradation with soil depth and its relationship with soil characteristics. Soil Biol. Biochem. 38(9): 2910–2918. doi: 10.1016/j.soilbio.2006.04.051.

Rose, M.T., T.R. Cavagnaro, C.A. Scanlan, T.J. Rose, T. Vancov, et al. 2016. Impact of Herbicides on Soil Biology and Function. Elsevier Inc.

Ruehlmann, J. 2020. Soil particle density as affected by soil texture and soil organic matter: 1. Partitioning of SOM in conceptional fractions and derivation of a variable SOC to SOM conversion factor. Geoderma 375(July): 114542. doi: 10.1016/j.geoderma.2020.114542.

Sadeghi, A.M., A.R. Isensee, and A. Shirmohammadi. 2000. Influence of soil texture and tillage on herbicide transport. Chemosphere 41(9): 1327–1332. doi: 10.1016/S0045-6535(00)00028-X.

Sánchez-Bayo, F., and K.A.G. Wyckhuys. 2019. Worldwide decline of the entomofauna: A review of its drivers. Biol. Conserv. 232(September 2018): 8–27. doi: 10.1016/j.biocon.2019.01.020.

Sandin, M., J. Koestel, N. Jarvis, and M. Larsbo. 2017. Post-tillage evolution of structural pore space and saturated and near-saturated hydraulic conductivity in a clay loam soil. Soil Tillage Res. 165: 161–168. doi: 10.1016/j.still.2016.08.004.

Schaap, M.G., F.J. Leij, and M.T. Van Genuchten. 2001. ROSETTA : A computer program for estimating soil hydraulic parameters with hierarchical pedotransfer functions. J. Hydrol. 251: 163–176. doi: 10.1016/S0022-1694(01)00466-8.

Schjønning, P., R.A. McBride, T. Keller, and P.B. Obour. 2017. Predicting soil particle density from clay and soil organic matter contents. Geoderma 286: 83–87. doi: 10.1016/j.geoderma.2016.10.020.

Scholtz, M.T., and T.F. Bidleman. 2007. Modelling of the long-term fate of pesticide residues in agricultural soils and their surface exchange with the atmosphere:

Part II. Projected long-term fate of pesticide residues. Sci. Total Environ. 377(1): 61–80. doi: 10.1016/j.scitotenv.2007.01.084.

Schuhmann, A., G. Klammler, S. Weiss, O. Gans, J. Fank, et al. 2019. Degradation and leaching of bentazone, terbuthylazine and S-metolachlor and some of their metabolites: A long-term lysimeter experiment. Plant, Soil Environ. 65(5): 273–281. doi: 10.17221/803/2018-PSE.

Schwärzel, K., S. Carrick, A. Wahren, K.-H. Feger, G. Bodner, et al. 2011. Soil Hydraulic Properties of Recently Tilled Soil under Cropping Rotation Compared with Two-Year Pasture. Vadose Zo. J. 10(1): 354–366. doi: 10.2136/vzj2010.0035.

Schwen, A., G. Bodner, P. Scholl, G.D. Buchan, and W. Loiskandl. 2011. Temporal dynamics of soil hydraulic properties and the water-conducting porosity under different tillage. Soil Tillage Res. 113(2): 89–98. doi: 10.1016/j.still.2011.02.005.

Siedt, M., A. Schäffer, K.E.C. Smith, M. Nabel, M. Roß-Nickoll, et al. 2021. Comparing straw, compost, and biochar regarding their suitability as agricultural soil amendments to affect soil structure, nutrient leaching, microbial communities, and the fate of pesticides. Sci. Total Environ. 751: 141607. doi: 10.1016/j.scitotenv.2020.141607.

Šimůnek, J., and M.T. Genuchten. 2008. Modeling Nonequilibrium Flow and Transport Processes Using HYDRUS. Vadose Zo. J. 7(2): 782–797. doi: 10.2136/vzj2007.0074.

Šimůnek, J., M.T. Genuchten, and M. Šejna. 2008a. Development and Applications of the HYDRUS and STANMOD Software Packages and Related Codes. Vadose Zo. J. 7(2): 587–600. doi: 10.2136/vzj2007.0077.

Šimůnek, J., M.T. Genuchten, and M. Šejna. 2016. Recent Developments and Applications of the HYDRUS Computer Software Packages. Vadose Zo. J. 15(7): 1–25. doi: 10.2136/vzj2016.04.0033.

Šimůnek, J.J.J., M.T. Genuchten, M. Šejna, B.P. Mohanty, M.H. Cosh, et al. 2008b. Impact of Data Quality and Model Complexity on Prediction of Pesticide Leaching (F. Führ, R. Hance, J. Plimmer, and J. Nelson, editors). J. Environ. Qual. 58(1): 628–640. doi: 10.2134/jeq2005.0257.

Šimůnek, J., M.T. van Genuchten, M.M. Gribb, and J.W. Hopmans. 1998. Parameter estimation of unsaturated soil hydraulic properties from transient flow processes. Soil Tillage Res. 47: 27–36. doi: 10.1016/S0167-1987(98)00069-5.

Šimunek, J., M.T. Van Genuchten, and Jacques. 2002. Solute Transport During Variably Saturated Flow — Inverse Methods. In: Dane, J.H. and Topp, G.C., editors, Methods of Soil Analysis. Part 4. Physical Method. Number 5 i. Soil Science Society of America, Inc., Madison, Wisconsin, USA. p. 1435–1449

Šimůnek, J., D. Jacques, G. Langergraber, S.A. Bradford, M. Šejna, et al. 2013. Numerical modeling of contaminant transport using HYDRUS and its specialized modules. J. Indian Inst. Sci. 93(2): 265–284.

Šimůnek, J., N.J. Jarvis, M.T. Van Genuchten, and A. Gärdenäs. 2003. Review and

comparison of models for describing non-equilibrium and preferential flow and transport in the vadose zone. J. Hydrol. 272(1–4): 14–35. doi: 10.1016/S0022-1694(02)00252-4.

Šimůnek, J., M. Šejna, H. Saito, M. Sakai, and M.T. Van Genuchten. 2009. The HYDRUS-1D Software Package for Simulating the One-Dimensional Movement of Water, Heat, and Multiple Solutes in Variably-Saturated Media. Version 4.08. Hydrus Software series. Department of environmental sciences, University of California Riverside, Riverside, California.

Simunek, J., O. Wendroth, N. Wypler, and M.T. van Genuchten. 2001. Non-equilibrium water flow characterized by means of upward infiltration experiments. Eur. J. Soil Sci. 52: 13–24.

Singh, G., G. Kaur, K. Williard, J. Schoonover, and J. Kang. 2018. Monitoring of Water and Solute Transport in the Vadose Zone: A Review. Vadose Zo. J. 17(1): 160058. doi: 10.2136/vzj2016.07.0058.

Singh, N., H. Kloeppel, and W. Klein. 2002. Movement of metolachlor and terbuthylazine in core and packed soil columns. Chemosphere 47(4): 409–415. doi: 10.1016/S0045-6535(01)00322-8.

van der Sluijs, J.P. 2020. Insect decline, an emerging global environmental risk. Curr. Opin. Environ. Sustain. 46: 39–42. doi: 10.1016/j.cosust.2020.08.012.

Smith, A.E., and D.M. Secoy. 1976. Early Chemical Control of Weeds in Europe. Weed Sci. 24(6): 594–597. doi: 10.1017/s0043174500063013.

Sniegowski, K., J. Mertens, J. Diels, E. Smolders, and D. Springael. 2009. Inverse modeling of pesticide degradation and pesticide-degrading population size dynamics in a bioremediation system: Parameterizing the Monod model. Chemosphere 75(6): 726–731. doi: 10.1016/j.chemosphere.2009.01.050.

Soto-Gómez, D., P. Pérez-Rodríguez, L. Vázquez Juíz, J.E. López-Periago, and M. Paradelo Pérez. 2019. A new method to trace colloid transport pathways in macroporous soils using X-ray computed tomography and fluorescence macrophotography. Eur. J. Soil Sci. 70(3): 431–442. doi: 10.1111/ejss.12783.

SPW ARNE. 2022. Etat des nappes et des masses d'eau souterraine de la Wallonie. Namur.

Strudley, M.W., T.R. Green, and J.C. Ascough. 2008. Tillage effects on soil hydraulic properties in space and time: State of the science. Soil Tillage Res. 99(1): 4–48. doi: 10.1016/j.still.2008.01.007.

Su, W., H. Hao, R. Wu, H. Xu, F. Xue, et al. 2017. Degradation of Mesotrione Affected by Environmental Conditions. Bull. Environ. Contam. Toxicol. 98(2): 212–217. doi: 10.1007/s00128-016-1970-9.

Sur, R., C. Kley, and S. Sittig. 2022. Field leaching study - Inverse estimation of degradation and sorption parameters for a mobile soil metabolite and its pesticide parent. Environ. Pollut. 310(March): 119794. doi: 10.1016/j.envpol.2022.119794.

Swartjes, F.A., and M.A. Van Der. 2020. Measures to reduce pesticides leaching into groundwater-based drinking water resources : An appeal to national and local

governments , water boards and farmers. Sci. Total Environ. 699: 134186. doi: 10.1016/j.scitotenv.2019.134186.

Szabó, B., M. Weynants, and T.K.D. Weber. 2021. Updated European hydraulic pedotransfer functions with communicated uncertainties in the predicted variables (euptfv2). Geosci. Model Dev. 14(1): 151–175. doi: 10.5194/gmd-14-151-2021.

Tian, Z., J. Chen, C. Cai, W. Gao, T. Ren, et al. 2021. New pedotransfer functions for soil water retention curves that better account for bulk density effects. Soil Tillage Res. 205: 1–40. doi: 10.1016/j.still.2020.104812.

Tifafi, M., R. Bouzouidja, S. Leguédois, S. Ouvrard, and G. Séré. 2017. How lysimetric monitoring of Technosols can contribute to understand the temporal dynamics of the soil porosity. Geoderma 296: 60–68. doi: 10.1016/j.geoderma.2017.02.027.

Tilman, D., J. Fargione, B. Wolff, C. D'Antonio, A. Dobson, et al. 2001. Forecasting agriculturally driven global environmental change.

Toccalino, P.L., R.J. Gilliom, B.D. Lindsey, and M.G. Rupert. 2014. Pesticides in Groundwater of the United States : Decadal-Scale Changes , 1993 – 2011. 52: 112–125. doi: 10.1111/gwat.12176.

Tóth, B., M. Weynants, A. Nemes, A. Makó, G. Bilas, et al. 2015. New generation of hydraulic pedotransfer functions for Europe. Eur. J. Soil Sci. 66(January): 226–238. doi: 10.1111/ejss.12192.

Ullucci, S., L. Menaballi, S. Di, M. Luini, C. Riva, et al. 2022. Science of the Total Environment Pesticides groundwater modelling relies on input data characterised by a high intrinsic variability : Is the resulting risk for groundwater credible ? Sci. Total Environ. 839(February): 156314. doi: 10.1016/j.scitotenv.2022.156314.

USEPA. 2008. Fate, transport and transformation test guidelines. OPPTS 835.1240 Leaching Studies. Washington DC.

Vandenberghe, C., A. Blondel, C. Lacroix, K. Lefébure, B. Krings, et al. 2024. Evaluation du devenir des produits phytopharmaceutiques en plein champ en fonction des pratiques culturales & évaluation du désherbage mécanique en culture de céréales avec ou sans combinaison avec du désherbage chimique pour le développement d'une agricu.

Vanderborght, J., and H. Vereecken. 2007. Review of Dispersivities for Transport Modeling in Soils. Vadose Zo. J. 6(1): 29–52. doi: 10.2136/vzj2006.0096.

Varvaris, I., B. V Iversen, Z. Pittaki-chrysodonta, and C.D. Børgesen. 2021a. Parameterization of two-dimensional approaches in HYDRUS-2D : Part 1 . Simulating water flow dynamics at the field scale. (December 2020): 1578–1599. doi: 10.1002/saj2.20307.

Varvaris, I., Z. Pittaki-Chrysodonta, C. Duus Børgesen, and B. V. Iversen. 2021b. Parameterization of two-dimensional approaches in HYDRUS-2D: Part 1. Simulating water flow dynamics at the field scale. Soil Sci. Soc. Am. J. 85(5): 1578–1599. doi: 10.1002/saj2.20307.

Varvaris, I., Z. Pittaki-Chrysodonta, C. Duus Børgesen, and B.V. Iversen. 2021c. Parameterization of two-dimensional approaches in HYDRUS-2D: Part 2. Solute transport at the field and column scale. Soil Sci. Soc. Am. J. 85(5): 1496–1518. doi: 10.1002/saj2.20262.

Vereecken, H., J.A. Huisman, N. Hendricks Franssen, H.J. Brüggemann, H.R. Bogena, S. Kollet, et al. 2015. Soil hydrology: Recent methodological advances, challenges, and perspectives. Water Resour. Res. 51(2616–2633). doi: 10.1111/j.1752-1688.1969.tb04897.x.

Vereecken, H., M. Weynants, M. Javaux, Y. Pachepsky, M.G. Schaap, et al. 2010. Using Pedotransfer Functions to Estimate the van Genuchten–Mualem Soil Hydraulic Properties: A Review. Vadose Zo. J. 9(4): 795–820. doi: 10.2136/vzj2010.0045.

Verhulst, N., B. Govaerts, E. Verachtert, A. Castellanos-Navarrete, M. Mezzalama, et al. 2010. Conservation Agriculture, Improving Soil Quality for Sustainable Production Systems? Food Secur. Soil Qual. (June): 137–208. doi: 10.1201/ebk1439800577-7.

Vincent, A., P. Benoit, V. Pot, I. Madrigal, L. Delgado-Moreno, et al. 2007. Impact of different land uses on the migration of two herbicides in a silt loam soil: Unsaturated soil column displacement studies. Eur. J. Soil Sci. 58(1): 320–328. doi: 10.1111/j.1365-2389.2006.00844.x.

Vogel, H. 2019. Scale Issues in Soil Hydrology. Vadose Zo. J. 18(1): 1–10. doi: 10.2136/vzj2019.01.0001.

Vogel, H.J., H.H. Gerke, R. Mietrach, R. Zahl, and T. Wöhling. 2023. Soil hydraulic conductivity in the state of nonequilibrium. Vadose Zo. J. 22(2): 1–12. doi: 10.1002/vzj2.20238.

Wahren, A., K.H. Feger, K. Schwärzel, and A. Münch. 2009. Land-use effects on flood generation - Considering soil hydraulic measurements in modelling. Adv. Geosci. 21: 99–107. doi: 10.5194/adgeo-21-99-2009.

Wanders, N., D. Karssenberg, A. De Roo, S.M. De Jong, and M.F.P. Bierkens. 2014. The suitability of remotely sensed soil moisture for improving operational flood forecasting. Hydrol. Earth Syst. Sci. 18(6): 2343–2357. doi: 10.5194/hess-18-2343-2014.

Wauchope, R.D., S. Yeh, J.B.H.J. Linders, R. Kloskowski, K. Tanaka, et al. 2002. Pesticide soil sorption parameters: Theory, measurement, uses, limitations and reliability. Pest Manag. Sci. 58(5): 419–445. doi: 10.1002/ps.489.

Weber, J.B., G.G. Wilkerson, and C.F. Reinhardt. 2004. Calculating pesticide sorption coefficients (Kd) using selected soil properties. Chemosphere 55(2): 157–166. doi: 10.1016/j.chemosphere.2003.10.049.

Weihermüller, L., P. Lehmann, M. Herbst, M. Rahmati, A. Verhoef, et al. 2021. Choice of Pedotransfer Functions Matters when Simulating Soil Water Balance Fluxes. J. Adv. Model. Earth Syst. 13(3): 1–30. doi: 10.1029/2020MS002404.

Weynants, M., L. Montanarella, G. Tóth, P. Strauss, F. Feichtinger, et al. 2013. European HYdropedological Data Inventory (EU-HYDI). Luxembourg.

Whalley, W.R., E.S. Ober, and M. Jenkins. 2013. Measurement of the matric potential of soil water in the rhizosphere. J. Exp. Bot. 64(13): 3951–3963. doi: 10.1093/jxb/ert044.

De Wilde, T., J. Mertens, J. Šimunek, K. Sniegowksi, J. Ryckeboer, et al. 2009. Characterizing pesticide sorption and degradation in microscale biopurification systems using column displacement experiments. Environ. Pollut. 157(2): 463–473. doi: 10.1016/j.envpol.2008.09.008.

Willkommen, S., J. Lange, U. Ulrich, M. Pfannerstill, and N. Fohrer. 2021. Field insights into leaching and transformation of pesticides and fluorescent tracers in agricultural soil. Sci. Total Environ. 751: 141658. doi: 10.1016/j.scitotenv.2020.141658.

Wołejko, E., A. Jabłońska-Trypuć, U. Wydro, A. Butarewicz, and B. Łozowicka. 2020. Soil biological activity as an indicator of soil pollution with pesticides – A review. Appl. Soil Ecol. 147(September 2019). doi: 10.1016/j.apsoil.2019.09.006.

WWDR. 2015. Water for a sustainable world. Paris.

Zhang, M., Y. Lu, J. Heitman, R. Horton, and T. Ren. 2017. Temporal Changes of Soil Water Retention Behavior as Affected by Wetting and Drying Following Tillage. Soil Sci. Soc. Am. J. 81(6): 1288–1295. doi: 10.2136/sssaj2017.01.0038.

Zhang, M., Y. Lu, R. Horton, and T. Ren. 2018. Temporal Changes of Soil Water Retention Behavior as Affected by Wetting and Drying Following Tillage. Soil Phys. Hydrol. 81: 1288–1295. doi: 10.2136/sssaj2017.01.0038.

Zhang, Y., and M.G. Schaap. 2019. Estimation of saturated hydraulic conductivity with pedotransfer functions: A review. J. Hydrol. 575(May): 1011–1030. doi: 10.1016/j.jhydrol.2019.05.058.

Zhao, Y., T. Wen, L. Shao, R. Chen, X. Sun, et al. 2020. Predicting hysteresis loops of the soil water characteristic curve from initial drying. Soil Sci. Soc. Am. J. 84(5): 1642–1649. doi: 10.1002/saj2.20125.

Zink, M., J. Mai, M. Cuntz, and L. Samaniego. 2018. Conditioning a Hydrologic Model Using Patterns of Remotely Sensed Land Surface Temperature. Water Resour. Res. 54(4): 2976–2998. doi: 10.1002/2017WR021346.